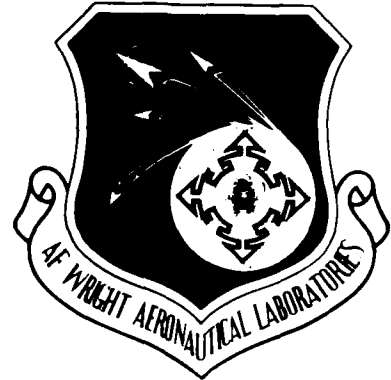


DTIC FILE COPY

2

AD-A195 145

AFWAL-TR-87-3069
VOLUME II



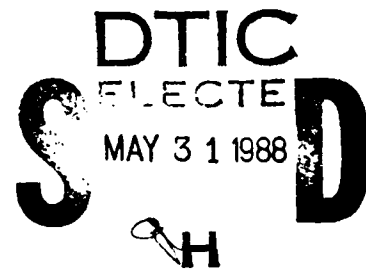
**EXPERIMENTAL MODAL ANALYSIS AND
DYNAMIC COMPONENT SYNTHESIS**

VOL. II Measurement Techniques for
Experimental Modal Analysis

Dr. Randall J. Allemang, Dr. David L. Brown, Dr. Robert W. Rost
Structural Dynamics Research Laboratory
Department of Mechanical and Industrial Engineering
University of Cincinnati
Cincinnati, Ohio 45221-0072

December 1987

Final Technical Report for Period November 1983 - January 1987



Approved for public release; distribution is unlimited


FLIGHT DYNAMICS LABORATORY
AIR FORCE WRIGHT AERONAUTICAL LABORATORIES
AIR FORCE SYSTEMS COMMAND
WRIGHT-PATTERSON AIR FORCE BASE, OHIO 45533-6553

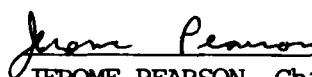
NOTICE

When Government drawings, specifications, or other data are used for any purpose other than in connection with a definitely Government-related procurement, the United States Government incurs no responsibility or any obligation whatsoever. The fact that the Government may have formulated or in any way supplied the said drawings, specifications, or other data, is not to be regarded by implication, or any other person or corporation; or as conveying any rights or permission to manufacture, use, or sell any patented invention that may in any way be related thereto.

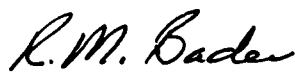
This report has been reviewed by the Office of Public Affairs (ASD/PA) and is releasable to the National Technical Information Service (NTIS). At NTIS, it will be available to the general public, including foreign nations.

This technical report has been reviewed and is approved for publication.


OTTO F. MAURER, Principal Engineer
Structural Dynamics Branch
Structures Division


JEROME PEARSON, Chief
Structural Dynamics Branch
Structures Division

FOR THE COMMANDER


ROBERT M. BADER, Ass't Chief
Structures Division
Flight Dynamics Laboratory

If your address has changed, if you wish to be removed from our mailing list, or if the addressee is no longer employed by your organization please notify AFWAL/FIBG, Wright-Patterson AFB, OH 45433-6553 to help us maintain a current mailing list.

Copies of this report should not be returned unless return is required by security considerations, contractual obligations, or notice on a specific document.

UNCLASSIFIED

SECURITY CLASSIFICATION OF THIS PAGE

REPORT DOCUMENTATION PAGE

1a. REPORT SECURITY CLASSIFICATION UNCLASSIFIED			1b. RESTRICTIVE MARKINGS									
2a. SECURITY CLASSIFICATION AUTHORITY			3. DISTRIBUTION/AVAILABILITY OF REPORT APPROVED FOR PUBLIC RELEASE; DISTRIBUTION IS UNLIMITED									
2b. DECLASSIFICATION/DOWNGRADING SCHEDULE												
4. PERFORMING ORGANIZATION REPORT NUMBER(S)			5. MONITORING ORGANIZATION REPORT NUMBER(S) AFWAL-TR-87-3069 VOL. II									
6a. NAME OF PERFORMING ORGANIZATION UNIVERSITY OF CINCINNATI		6b. OFFICE SYMBOL (If applicable)	7a. NAME OF MONITORING ORGANIZATION AIR FORCE WRIGHT AERONAUTICAL LABORATORIES, FLIGHT DYNAMICS LABORATORY									
6c. ADDRESS (City, State and ZIP Code) CINCINNATI OH 45221-0072			7b. ADDRESS (City, State and ZIP Code) AFWAL/FIBG Wright-Patterson AFB OH 45433-6553									
8a. NAME OF FUNDING/SPONSORING ORGANIZATION Armament Test Laboratory		8b. OFFICE SYMBOL (If applicable) AFATL	9. PROCUREMENT INSTRUMENT IDENTIFICATION NUMBER F33615-83-C-3218									
8c. ADDRESS (City, State and ZIP Code) Eglin AFB FL 32542			10. SOURCE OF FUNDING NOS. <table border="1"><thead><tr><th>PROGRAM ELEMENT NO.</th><th>PROJECT NO.</th><th>TASK NO.</th><th>WORK UNIT NO.</th></tr></thead><tbody><tr><td>62201F</td><td>2401</td><td>04</td><td>16</td></tr></tbody></table>		PROGRAM ELEMENT NO.	PROJECT NO.	TASK NO.	WORK UNIT NO.	62201F	2401	04	16
PROGRAM ELEMENT NO.	PROJECT NO.	TASK NO.	WORK UNIT NO.									
62201F	2401	04	16									
11. TITLE (Include Security Classification) EXPERIMENTAL MODAL ANALYSIS AND DYNAMIC COMPONENT SYNTHESIS (UNCLASSIFIED) Vol. II - Measurement Techniques for Experimental Modal Analysis												
12. PERSONAL AUTHOR(S) DR. RANDALL J. ALLEMANG DR. DAVID L. BROWN												
13a. TYPE OF REPORT FINAL		13b. TIME COVERED FROM NOV 1983 TO JAN 1987	14. DATE OF REPORT (Yr., Mo., Day) DECEMBER 1987	15. PAGE COUNT 227								
16. SUPPLEMENTARY NOTATION The computer software contained herein are theoretical and/or references that in no way reflect Air Force-owned or developed computer software.												
17. COSATI CODES <table border="1"><thead><tr><th>FIELD</th><th>GROUP</th><th>SUB. GR.</th></tr></thead><tbody><tr><td>22</td><td>01</td><td></td></tr></tbody></table>			FIELD	GROUP	SUB. GR.	22	01		18. SUBJECT TERMS (Continue on reverse if necessary and identify by block number) MODAL TESTING VIBRATION TESTING DYNAMICS			
FIELD	GROUP	SUB. GR.										
22	01											
19. ABSTRACT (Continue on reverse if necessary and identify by block number) <p>This technical report presents the theory and practical aspects of acquiring data used in an experimental modal analysis. Always keeping in mind that a modal analysis is an experimental technique to determine the dynamic properties of a system, this report describes the procedures to collect data that can be used in parameter estimation algorithms that estimate natural frequency, damping, and mode shapes. The potential errors are discussed as well as techniques for reducing these errors. Several mathematical models for the computation of frequency response functions for single and multiple inputs are presented. Some new considerations in the area of nonlinear vibrations is presented.</p>												
20. DISTRIBUTION/AVAILABILITY OF ABSTRACT UNCLASSIFIED/UNLIMITED <input checked="" type="checkbox"/> SAME AS RPT. <input type="checkbox"/> DTIC USERS <input type="checkbox"/>			21. ABSTRACT SECURITY CLASSIFICATION UNCLASSIFIED									
22a. NAME OF RESPONSIBLE INDIVIDUAL OTTO F. MAURER		22b. TELEPHONE NUMBER (Include Area Code) (513)255-5236	22c. OFFICE SYMBOL AFWAL/FIBG									

SUMMARY

When attempting to experimentally determine the dynamic properties (natural frequency, damping, and mode shapes) of a structure, one of the most important aspects is to collect and process data that represents the structure as accurately as possible. This means that "clean" and error free data must be collected. This data must be processed by an appropriate frequency response function model. This data can then be used as input to an number of parameter estimation algorithms and could also be used in modal modeling algorithms.

This technical report describes the procedure used to collect this data. Many of the potential errors are discussed as well as techniques to eliminate or reduce the effects of these errors on the quality of the results.

Throughout the time frame of this contract, it was determined, that if the procedures described in this technical report are followed, data can be collected, as input to modal parameter estimation algorithms, that will yield accurate dynamic properties of the test structure. With care and attention to theoretical limitations, these dynamic properties can be used to construct a modal model.



Accession For	
NTIS GRA&I	<input checked="" type="checkbox"/>
DTIC TAB	<input type="checkbox"/>
Unannounced	<input type="checkbox"/>
Justification	
By _____	
Distribution/	
Availability Codes	
Dist	Avail and/or Special
A-1	

PREFACE

This report is one of six Technical Reports that represent the final report on the work involved with United States Air Force Contract F33615-83-C-3218, Experimental Modal Analysis and Dynamic Component Synthesis. The reports that are part of the documented work include the following:

AFWAL-TR-87-3069

VOLUME I Summary of Technical Work
VOLUME II Measurement Techniques for Experimental Modal Analysis
VOLUME III Modal Parameter Estimation
VOLUME IV System Modeling Techniques
VOLUME V Universal File Formats
VOLUME VI Software User's Guide

For a complete understanding of the research conducted under this contract, all of the Technical Reports should be referenced.

ACKNOWLEDGEMENTS

The University of Cincinnati Structural Dynamics Research Laboratory (UC-SDRL) would like to acknowledge the numerous people who have contributed to the Measurement Techniques for Experimental Modal Analysis Technical Report. Instrumental in providing technical assistance and guidance in both theoretical and practical implementation were Jan Leuridan of Leuven Measurement and Systems, and Havard Vold of the Structural Dynamics Research Corporation. Also, the UC-SDRL would like to acknowledge the contract monitor, Otto Maurer, for guidance and assistance during the course of the contract.

The section on non-linear evaluation is directly attributable to Greg Hopton of Defiance - SMC.

In addition, the following people on the staff of the UC-SDRL have contributed to the preparation of this volume: Kelly Allen, C. Y. Shih, Tony Severyn, Vivian Walls, Hiroshi Kanda, Phil Weber, Stu Shelly, Max Wei, Filip Deblawue, and Jeff Poland.

TABLE OF CONTENTS

Section	page
Report Documentation Page - DD Form 1473	iii
SUMMARY	iv
PREFACE	v
ACKNOWLEDGEMENTS	vi
1. INTRODUCTION	1
1.1 Objectives	1
1.2 Terminology	2
2. MODAL TESTING	3
2.1 Test Structure Set-up	3
2.2 Hardware Set-up	4
2.3 Initial Measurements	5
2.4 Non-linear Check	5
2.5 Modal Test	5
3. MODAL DATA ACQUISITION	6
3.1 Digital Signal Processing	6
3.1.1 Sampling	6
3.1.2 Sampling Theory	7
3.1.3 Quantization	7
3.1.4 Discrete Fourier Transform	9
3.1.5 Errors	12
3.1.6 Leakage Error	13
3.1.7 Aliasing Error	20
3.1.8 Quantization Error	25
3.1.9 Differential Nonlinearity	25
3.1.10 Bit Dropout	25
3.1.11 Reference Voltage	25
3.1.12 Overload and Overload Recovery	25
3.1.13 Aperture Error - Clock Jitter	25
3.1.14 Digitizer Noise	26
3.2 Transducer Considerations	26
3.3 Error Reduction Methods	29
3.3.1 Signal Averaging	29
3.3.2 Excitation	40
3.3.3 Increased Frequency Resolution	40
3.3.4 Weighting Functions	41
4. EXCITATION TECHNIQUES	44
4.1 Excitation Constraints	44
4.2 Excitation Signals	45
4.2.1 Slow Swept Sine	46
4.2.2 Periodic Chirp	46
4.2.3 Impact (Impulse)	46
4.2.4 Step Relaxation	46
4.2.5 Pure Random	49
4.2.6 Pseudorandom	49
4.2.7 Periodic Random	49
4.2.8 Burst Random	50
5. FREQUENCY RESPONSE FUNCTION ESTIMATION	52
5.1 Introduction	52
5.2 Theory	52
5.3 Mathematical Models	54

TABLE OF CONTENTS (continues)

Section	page
5.3.1 H_1 Technique	54
5.3.1.1 Dual Input Case	57
5.3.1.2 Multiple Inputs	59
5.3.2 H_2 Technique	59
5.3.2.1 Two Inputs/Two Response	60
5.3.2.2 Two Inputs/Three Responses	61
5.3.3 H_e Technique	61
5.4 H_e Technique	62
5.5 Comparison of H_1 , H_2 , and H_e	63
5.6 Examples	64
5.6.1 Single Input	68
5.6.2 Dual Inputs	68
5.6.3 Three Inputs	68
5.7 Calculation Techniques	75
5.7.1 H_1 Technique	75
5.7.1.1 Trivial Solution	75
5.7.1.2 Matrix Inversion	75
5.7.1.3 Gauss Elimination	77
6. MULTIPLE INPUT CONSIDERATIONS	80
6.1 Optimum Number Of Inputs	80
6.2 Input Evaluation	81
6.2.1 Coherence Functions	81
6.2.1.1 Vector Representation	83
6.2.2 Principal Input Forces	85
6.3 Examples	89
7. NON-LINEAR CONSIDERATIONS	115
7.1 Overview	115
7.2 Research Objectives	115
7.3 Modal Analysis and Nonlinearities	116
7.3.1 System Assumptions	116
7.3.2 Basic Nonlinear Systems	117
7.3.3 Excitation Techniques	121
7.4 Nonlinear Detection Techniques	124
7.4.1 Distortion of The Characteristic Function	124
7.4.1.1 The Nyquist Plot	124
7.4.1.2 Damping Values	125
7.4.2 Reciprocity	126
7.4.3 Coherence	127
7.4.4 The 'Sig-function'	128
7.4.5 The Hilbert Transform	129
7.4.6 Volterra and Wiener Functional Series	138
7.4.7 Bispectral Analysis	139
7.5 Nonlinearities and Multiple Inputs	140
7.5.1 The Multiple Input Estimation Technique	140
7.5.2 Higher Order Function Estimates	141
7.5.3 Research Approach	142
7.5.4 Research Application	143
7.5.4.1 Duffing's Equation Simulated	145
7.5.5 Effects of Varying Test Parameters	146
7.5.6 Dead Zone Gap Simulated	151
7.5.7 Nonlinear Damping Effects Simulated	170
7.5.8 Two Degree of System Simulated	170
7.5.9 Application to Physical Systems	178
7.6 CONCLUSIONS AND RECOMMENDATIONS	185

TABLE OF CONTENTS (concluded)

Section	page
REFERENCES	186
BIBLIOGRAPHY	191
Nomenclature	201
Appendix A: Least Squares Method	A-1
A.1 Least Squares Method	A-1
A.2 Correlation Coefficient	A-4
A.3 Examples	A-5
A.3.1 Example 1	A-5
A.3.2 Example 2	A-6
A.4 References	A-7
Appendix B: Singular Value Decomposition	B-1

LIST OF ILLUSTRATIONS

	page
Figure 1. Digitization Equations	8
Figure 2. Quantization: 3 Bit Analog to Digital Converter	9
Figure 3. Quantization: ADC Input Optimization	10
Figure 4. Quantization: ADC Input Optimization	11
Figure 5. Time Domain Function: Theoretical Harmonic	14
Figure 6. Time Domain Function: Theoretical Window	15
Figure 7. Time Domain Function: Multiplication of Signals	16
Figure 8. Frequency Domain: Theoretical Harmonic	17
Figure 9. Frequency Domain: Theoretical Window	18
Figure 10. Frequency Domain: Convolved Signals	19
Figure 11. Frequency Domain: Periodic Signal	21
Figure 12. Frequency Domain: Nonperiodic Signal	22
Figure 13. Aliasing Example	23
Figure 14. Aliasing Contribution	24
Figure 15. Transducer Mounting Methods	27
Figure 16. Calibration Methods	28
Figure 17. Asynchronous Averaging: (N = 1, M = 1)	32
Figure 18. Asynchronous Averaging With Hann: (N = 1, M = 80)	33
Figure 19. Cyclic Averaging (N = 4, M = 20)	35
Figure 20. Cyclic Averaging With Hann (N = 4, M = 20)	36
Figure 21. Overlap Processing: Zero Overlap	37
Figure 22. Overlap Processing: Fifty Percent Overlap	38
Figure 23. Random Decrement Averaging	39
Figure 24. Increased Frequency Resolution	42
Figure 25. Typical Weighting Functions	43
Figure 26. Typical Test Configuration: Shaker	47
Figure 27. Typical Test Configuration: Impact Hammer	48
Figure 28. Summary of Excitation Signals	51
Figure 29. Multiple Input System Model	53
Figure 30. Dual Input System Model, H_1 Technique	57
Figure 31. System Model for H_2 Technique	60
Figure 32. Geometrical Interpretation at Resonance	65
Figure 33. Geometrical Interpretation at Anti-resonance	66

LIST OF ILLUSTRATIONS (continues)

	page
Figure 34. Body-in-white Test Structure	67
Figure 35. Frequency Response Estimate H_{11} - Single Input	69
Figure 36. Coherence and Auto Power Spectrum for H_{11} - Single Input	70
Figure 37. Frequency Response Estimate H_{11} - Dual Input Case	71
Figure 38. Multiple Coherence Function - Dual Input Case	72
Figure 39. Frequency Response Estimate H_{11} - Three Input Case	73
Figure 40. Multiple Coherence Function - Three Input Case	74
Figure 41. Frequency Response and Coherence Estimated With Two Driven Exciters but Only One Measured Force	76
Figure 42. Three Inputs As Vectors - F_1 Used As The Reference	84
Figure 43. Remaining Vectors - F_1 Used As The Reference	86
Figure 44. Three Inputs As Vectors - F_2 Used As The Reference	87
Figure 45. Remaining Vectors - F_2 Used As The Reference	88
Figure 46. Ordinary Coherence Function Between Forces Dual Input Case	90
Figure 47. Principal Auto Power Spectra of Input Forces Dual Input Case	91
Figure 48. Input Auto Power Spectrum Dual Input Case	92
Figure 49. Determinant of Input Cross Spectrum Matrix Dual Input Case	93
Figure 50. Frequency Response Estimates Dual Input Case	94
Figure 51. Input Auto Power Spectrum, One Input Not Driven, Dual Input Case	96
Figure 52. Ordinary Coherence Function Between Forces One Input Not Driven, Dual Input Case	97
Figure 53. Principal Auto Power Spectra of the Input Forces, One Input Not Driven, Dual input Case	98
Figure 54. Determinant Function, One Input Not Driven, Dual Input Case	100
Figure 55. Frequency Response Estimates, One Input Not Driven, Dual Input Case	101
Figure 56. Auto Power Spectrum of Inputs, Same Signal Driving Both Exciters, Dual Input Case	102
Figure 57. Ordinary Coherence Between Forces, Same Signal Driving Both Exciters, Dual Input Case	103
Figure 58. Principal Auto Power Spectra of Inputs, Same Signal Driving Both Exciters, Dual Input Case	104
Figure 59. Frequency Response Estimates, Same Signal Driving Both Exciters, Dual Input Case	105
Figure 60. Ordinary Coherence Function COH_{12} Three Input Case	106
Figure 61. Conditioned Partial Coherence COH_{23}^1 Three Input Case	107
Figure 62. Principal Auto Power Spectra of Inputs, Three Input Case	108
Figure 63. Ordinary Coherence Function COH_{12} Input 2 off, Three Input Case	109
Figure 64. Conditioned Partial Coherence COH_{23}^1 Input 2 off, Three Input Case	110

LIST OF ILLUSTRATIONS (continues)

	page
Figure 65. Principal Auto Power Spectra of Inputs, Shaker 2 off, Three Input Case	111
Figure 66. Ordinary Coherence Function COH_{12} , Input 3 off, Three Input Case	112
Figure 67. Conditioned Partial Coherence COH_{23}^1 , Input 3 Off, Three Input Case	113
Figure 68. Principal Auto Power Spectra of Inputs, Input 3 off, Three Input Case	114
Figure 69. Evaluation of Linear and Nonlinear Systems	116
Figure 70. Linear Network	117
Figure 71. Simple Pendulum	119
Figure 72. Simple Spring-Mass System	120
Figure 73. Force Characteristic Curves	121
Figure 74. F.R.F. of a Hardening and Softening Spring	122
Figure 75. Simple Spring-Mass System with Dashpot	123
Figure 76. Nyquist Plot	125
Figure 77. Distorted Nyquist Plots	126
Figure 78. Carpet Plot of a Linear System	127
Figure 79. Carpet Plots of Nonlinear Systems	128
Figure 80. Complex Frequency Plane	131
Figure 81. Cross Bispectrum Plot	141
Figure 82. Process Flow Diagram	144
Figure 83. Nonlinear Stiffness Model	146
Figure 84. BOSS Nonlinear Stiffness Model	147
Figure 85. Linear Stiffness Model - BLRA	148
Figure 86. Nonlinear Stiffness Model - BNRA	149
Figure 87. Nonlinear Stiffness Model - BNRC	150
Figure 88. Linear Stiffness Model - BLBA	152
Figure 89. Nonlinear Stiffness Model - BNB100	153
Figure 90. Linear Stiffness Model - BLBA	154
Figure 91. Nonlinear Stiffness Model - BNBA	155
Figure 92. Nonlinear Stiffness Model - BNBB	156
Figure 93. Nonlinear Stiffness Model - BNBC	157
Figure 94. Nonlinear Stiffness Model - BNBD	158
Figure 95. Linear Stiffness Model - BLBLF	159
Figure 96. Nonlinear Stiffness Model - BNLF1	160
Figure 97. Nonlinear Stiffness Model - BNLF8	161
Figure 98. Linear Stiffness Model - BNHF0	162
Figure 99. Nonlinear Stiffness Model - BNHF1	163
Figure 100. Nonlinear Stiffness Model - BNHF8	164

LIST OF ILLUSTRATIONS (concluded)

	page
Figure 101. Nonlinear Clearance Model	165
Figure 102. BOSS Nonlinear Clearance Model	166
Figure 103. Linear Clearance Model - BLK2	167
Figure 104. Nonlinear Clearance Model - BNK21	168
Figure 105. Nonlinear Clearance Model - BNK25	169
Figure 106. Linear Clearance Model - BLK2H0	171
Figure 107. Nonlinear Clearance Model - BNK2H1	172
Figure 108. Nonlinear Clearance Model - BNK2H5	173
Figure 109. BOSS Nonlinear Damping Model	174
Figure 110. Nonlinear Damping Model - BNDA	175
Figure 111. Function Simulator - Low Force	176
Figure 112. Function Simulator - High Force	177
Figure 113. Modified Body-in-White - 2.5 lbs	179
Figure 114. Modified Body-in-White - 5.0 lbs	180
Figure 115. Modified Body-in-White - 10.0 lbs	181
Figure 116. AMC Jeep - 5.0 lbs	182
Figure 117. AMC Jeep - 10.0 lbs	183
Figure 118. AMC Jeep - 15.0 lbs	184
Figure 119. Straight Lines Fitting the Data	A-1
Figure 120. Errors in Least Squares Estimation	A-2
Figure 121. Variations in Data	A-4
Figure 122. Least Squares Fit of Data	A-6

LIST OF TABLES

	page
TABLE 1. Comparison of H_1, H_2 , and H_e	63
TABLE 2. Frequency Response Measurements	118
TABLE 3. Excitation Signal Summary	123
TABLE 4. BOSS Input Files	145
TABLE 5. x and y Values for Least Squares Fit	A-5

1. INTRODUCTION

The most fundamental phase of any experimental analysis is to acquire data that are relevant to defining, understanding, and solving the problem. When attempting to define a structure dynamically (usually in terms of impedance functions or in terms of natural frequencies, damping ratios, and modal vectors), this normally involves measuring a force input to the structure and the system response to that input as either displacement, velocity or acceleration (all of which are related through differentiation and/or integration).

This data are sometimes observed, measured and analyzed in the time domain using equipment as simple as a volt meter and an oscilloscope and forcing functions that are well defined such as single frequency sine waves. The natural frequencies are estimated by observing peaks in the response amplitude. Damping can be estimated by a log decrement equation and mode vectors are estimated by measuring the response at various points of interest on the structure. Phase resonance testing, or forced normal mode testing, used extensively in the aircraft industry, is a sophisticated version of this method.

Advances in hardware and software allowed for the computation of the fast Fourier transform (FFT), the single input, single output frequency response function and the ability to use these measured and stored frequency response functions as inputs to parameter estimation algorithms which could "automatically" estimate natural frequency, damping, and mode shapes and even display "animated" mode shapes on display terminals. The digital computer, mass storage medium, and the FFT allowed band limited random noise to be used as the forcing function so that the structure could be tested faster and the data analyzed or re-analyzed at a later time. But these new techniques also caused many potential errors, particularly signal processing errors.

In recent years, more advances in the speed, size and cost of mini-computers and other test related hardware have made multi-input, multi-output frequency response function testing a desirable testing technique.

This volume is concerned with the measurement techniques that are widely used in modal analysis. Although some history is presented, a more complete history can be found by reviewing the literature identified in the Bibliography that is presented as part of this report. Also, some present research in the areas of frequency response function estimation, multiple input considerations, and non-linear vibration considerations is presented as part of this report.

1.1 Objectives

The objectives of a modal test are to make measurements that as accurately as possible represent the true force input and system response so that accurate frequency response functions are computed. These frequency response functions are the input to parameter estimation algorithms. If the data used as input to these algorithms are not accurate, the parameters that the algorithms estimate are also not accurate.

1.2 Terminology

Throughout this report, the nomenclature will follow, as close as possible, the nomenclature found at the end of this report. Any exceptions will be noted at the time they are introduced.

One potential point of confusion is the concept of system degree of freedom versus a measurement degree of freedom.

A system degree of freedom is the more classical definition of the number of independent coordinates needed to describe the position of the structure at any time with respect to an absolute coordinate frame. Therefore, every potential physical point has six (three linear and three rotational) degrees of freedom. Therefore, the structure has an infinite number of system degrees of freedom. While the theoretical number of system degrees of freedom is infinite, the number of system degrees of freedom can be considered to be finite since a limited frequency range will be considered. This number of system degrees of freedom in the frequency range of interest is referred to in the following sections as N .

A measurement degree of freedom is a physical measurement location (both in terms of structure coordinates as well as measurement direction) where data will be collected. Therefore, for a typical modal test, the number of measurement degrees of freedom will not necessarily be related to the number of system degrees of freedom. It is apparent that the number of measurement degrees of freedom must be at least as large as the number of system degrees of freedom. In general, since three translational motions are measured at every physical measurement location and since these physical locations are distributed somewhat uniformly over the system being tested, the number of measurement degrees of freedom will be much larger than the number of system degrees of freedom expected in the frequency range of interest. This, though, does not guarantee that all modal information in the frequency range of interest will be found.

The number of measurement degrees of freedom (the number of physical measurement locations multiplied times the number of transducer orientations at each physical measurement location) is referred to in the following sections as m . Note that the number of measurement degrees of freedom can be used to describe input or output characteristics.

2. MODAL TESTING

The basic purpose of any modal test is to determine the damped natural frequency, damping, and in most cases mode shapes, of a test structure. These are known as the *modal properties* or *dynamic properties* of a system and are unique to the system and the boundary conditions under which it was tested. In some cases it is also necessary to compute generalized or modal mass and modal stiffness. Therefore, by measuring these dynamic properties, we define the system.

The results from the modal test are historically used for three purposes. These are:

- Finite Element model verification
- Troubleshooting
- Modal modeling

In all cases, the modal tests start with acquiring data (usually input and output) from the structure. Because of the one to one relationship between the time domain and the frequency domain, the data, which is always measured in the time domain, may be converted to the frequency domain.

In the time domain, free decay data or impulse response functions, $h(t)$, are used in the estimation the dynamic properties.

In the frequency domain, frequency response functions, $H(\omega)$, are estimated. The frequency response function is then the input to a parameter estimation algorithm used to estimate the dynamic properties.

There are also modal parameter estimation methods that do not require that intermediate functions be computed; these methods utilize long time records. Due to practical limitations concerning archival and retrieval of data in this format, these methods are not addressed in this report.

2.1 Test Structure Set-up

The first decision that must be made before any data is collected is the test configuration. Since the modal parameters that are estimated are for the test structure in the configuration in which it is tested, the test structure should be in a configuration that, as close as possible, represents the desired data. This means that the boundary conditions are an important consideration when setting up the test. If the structure is in a free-free configuration, then the modal parameters estimated are for the free-free case. This is especially important when attempting to verify a finite element model. If the structure is tested in a configuration that is different from the configuration that was modeled, there is no chance of correlation. Since the modal parameters that are estimated are for that configuration, a structure may need to be tested more than once to completely define the structure in its various operating configurations.

Also in this initial phase of the test, the points to be tested are identified, marked, and measured in physical coordinates. In most cases, the physical points and associated directions where acceleration (displacement) is to be measured are selected to give physical significance to the animation. But it is important that any critical points that need to be measured are also identified.

Another factor that may need to be considered at this time is the ability to access the measurement

degrees of freedom that need to be tested. This may require some ingenuity so that the test configuration is changed as little as possible during the data collection.

2.2 Hardware Set-up

In all cases, it is only possible to *estimate* the dynamic properties of the system. This is directly a result of only being able to *estimate* "true" inputs and responses of the system. It is therefore imperative that the "best" possible data is collected.

For single input, single output frequency response function testing, a force input to the system must be measured as well as the system response to that input.

One of the first decisions to be made is the frequency range (f_{min} to f_{max}) for the test. The frequency range must, of course, include all important modes that are to be identified. But, because of the constraints of the parameter estimation algorithms, the number of modes (modal density) should be kept to a minimum. This may mean that more than one test, using different frequency ranges, needs to be conducted. Many times, the test frequency range cannot be determined until initial measurements have been made. An important consideration is that, when using modal modeling techniques, it is important to identify modes that are higher or lower in frequency than the test frequency. This will yield more accurate modal models.

Next, the type of excitation and the form of the forcing function must be selected. Sometimes, the structure may determine the type of excitation. Other times, the use of the data may determine the excitation. If the purpose of the test is troubleshooting, an impact test may be the best form of excitation. If a modal model is to be built, more precise form of input must be used.

If an impact test is to be conducted, the size of hammer and hardness of the impact surface must be selected. This will determine the frequency range of the usable frequency response.

If a shaker is to be used to excite the structure, a forcing signal needs to be selected. This could include sine, pure random, periodic random, or burst random as well as others that may more closely match operating conditions. Section 4 presents many common excitation signals and their strong and weak points.

The force input location(s) must be selected to excite all the important modes in the frequency range to be tested. For multi-input testing, there are other constraints that must be satisfied. Section 6 has a complete review of these constraints.

In a typical test, load cells are used to measure the force input and accelerometers to measure acceleration values which can be related to displacement.

The transducers generally have their own power supply and signal conditioning hardware. Accelerometers need to be selected such that they have sufficient sensitivity but also low mass to make measurements of acceleration that accurately define the acceleration of the structure at that point.

These signals, force and acceleration, are then passed through low-pass anti-aliasing filters, analog-to-digital converters, and into the analysis computer.

The computer calculates fast Fourier transforms and all necessary auto and cross spectra needed to compute a single frequency response function. This is normally stored to disc and another output selected.

In the case of multiple inputs, many of the potential errors arise from the additional hardware needed to collect the data required to compute frequency response functions. The potential "bookkeeping" to be certain that the correct auto and cross spectra are being used in the computations can in itself be bothersome. A two input, 6 response test necessitates the calculation of 8 auto spectra and 13 cross spectra, each with a real and imaginary part, in addition to the 12 frequency response functions that are estimated in one acquisition session. There are also 2 load cells, 6 accelerometers, 16 cables, 8 transducer power supplies, 2 exciter systems, 2 signal generators, 8 anti-aliasing filters, and 8 ADC channels that all have the possibility of failure during the test. It is therefore important to have a technique to check various components used in the test at selected intervals. Most of these errors can be eliminated by good measurement practice.

2.3 Initial Measurements

Once the structure is defined and an input point(s) selected, it is necessary to take initial measurements to be certain that the input point excites the structure reasonably well over the analysis range and to be certain that all hardware is operating properly.

Usually, the "driving point" is measured first. This is because the form of the driving point measurement is well known and defined and also because this should be a "clean" measurement. In a driving point frequency response function, all peaks in the imaginary part should be of the same sign (positive or negative), each resonance should be followed by an anti-resonance, and all circles in the Argand plot lie on the same half of the plane. Many potential problems can be averted from this one measurement.

Once the driving point measurement is satisfactory, measurements at remote points are made. This will ensure that the structure is satisfactorily excited at all points for that force level. In a typical test, the level of excitation is not changed over the duration of the test. In fact, if the structure is highly non-linear, this would make the analysis overly complicated.

2.4 Non-linear Check

Another important step in a successful modal test is to check for linearity. The basic theory of modal analysis requires a linear structure. Seldom is the structure under test linear over all but a limited force range. Linearity is easily checked by exciting the structure at various force levels. If a shift in natural frequency occurs for different force levels, the structure exhibits some form of non-linear stiffness. If the amplitude of the frequency response function changes, the structure exhibits non-linear damping. Section 7 is an extensive review of non-linear considerations.

2.5 Modal Test

Once the initial set up is complete, the actual testing phase is simply a process of collecting, processing, and storing the relevant information. This data will then be used in parameter estimation algorithms and potentially modal modeling algorithms. For an in-depth review of these areas, other technical reports, found in the preface, should be consulted.

3. MODAL DATA ACQUISITION

Acquisition of data that will be used in the formulation of frequency response functions or in a modal model involves many important technical concerns. One primary concern is the digital signal processing or the converting of analog signals into a corresponding sequence of digital values that accurately describe the time varying characteristics of the inputs to and responses from a system. Once the data is available in digital form, the most common approach is to transform the data from the time domain to the frequency domain by use of a discrete Fourier transform algorithm. Since this algorithm involves discrete data over a limited time period, there are large potential problems with this approach that must be well understood.

3.1 Digital Signal Processing

The process of representing an analog signal as a series of digital values is a basic requirement of modern digital signal processing analyzers. In practice, the goal of the analog to digital conversion (ADC) process is to obtain the conversion while maintaining sufficient accuracy in terms of frequency, magnitude, and phase. When dealing strictly with analog devices, this concern was satisfied by the performance characteristics of each individual analog device. With the advent of digital signal processing, the performance characteristics of the analog device is only the first criteria of consideration. The characteristics of the analog to digital conversion now become of prime importance.

This process of analog to digital conversion involves two separate concepts, each of which are related to the dynamic performance of a digital signal processing analyzer. *Sampling* is the part of the process related to the timing between individual digital pieces of the time history. *Quantization* is the part of the process related to describing an analog amplitude as a digital value. Primarily, sampling considerations alone affect the frequency accuracy while both sampling and quantization considerations affect magnitude and phase accuracy.

3.1.1 Sampling

Sampling is the process of recording the independent variable (force, acceleration, etc.) of an analog process. This can be done in an absolute sense where the independent variable is in terms of time. Quite often, particular advantage can be gained if the sampling process proceeds in a relative sense where this independent variable is in terms of some event. This relative approach is the basis of the processing of data related to rotating equipment where the event is a revolution of a shaft. In either case, the same theories apply to the sampling process. In the relative approach, there is simply a change of variable associated with the independent axis (time versus event).

The process of sampling arises from the need to describe analog time histories in a digital fashion. This can be done, in general, by recording a digitized amplitude and a reference time of measurement or in the more common method of recording amplitudes at uniform increments of time (Δt). Since all analog to digital converters sample at constant sampling increments during each sample period, all further discussion will be restricted to this case.

3.1.2 Sampling Theory

Two theories or principles apply to the process of digitizing analog signals and recovering valid frequency information. Shannon's Sampling Theorem states, very simply, the following:

$$F_{\text{sampl}} \geq F_{\text{max}} * 2.0 \quad (1)$$

This theorem has to do with the maximum frequency which can be described accurately. It should be noted that Equation 1 establishes the lowest limit that can be used to digitize a signal and still identify a certain maximum frequency component. For reasons involving the practical limitation of the analog filters used prior to any digitization, the sampling frequency is often chosen to be four times the maximum frequency of interest. In this case, Equation 1 still applies as stated by the inequality. Note that in this situation the resulting frequency information must be displayed appropriately to avoid viewing the data that is considered invalid.

Rayleigh's criterion or principle was first formulated in the field of optics and has to do with being able to resolve two closely related spaced frequency components. For a time record of T seconds, the lowest frequency component measurable is:

$$\Delta f = \frac{1}{T} \quad (2)$$

It should be emphasized that Equation 2 is always true regardless of the absolute frequency involved.

With these two principles in mind, the selection of sampling parameters can be summarized as shown in Figure 1. Note that for this case, the equality in Equation 1 has been used.

3.1.3 Quantization

Quantization refers to the conversion of a specific analog value of amplitude to the nearest discrete value available in the analog to digital converter. This process involves representing a range of voltage by a fixed number of integer steps. Normally, the range of voltage is chosen to be between positive and negative limits for a given voltage limit. The number of discrete levels is a function of the number of bits in the analog to digital conversion. An ADC with an "M-BIT" converter is able to determine signal amplitude within one part in 2 raised to the M power. Ten and twelve bit converters are very common. An example of a three bit converter is shown in Figure 2. The most important consideration with respect to optimum quantization depends upon the concept of *actual* word size versus *effective* word size. The actual word size is the number of bits available in each word in the ADC or computer. The effective word size is the number of bits used in each word in any operation in the ADC or computer. The first consideration is that of dynamic range. This has to do with the input to the ADC in the digitization process. Since the actual word size of the ADC is fixed, the dynamic range of the ADC (60 db for 10 bits, 72 db for 12 bits) is only meaningful if the quantization of an input signal of interest involves all of the bits of the actual word. Two situations may exist where this is not true. First, if the input ranges for the ADC are not automatically or manually set to the optimum position, some loss of dynamic range will occur. This means that the maximum level of the data should not be less than one half of the input voltage range. Secondly, if the signal has more

Choose convenient round number for parameter shown.	Chosen parameter automatically fixes the value of parameter below, because of relationship in parentheses.	Then make either of the remaining two parameters (can't be both) as close as possible to the desired value by choosing N^* in the relationship shown.
Δt	$F_{\max} (F_{\max} = \frac{1}{2\Delta t})$	$T (T = N \Delta t)$ $\Delta f (\Delta f = \frac{1}{N\Delta t})$
F_{\max}	$\Delta t (\Delta t = \frac{1}{2F_{\max}})$	$T (T = N \Delta t)$ $\Delta f (\Delta f = \frac{1}{N\Delta t})$
Δf	$T (T = \frac{1}{\Delta f})$	$\Delta t (\Delta t = \frac{T}{N})$ $F_{\max} (F_{\max} = \frac{N}{2} \Delta f)$
T	$\Delta f (\Delta f = \frac{1}{T})$	$\Delta t (\Delta t = \frac{T}{N})$ $F_{\max} (F_{\max} = \frac{N}{2} \Delta f)$

N^* , the data block size, is always a power of 2.

Figure 1. Digitization Equations

dominant information content outside the band of interest, a significant portion of the dynamic range will be used to describe the unwanted characteristic. This will reduce the potential dynamic range available to the portion of the signal in which there is interest. Some common examples of this are a large mean value offset, Figure 3, or large harmonic component (such as 60 Hertz) as shown in Figure 4. Both of these situations cause the effective word size of the ADC to be smaller than the actual word size of the ADC with respect to the information of interest.

This dynamic range consideration with respect to quantization is particularly important when a multiplexer is used to obtain a large number of channels of data in parallel. Since a multiplexer configuration often involves only one ADC channel for a number of multiplexer channels, the dynamic range of all the channels must be similar or the effective word size for many of the channels will be much less than the actual word size. In this situation, the signals must be amplified prior to digitization so that each channel has approximately the same dynamic range. Naturally, this amplification factor must be taken into account in the final calibration of the data.

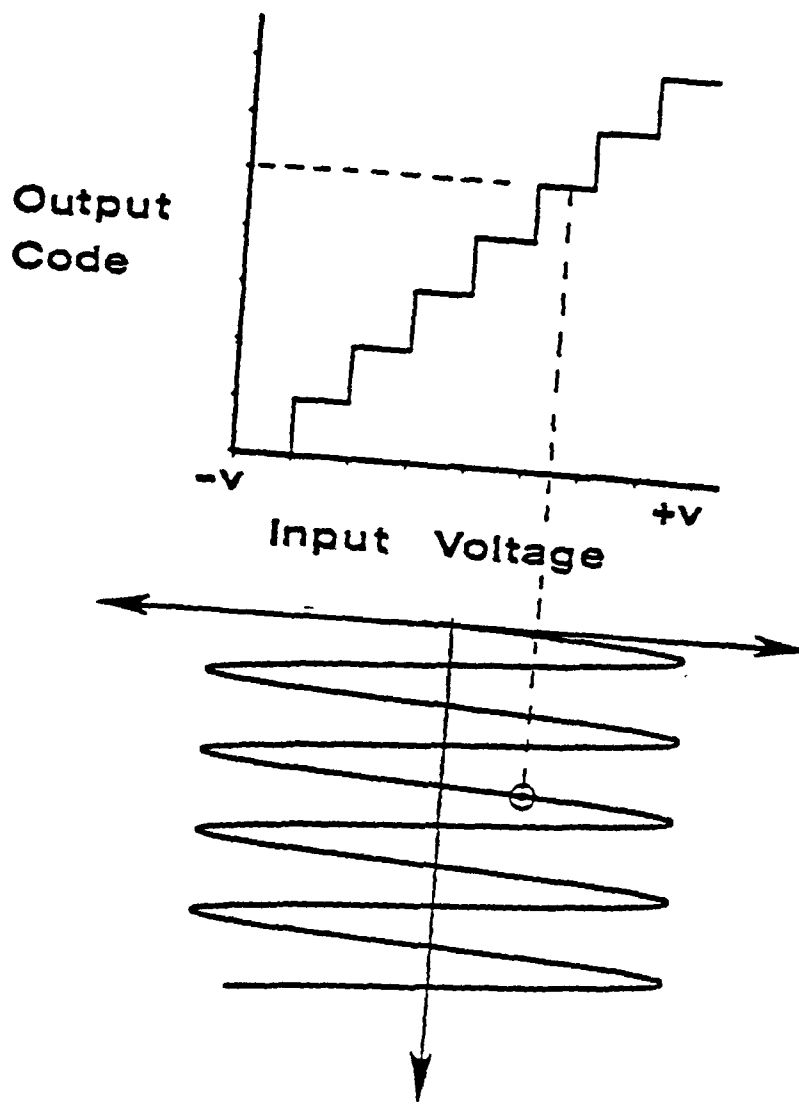


Figure 2. Quantization: 3 Bit Analog to Digital Converter

3.1.4 Discrete Fourier Transform

The discrete Fourier transform algorithm is the basis for the formulation of any frequency domain function in modern data acquisition systems. In terms of an integral Fourier transform, the function must exist for all time in a continuous sense in order to be evaluated. For the realistic measurement situation, data are available in a discrete sense over a limited time period. The discrete Fourier transform, therefore, is based upon a set of assumptions concerning this discrete sequence of values. The assumptions can be reduced to two situations that must be met by every signal processed by the discrete Fourier transform algorithm. The first assumption is that the signal must be a totally observed transient with respect to the time period of observation. If this is not true, then the signal

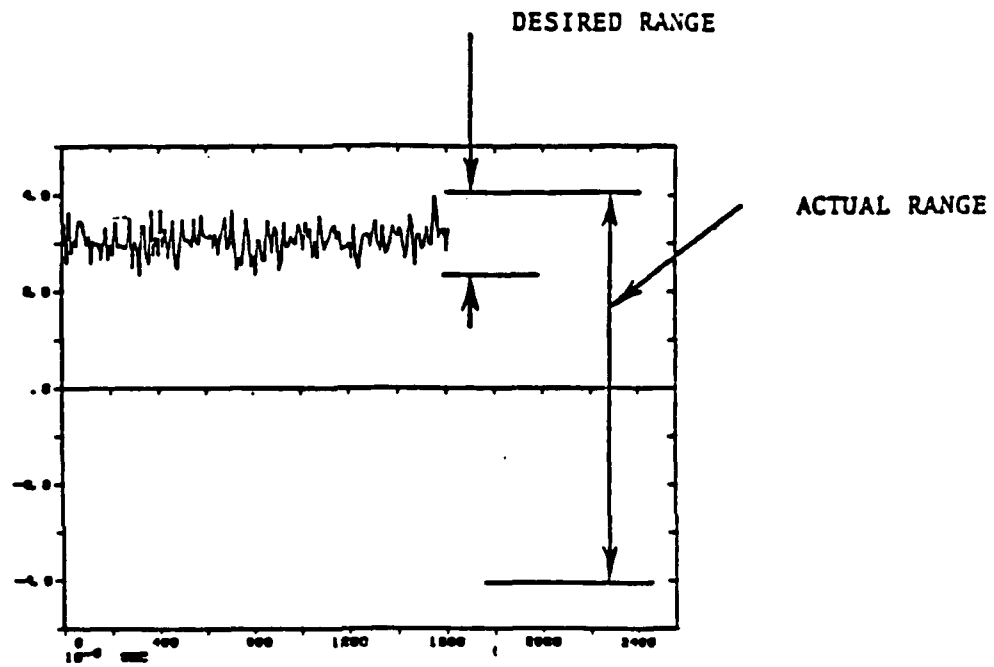


Figure 3. Quantization: ADC Input Optimization

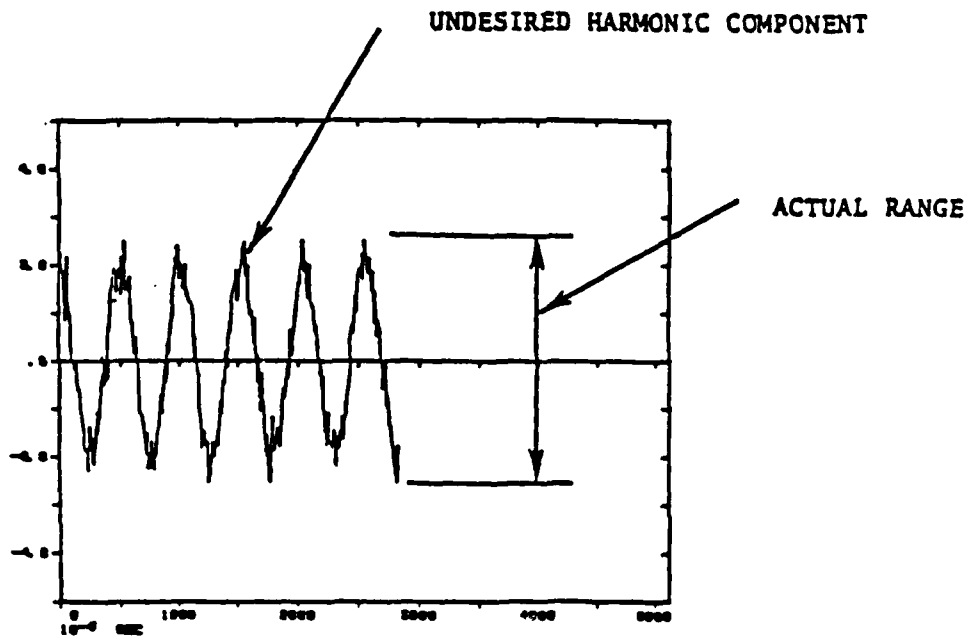


Figure 4. Quantization: ADC Input Optimization

must be composed only of harmonics of the time period of observation. If one of these two assumptions is not met by any discrete history processed by the discrete Fourier transform algorithm, then the resulting spectrum will contain bias errors accordingly. Much of the data processing that is considered with respect to acquisition of data with respect to the formulation of a modal model revolves around an attempt to assure that the input and response histories match one of these two assumptions. For a more complete understanding of the discrete Fourier transform algorithm and the associated problems, there are a number of good references which explain all of the pertinent details ^[1-3].

3.1.5 Errors

The accurate measurement of frequency response functions depends heavily upon the errors involved with the digital signal processing. In order to take full advantage of experimental data in the evaluation of experimental procedures and verification of theoretical approaches, the errors in measurement, generally designated noise, must be reduced to acceptable levels.

With respect to the frequency response function measurement, the errors in the estimate are generally grouped into two categories: variance and bias. The variance portion of the error is due to random deviations of each sample function from the mean. Statistically, then, if sufficient sample functions are evaluated, the estimate will closely approximate the true function with a high degree of confidence. The bias portion of the error, on the other hand, does not necessarily reduce as a result of many samples. The bias error is due to a system characteristic or measurement procedure consistently resulting in an incorrect estimate. Therefore, the expected value is not equal to the true value. Examples of this are system nonlinearities or digitization errors such as aliasing or leakage. With this type of error, knowledge of the form of the error is vital in reducing the resultant effect in the frequency response function measurement.

Specifically, two general categories of problems exist which may cause significant error even when great care has been taken to deal with inaccurate system assumptions and obvious measurement mistakes. The first category is concerned with the limitations of using finite information. Any measurement instrument is limited in time resolution, or frequency bandwidth. However, sampling a signal at discrete times also introduces a form of amplitude error (called aliasing) that converts high frequency energy to lower frequencies. This source of error would be classified as a bias. Thus, the time resolution and frequency bandwidth parameters are generally dictated by an anti-aliasing filter in front of the sampler. The shape of this filter influences the in-band accuracy and the stop-band rejection characteristics of the instrument. Obviously, filters are not perfect, and there is no such thing as absolute rejection. Strong signals with potential aliasing are often present to some extent. Another form of amplitude error is involved in the quantization of the analog signal to a digital signal. Since only discrete amplitude levels are possible, the amplitude will often be in error. This source of error is normally Gaussian distributed and therefore is part of the variance portion of the total error.

Analogous to time resolution limits, there is always a limit on frequency resolution. This is ultimately determined by the total effective time over which coherent data is collected. The effect of this finite collection time is the introduction of another type of non-linear error (called leakage), which converts energy at each frequency into energy within a relatively narrow band nearby. This type of error is controlled to some extent by weighting (or windowing) the original time domain data. However, this type of error will always cause a considerable bias in any portion of a measurement that is sufficiently close to a strong signal. In the situation of excitation of lightly damped structures, this leakage error, compared to all other sources of error, is usually the largest bias error and often will be much greater than the variance error.

3.1.6 Leakage Error

This error is basically due to a violation of an assumption of the fast Fourier transform algorithm. This assumption is that the true signal is periodic within the sample period used to observe the sample function. In the cases where both input and output are totally observable (transient input with completely observed decay output within the sample period) or are harmonic functions of the time period of observation (T), there will be no contribution to the bias error due to leakage.

Leakage is probably the most common and, therefore, the most serious digital signal processing error. Unlike aliasing and many other errors, the effects of leakage can only be reduced, not completely eliminated. The leakage error can be reduced by any of the following four methods:

- Cyclic averaging
- Periodic Excitation
- Increase in Frequency Resolution
- Windowing or Weighting Functions

In order to understand how each of these methods reduce the leakage error, the origin of leakage must be well understood.

The discrete Fourier transform algorithm assumes that the data to be transformed is periodic with respect to the frequency resolution of the sampling period. Since, in general, the real world does not operate on the basis of multiples of some arbitrary frequency resolution, this introduces an error known as leakage.

The following is one approach (there are many other equivalent presentations) used to explain leakage in terms of convolution.

The concept of multiplication and convolution represents a transform pair with respect to Fourier and Laplace transforms. More specifically, if two functions are multiplied in one domain, the result is the convolution of the two transformed functions in the other domain. Conversely, if two functions are convolved in one domain, the result is the multiplication of the two transformed functions in the other domain. When a signal is observed in the time domain with respect to a limited observation period, T, the signal that is observed can be viewed as the multiplication of two infinite time functions as shown in Figures 5 and 6. The resulting time domain function is, in the limit, the signal that is processed by the Fourier transform which is shown in Figure 7. Therefore, by this act of multiplication, the corresponding frequency domain functions of Figures 8 and 9 will be convolved to give the result equivalent to the Fourier transform of Figure 10. In this way, the difference between the infinite and the truncated signal can be evaluated theoretically.

In order to evaluate the frequency domain result, the concept of convolution must now be understood. First of all, the integral equation representing the convolution of two time domain signals $x(t)$ and $y(t)$ can be given by Equation 3.

$$W(\phi) = \int_{-\infty}^{\infty} X(\omega)Y(\phi-\omega) d\omega \quad (3)$$

Therefore, the evaluation of the convolution of two functions is a function as well. The value of the

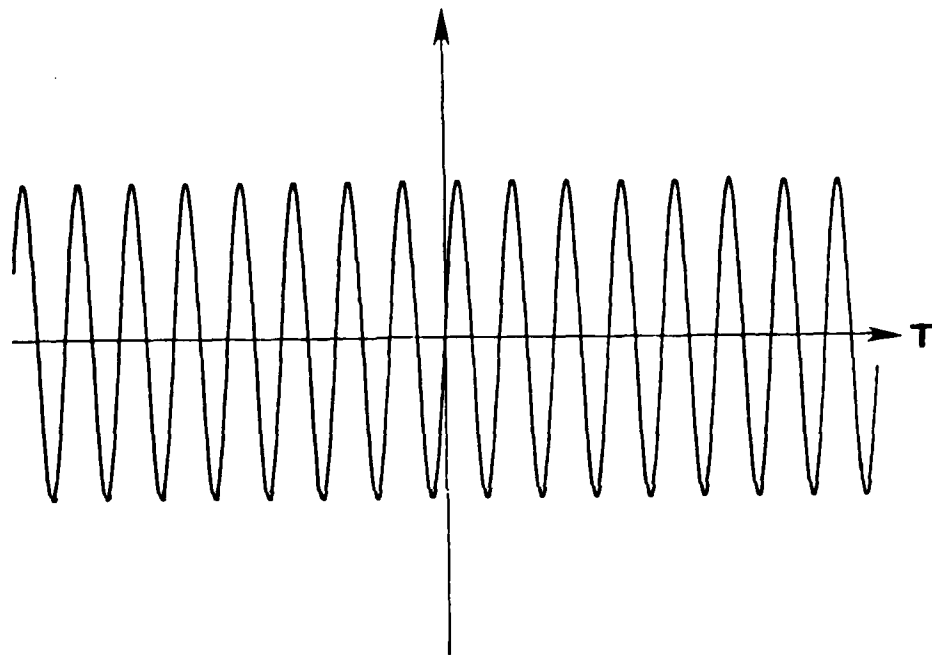


Figure 5. Time Domain Function: Theoretical Harmonic

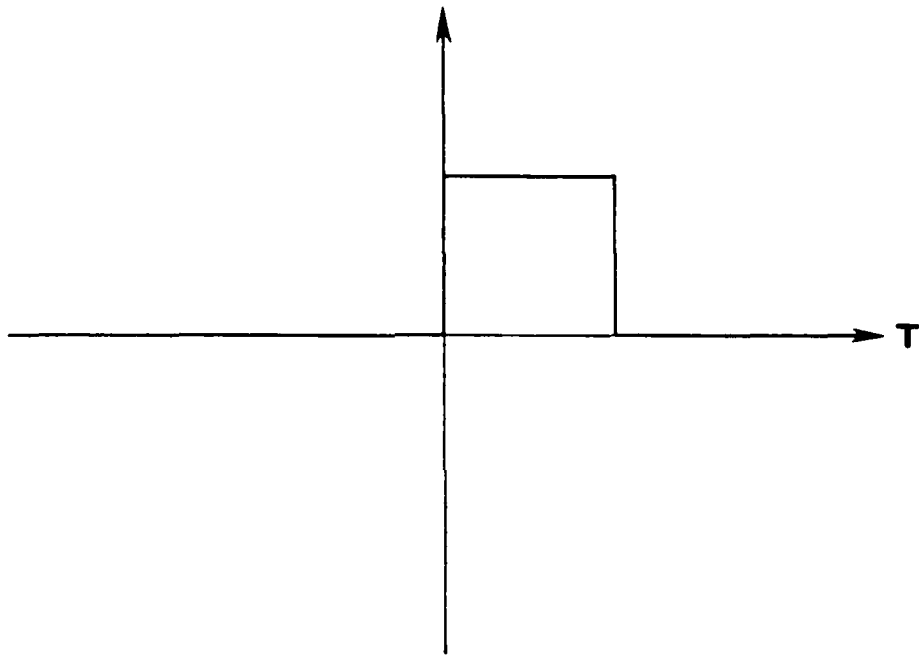


Figure 6. Time Domain Function: Theoretical Window

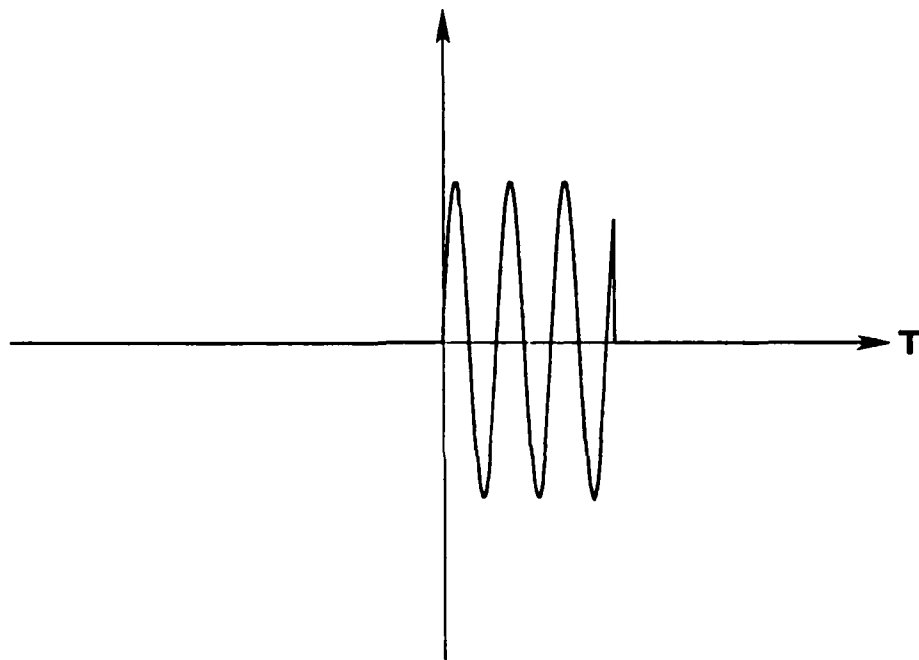


Figure 7. Time Domain Function: Multiplication of Signals

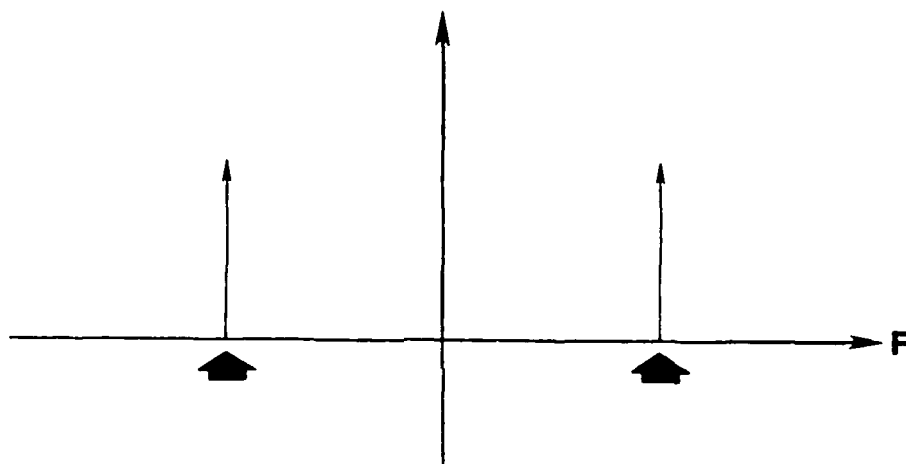


Figure 8. Frequency Domain: Theoretical Harmonic

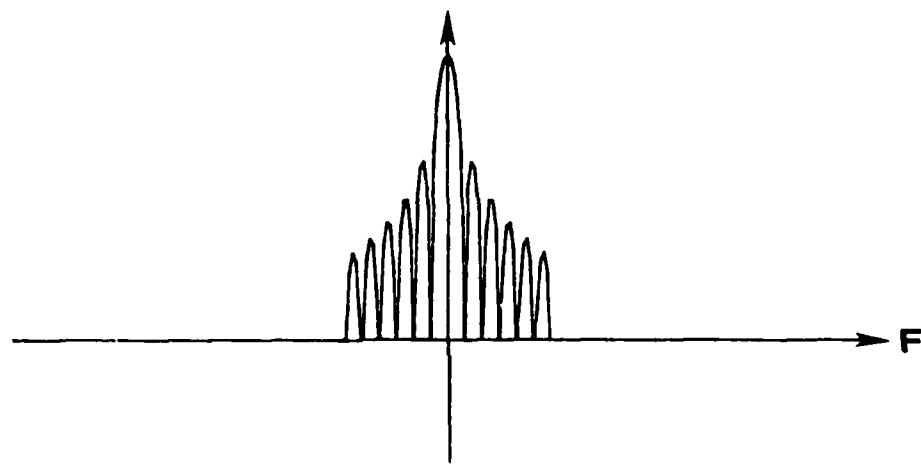


Figure 9. Frequency Domain: Theoretical Window

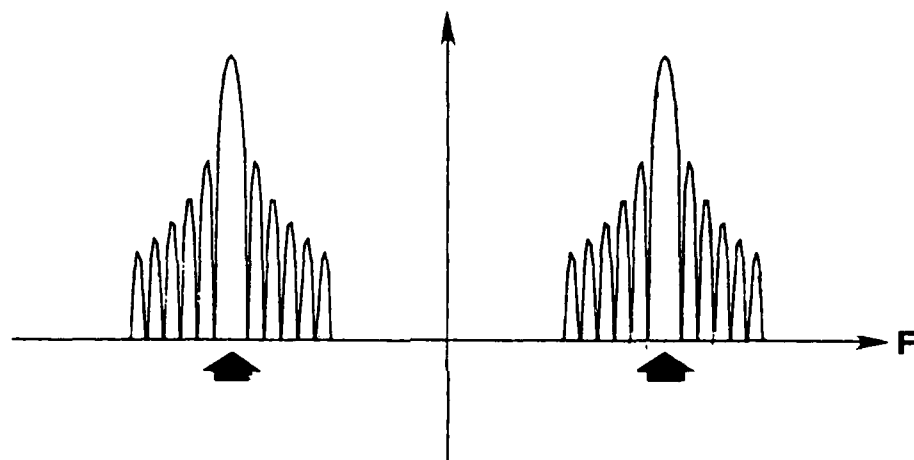


Figure 10. Frequency Domain: Convolved Signals

new function can be viewed as the integration (or summation) over all frequencies of the product of the two frequency domain functions, where one function has been shifted in frequency. This result is shown in Figure 10. Note that only the amplitude results are shown for simplicity. For a complete understanding of the bias error, a discussion of the phase effects is also needed. Figure 8 is the Fourier transform of Figure 5. Figure 9 is the Fourier transform of Figure 6. Figure 10 is the convolution of Figure 8 and Figure 9.

For the practical case, the resulting functions shown in Figure 7 and Figure 10 are not continuous but occur in a digital sense. For this case, Equation 3 can be adjusted accordingly as shown in Equation 4.

$$W(\phi) = \sum_{i=-N}^{+N} X(i \Delta \omega) Y(\phi - i \Delta \omega) \quad (4)$$

Where: $\phi = s \Delta \omega$
 $s = -N \longleftrightarrow +N$

With this in mind, two cases must be evaluated with respect to whether the theoretical harmonic chosen for the example is periodic or not with respect to the window period, T. These cases are shown in Figure 11 and Figure 12. Note that a harmonic signal was chosen for this example since any other signal can be thought to be simply a linear sum of such harmonics. Since the Fourier transform is also linear in this sense, the result shown is valid for any theoretical signal satisfying the Dirichlet conditions.

Therefore, when an analog signal is digitized in a Fourier analyzer, the analog signal has been multiplied by a function of unity (for a period of time T) in the time domain. This results in a convolution of the two signals in the frequency domain. This process of multiplying an analog signal by some sort of weighting function is loosely referred to as "windowing". Whenever a time function is sampled, the transform relationship between multiplication and convolution must be considered. Likewise, whenever an additional weighting function such as a Hanning window is utilized, the effects of such a window can be evaluated in the same fashion.

3.1.7 Aliasing Error

If frequency components larger than one half the sampling frequency occur in the analog time history, amplitude and frequency errors will result. These errors are a result of the inability of the Fourier transform to decide which frequencies are within the analysis band and which frequencies are outside the analysis band. This problem is explained graphically in Figure 13.

A summary of what happens to signals above the F_{max} defined by the equality in Equation 1 is shown graphically in Figure 14. This demonstrates that a signal above F_{max} will appear after being digitized as a frequency below F_{max} . This serious error is controlled by using analog filters prior to digitization to low pass only the information below F_{max} . Naturally, since filters have a limited out of band rejection, the positioning of the cutoff frequency of the filters must be made with respect to the F_{max} and the roll-off characteristic of the filter.

A number of other errors must be discussed in order to understand that the possibility for error originates at every step in the measurement process. While all of the following errors are possible, many of the errors are a function of the way in which the ADC hardware operates or often malfunctions. Many of these errors can be evaluated by performing a histogram on a signal with

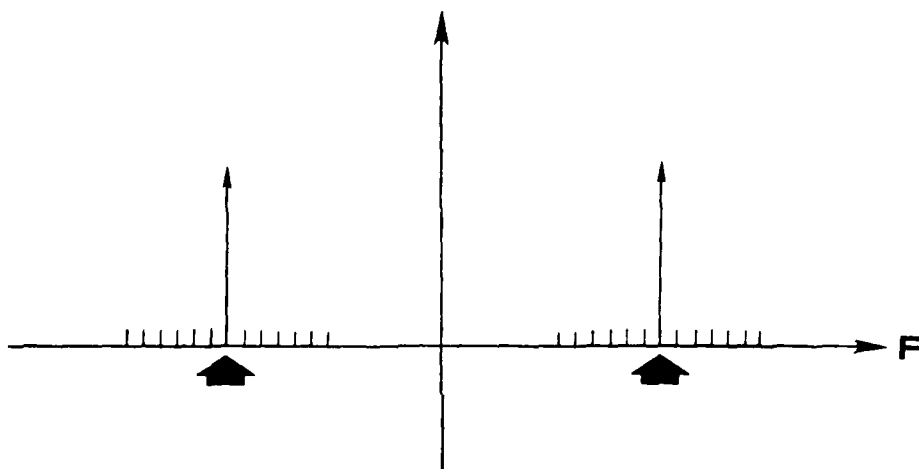


Figure 11. Frequency Domain: Periodic Signal

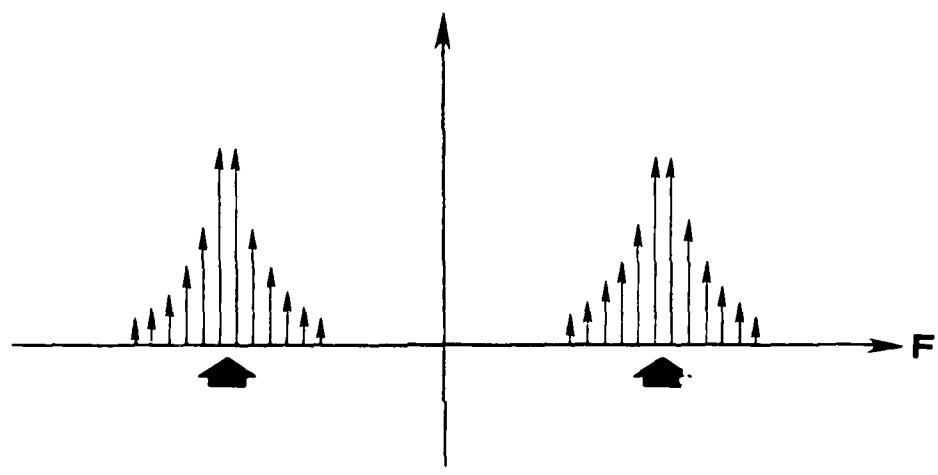


Figure 12. Frequency Domain: Nonperiodic Signal

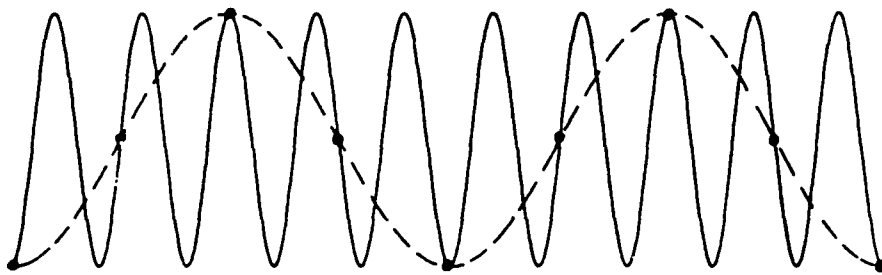
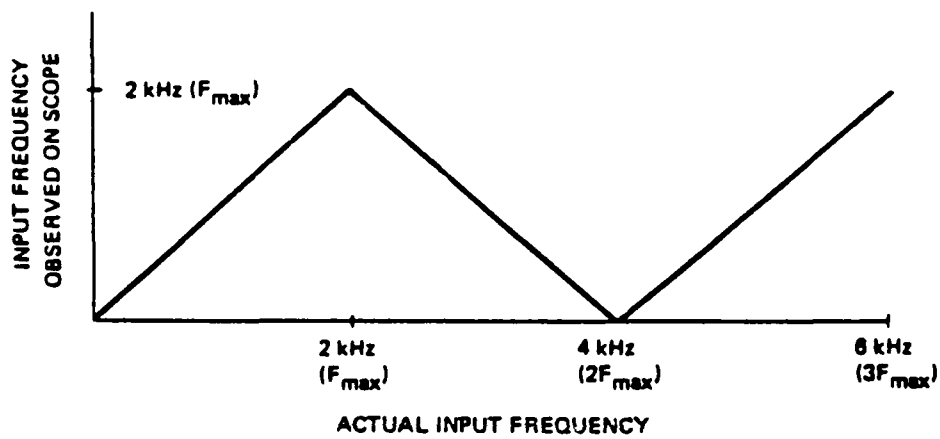


Figure 13. Aliasing Example



*THUS 2.2 kHz will be seen as 1.8 kHz
 4.0 kHz will be seen as 0 kHz
 etc.*

Figure 14. Aliasing Contribution

known characteristics.

3.1.8 Quantization Error

The difference between the actual analog signal and the measured digitized value. Normally this is plus or minus one half of one part in 2^M . Since this error is a random event, averaging will minimize the effect on the resulting measurements.

3.1.9 Differential Nonlinearity

If the roundoff that occurs to cause quantization error is not regular (some of the spacing between counts varies) this type of error results. This causes the "noise" from quantization error to be biased.

3.1.10 Bit Dropout

One bit in the ADC may never be set. Obviously, any sample requiring this bit in the ADC word to be set will be in error and the error will be biased. A similar problem exists if one bit of the ADC word is always set.

3.1.11 Reference Voltage

The reference voltage used by the ADC may drift within or between sample periods. Since this drift is not known or measured, this error will cause a bias in any resulting estimate of the dependent variable.

3.1.12 Overload and Overload Recovery

When the ADC is overloaded, it may take several sampling increments to recover. This is normally only a problem under severe overloads but if it occurs the result will be a bias in the estimate of the amplitude.

3.1.13 Aperture Error - Clock Jitter

The value of amplitude recorded does not correspond to the assumed instant in time, t . This type of error will result in a bias in the estimate of time and frequency parameters.

3.1.14 Digitizer Noise

The random setting of plus or minus one bit when the input is zero is referred to as digitizer noise. This error may become dominant in transient excitation since a large part of the observed histories may be very small or actually zero as in the case of impact testing. This error can be controlled to some extent by averaging and the use of special window functions.

3.2 Transducer Considerations

The transducer considerations are often the most overlooked aspect of the experimental modal analysis process. Considerations involving the actual type and specifications of the transducers, mounting of the transducers, and calibration of the transducers will often be some of the largest sources of error.

Transducer specifications are concerned with the magnitude and frequency limitations that the transducer is designed to meet. This involves the measured calibration at the time that the transducer was manufactured, the frequency range over which this calibration is valid, and the magnitude and phase distortion of the transducer, compared to the calibration constant over the range of interest. The specifications of any transducer signal conditioning must be included in this evaluation.

Transducer mounting involves evaluation of the mounting system to ascertain whether the mounting system has compromised any of the transducers specifications. This normally involves the possibility of relative motion between the structure under test and the transducer. Very often, the mounting systems which are convenient to use and allow ease of alignment with orthogonal reference axes are subject to mounting resonances which result in substantial relative motion between the transducer and the structure under test in the frequency range of interest. Therefore, the mounting system which should be used depends heavily upon the frequency range of interest and upon the test conditions. Test conditions are factors such as temperature, roving or fixed transducers, and surface irregularity. A brief review of many common transducer mounting methods is shown in Figure 15.

Transducer calibration refers to the actual engineering unit per volt output of the transducer and signal conditioning system. Calibration of the complete measurement system is needed to verify that the performance of the transducer and signal conditioning system is proper. Obviously, if the measured calibration differs widely from the manufacturers specifications, the use of that particular transducer and signal conditioning path should be questioned. Also, certain applications, such as impact testing, involve slight changes in the transducer system (such as adding mass to the tip of an instrumented hammer) that affect the associated calibration of the transducer.

Ideally, on-site calibration should be performed both before and after every test to verify that the transducer and signal conditioning system is operating as expected. The calibration can be performed using the same signal processing and data analysis equipment that will be used in the data acquisition. There are a number of calibration methods which can be used to calibrate the transducer and signal conditioning. Some of these methods yield a calibration curve, with magnitude and phase, as a function of frequency while other methods simply estimate a calibration constant. Most of the current calibration methods are reviewed in Figure 16. Note that some of the methods are more suited for field calibration while other methods are more suited for permanent installations in calibration laboratories^[4-9].

Method	Frequency range (Hz)	Main advantage	Main disadvantage
Hand-held	20-1000	"Quick look"	Poor measuring quality for long sample periods
Putty	0-200	Alignment, ease of mounting	Low-frequency range, creep problem during measurement
Wax	0-2000	Ease of application	Temperature limitations, frequency range limited by wax thickness, alignment
Hot glue	0-2000	Quick setting time, good alignment	Temperature-sensitive transducers
Magnet	0-2000	Quick setup	Requires magnetic material, alignment, bounce a problem during impact, surface preparation important
Adhesive film	0-2000	Quick setup	Alignment, flat surface
Epoxy-cement	0-5000	Mounts on irregular surface, alignment	Long curing time
Stud mount	0-10,000	Accurate alignment if carefully machined Approximate freq ranges, depends on transducer mass, and contact conditions	Difficult setup

Figure 15. Transducer Mounting Methods


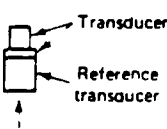
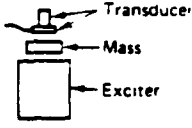
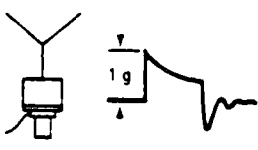
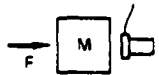
Method			Remarks
Inversion test		Constant	Can only be used with transducer that has stable dc output; calibration against local earth's gravity
Comparison method		Frequency response	Calibration against reference transducer
Reciprocity method		Constant and/or frequency response	Calibration against mass-loaded shaker
Drop method		Constant	Calibration against local earth and gravity; used for ac-coupled transducers
Ratio method	 $\frac{a}{F} = \frac{1}{m} \text{ (Rigid mass)}$	Frequency-response ratio	Calibration against known a/F for a rigid mass

Figure 16. Calibration Methods

3.3 Error Reduction Methods

There are several factors that contribute to the quality of actual measured frequency response function estimates. Some of the most common sources of error are due to measurement mistakes. With a proper measurement approach, most of this type of error, such as overloading the input, extraneous signal pick-up via ground loops or strong electric or magnetic fields nearby, etc., can be avoided. Violation of test assumptions are often the source of another inaccuracy and can be viewed as a measurement mistake. For example, frequency response and coherence functions have been defined as parameters of a linear system. Nonlinearities will generally shift energy from one frequency to many new frequencies, in a way which may be difficult to recognize. The result will be a distortion in the estimates of the system parameters, which may not be apparent unless the excitation is changed. One way to reduce the effect of nonlinearities is to randomize these contributions by choosing a randomly different input signal for each of the n measurements. Subsequent averaging will reduce these contributions in the same manner that random noise is reduced. Another example involves control of the system input. One of the most obvious requirements is to excite the system with energy at all frequencies for which measurements are expected. It is important to be sure that the input signal spectrum does not have "holes" where little energy exist. Otherwise, coherence will be very low, and the variance on the frequency response function will be large.

Assuming that the system is linear, the excitation is proper, and obvious measurement mistakes are avoided, some amount of noise will be present in the measurement process. Noise is a general designation describing the difference between the true value and the estimated value. A more exact designation is to view this as the total error comprised of two terms, variance and bias. Each of these classifications are merely a convenient grouping of many individual errors which cause a specific kind of inaccuracy in the function estimate. The variance portion of the error essentially is Gaussian distributed and can be reduced by any form of synchronization in the measurement or analysis process. The bias or distortion portion of the error causes the expected value of the estimated function to be different from the true value. Normally, bias errors are removed if possible but, if the form and the source of a specific bias error is known, many techniques may be used to reduce the magnitude of the specific bias error.

Four different approaches can be used to reduce the error involved in frequency response function measurements in current fast Fourier transform (FFT) analyzers. The use of averaging can significantly reduce errors of both variance and bias and is probably the most general technique in the reduction of errors in frequency response function measurement. Selective excitation is often used to verify nonlinearities or randomize characteristics. In this way, bias errors due to system sources can be reduced or controlled. The increase of frequency resolution through the zoom fast Fourier transform can improve the frequency response function estimate primarily by reduction of the leakage bias error due to the use of a longer time sample. The zoom fast Fourier transform by itself is a linear process and does not involve any specific error reduction characteristics compared to a baseband fast Fourier transform(FFT). Finally, the use of weighting functions(windows) is widespread and much has been written about their value ^[1-3,10,11]. Primarily, weighting functions compensate for the bias error(leakage) caused by the analysis procedure.

3.3.1 Signal Averaging

The averaging of signals is normally viewed as a summation or weighted summation process where each sample function has a common abscissa. Normally, the designation of "history" is given to sample functions with the abscissa of absolute time and the designation of "spectrum" is given to sample functions with the abscissa of absolute frequency. The spectra are normally generated by

Fourier transforming the corresponding history. In order to generalize and consolidate the concept of signal averaging as much as possible, the case of relative time could also be considered. In this way "relative history" could be discussed with units of the appropriate event rather than seconds and a "relative spectrum" would be the corresponding Fourier transform with units of cycles per event. This concept of signal averaging is used widely in structural signature analysis where the event is a revolution. This kind of approach simplifies the application of many other concepts of signal relationships such as Shannon's sampling theorem and Rayleigh's criterion of frequency resolution.

The process of signal averaging as it applies to frequency response functions is simplified greatly by the intrinsic uniqueness of the frequency response function. Since the frequency response function can be expressed in terms of system properties of mass, stiffness, and damping, it is reasonable to conclude that in most realistic structures, the frequency response functions are considered to be constants just like mass, stiffness, and damping. This concept means that when formulating the frequency response function using cross and auto power spectrums, the estimate of frequency response is *intrinsically unique*, as long as the system is linear. In general, the auto- and cross-power spectrums are statistically unique only if the input is stationary and sufficient averages have been taken. Nevertheless, the estimate of frequency response is valid whether the input is stationary, non-stationary, or deterministic (see Section 5).

The concept of the *intrinsic uniqueness* of the frequency response function also permits a greater freedom in the testing procedure. Each function can be derived as a result of a separate test or as the result of different portions of the same continuous test situation. In either case, the estimate of frequency response function will be the same as long as the time history data is acquired simultaneously for the auto- and cross-power spectrums that are utilized in any computation for frequency response or coherence function.

The approaches to signal averaging vary only in the relationship between each sample function used. Since the Fourier transform is a linear function, there is no theoretical difference between the use of histories or spectra. (Practically, though, there are precision considerations which will be discussed later). With this in mind, the signal averaging useful to frequency response function measurements can be divided into three classifications:

- Asynchronous
- Synchronous
- Cyclic

These three classifications refer to the trigger and sampling relationships between sample functions.

Asynchronous Signal Averaging - The classification of asynchronous signal averaging refers to the case where no known relationship exists between individual sample functions except for the intrinsic uniqueness of the frequency response function. In this case the least squares approach to the estimate of frequency response must be used since no other way of preserving phase and improving the estimate is available. In this situation, the trigger for digitization (sampling and quantization) takes place in a random fashion dependent only upon the equipment availability. The digitization is said to be in a free-run mode.

Synchronous Signal Averaging - The synchronous classification of signal averaging adds an additional constraint that each sample function must be initiated with respect to a system input. This fact, together with the intrinsic uniqueness, would allow the frequency response function to be formed as a summation of ratios of Y divided by X since phase is preserved. Even so, the reduction of variance and the value of coherence available with the power spectra approach would preclude the use of any other technique in most cases. The ability to synchronize the initiation of digitization

allows for use of non-stationary or deterministic inputs with a resulting increased signal to noise ratio and reduced leakage. Both of these improvements in the frequency response function estimate are due to more of the input and output being observable in the limited time window.

The synchronization takes place as a function of a trigger signal occurring in the input (internally) or in some event related to the input (externally). An example of an internal trigger would be the case where an impulsive input is used to estimate the frequency response. All sample functions would be initiated when the input reached a certain amplitude and slope. A similar example of an external trigger would be the case where the impulsive excitation to a speaker is used to trigger the estimate of frequency response between two microphones in the sound field. Again, all sample functions would be initiated when the trigger signal reached a certain amplitude and scope.

Cyclic Signal Averaging - The cyclic classification of signal averaging involves the added constraint that the digitization is coherent between sample functions. This means that the exact time (absolute or relative) between each sample function is used to enhance the signal averaging process. Rather than trying to keep track of elapsed time between sample functions, the normal procedure is to allow no time to elapse between successive sample functions. This process can be described as a comb digital filter in the frequency domain with the teeth of the comb at frequency increments dependent upon the periodic nature of the sampling with respect to the event measured. The result is an attenuation of the spectrum between the teeth not possible with other forms of averaging.

This form of signal averaging is very useful for filtering periodic components from a noisy signal since the teeth of the filter are positioned at harmonics of the frequency of the sampling reference signal. This is of particular importance in signature applications where it is desirable to extract signals connected with various rotating members. This same form of signal averaging is particularly useful for reducing leakage during frequency response measurements and also has been used extensively for evoked response measurements in biomedical studies.

A very common application of cyclic signal averaging is in the area of analysis of rotating structures. In such a signature analysis application, the peaks of the comb filter are positioned to match the fundamental and harmonic frequencies of a particular rotating shaft or component. This is particularly powerful, since in one measurement it is possible to filter all of the possible frequencies generated by the rotating member from a given data signal. With a zoom Fourier transform type of approach, potentially only one shaft frequency at a time can be examined depending upon the zoom power necessary to extract the shaft frequencies from the surrounding noise.

In the application of cyclic signal averaging to frequency response function estimates, the corresponding fundamental and harmonic frequencies are now simply the frequency resolution, Δf , and integer multiples of Δf . In this case, the spectra between each Δf is reduced with an associated reduction of the bias error called leakage.

The implementation of cyclic signal averaging proceeds in a manner easily applicable to most fast Fourier transform analyzers. The cyclic averaged inputs and outputs are normally computed by simply summing successive time records. The important requirement of the successive time records is that no data is lost. Therefore, these successive time records could be laid end to end to create a digitized time record of length NT . The cyclic averaged records are then created by simply adding each time record of length T together in a block mode.

While the basic approach to cyclic averaging involves using the data weighted uniformly over the total sample time NT , the benefits that can be gained by using weighting functions can also be applied. The application of a Hann window to the successive time records before the summation occurs yields an even greater reduction of the bias error. Therefore, for frequency response measurements Hann weighted signal averaging should drastically reduce the leakage errors which can exist when using broadband random excitation techniques to measure frequency response. In Figure 17 through Figure 20, a series of measurements were performed by measuring the frequency response of a very

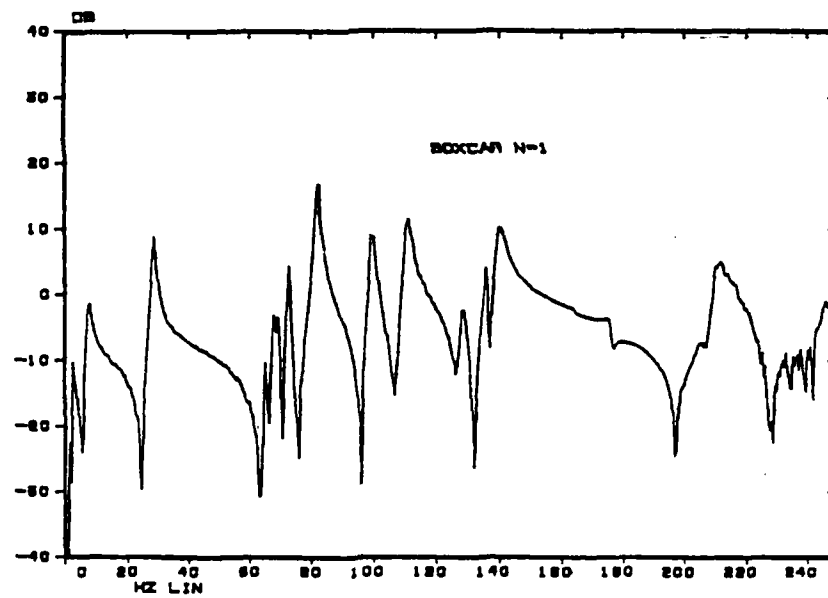
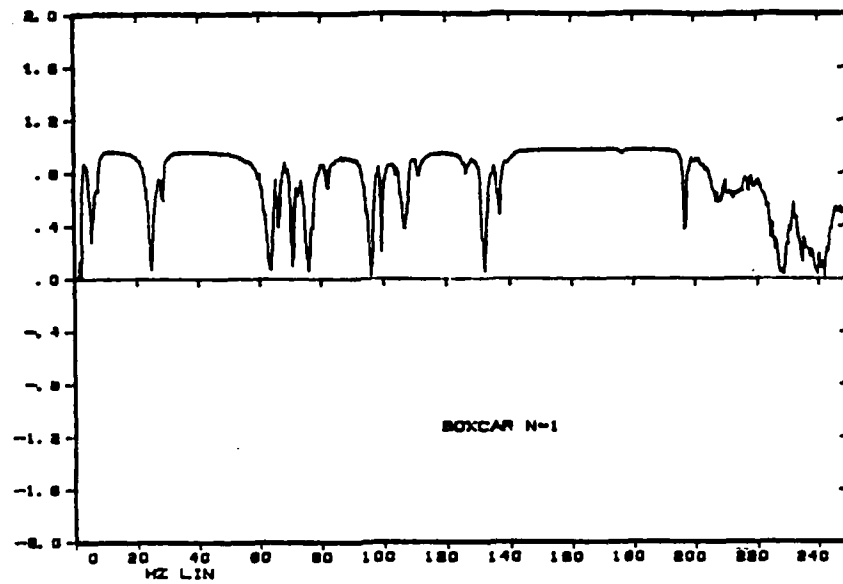


Figure 17. Asynchronous Averaging: (N = 1, M = 1)

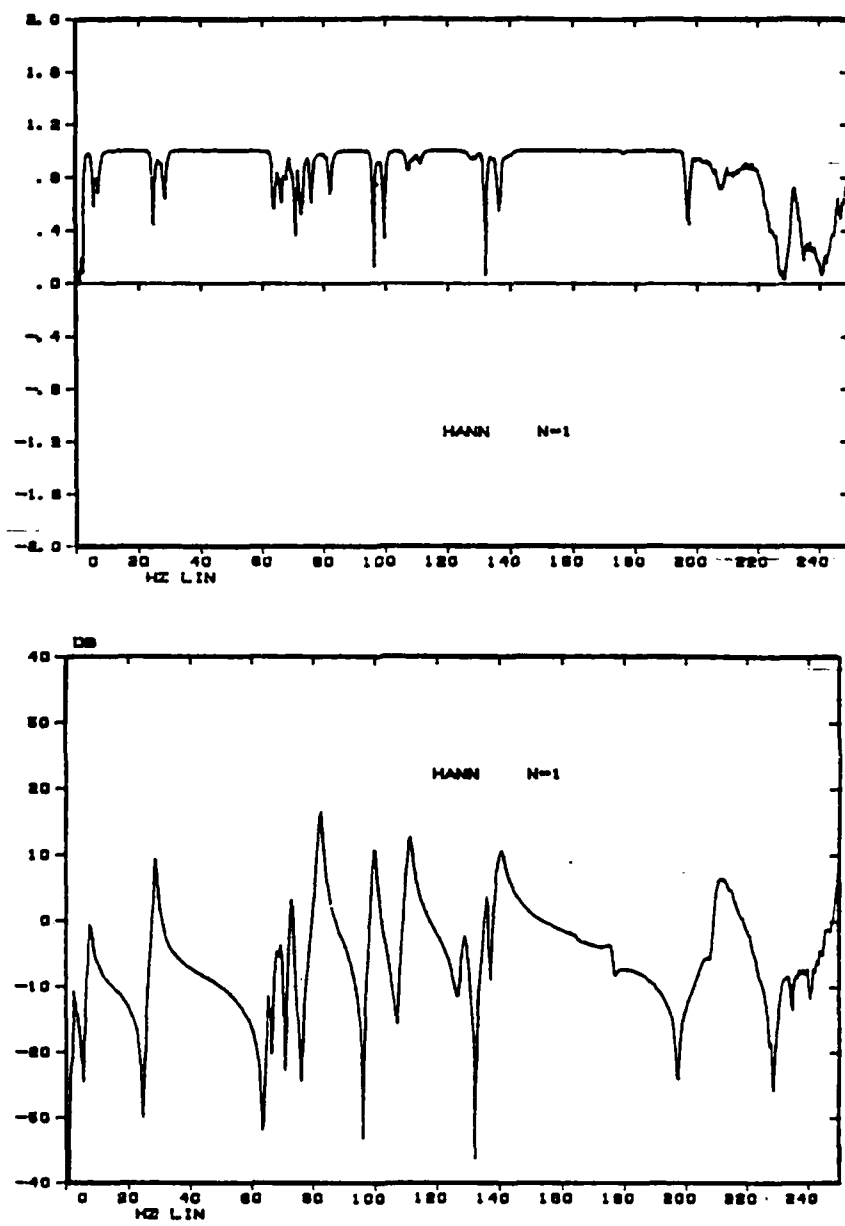


Figure 18. Asynchronous Averaging With Hann: (N = 1, M = 80)

lightly damped automotive frame. The value of N indicates the number of cyclic time records averaged together and M is the number of asynchronous auto and cross spectrum averages: a total of NM time records were sampled. This is done so that, statistically, the same amount of independent information is available in each averaging case. Note that for every case, the total time required to acquire the measurement is the same and no change has been made in the placement of the transducers or the form of the excitation. Clearly, the measurement using cyclic averaging with the Hann weighting show a significant reduction of the bias error. An interesting point is that the data near the antiresonance is also drastically improved due to the sharp roll off of the line shape of the Hann weighted averaging.

Overlapping Time Records - There are at least two common averaging techniques that use histories which may or may not overlap. In both cases, the averaging techniques involve processing random data histories in order to enhance the data. The first case is that of overlap processing. Overlap processing involves using individual sample histories which are not totally independent from one another. The dependence that occurs results from each successive history starting before the previous history ends. For the general case where the time data is not weighted in any fashion, it should be obvious that this averaging procedure does not involve any new data and, therefore, statistically does not improve the estimation process. In the special case where weighting functions are involved, this technique can utilize data that is otherwise ignored. Figure 21 is an example of a data record that has been weighted to reduce the leakage error using a Hann weighting function. The data prior to twenty percent of each sample period and after eighty percent of each sample period is nearly eliminated by the Hanning window used. Using an overlap factor of at least twenty to thirty percent as in Figure 22 involves this data once again in the averaging process.

The second case involving overlapping histories is that of random decrement analysis [12-15]. This process involves the overlapping of histories in order to enhance the deterministic portion of the random record. In general, the random response data can be considered to be made up of two parts: a deterministic part and a random part. Since averaging takes place in the time domain, the random part can be reduced if a trigger signal with respect to the information of interest exists. In the previous discussions, this trigger signal has been a function of the input (asynchronous or synchronous averaging) or of the sampling frequency (cyclic averaging). More generally, though, the trigger function can be any function with characteristics related to the response history. Specifically, then, the random decrement technique utilizes the assumption that the deterministic part of the random response signal itself contains free decay step and impulse response functions and can be used as the trigger function. Therefore, by starting each history at a specific value and slope of the random response function, characteristics related to the deterministic portion of the history will be enhanced.

There are three specific cases of random decrement averaging that represent the limiting results of its use [16]. The first case occurs when each starting value is chosen when the random response history reaches a specific constant level with alternating slopes for each successive starting value. The random decrement history for this case becomes the free decay step response function. An example of this case for the first few averages is shown in Figure 23. The second case occurs when each starting value is chosen when the random response history crosses the zero axis with positive slope. The random decrement history for this case becomes the free decay positive impulse response function.

The third case occurs when each starting value is chosen when the random response history crosses zero with negative slope. The random decrement history for this case becomes the free decay negative impulse response function.

Therefore, in each of these cases, the random decrement technique acts like a notched digital filter with pass bands at the poles of the trigger function. This tends to eliminate spectral components not coherent with the trigger function.

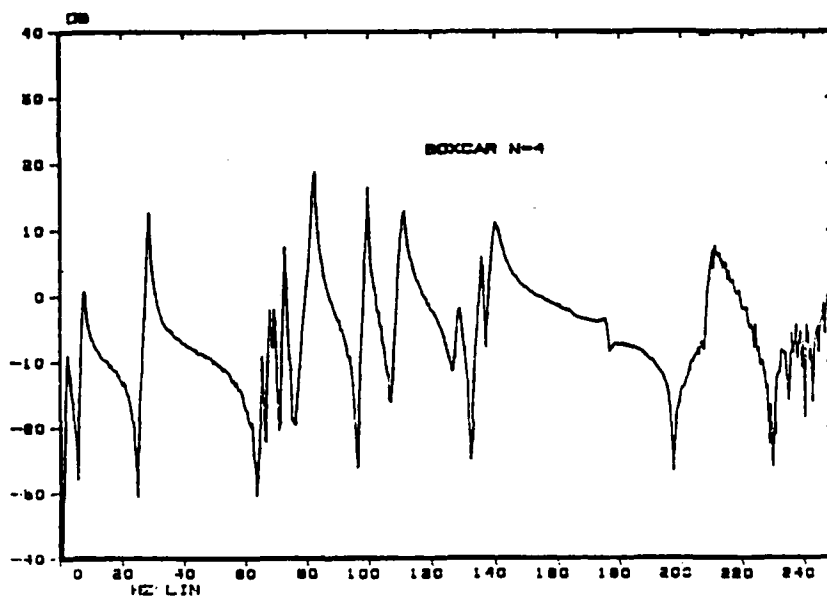
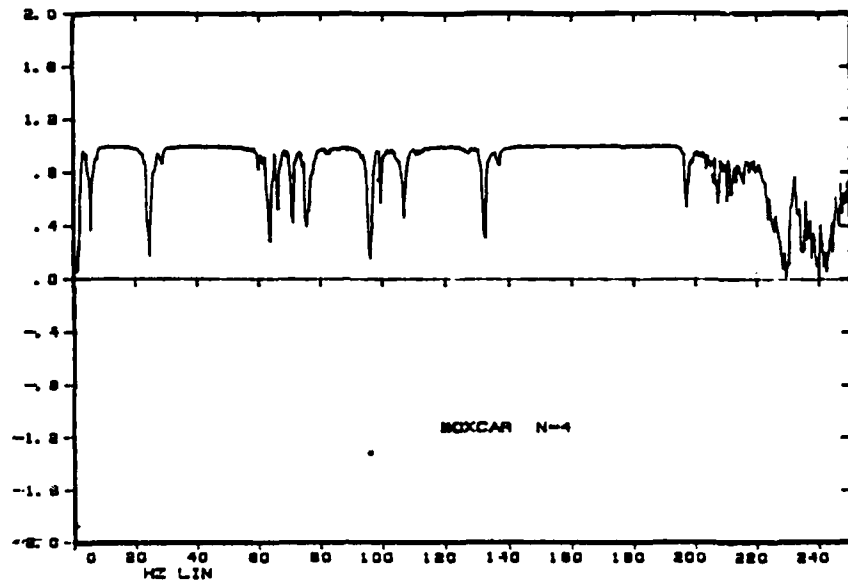


Figure 19. Cyclic Averaging (N = 4, M = 20)

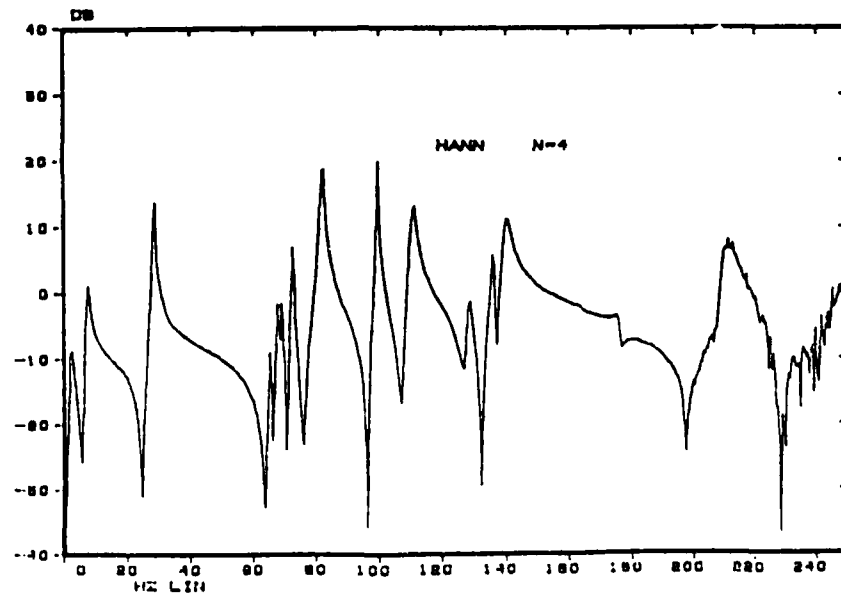
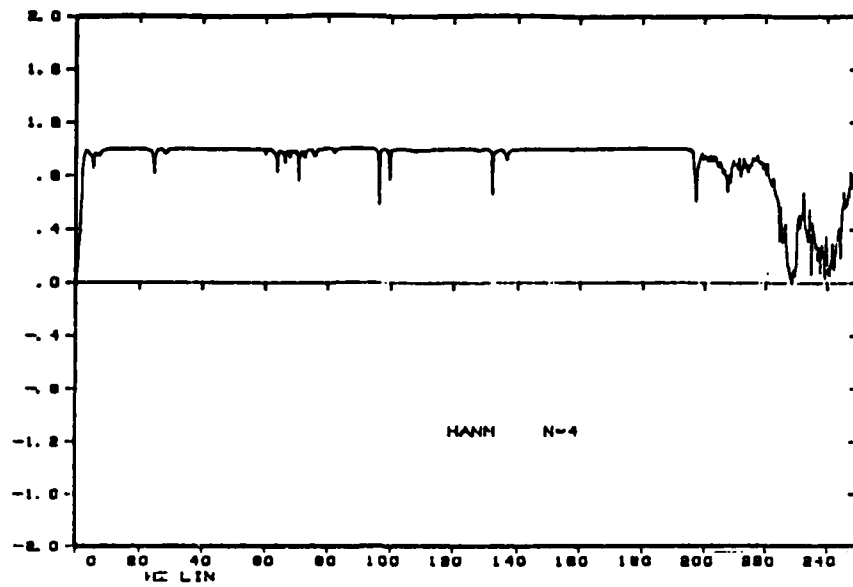


Figure 20. Cyclic Averaging With Hann ($N = 4$, $M = 20$)

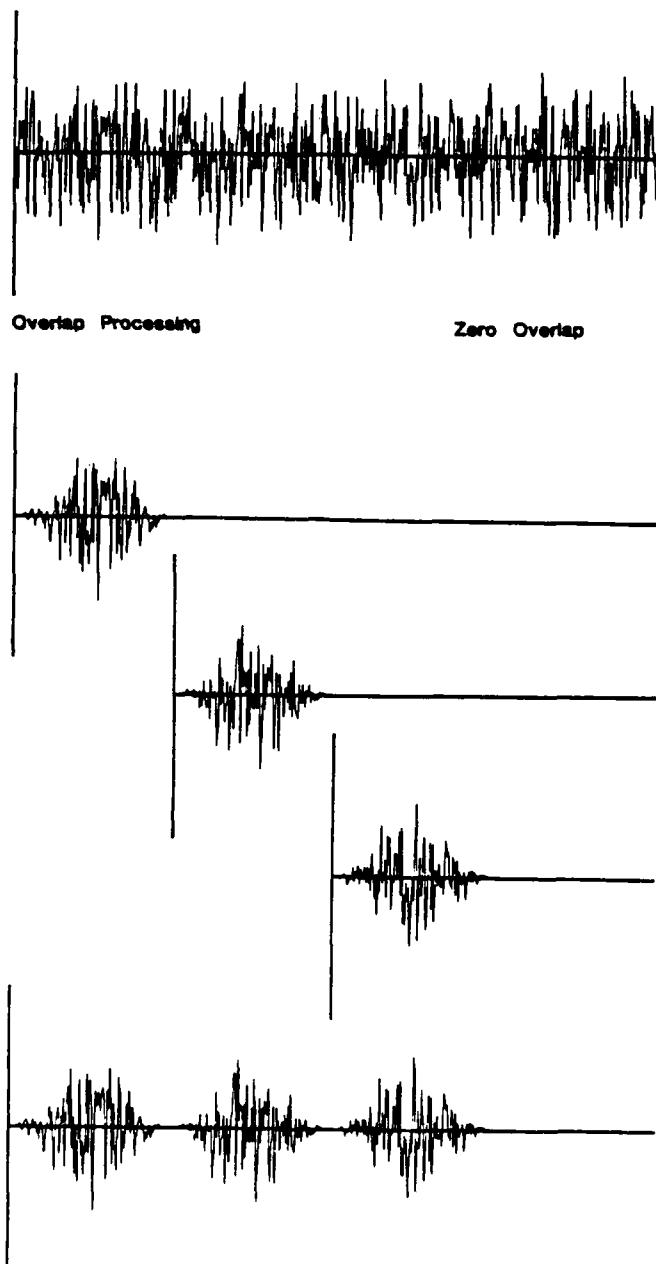
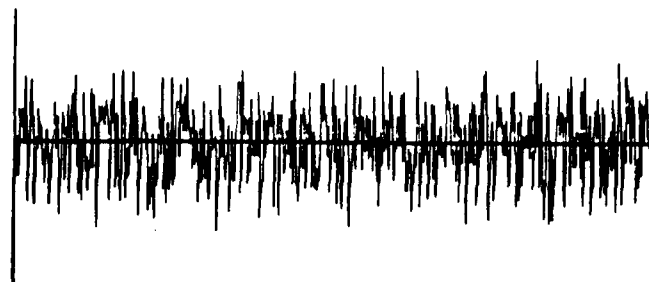


Figure 21. Overlap Processing: Zero Overlap



Overlap Processing

50 % Overlap

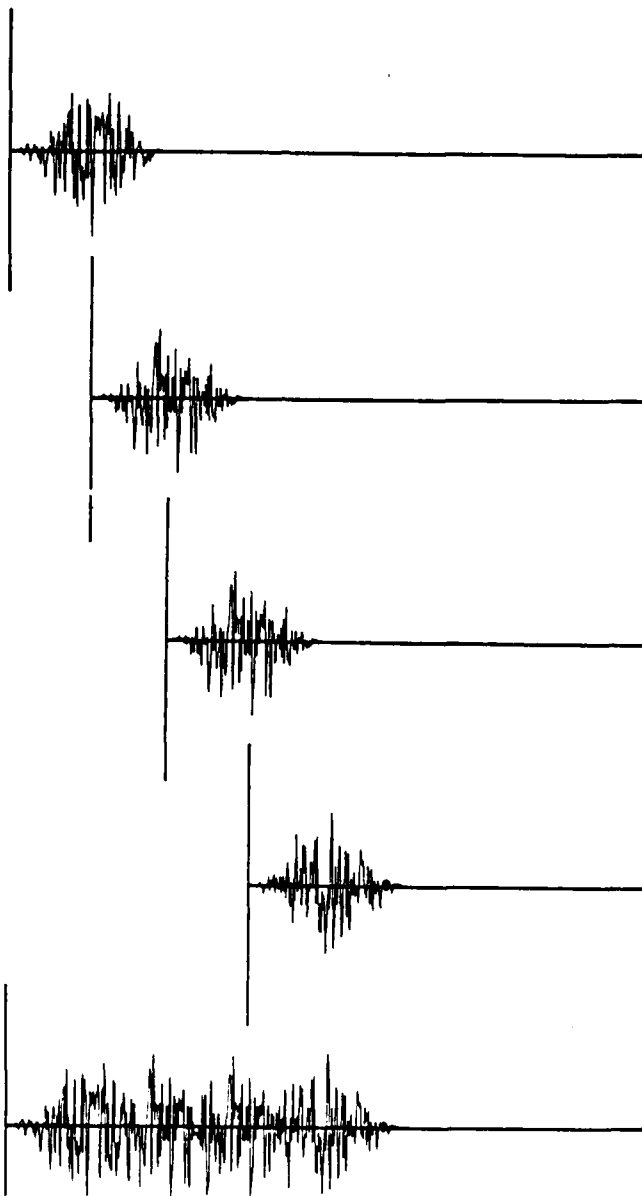
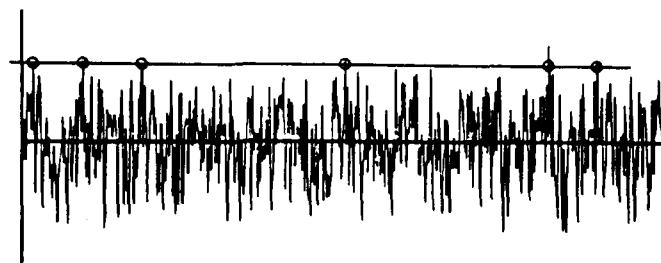


Figure 22. Overlap Processing: Fifty Percent Overlap



Random Decrement History

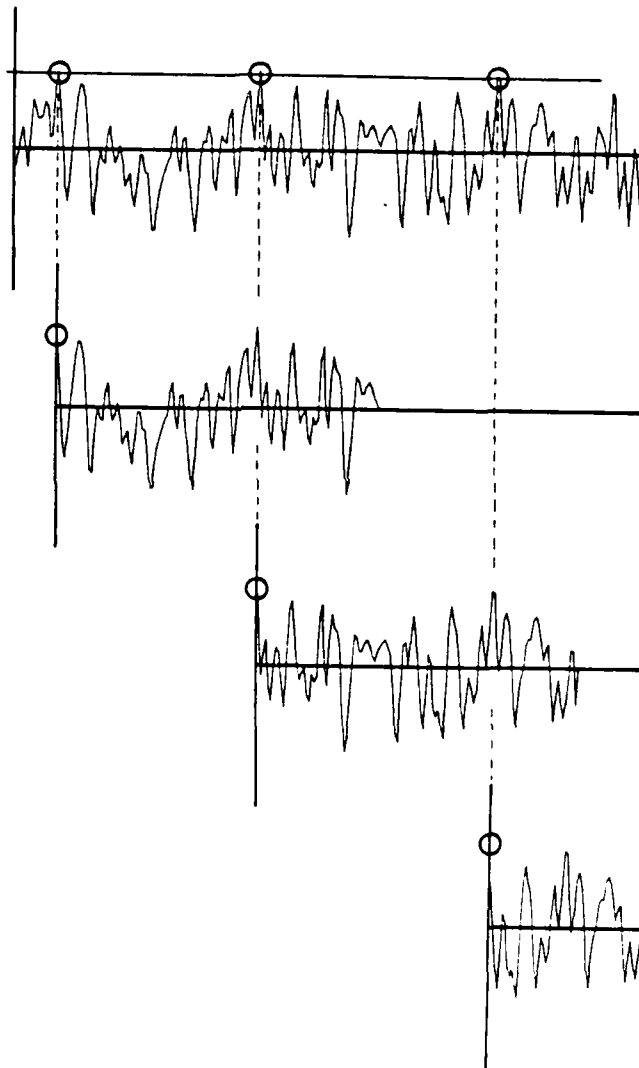


Figure 23. Random Decrement Averaging

If a secondary function is utilized as the trigger function, only the history related to the poles of the secondary function will be enhanced by this technique. If the trigger function is sinusoidal, the random decrement history will contain information related only to that sinusoid. Likewise, if the trigger function is white noise, the random decrement history will be a unit impulse function at time zero. One useful example of this concept was investigated for conditioning random response histories so that information unrelated to the theoretical input history is removed. In this situation, the theoretical input history serves as the trigger function. The random decrement history formed on the basis of this trigger function represents the random response function that would be formed if the theoretical input history were truly the system input. In reality, the measured input history may vary due to noise, impedance mismatch, etc.

3.3.2 Excitation

Another effective error reduction technique is the use of excitation signals that match the signal processing constraints. These signals will be more fully discussed in Section 4.

3.3.3 Increased Frequency Resolution

An increase in the frequency resolution of a frequency response function affects measurement errors in several ways. Obviously, finer frequency resolution allows more exact determination of the damped natural frequency of each modal vector. The increased frequency resolution means that the level of a broadband signal is reduced. The most important benefit of increased frequency resolution, though, is a reduction of the leakage error. Since the distortion of the frequency response function due to leakage is a function of frequency spacing, not frequency, the increase in frequency resolution will reduce the true bandwidth of the leakage error centered at each damped natural frequency. In order to increase the frequency resolution, the total time per history must be increased in direct proportion. The longer data acquisition time will increase the variance error problem when transient signals are utilized for input as well as emphasizing any nonstationary problem with the data. The increase of frequency resolution will often require multiple acquisition and/or processing of the histories in order to obtain an equivalent frequency range. This will increase the data storage and documentation overhead as well as extending the total test time.

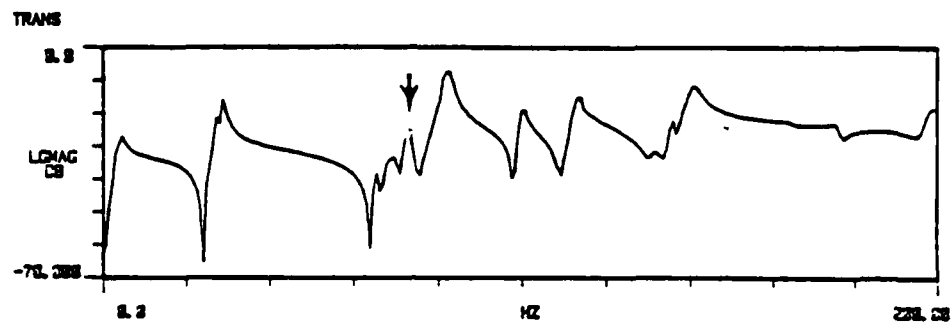
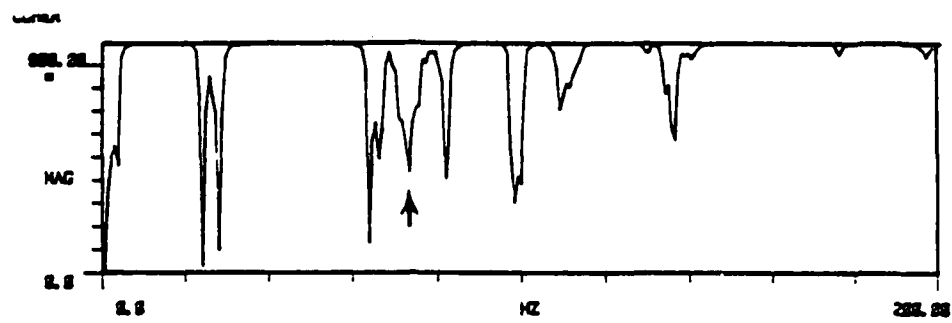
There are two approaches for increasing the frequency resolution of a frequency response function. The first approach involves increasing the number of spectral lines in a baseband measurement. The advantage of this approach, is that no additional hardware or software is required. Often, FFT analyzers do not have the capability to alter the number of spectral lines used in the measurement. The second approach involves the reduction of the bandwidth of the measurement while holding the number of spectral lines constant. If the lower frequency limit of the bandwidth is always zero, no additional hardware or software is required. Ideally, though, for an arbitrary bandwidth, hardware and/or software to perform a frequency shifted, or digitally filtered, FFT will be required.

The frequency shifted FFT process for computing the frequency response function has additional characteristics pertinent to the reduction of errors. Primarily, more accurate information can be obtained on weak spectral components if the bandwidth is chosen to avoid strong spectral components. The out-of-band rejection of the frequency shifted FFT is better than most analog filters that could be used in a measurement procedure to attempt to achieve the same results. Additionally, the precision of the resulting frequency response function will be improved due to processor gain inherent in the frequency shifted FFT calculation procedure. An example of the improvement of the frequency response function using a frequency shifted FFT can be seen in Figure

3.3.4 Weighting Functions

Weighting functions, or data windows, are probably the most common approach to the reduction of the leakage error in the frequency response function. While weighting functions are sometimes desirable and necessary, weighting functions are often utilized when one of the other approaches to error reduction would give superior results. Averaging, selective excitation, and increasing the frequency resolution all act to reduce the leakage error by the elimination of the cause of the error. Weighting functions, on the other hand, attempt to compensate for the leakage error after the fact. This compensation for the leakage error causes an attendant distortion of the frequency and phase information of the frequency response function, particularly in the case of closely spaced, lightly damped system poles. This distortion is a direct function of the width of the main lobe and the size of the side lobes of the spectrum of the weighting function. Examples of some common weighting functions are given in Figure 25. Complete details concerning these and many other weighting functions are available from many sources ^[1,2,10,11].

Weighting functions may be applied to all classifications of signal averaging. The most common case is a weighting function equal to the inverse of the number of averages used in the estimate. When this weight is used, the individual power spectra can be weighted at the end of the signal averaging or as an ongoing procedure referred to as stable averaging. This type of weighting introduces no further distortion in the frequency response function estimate but, also, does not act to compensate for the leakage error.



Increased Frequency Resolution

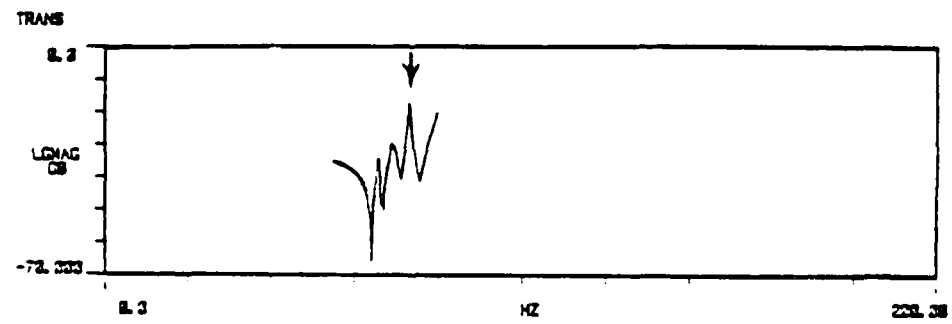
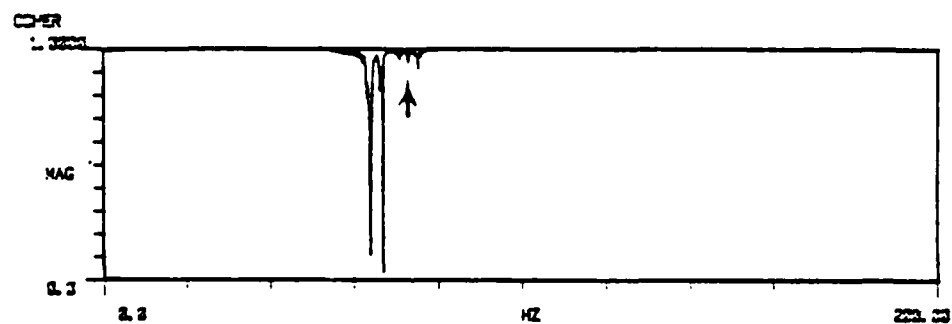


Figure 24. Increased Frequency Resolution

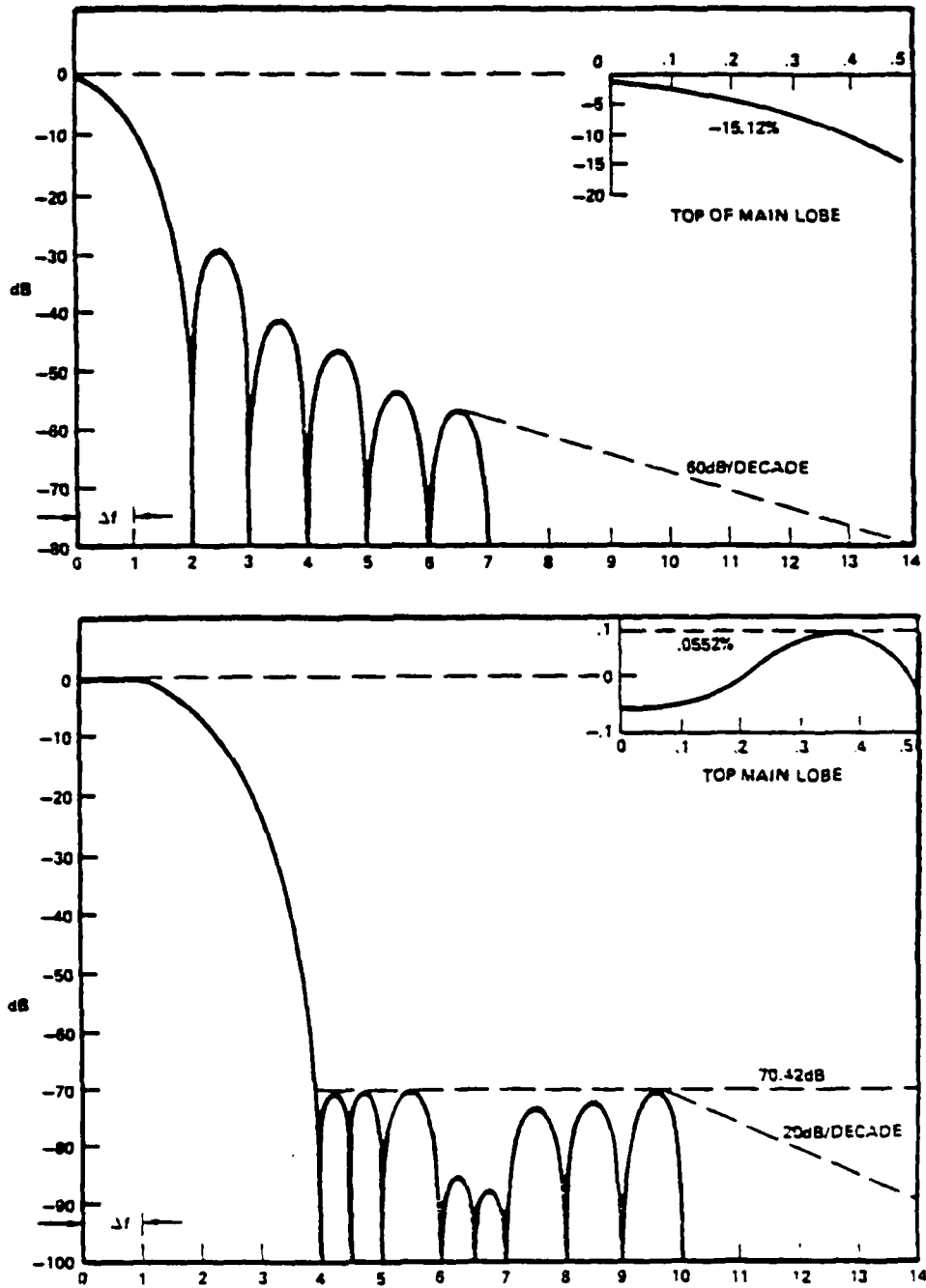


Figure 25. Typical Weighting Functions

4. EXCITATION TECHNIQUES

When exciting a structure to determine its modal properties, it is important to remember that the form of the excitation will have an effect on the validity of the estimates of the modal properties. If the frequency response estimates contain errors, then the estimates of the modal properties will also contain errors. There are at many signals that can be used to excite structures for modal testing. Some have many advantages over others. The accuracy of the estimates of the frequency response functions and the time to acquire the data are different are only some of the differences between the signals.

4.1 Excitation Constraints

While there is no well developed theory involving the excitation of structures for the purpose of estimating the frequency response functions, there are a number of constraints that must be considered in order to yield an estimate of the frequency response function that is unbiased ^[17-23].

The first constraint that is important to the estimation of the frequency response function is concerned with digital signal processing. Since most modern data acquisition equipment is based upon digital data acquisition and Discrete Fourier Transforms, unique requirements are placed on the excitation signal characteristics. This digital approach to processing the input and response signals, with respect to the frequency domain, assumes that starting at a minimum frequency and ending at a maximum frequency the analysis is going to proceed only at integer multiples of the frequency resolution, therefore matching the limits of the Discrete Fourier Transform. Therefore, this constraint first indicates that any excitation signal should only contain frequency information between the minimum and maximum frequency. This constraint also implies that, ideally, either the frequency content should be discrete and located only at integer multiples of the frequency resolution or that the excitation should be a totally observed transient.

Both of these methods match the Discrete Fourier Transform equally well, but there are advantages and disadvantages to both. If the data contains information only at multiples of the frequency resolution, it is impossible to use a zoom Fourier Transform to achieve a smaller frequency resolution on the same excitation function. If a new excitation function is created that contains information only at integer multiples in the zoom band, it is possible to zoom. If the data is a transient, the signal-to-noise ratio may become a problem.

The second constraint that is important to the estimation of the frequency response function is concerned with the requirements of the modal parameter estimation algorithms. A fundamental assumption in modal analysis is that the structure under evaluation is a linear system or at least behaves linearly for some force level. While this is never absolutely true, parameter estimation algorithms are written as though this assumption is valid. With the increasing complexity of the modal parameter estimation algorithms, violation of this characteristic within the frequency response function data base renders these algorithms impotent. Therefore, the modal parameter estimation constraint requires that the excitation signal yield the best linear estimate of the frequency response function even in the presense of small nonlinear characteristics or a significant nonlinear characteristic being evaluated around an operating point.

An additional constraint that is important when using multiple inputs is the requirement that the inputs be uncorrelated. This can be achieved by using deterministic signals, such as sinusoids, with different magnitude, phases, and frequencies for each input during each average involved with the estimation of the frequency response function. Normally, uncorrelated inputs are achieved by using a

different random excitation signal for each input. Assuming that a significant number of averages is involved, the use of uncorrelated random signals, then, is a simple solution to the requirement that the excitation signals be uncorrelated.

4.2 Excitation Signals

Inputs which can be used to excite a system in order to determine frequency response functions belong to one of two classifications. The first classification is that of a random signal. Signals of this form can only be defined by their statistical properties over some time period. Any subset of the total time period is unique and no explicit mathematical relationship can be formulated to describe the signal. Random signals can be further classified as stationary or non-stationary. Stationary random signals are a special case where the statistical properties of the random signals do not vary with respect to translations with time. Finally, stationary random signals can be classified as ergodic or non-ergodic. A stationary random signal is ergodic when a time average on any particular subset of the signal is the same for any arbitrary subset of the random signal. All random signals which are commonly used as input signals fall into the category of ergodic, stationary random signals.

The second classification of inputs which can be used to excite a system in order to determine frequency response functions is that of a deterministic signal. Signals of this form can be represented in an explicit mathematical relationship. Deterministic signals are further divided into periodic and non-periodic classifications. The most common inputs in the periodic deterministic signal designation are sinusoidal in nature while the most common inputs in the non-periodic deterministic designation are transient in form.

The choice of input to be used to excite a system in order to determine frequency response functions depends upon the characteristics of the system, upon the characteristics of the parameter estimation, and upon the expected utilization of the data. The characterization of the system is primarily concerned with the linearity of the system. As long as the system is linear, all input forms should give the same expected value. Naturally, though, all real systems have some degree of nonlinearity. Deterministic input signals result in frequency response functions that are dependent upon the signal level and type. A set of frequency response functions for different signal levels can be used to document the nonlinear characteristics of the system. Random input signals, in the presence of nonlinearities, result in a frequency response function that represents the best linear representation of the nonlinear characteristics for a given level of random signal input. For small nonlinearities, use of a random input will not differ greatly from the use of a deterministic input.

The characterization of the parameter estimation is primarily concerned with the type of mathematical model being used to represent the frequency response function. Generally, the model is a linear summation based upon the modal parameters of the system. Unless the mathematical representation of all nonlinearities is known, the parameter estimation process cannot properly weight the frequency response function data to include nonlinear effects. For this reason, random input signals are prevalently used to obtain the best linear estimate of the frequency response function when a parameter estimation process using a linear model is to be utilized.

The expected utilization of the data is concerned with the degree of detailed information required by any post-processing task. For experimental modal analysis, this can range from implicit modal vectors needed for trouble-shooting to explicit modal vectors used in an orthogonality check. As more detail is required, input signals, both random and deterministic, will need to match the system characteristics and parameter estimation characteristics more closely. In all possible uses of frequency response function data, the conflicting requirements of the need for accuracy, equipment availability, testing time, and testing cost will normally reduce the possible choices of input signal.

With respect to the reduction of the variance and bias errors of the frequency response function, random or deterministic signals can be utilized most effectively if the signals are periodic with respect to the sample period or totally observable with respect to the sample period. If either of these criteria are satisfied, regardless of signal type, the predominant bias error, leakage, will be eliminated. If these criteria are not satisfied, the leakage error may become significant. In either case, the variance error will be a function of the signal-to-noise ratio and the amount of averaging.

Many signals are appropriate for use in experimental modal analysis. Some of the most commonly used signals are described in the following sections. For those excitation signals that require the use of a shaker, Figure 26 shows a typical test configuration; Figure 27 shows a typical test configuration when an impact form of excitation is to be used. The advantages and disadvantages of each excitation signal are summarized in Figure 28.

4.2.1 Slow Swept Sine

The slow swept sine signal is a periodic deterministic signal with a frequency that is an integer multiple of the FFT frequency increment. Sufficient time is allowed in the measurement procedure for any transient response to the changes in frequency to decay so that the resultant input and response histories will be periodic with respect to the sample period. Therefore, the total time needed to compute an entire frequency response function will be a function of the number of frequency increments required and the system damping.

4.2.2 Periodic Chirp

The periodic chirp is a fast swept sine signal that is a periodic deterministic signal and is formulated by sweeping a sine signal up or down within a frequency band of interest during a single sample period. Normally, the fast swept sine signal is made up of only integer multiples of the FFT frequency increment. This signal is repeated without change so that the input and output histories will be periodic with respect to the sample period.

4.2.3 Impact (Impulse)

The impact signal is a transient deterministic signal which is formed by applying an input pulse to a system lasting only a very small part of the sample period. The width, height, and shape of this pulse will determine the usable spectrum of the impact. Briefly, the width of the pulse will determine the frequency spectrum while the height and shape of the pulse will control the level of the spectrum. Impact signals have proven to be quite popular due to the freedom of applying the input with some form of an instrumented hammer. While the concept is straight forward, the effective utilization of an impact signal is very involved ^[21].

4.2.4 Step Relaxation

The step relaxation signal is a transient deterministic signal which is formed by releasing a previously

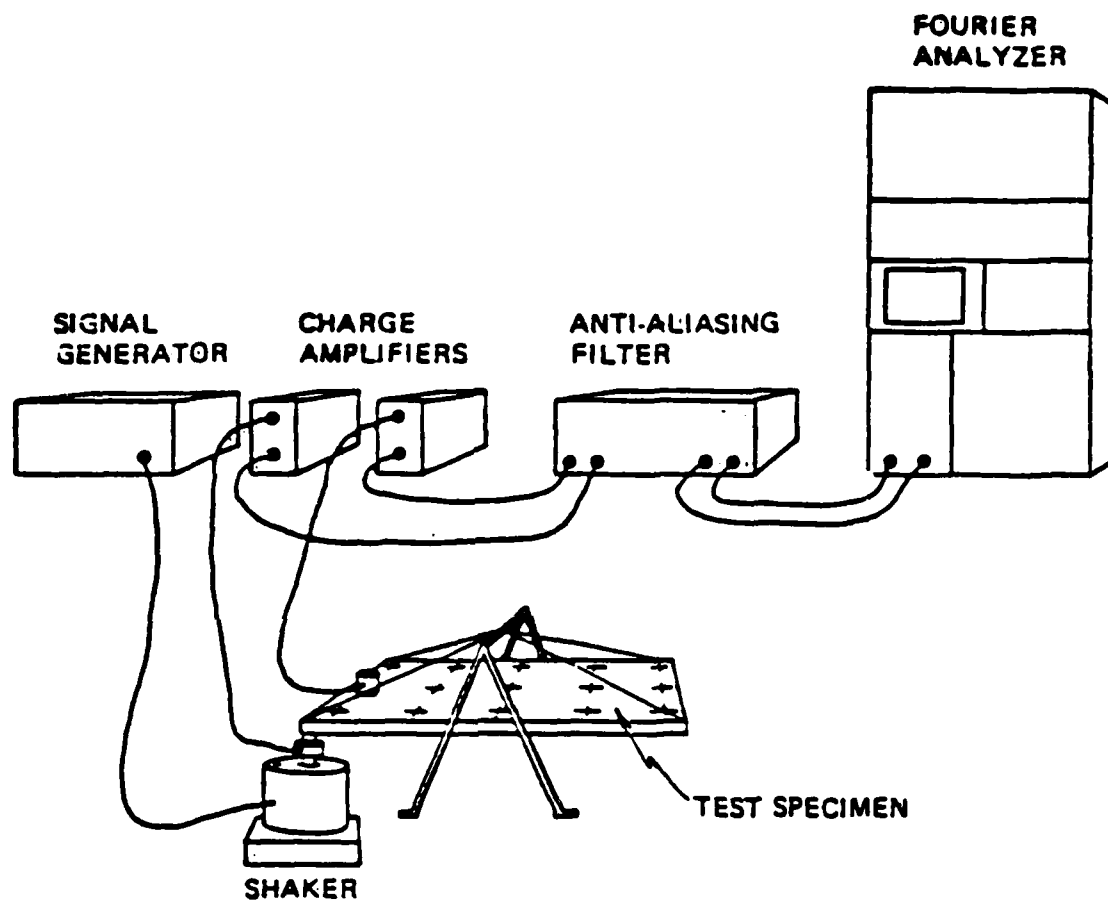


Figure 26. Typical Test Configuration: Shaker

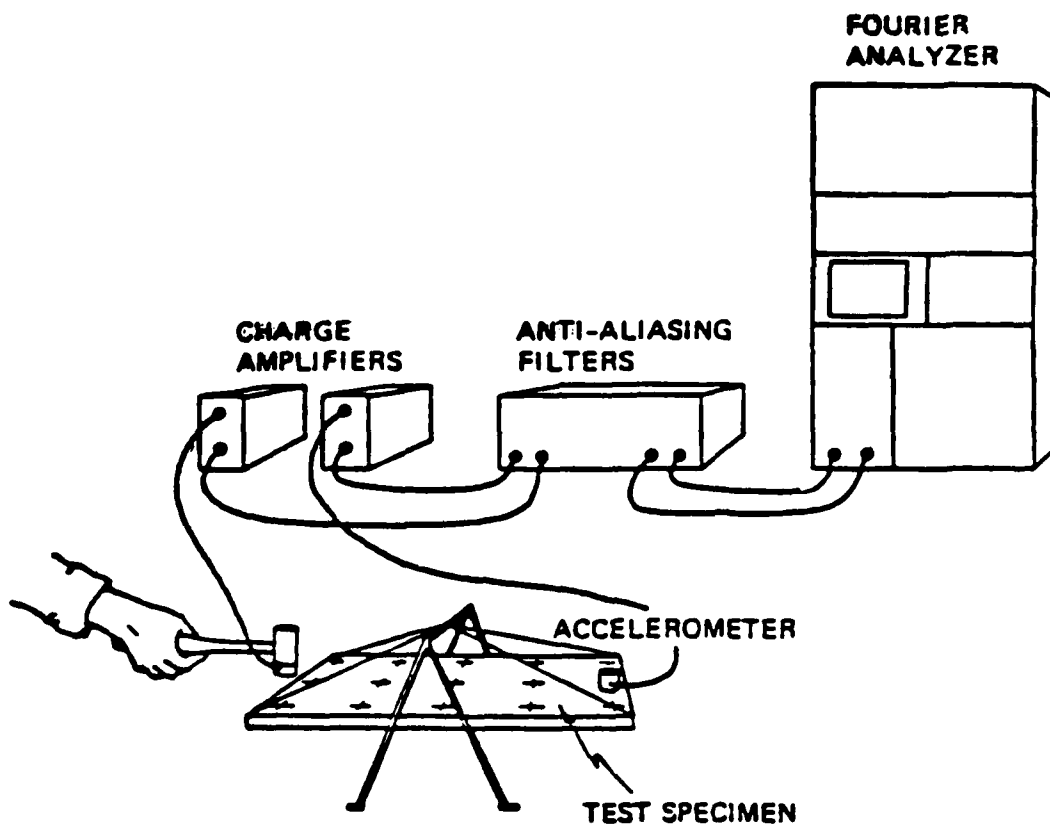


Figure 27. Typical Test Configuration: Impact Hammer

applied static input. The sample period begins at the instant that the release occurs. This signal is normally generated by the application of a static force through a cable. The cable is then cut or allowed to release through a shear pin arrangement ^[22].

4.2.5 Pure Random

The pure random signal is an ergodic, stationary random signal which has a Gaussian probability distribution. In general, the frequency content of the signal contains all frequencies (not just the integer multiples of the frequency resolution used by the Discrete Fourier Transform) but may be filtered to include only information in a frequency band of interest. The measured input spectrum will be altered by any impedance mismatch between the excitation system and the structural system under evaluation. There are many important characteristics of the pure random signal relevant to the estimation of frequency response functions. Since neither the input nor the response to this input is periodic with respect to the frequency resolution used in the digital signal processing, the bias error due to the truncation of the signal will be present if the structure being evaluated has light to moderate damping. Normally, weighting functions such as a Hanning window are used to try to reduce the effects of this truncation error but weighting functions cannot eliminate completely the bias of this error. The pure random signal type yields a peak-to-RMS ratio that is sufficiently low so that most problems with noncoherent noise can be eliminated through averaging. The data is well suited for use with the zoom Fourier Transform to achieve a smaller frequency resolution.

4.2.6 Pseudorandom

The pseudorandom signal is an ergodic, stationary random signal consisting only of integer multiples of the FFT frequency increment. The frequency spectrum of this signal has a constant amplitude with random phase. If sufficient time is allowed in the measurement procedure for any transient response to the initiation of the signal to decay, the resultant input and response histories are periodic with respect to the sample period. The number of averages used in the measurement procedure is only a function of the reduction of the variance error. In a noise free environment, only one average may be necessary.

4.2.7 Periodic Random

The periodic random signal is an ergodic, stationary random signal consisting of discrete frequencies containing only integer multiples of the frequency resolution used by the Discrete Fourier Transform. The frequency spectrum of this signal has random amplitude and random phase distribution. Since a single history will not contain information at all frequencies, a number of histories must be involved in the estimation process. For each average, an input history is created with random amplitude and random phase characteristics at each of the discrete frequencies involved in the Discrete Fourier Transform. The structure under evaluation is excited with this input in a repetitive cycle until the transient response to the change in excitation signal decays. The input and response histories should then contain only frequency information that will be involved in the Discrete Fourier Transform and are now recorded as one average in the total process. Since the input and response contain information only at integer multiples of the frequency resolution, there is no leakage in the measurement. With each new average, a new history, uncorrelated with the previous histories but constructed in the same manner, is generated so that the resulting

measurement will be completely randomized.

There are many important characteristics of the periodic random signal with respect to its use in the estimation of frequency response functions. The periodic random signal determines the best linear estimate of the frequency response function consistent with current modal parameter estimation algorithms since the leakage error is eliminated so effectively. The obvious disadvantage of this method is that it is at least twice as slow, because of the wait of at least one measurement cycle for the transient part of the response to decay to zero, as any other excitation signal with the same statistical parameters. A secondary disadvantage is that more sophisticated hardware is required in order to generate periodic signals synchronous with the measurement process. Another disadvantage of the periodic random signal is that it is not possible to post process time domain periodic random data using the zoom Fourier Transform. This is because the data contains information only at the frequency resolution of the original frequency range.

4.2.8 Burst Random

The burst random signal, often referred to as a random transient, is neither a completely transient deterministic signal nor a completely ergodic, stationary random signal but contains properties of both signal types. The frequency spectrum of this signal has random amplitude and random phase distribution and contains energy throughout the frequency spectrum. The difference between this signal and the pure random signal is that the random transient signal is truncated to zero after some portion of the sample period (normally fifty to eighty percent depending on the damping in the system). Because the input and response are totally observable transients, the measurement procedure duplicates the results of the periodic random procedure but without the need to wait for the transient part of the response to decay. The point at which the input history is truncated to zero is chosen so that the response history decays to zero within the sample period. Even for lightly damped structures, the response history will decay to zero very quickly due to the damping provided by the excitation system trying to maintain a zero input force. This will work best when the excitation system utilizes a voltage feedback amplifier. This damping, provided by the excitation system, is often overlooked in the analysis of the characteristics of the signal type since many excitation systems utilize a current feedback amplifier. Since the measured input history, although not exactly like the generated input signal, includes the variation of the input during decay of the response history, the input and response histories are totally observable within the sample period. This yields an unbiased estimate of the frequency response function, with respect to leakage, and does not affect the estimates of structural damping parameters.

There are many important characteristics of the burst random signal relevant to its use in the estimation of frequency response functions. The signal-to-noise ratio is much larger as well as the peak-to-RMS ratio being much lower than other forms of transient signals. The random aspect of the signal type provides a linear representation of the frequency response function that is consistent with the periodic random signal but in at least half of the measurement time. In addition, compared to the periodic random signal, the random transient signal is continuous in the frequency range of interest which allows zoom Fourier Transforms to be used on the same data to achieve a smaller frequency resolution when required. While some additional hardware is required to generate the random transient signal, the hardware does not require the sophistication involved with the periodic random signal.

	Type of Excitation							
	Steady State Sine	Pure Random	Pseudo Random	Random	Fast Sine	Impact	Burst Sine	Burst Random
Minimize Leakage	No	No	Yes	Yes	Yes	Yes	Yes	Yes
Signal-to-Noise Ratio	Very High	Fair	Fair	Fair	High	Low	High	Fair
RMS-to-Peak Ratio	High	Fair	Fair	Fair	High	Low	High*	Fair
Test Measurement Time	Very Long	Good	Very Short	Fair	Fair	Very Good	Very Good	Very Good
Controlled Frequency Content	Yes	Yes •	Yes •	Yes •	Yes •	No	Yes •	Yes •
Controlled Amplitude Content	Yes	No	Yes •	No	Yes •	No	Yes •	No
Removes Distortion	No	Yes	No	Yes	No	No	No	Yes
Characterize Nonlinearity	Yes	No	No	No	Yes	No	Yes	No

* Requires special hardware

Figure 28. Summary of Excitation Signals

5. FREQUENCY RESPONSE FUNCTION ESTIMATION

5.1 Introduction

The theoretical foundation for the estimation of modal parameters has been well documented. Historically, modal testing was first done using the phase resonance, or forced normal mode testing method. Using this method, the structure was forced into a normal mode by a number of single frequency force inputs. The frequency, damping, and modal vector could then be estimated.

With advances in computer technology (both hardware and software), and especially the development of the Fast Fourier Transform, it became practical to estimate frequency response functions for random data. The theoretical foundation for the computation of frequency response functions for any number of inputs has been well documented [1-3,25-29]. A single input, single output frequency response function was estimated for all test points. This greatly reduced test time. But, in order to insure that no modes had been missed, more than one input location should be used.

Starting in about 1979, the estimation of frequency response functions for multiple inputs has been investigated [27,30-36]. The multiple input approach has proven to have advantages over the single input approach. When large numbers of responses are measured simultaneously, the estimated frequency response functions are consistent with each other.

5.2 Theory

Consider the case of n inputs and m outputs measured during a modal test on a dynamic system as shown in Figure 29. Equation 5 is the governing equation.

$$X(\omega) = H(\omega) * F(\omega) \quad (5)$$

For simplicity, the ω will be dropped from the equations. Since the actual measured values for input and output may contain noise, the measured values are:

$$F = \hat{F} - v$$

and

$$X = \hat{X} - \eta$$

Therefore, a more general model for the computation of frequency response functions for N_i inputs and N_o outputs could be at response location p:

$$\hat{X}_p - \eta_p = \sum_{q=1}^{N_i} H_{pq} * (\hat{F}_q - v_q) \quad (6)$$

Where:

- F = $\hat{F} - v$ Actual input
- X = $\hat{X} - \eta$ Actual output
- \hat{X}_p = Spectrum of the p-th output, measured
- \hat{F}_q = Spectrum of the q-th input, measured
- H_{pq} = Frequency response function of output p with respect to input q
- v_q = Spectrum of the noise part of the input
- η_p = Spectrum of the noise part of the output

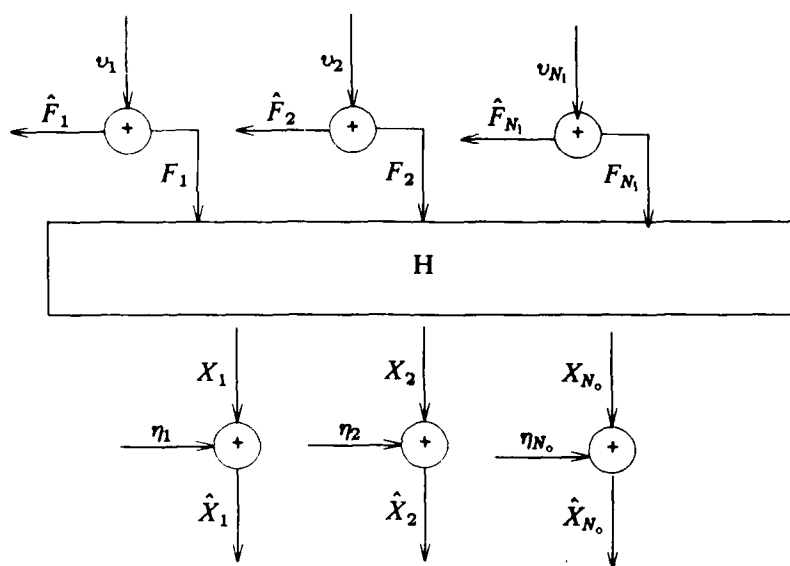


Figure 29. Multiple Input System Model

If $N_i = N_o = 1$, Equation 6 reduces to the classic single input, single output case. With N_i not equal 1, the equation is for the multiple input case.

For the multiple input case, the concept of coherence must be expanded to include ordinary, partial, and multiple coherence functions^[30,35]. Each of the coherence functions is useful in determining the validity of the model used to describe the system under test or, as discussed in Section 6, to evaluate how well the inputs conform to the theory.

Ordinary coherence is defined as the correlation coefficient describing the possible causal

relationship between any two signals. Ordinary coherence can be calculated between any two forces or between any force and any response. In this calculation, the contribution of all other signals is ignored. Therefore, the interpretation of the ordinary coherence functions must be made with great care. The use and interpretation of the ordinary coherence function between forces will be discussed in Section 6. The ordinary coherence function between an input and an output is of little use in determining the validity of the model. This is because the output in the multiple input case is due to a number of inputs so that the ordinary coherence will not have the same useful interpretation as in the single input case.

Partial coherence is defined as the ordinary coherence between any two conditioned signals. The signals are conditioned by removing, in a systematic manner, the contribution(s) of other signals. The order of conditioning has an effect on the degree of correlation. A partial coherence function can be calculated between conditioned inputs, a conditioned output and a conditioned input, or, with multiple outputs, between conditioned outputs. Typically, the input and output are conditioned by removing the potential contributions to the output and input from other input(s). The removal of the effects of the other input(s) is formulated on a linear least squares basis. There will be a partial coherence function for every input/output combination for all permutations of conditioning. The usefulness of partial coherence with respect to frequency response function estimation is to determine the degree of correlation between inputs. The use and interpretation of the partial coherence will be discussed in Section 6.

Multiple coherence is defined as the correlation coefficient describing the possible causal relationship between an output and all known inputs. There will be one multiple coherence function for every output. Multiple coherence is used similarly to the ordinary coherence in the single input case. The multiple coherence function should be close to unity throughout the entire frequency range of the estimated frequency response function. A low value of multiple coherence at resonance indicates possible measurement error, unknown inputs, unmeasured inputs, or signal processing errors such as leakage. However, a low value of multiple coherence is not expected at an antiresonance since there should be sufficient signal-to-noise ratio at these frequencies (antiresonance is not a global property of the system).

5.3 Mathematical Models

Depending on where the noise is assumed to enter the measurement process, there are at least three different mathematical models that can be used to estimate the frequency response functions. It is important to remember that the system determines its own frequency response function for a given input/output pair and the boundary conditions for the test. In the limit, if all noise were removed, any estimation technique must give the same result.

5.3.1 H_1 Technique

Assuming that there are no measurement errors on the input forces, let the measurement errors on the response signal be represented by $\{\eta\}$. The H_1 least squares technique aims at finding the solution $\{H\}$ of Equation 7 that minimizes the Euclidean length of $\{\eta\}$, the "squared error". This solution is also called the least squares estimate. Writing Equation 6, using all measured values (*the η has been dropped for simplicity*) in a form more readily recognized yields ^[31-34,36].

$$[H]_{N_o \times N_i} \{F\}_{N_i \times 1} = \{X\}_{N_o \times 1} - \{\eta\}_{N_o \times 1} \quad (7)$$

The subscripts refer to the size of the matrix. It is well known that the solution $[H]$ can be found as the solution of the set of "normal equations" formed by post multiplying by $\{F\}^H$ [37-39].

$$[H] \{F\} \{F\}^H = \{X\} \{F\}^H - \{\eta\} \{F\}^H \quad (8)$$

$\|\eta\|_2$ is minimum

Where:

H : complex conjugate transpose (Hermitian)

$\|\dots\|_2$: Euclidean norm

Equation 8 can be reduced to Equation 9 by assuming that the noise on the outputs are uncorrelated with the inputs and that with sufficient averages, the normalized noise spectra are close to zero.

$$[H]_{N_o \times N_i} \{F\}_{N_i \times 1} \{F\}_{1 \times N_i}^H = \{X\}_{N_o \times 1} \{F\}_{1 \times N_i}^H \quad (9)$$

The elements of the coefficient matrix and right hand matrix in Equation 9 are readily identified, when expanded, with the auto and cross power spectra of input forces and response signals [30-35].

When the matrix multiplications of Equation 9 are expanded to form Equations 10 or 11, the form is more readily recognized as a frequency response function estimation.

$$[H][GFF]=[GXF] \quad (10)$$

or

$$[H]=[GXF][GFF]^{-1} \quad (11)$$

Where:

$[H]$ = Frequency response function matrix

$$= \begin{bmatrix} H_{11} & H_{12} & \dots & H_{1N_i} \\ H_{21} & \cdot & \cdot & \cdot \\ \cdot & \cdot & \cdot & \cdot \\ H_{N_o1} & \cdot & \cdot & H_{N_oN_i} \end{bmatrix}$$

$[GXF]$ = Input/output cross spectra matrix

$$= \{X\} \{F\}^H$$

$$= \begin{Bmatrix} X_1 \\ X_2 \\ \vdots \\ X_{N_o} \end{Bmatrix} [F_1^* \ F_2^* \ \dots \ F_{N_i}^*]$$

* : complex conjugate

$[GFF]$ = Input cross spectra matrix

$$= \{F\} \{F\}^H$$

$$= \begin{Bmatrix} F_1 \\ F_2 \\ \vdots \\ F_{N_i} \end{Bmatrix} [F_1^* \ F_2^* \ \dots \ F_{N_i}^*]$$

$$= \begin{bmatrix} GFF_{11} & \dots & GFF_{1N_i} \\ \vdots & \ddots & \vdots \\ GFF_{N_i1} & \dots & GFF_{N_iN_i} \end{bmatrix}$$

$GFF_{ik} = GFF_{ki}^*$ (Hermitian matrix)

The ordinary coherence function can be formulated in terms of the elements of the matrices defined previously. The ordinary coherence function between the p-th output and the q-th input can be computed from Equation 12.

$$COH_{pq} = \frac{|GXF_{pq}|^2}{GFF_{qq} GXX_{pp}} \quad (12)$$

Where:

GXX_{pp} = Auto power spectrum of the output

The magnitude of the error vector that corresponds to the least squares solution is a measure of how

well the response signal is predicted by the input forces. When compared with the magnitude of the response signal, a normalized measure, known as the multiple coherence function, can be defined by Equation 13 [34,35].

$$MCOH_p = \sum_{s=1}^{N_i} \sum_{t=1}^{N_i} \frac{H_{ps} GFF_{st} H_{pt}^*}{GXX_{pp}} \quad (13)$$

Where:

H_{ps} = Frequency Response Function for output p and input s

H_{pt} = Frequency Response Function for output p and input t

5.3.1.1 Dual Input Case

The natural place to begin the investigation of the practicality of the multiple input frequency response function estimation is with the two input case.

The model used for the H_1 technique is shown in Figure 30. By expanding Equation 6 with N_i equal to 2 and N_o equal to 1, the equations for the two input single output case can be put in a form that reduces the matrix equation to Equation 14 [30-35].

$$\hat{X}_p - \eta_p = H_{p1} F_1 + H_{p2} F_2 \quad (14)$$

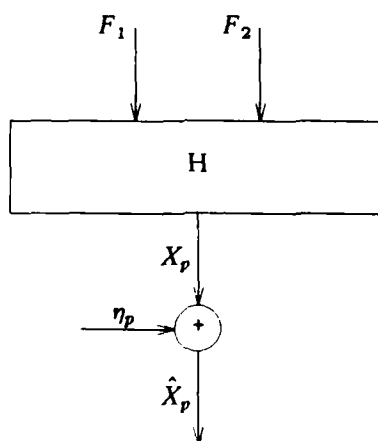


Figure 30. Dual Input System Model, H_1 Technique

Again, if the noise on the output is uncorrelated with the inputs and if sufficient averages are taken,

Equation 14 can be put in the form of Equation 10 to compute the least squares estimate of the frequency response functions. The result is Equation 15.

$$\{X_p\} [F_1^* \ F_2^*] = [H_{p1} \ H_{p2}] \begin{Bmatrix} F_1 \\ F_2 \end{Bmatrix} [F_1^* \ F_2^*] \quad (15)$$

Forming the matrix products for N_o outputs, Equation 15 can be expanded to Equation 16 in the form of Equation 11.

$$\begin{bmatrix} H_{11} & H_{12} \\ H_{21} & H_{22} \\ H_{31} & H_{32} \\ \vdots & \vdots \\ H_{N_o,1} & H_{N_o,2} \end{bmatrix} = \begin{bmatrix} GFX_{11} & GFX_{12} \\ GFX_{21} & GFX_{22} \\ GFX_{31} & GFX_{32} \\ \vdots & \vdots \\ GFX_{N_o,1} & GFX_{N_o,2} \end{bmatrix} \begin{bmatrix} GFF_{11} & GFF_{12} \\ GFF_{21} & GFF_{22} \end{bmatrix}^{-1} \quad (16)$$

When the input cross spectra matrix [GFF] is inverted, Equation 16 can be simplified to yield Equation 17 and Equation 18 that are for estimates of two frequency response functions.

$$H_{p1} = \frac{GFX_{p1} GFF_{22} - GFX_{p2} GFF_{21}}{\det[GFF]} \quad (17)$$

$$H_{p2} = \frac{GFX_{p2} GFF_{11} - GFX_{p1} GFF_{12}}{\det[GFF]} \quad (18)$$

Where:

$$\begin{aligned} \det[GFF] &= \text{Determinant of [GFF] matrix} \\ &= GFF_{11} GFF_{22} - GFF_{21} GFF_{12} \end{aligned}$$

There are three ordinary coherence functions that can be computed for the dual input case. The interpretation of the ordinary coherence functions is now not completely consistent with the single input case. As discussed in Section 6, the coherence between the forces, COH_{12} , should be as close to zero as possible. The ordinary coherence between the response and either force (COH_{p1} , COH_{p2}) is of limited use because the output is now caused by the two input forces.

$$COH_{p1} = \frac{|GFX_{p1}|^2}{GFF_{11} GXX_{pp}} \quad (19)$$

$$COH_{p2} = \frac{|GFX_{p2}|^2}{GFF_{22} GXX_{pp}} \quad (20)$$

$$COH_{12} = \frac{|GFX_{12}|^2}{GFF_{11} GFF_{22}} \quad (21)$$

The multiple coherence function can be defined by Equation 13.

5.3.1.2 Multiple Inputs

For more than 2 inputs, Equation 10 can be expanded, as an example, for six inputs to yield Equation 22. Note that Equation 22 has been put in transposed form in which the frequency response functions appear as a column instead of a row. Equation 22 is recognized as a set of simultaneous equations with the frequency response functions as the unknowns.

$$\begin{bmatrix} GFF_{11} & \dots & GFF_{61} \\ GFF_{12} & & \cdot \\ \cdot & & \cdot \\ \cdot & & \cdot \\ GFF_{16} & \dots & GFF_{66} \end{bmatrix} \begin{bmatrix} H_{p1} \\ H_{p2} \\ \cdot \\ \cdot \\ H_{p6} \end{bmatrix} = \begin{bmatrix} GXF_{p1} \\ GXF_{p2} \\ \cdot \\ \cdot \\ GXF_{p6} \end{bmatrix} \quad (22)$$

Equation 22 could be solved for the frequency response functions by the technique of Section 5.3.1, inversion of the [GFF] matrix, but the computational time and possible dynamic range errors may make the inversion technique undesirable [34,40]. Computational techniques for solution of the equation will be discussed later in this Section.

As before, ordinary coherence functions can be defined between any two forces or any force with the response giving a total of 21 possible ordinary coherence functions. In a systematic way, 4 partial coherence functions between forces can also be defined and one multiple coherence function can be defined by Equation 13. The partial coherence functions are defined and discussed in Section 6.

5.3.2 H_2 Technique

If all measurement errors are assumed to be confined to the inputs, let the errors associated with the inputs be represented by $\{v\}$. The H_2 least squares technique aims at finding the solution $[H]$ of Equation 23 that minimizes the length of $\{v\}$. The basic model for the H_2 technique is shown in Figure 31 [41,42].

$$[H]_{N_o \times N_i} \{ \{F\}_{N_i \times 1} + \{v\}_{N_i \times 1} \} = \{X\}_{N_o \times 1} \quad (23)$$

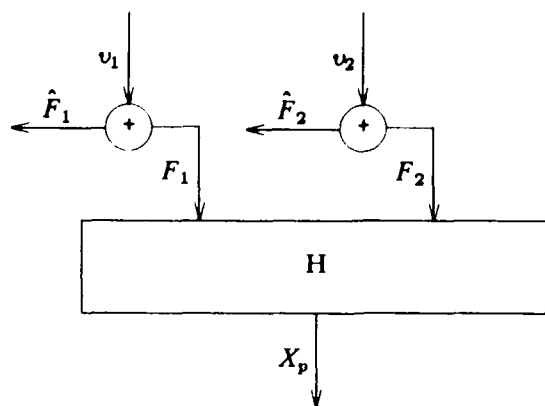


Figure 31. System Model for H_2 Technique

To find the solution of Equation 23 in a similar manner as in the H_1 case, postmultiply by $\{X\}^H$.

$$[H] \{ \{F\} + \{v\} \} \{X\}^H = \{X\} \{X\}^H \quad (24)$$

If the noise on the input $\{v\}$ is assumed not correlated with the output and if sufficient averages are taken so that the noise matrix approaches zero, Equation 24 can be written as:

$$[H]_{N_o \times N_i} \{F\}_{N_i \times 1} \{X\}_{N_o \times 1}^H = \{X\}_{N_o \times 1} \{X\}_{1 \times N_o}^H \quad (25)$$

The elements of the matrices are now identified as the cross power spectra between inputs and outputs and the output auto power spectra.

To investigate the potential uses of the H_2 technique for multiple inputs, it will be helpful to expand the equations for two cases. One is when the number of inputs and the number of outputs are equal and another when the number of outputs is greater than the number of inputs.

5.3.2.1 Two Inputs/Two Response

For the case of two inputs and two responses, $N_o = N_i = 2$. Expanding Equation 24 for this case yields:

$$[H]_{2 \times 2} [GFX]_{2 \times 2} = [GXX]_{2 \times 2} \quad (26)$$

or

$$[H]_{2 \times 2} = [GXX]_{2 \times 2} [GFX]_{2 \times 2}^{-1} \quad (27)$$

Equation 26 can be solved for the frequency response functions by inverting the input/output cross spectra matrix at every frequency in the analysis range and solving the set of simultaneous equations.

5.3.2.2 Two Inputs/Three Responses

For the case of two inputs and three responses, $N_o = 3$ and $N_i = 2$. Equation 25 is expanded to yield:

$$[H]_{3 \times 2} [GFX]_{2 \times 3} = [GXX]_{3 \times 3} \quad (28)$$

or

$$[H]_{3 \times 2} = [GXX]_{3 \times 3} [GFX]_{2 \times 3}^{-1} \quad (29)$$

For Equation 29 to be valid, a 3×3 matrix must be multiplied by a 2×3 matrix. For the equation to be valid, a generalized inverse must be used. Therefore, unique frequency response function can not be estimated from this set of data. Therefore, an added constraint on the H_2 technique is that the number of outputs must equal the number of inputs^[42,43]. For the single input, single output case, this constraint is not a disadvantage. But, for the multiple input technique, this constraint makes the H_2 technique impractical for many testing situations (for example a 2 triaxial response test with 2 inputs). Also, the major advantage of the H_2 technique is to reduce the effects of noise on the input. This can also be accomplished by selective excitation that is investigated in Section 4 or by formulating the H_v frequency response estimate which is better suited for multiple inputs. Therefore, the H_2 technique was not heavily investigated for the multiple input case.

5.3.3 H_v Technique

Assume now that measurement errors are present on both the input and the response signals, represented by $\{v\}$ for the noise on the input and $\{\eta\}$ for the noise on the output. The H_v least squares technique aims at finding the solution $[H]$ in Equation 29 that minimizes the sum of the Euclidean lengths of $\{\eta\}$ and $\{v\}$, or the "total squared error"^[42,44-46]. This solution is referred to as the Total Least Squared estimate. It is proved in the literature that it can be identified with the elements of the matrix $[GFFX]$ defined by Equation 30. Again the elements of this matrix are readily identified with the auto and cross power spectra of input forces and response signals.

$$[H] \{ \{F\} - \{v\} \} = \{X\} - \{\eta\} \quad (29)$$

$$[GFFX] = \{ \{F\} \{X\} \}^H \{ \{F\} \{X\} \} \quad (30)$$

$$[GFFX] = \begin{bmatrix} [GFF] & [GFX] \\ [GFX]^H & [GXX] \end{bmatrix} \quad (30)$$

The matrix $[GFFX]$ is Hermitian; its eigenvalue decomposition is therefore defined by Equation 31. The Total Least Squared estimate for $[H]$ is then defined by Equation 32.

$$[GFFX] = [V] \Lambda [V]^H \quad (31)$$

Where:

$$\Lambda = \text{diag}(\lambda_1, \lambda_2, \dots, \lambda_m)$$

$$[V]^H [V] = I$$

$$\{H\} = \begin{Bmatrix} -V_{1 \ p+1} / V_{p+1 \ p+1} \\ \vdots \\ -V_{p \ p+1} / V_{p+1 \ p+1} \end{Bmatrix} \quad (32)$$

Notice that the Total Least Squares solution does not exist if $V_{p+1 \ p+1}$ equals 0. This however can only happen if the submatrix $[GFF]$ of $[GFFX]$ is singular^[44]; that is, if the input forces are correlated. Verifying that the input forces are not correlated is therefore sufficient to warrant the existence of the Total Least Squares solution.

Corresponding to the Total Least Squares estimate, there will be errors on both input forces and response signals. The magnitude of the errors on the response signal can be expressed by Equation 33. If this error is substituted into Equation 34, one calculates a measure of how well the response signal is predicted by the input forces, considering now however also errors on the input forces.

$$G\eta = \lambda_{p+1} V_{p+1 \ p+1}^2 V_{p+1 \ p+1} \quad (33)$$

$$MCOH = 1 - \frac{G\eta}{GXX} \quad (34)$$

5.4 H_s Technique

In a similar fashion, a "scaled" frequency response function has been proposed by Wicks and Vold^[47].

Starting with Equation 6 for a single input (the equations can be readily expanded to the multiple

input case):

$$\hat{X} - \eta = H^*(\hat{F} - v) \quad (35)$$

Expanding for the single input case and collecting error terms yields:

$$\eta \eta^* + (H H^*) (v v^*) = (H \hat{F} - \hat{X}) (H \hat{F} - \hat{X})^* \quad (36)$$

If the error terms of Equation 36 are equal in magnitude, a least squares minimization can be applied to Equation 36. To insure that the magnitudes are equal, either the input or the output can be scaled. Assuming that the input is scaled by S , Equation 35 can be written as:

$$\hat{X} - \eta = H S^*(\hat{F} - v)$$

If the scaling constant is carried throughout the development, an equation can be written for a "scaled" frequency response function.

$$H_S = \frac{(\hat{X} \hat{X}^* - S^2 \hat{F} \hat{F}^*) + \sqrt{(S^2 \hat{F} \hat{F}^* - \hat{X} \hat{X}^*)^2 + 4 S^2 \hat{X}^* \hat{F} \hat{F}^* \hat{X}}}{2 S \hat{X}^* \hat{F}} \quad (37)$$

5.5 Comparison of H_1 , H_2 , and H_v

The assumption that measurement errors are confined totally to the input forces or totally to the response signals is sometimes unrealistic. But, it is important to understand why H_1 , H_2 , and H_v yield different estimates of the same input/output frequency response function for a given system. It is important also to remember that a linear system has only one theoretical frequency response for any given input/output pair. Table 1 compares the different assumptions and solution techniques.

TABLE 1. Comparison of H_1 , H_2 , and H_v

Technique	Solution		
	Method	Assumed location of noise	
		Force Inputs	Response
H_1	LS	no noise	noise
H_2	LS	noise	no noise
H_v	TLS	noise	noise

It is also important to realize that if the noise on the inputs $\{\eta\}$ and the noise on the responses $\{v\}$ are eliminated, H_1 equals H_2 and they are approximately equal to H_v . Therefore, it is important to

spend time to acquire data that is noise free and that fits the assumptions of the Discrete Fourier Transform rather than accept the errors and try to minimize their effect by the solution technique.

The mechanism of the least squares solution of H_1 and H_2 and the Total Least Squares solution of H_o can be compared using the following geometric interpretation^[44]. Assume that m equals 1 for a single input, and real-valued input forces and response spectra. Figure 32 is a measure of the goodness-of-fit for one frequency, magnitude only, of the frequency response estimate. F represents the input at that frequency and X the corresponding response. In the H_1 technique only X is assumed inaccurate, and it is the vertical distance that is minimized. Likewise, for the H_2 technique, only F is assumed to contain errors and so the horizontal distance is minimized. In the H_o technique, both F and X are assumed inaccurate. The Total Least Squares technique aims at minimizing the total error on F and X so that the perpendicular distance is minimized. Figure 32 depicts the Least Squares and Total Least Squares measure of goodness-of-fit at a resonance of the system. As can be seen, because the H_1 technique is minimizing a large vertical distance, therefore the slope of the line will be pulled down, meaning that the value at resonance will be low. Since the H_2 technique minimizes a horizontal distance, the slope of the line will be steeper than for the H_1 technique. Figure 33 shows the same goodness-of-fit for an anti-resonance condition. In this case, the reverse is true. The H_2 technique minimizes a large horizontal distance giving a value in the anti-resonance that is too high. The H_1 technique minimizes a smaller vertical distance giving a sharper anti-resonance. The H_o technique in both cases minimizes a distance that is between the H_1 and H_2 techniques. Away from a resonance or anti-resonance where the errors are likely to be less, the H_1 , H_2 , and H_o techniques are almost identical.

From the standpoint of frequency response function estimation, the H_1 technique, at resonances, underestimates the height of the peak amplitude and therefore overestimates the damping. In the Argand plane, the circles look "flat". The H_2 technique, at resonances, overestimates the amplitude and therefore underestimates damping. The circles look oblong in the H_2 technique. The H_o technique gives, at resonance, an estimate of the frequency response function that is between the H_1 and H_2 estimates. At antiresonances, the reverse is true, H_1 gives the lowest estimate and H_2 gives the highest estimate with H_o in the middle. Away from resonance, all three give the same estimate. It is important to remember that in all three cases, the value computed is only an estimate of the theoretical frequency response function. If other measurement errors or violation of system assumptions are present, all three estimators will give erroneous results. It is therefore important to spend as much time as possible to reduce known errors before data acquisition begins.

5.6 Examples

To investigate the potential improvements and limitations of the multiple input frequency response function estimation, a base line set of data is needed for comparison. For this set of data, an automobile body-in-white, shown in Figure 34 was chosen as a representative structure. The structure is lightly damped so that leakage is expected to be a problem. The body was mounted on air rides to simulate a free-free condition. In an attempt to reduce as many measurement errors as possible, an accelerometer was permanently mounted at point #1 and left in the same position throughout the entire data collection period. Also, all cabling, power supplies, load cells, and signal generation equipment was kept constant. Therefore, any variation in the data should be caused by the multiple input technique and not because of differences in the equipment or poor data collection techniques. In all cases, 25 stable frequency domain averages were collected in the range from 0 to 50 Hertz. The anti-aliasing filters were set at 40 Hertz. The low frequency characteristics of the accelerometers is about 5 Hertz. Therefore, the data below 5 Hertz is not expected to be of good quality. But, the accelerometers were chosen because of their low mass.

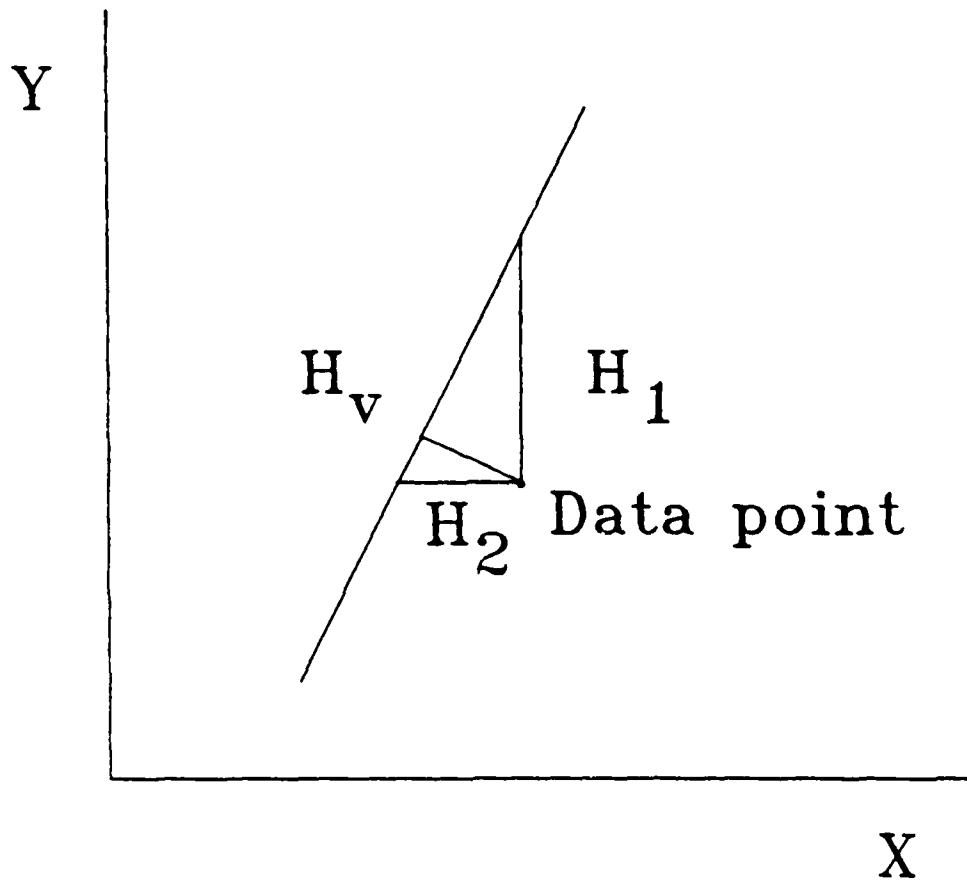


Figure 32. Geometrical Interpretation at Resonance

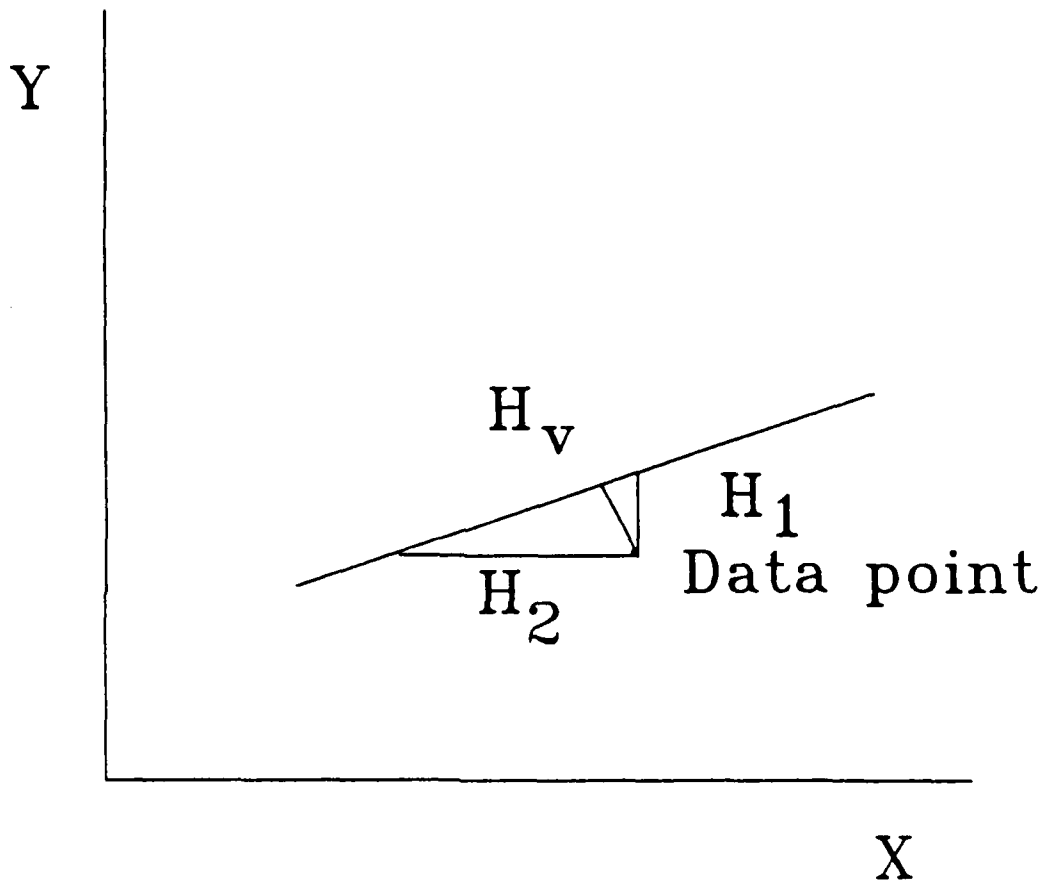


Figure 33. Geometrical Interpretation at Anti-resonance

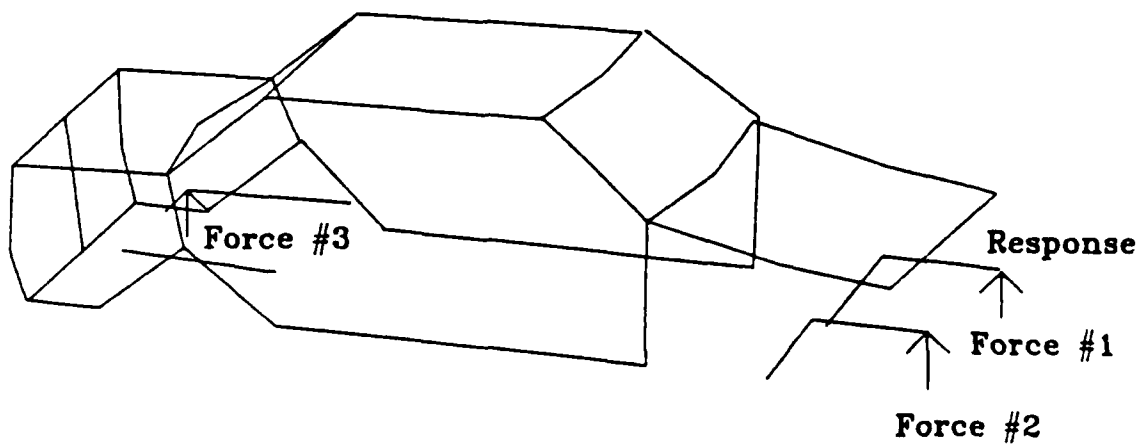


Figure 34. Body-in-white Test Structure

5.6.1 Single Input

Figures 35 and 36 show frequency response function estimates (log magnitude and phase), their associated ordinary coherence function, and input auto power spectrum taken on the body-in-white, using existing single input, H_1 technology. The excitation was pure random and a Hanning window applied to both the excitation and the response signals. The data was collected by attaching one shaker and estimating the associated frequency response function of that input location versus the response at location #1. As can be seen by the ordinary coherence functions, leakage at the resonances appears to be a problem. The low value of the coherence function at the anti-resonance is expected because of the low signal-to-noise at those frequencies.

5.6.2 Dual Inputs

Next, two forces were input at points #1 and #2. In this case, frequency response function H_{11} was estimated. Figure 37 is the associated estimate of the frequency response function. Figure 38 is the multiple coherence function for this case. Also computed during this measurement cycle is frequency response function H_{21} . Both input auto power spectra were flat from 0 to 40 Hertz. This indicates that sufficient energy should be present to excite all modes in the 0 to 50 Hertz range. As can be seen by comparing Figure 35 with Figure 37 the estimates for the dual input case are comparable with the associated single input case. But, for the dual input case, the estimates of the frequency response functions are computed from data that is taken simultaneously. Therefore, the estimates of the damped natural frequency and damping for these two functions are consistent with each other. Also, since these two functions are estimated from symmetric input locations, the two estimates could be added to enhance symmetric modes and subtracted to enhance anti-symmetric modes.

Noting that the multiple coherence function exhibits drops from unity at system poles may indicate that leakage is a problem. But, the multiple coherence function does not exhibit the drops at anti-resonances because there is now sufficient signal-to-noise at these frequencies. Therefore, the estimate of the frequency response function should contain less errors at these frequencies.

5.6.3 Three Inputs

For the body-in-white, three inputs approach the limits of the optimum number of inputs. Therefore, an exciter was attached at point #3, and three frequency response functions were estimated simultaneously. Figure 39 is the frequency response function that was estimated in this case. Figure 40 is the associated multiple coherence function. Again, when comparing the associated frequency response estimates for the single, dual, and three input case, the estimates are very similar. For the three input case, the estimates are computed from data that is taken simultaneously, therefore consistency between the three rows is guaranteed for these three estimates.

The multiple coherence function again indicate that leakage may still be a problem. But, as expected, the multiple coherence function is unity at anti-resonances

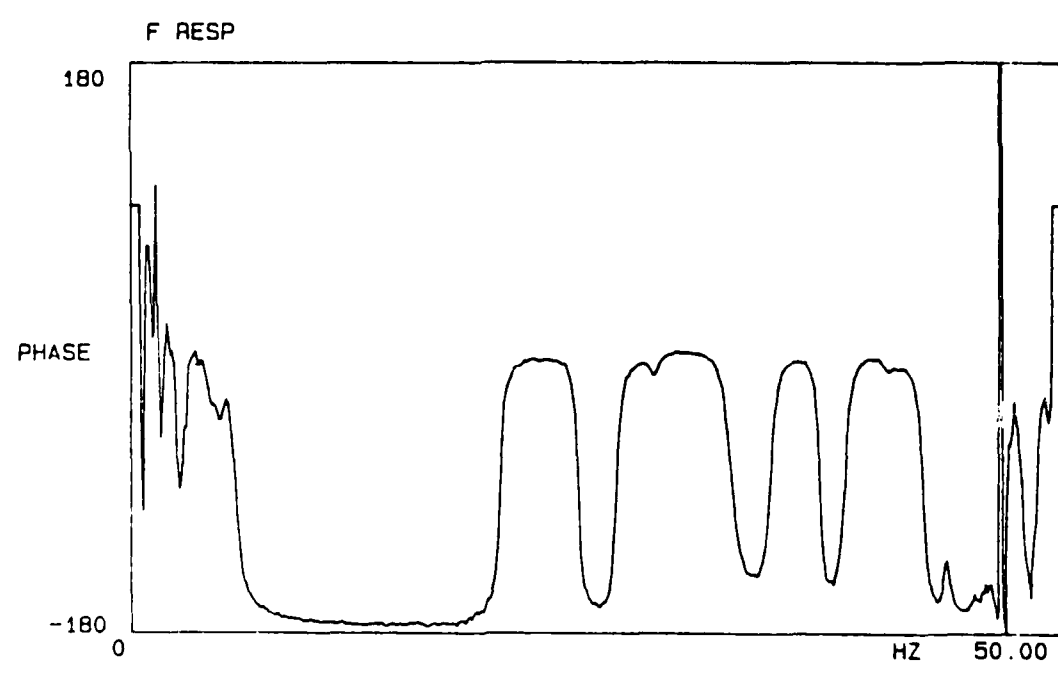
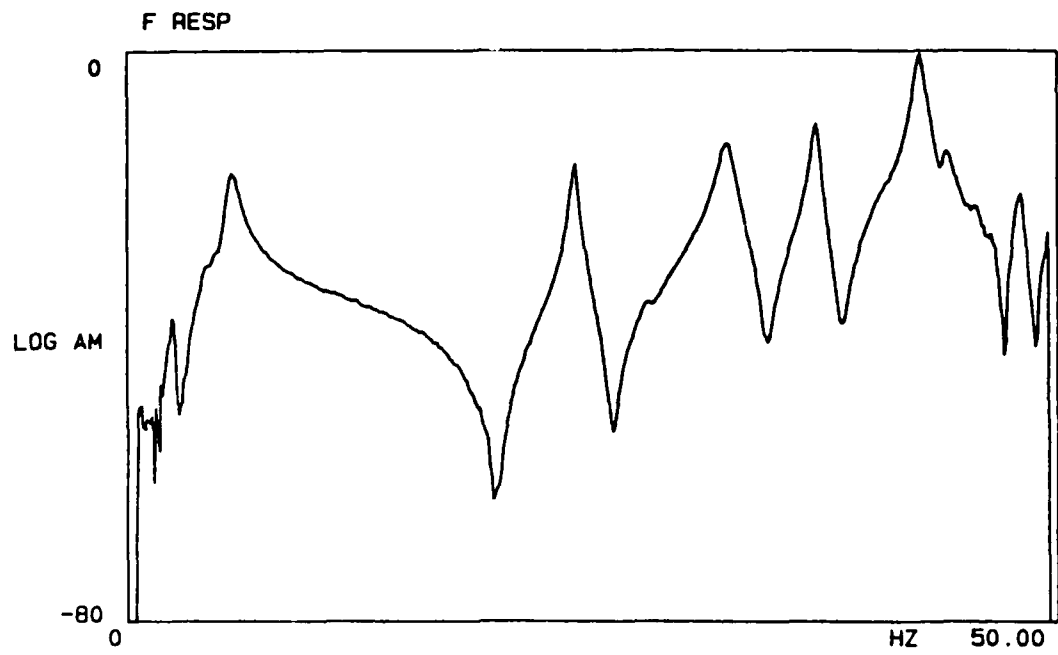


Figure 35. Frequency Response Estimate H_{11} - Single Input

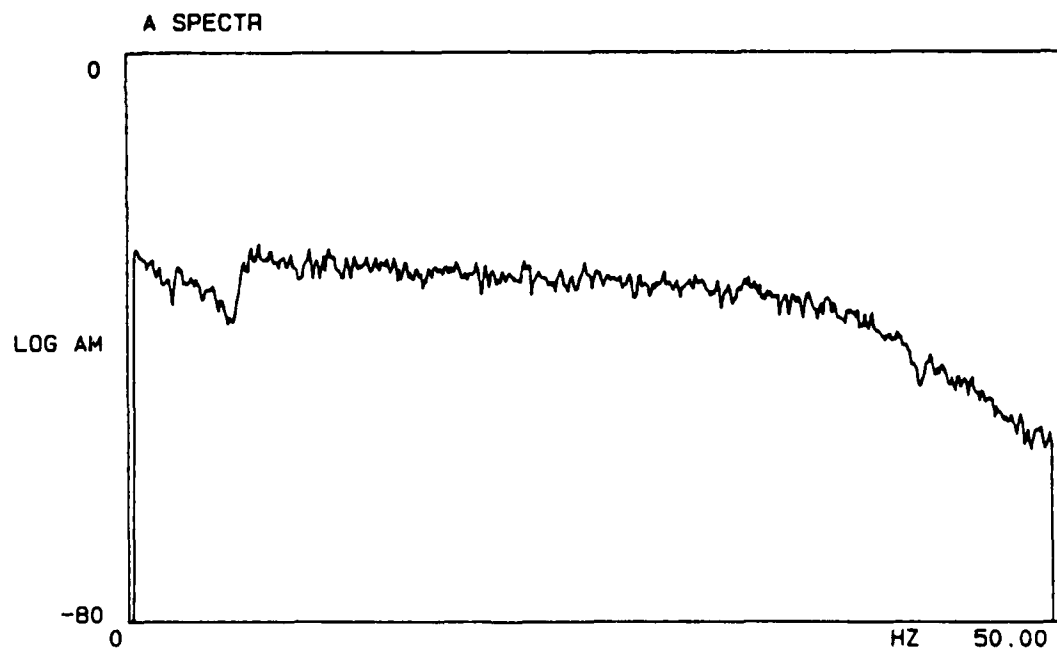


Figure 36. Coherence and Auto Power Spectrum for H_{11} - Single Input

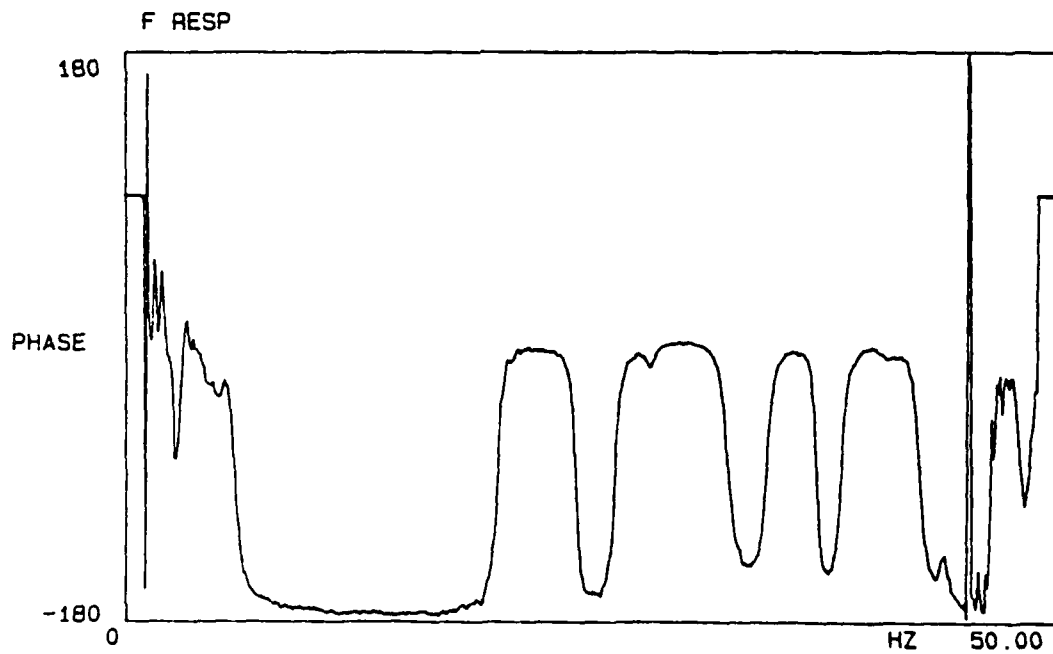
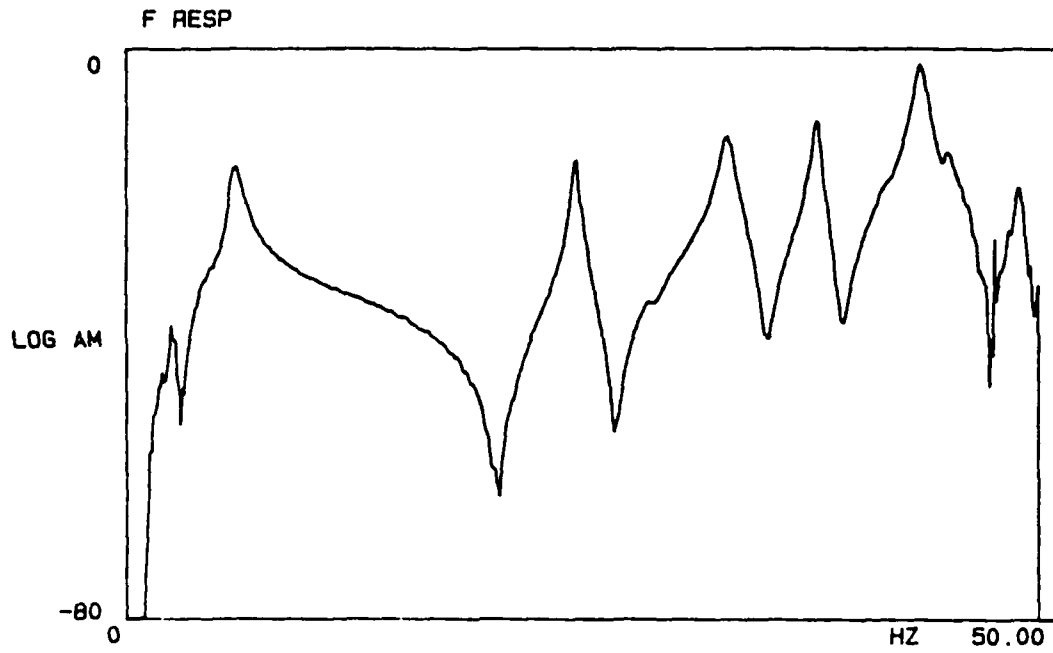


Figure 37. Frequency Response Estimate H_{11} - Dual Input Case

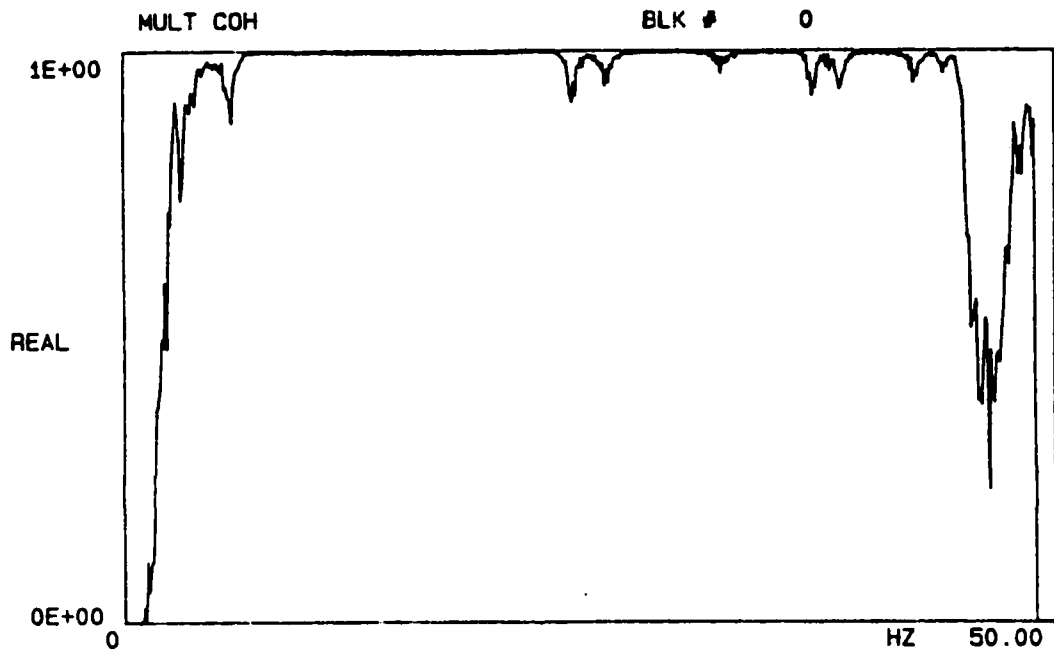


Figure 38. Multiple Coherence Function - Dual Input Case

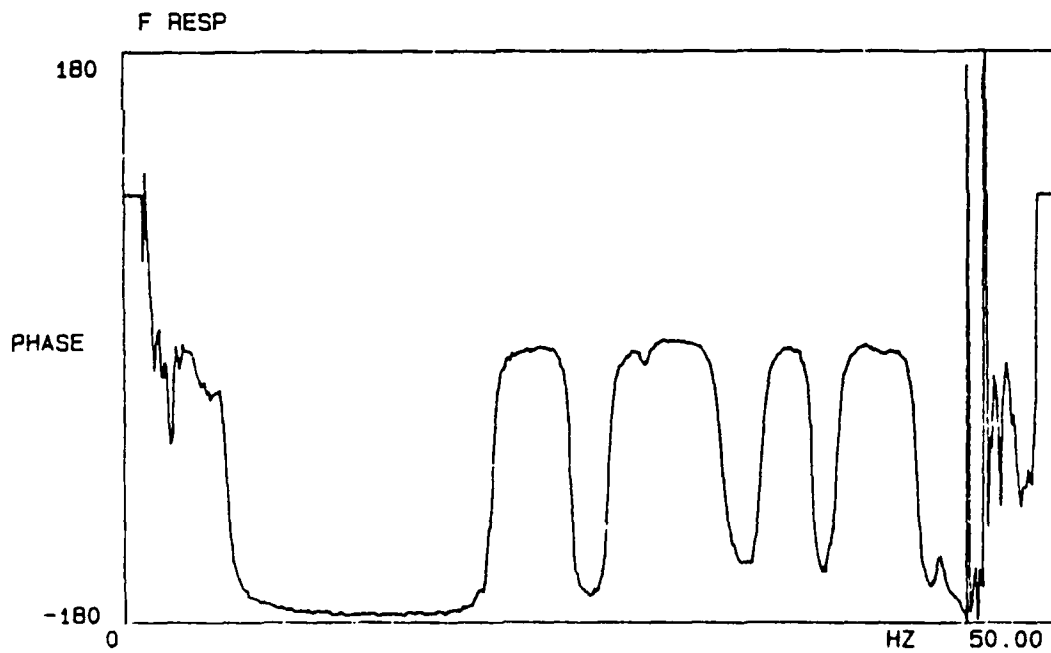
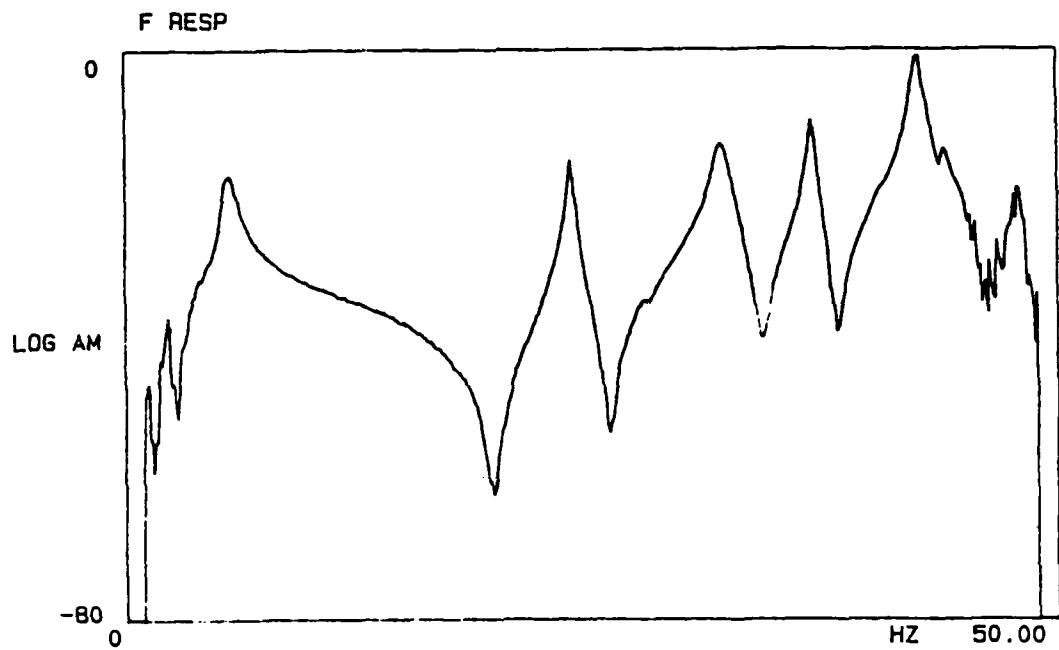


Figure 39. Frequency Response Estimate H_{11} - Three Input Case

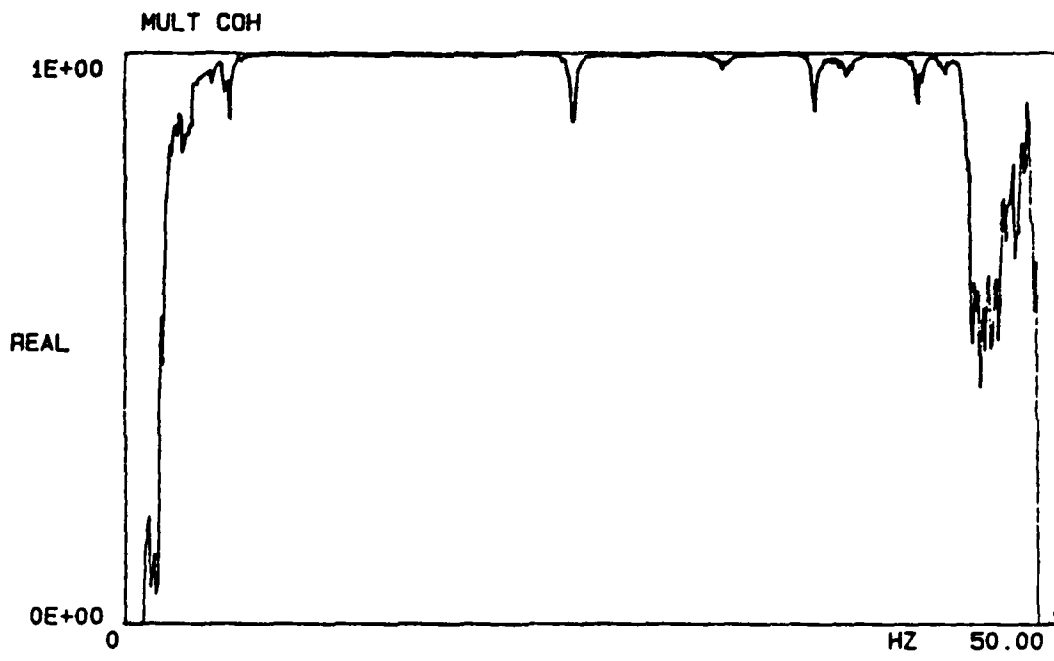


Figure 40. Multiple Coherence Function - Three Input Case

5.7 Calculation Techniques

Once the acquisition of the required auto and cross spectrum has been completed, the solution of the pertinent equations can proceed in a variety of ways. Since the H_2 technique is not practically adaptable to the multiple input technique, it will not be discussed.

It should be noted, from regression analysis, that in order to compute a direct estimate of the frequency response function, the number of averages must be equal to the number of inputs. To compute a least squares estimate of the frequency response function, the number of averages must be greater than the number of inputs.

5.7.1 H_1 Technique

5.7.1.1 Trivial Solution

Starting with Equation 11, the solution for the estimate of the frequency response function can proceed in at least 3 ways. Equation 11 is restated for clarity as Equation 38.

$$[H] = [GFX] [GFF]^{-1} \quad (38)$$

If the off diagonal terms in Equation 38 were to average to exactly zero, the solution would be exactly the same as for the single input case. This situation would occur if the inputs were totally uncorrelated. This approach was investigated but the resulting frequency response functions were of poor quality when compared to the single input case. Figure 41 shows a frequency response and coherence function that was estimated with two driven inputs, measuring only one, and using the existing single input equations. As can be seen, the data is of unacceptable quality.

5.7.1.2 Matrix Inversion

If the off diagonal terms of the input cross spectrum matrix do not average to zero, and the input cross spectrum matrix is not singular, the frequency response functions could be estimated by inversion of the input cross spectrum matrix. This approach yields no computational problems but, as the number of inputs is increased, the amount of memory needed to store intermediate results is sometimes more than is available in a mini-computer. Therefore, the results need to be stored to disk making the inversion for more than two inputs inefficient from a computer standpoint. The inversion technique is straight forward except for the need to have a generalized inversion algorithm for a variable number of inputs.

In the initial stages of the research, the inversion technique was used exclusively. As long as the ordinary coherence between forces was not exactly unity or if the determinant of the input cross spectrum matrix was not zero, Equation 38 is solvable. The input cross spectrum matrix needs to be inverted at each frequency in the analysis range and then Equations 17 and 18 were solved for the frequency response functions. This inversion of a matrix as opposed to a single input auto spectrum

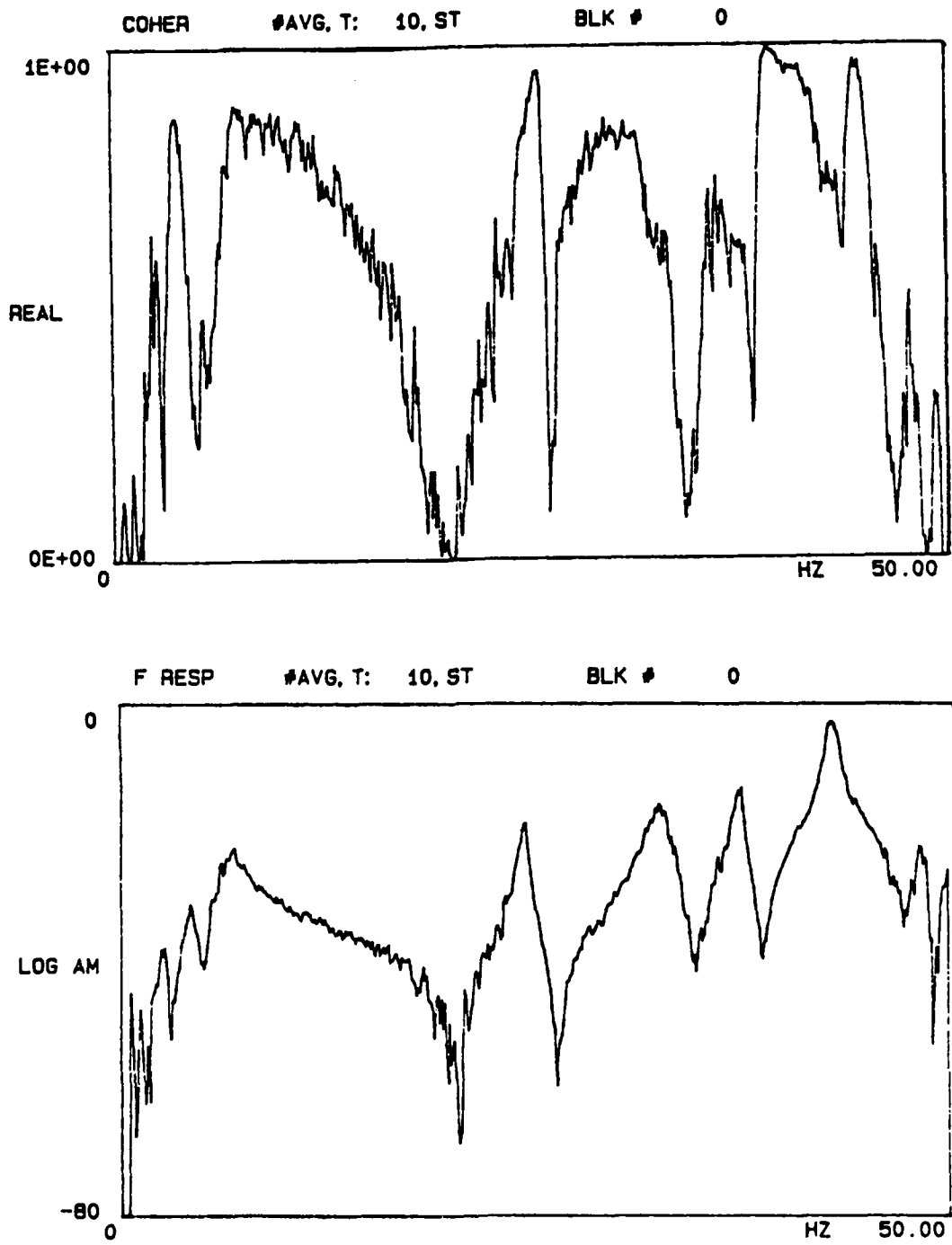


Figure 41. Frequency Response and Coherence Estimated With Two Driven Exciters but Only One Measured Force

for the single input case places an additional load on the analysis computer. As the number of inputs was increased, it became apparent, for the equipment at the University of Cincinnati Structural Dynamics Research Laboratory (SDRL), that the inversion technique would be computationally cumbersome. But, others in the field who have virtual memory mini-computers, have used the inversion technique with satisfactory results.

5.7.1.3 Gauss Elimination

As an alternative to the matrix inversion technique, an algorithm was developed based upon a Gaussian elimination approach to the solution of Equation 38. This approach was found to be well suited for the mini-computer hardware with limited memory and is often the method used within an inversion subroutine.

As an example of the algorithm, start with Equation 22 which is restated as Equation 39.

$$\begin{bmatrix} GFF_{11} & \dots & GFF_{61} \\ GFF_{12} & & GFF_{62} \\ \vdots & & \vdots \\ GFF_{16} & \dots & GFF_{66} \end{bmatrix} \begin{bmatrix} H_{p1} \\ H_{p2} \\ \vdots \\ H_{p6} \end{bmatrix} = \begin{bmatrix} GXF_{p1} \\ GXF_{p2} \\ \vdots \\ GXF_{p6} \end{bmatrix} \quad (39)$$

This equation is for the six input and one response case. The form of Equation 39 can be recognized as a set of simultaneous equations with the frequency response functions as the unknowns. The input cross spectrum matrix $[GFF]$ is well suited for a Gauss elimination procedure since the terms along the diagonal should always be positive values as well as being the largest values in the $[GFF]$ matrix. Therefore, it is not necessary to pivot during this elimination. In order to proceed, the $[GFFX_p]$ matrix is defined in Equation 40. The form of this matrix is required so that multiple coherence can be computed if required.

$$\begin{bmatrix} GFF_{11} & GFF_{21} & \dots & GFF_{61} & GXF_{p1} \\ GFF_{12} & \cdot & & \cdot & GXF_{p2} \\ \vdots & \vdots & & \vdots & \vdots \\ GFF_{16} & \cdot & & GFF_{66} & GXF_{p6} \\ GXF_{1p} & \cdot & \dots & GXF_{6p} & GFF_p \end{bmatrix} \quad (40)$$

The $[GFFX_p]$ matrix is processed by first dividing row one by GFF_{11} , multiplying by GFF_{12} and subtracting the conditioned row one from row two. Note that the superscripts refer to the number of times that the particular matrix element has been conditioned. When the conditioning is complete, the notation LFF or LXF is used.

$$LFF_{11} = \frac{GFF_{11}}{GFF_{11}} = 1 \quad (41)$$

$$LFF_{21} = \frac{GFF_{21}}{GFF_{11}} \quad (42)$$

$$GFF_{22}^1 = GFF_{22} - GFF_{12} LFF_{21} \quad (43)$$

This results in Equation 44.

$$\begin{bmatrix} 1 & LFF_{21} & \dots & LFF_{61} & LXF_{p1} \\ 0 & GFF_{22}^1 & \dots & GFF_{62}^1 & GXF_{p2}^1 \\ \vdots & \vdots & \ddots & \vdots & \vdots \\ 0 & GXF_{2p}^1 & \dots & GXF_{6p}^1 & GXX_p^1 \end{bmatrix} \quad (44)$$

Rows 3 through 7 ($i = 3 - 7$) are then conditioned by dividing each row by GFF_{11} , multiplying by GFF_{1i} , and subtracting from each element. This would result in Equation 45.

$$\begin{bmatrix} 1 & LFF_{21} & \dots & LFF_{61} & LXF_{p1} \\ 0 & \cdot & \cdot & GFF_{62}^1 & GXF_{p2}^1 \\ \vdots & \vdots & \ddots & \vdots & \vdots \\ 0 & GXF_{2p}^1 & \dots & GXF_{6p}^1 & GXX_p^1 \end{bmatrix} \quad (45)$$

Rows 3 through 7 are then conditioned in a similar manner using GFF_{22}^1 as the pivot element. When the conditioning is completed, the matrix takes on the form of Equation 46. In practice, the form of the diagonal (1) and the lower triangle (0) is known. Therefore, these elements are not actually conditioned in the algorithm but, saved in their conditioned intermediate form so that other responses collected simultaneously with this set of forces can be processed without reprocessing the $[GFF]$ portion of the $[GFFY]$ matrix.

$$\begin{bmatrix} 1 & LFF_{21} & \dots & LFF_{61} & LXF_{p1} \\ 0 & 1 & \cdot & LFF_{62} & LXF_{p2} \\ \vdots & \vdots & \ddots & \vdots & \vdots \\ 0 & & & 1 & LXY_{p6} \\ 0 & 0 & \dots & 0 & GXX_p^6 \end{bmatrix} \quad (46)$$

Once the form of Equation 46 has been achieved, the frequency response estimates can be found through back substitution using the conditioned equations as follows:

$$H_{i6} = LXF_{i6} \quad (47)$$

$$H_{i5} = LXF_{i5} - H_{i6} LXF_{65} \quad (48)$$

$$H_{i4} = LXF_{i4} - H_{i6} LXF_{64} - H_{i5} LXF_{54} \quad (49)$$

$$H_{i3} = LXF_{i3} - H_{i6} LXF_{63} - H_{i5} LXF_{53} - H_{i4} LXF_{43} \quad (50)$$

$$H_{i2} = LXF_{i2} - H_{i6} LXF_{62} - H_{i5} LXF_{52} - H_{i4} LXF_{42} - H_{i3} LXF_{32} \quad (51)$$

$$H_{i1} = LXF_{i1} - H_{i6} LXF_{61} - H_{i5} LXF_{51} - H_{i4} LXF_{41} - H_{i3} LXF_{31} - H_{i2} LXF_{21} \quad (52)$$

From the form of the [GFFY] matrix, either before, during, or after conditioning, the ordinary, conditioned, and multiple coherence functions as defined in Section 6 can be calculated. The multiple coherence function can be redefined as in Equation 53.

$$MCOH_p = \frac{GXX_p^6}{GXX_p} \quad (53)$$

An added benefit of the Gauss Elimination procedure is that the conditioned terms may be left in the lower half of the input cross spectra matrix. Therefore, if more than one response is measured simultaneously, the input cross spectra matrix is only conditioned once for those responses. Each response is then used to estimate frequency response functions with those forces. This can greatly reduce computation time. For the next measurement cycle, the input cross spectra matrix is again conditioned and the next set of responses is used.

Both the inversion technique and the Gauss Elimination techniques have been used with equal results at the UC-SDRL. The actual numerical procedure is often a function of the hardware involved.

6. MULTIPLE INPUT CONSIDERATIONS

From the theory in Section 5, the equations for the computation of the frequency response functions all require that the input cross spectra matrix $[GFF]$ not be singular^[1-3,25-30]. Unfortunately, there are a number of situations where the input cross spectra matrix $[GFF]$ may be singular at specific frequencies or frequency intervals. When this happens, the equations for the frequency response functions cannot be used to solve for unique frequency response functions at those frequencies or in those frequency intervals even though the equations are still valid.

One potential reason for the input cross spectra matrix $[GFF]$ to be singular is when one or more of the input force auto power spectrum is zero at some frequency or some frequency interval. If an input has a zero in the auto power spectrum, the associated cross spectrums calculated with that force will also have zeros at the same frequency or frequency interval. The primary reason for this to occur would be because of an impedance mismatch between the exciter system and the system under test. Unfortunately, this situation occurs at system poles that have a low value of damping where a good estimate of the frequency response is desired. Therefore, it is imperative to check the input cross spectra matrix for zeros. For the two input case where the determinant is calculated, a good check is to be sure that the determinant does not have zeros in it.

Another way that the input cross spectra matrix may be singular is if two or more of the inputs are totally coherent at some frequency or over some frequency interval. A good method to check for coherent forces is to compute the ordinary and conditioned partial coherence functions among the inputs^[25-30]. A technique is also presented in Section 6.2.2 that computes the principal auto power spectra of the input forces^[48]. This technique uses an eigenvalue decomposition to determine the dimensionality of the input cross spectra matrix $[GFF]$. If two of the inputs are fully coherent, then there are no unique frequency response functions associated with those inputs at those frequencies even though the Equation 11 is still valid. This is because the frequency response is now estimated using a singular matrix that will yield infinite solutions that are combinations of each other. Although the signals used as inputs to the exciter system are uncorrelated random signals, the response of the structure at resonance, combined with the inability to completely isolate the exciter systems from this response will result in the ordinary or conditioned partial coherence functions to have values other than zero, particularly, at the system poles. As long as the coherence functions are not unity at any frequency, the equations will give a correct estimate of the frequency response function. It is therefore necessary to have a method to evaluate the inputs to assure that there are neither holes in the auto power spectrum nor perfectly coherent inputs.

6.1 Optimum Number Of Inputs

When considering the estimation of frequency response functions in the presence of multiple inputs, more time must be spent to determine the number of inputs, the input directions, and the input locations.

An advantage of the multiple input technology is that, for most structures, all important modes can be excited in one test cycle. For example, in a typical test of an aircraft structure, if existing single input technology is used, at least two complete tests must be conducted in order to get sufficient energy into both the vertical and lateral fuselage modes. If two symmetric, correlated inputs with zero or 180 degree phase difference are used, even though the number of degrees of freedom that the parameter estimation algorithm must deal with is reduced, at least two complete tests must also be conducted to define all the modes of the structure. With uncorrelated random multiple inputs, since there is no constraint on the input directions, one input could be vertical and the other horizontal. In

this way, both the vertical and lateral modes will be excited in the same test cycle. By exciting at symmetric locations, the frequency response estimates can be added or subtracted to enhance in phase and out of phase modes. Since the original frequency response estimates are not destroyed, effectively, four pieces of useful information have been estimated for the structure under test in one test cycle.

But, as the number of inputs is increased, so too is the potential for problems with the excitation forces. One such problem is that, due to the structural response, the inputs may be correlated by one or more exciters driving the other exciters. This happens most often if the exciters are placed at locations that have a high amplitude of motion particularly at resonance. Also, depending on the size of the structure, there is a diminishing return on more inputs. The advantage of two inputs to one input has been apparent in almost every test case. For more than two inputs, particularly on smaller structures, the added inputs mean that more averages must be taken to compute "clean" frequency response functions. In practice, fighter aircraft have been tested with as many as six inputs with no adverse effects. For automobiles, three inputs appears to be a practical limit.

6.2 Input Evaluation

Let F_1, \dots, F_{N_i} represent the spectra of N_i input forces at a particular frequency. The input forces are correlated at this frequency when the input cross spectra matrix $[GFF]$, defined by Equation 54 is singular.

$$[GFF] = \begin{bmatrix} GFF_{11} & \dots & GFF_{N_i,1} \\ \vdots & & \vdots \\ GFF_{1N_i} & \dots & GFF_{N_i,N_i} \end{bmatrix} \quad (54)$$

Where:

$$GFF_{ik} = GFF_{ki}^* \text{ (Hermitian Matrix)}$$

$$GFF_{ik} = \sum F_i F_k^*$$

6.2.1 Coherence Functions

The ordinary coherence function measures the degree of linear dependence (or correlation) between the spectra of two signals. The partial coherence function measures the degree of linear dependence between the spectra of two signals, after eliminating in a least squares sense, the contribution of some other signals. Both functions can be used in systematic procedure to verify that the forces are not correlated or that the input cross spectra matrix $[GFF]$ is not singular.

The ordinary coherence function between any input i and any other input k can be defined by Equation 55. If F_i and F_k are linearly dependent at any frequency, then COH_{ik} equals 1.0 at that frequency and a unique frequency response functions cannot be computed at that frequency even though the equations are still valid. If the coherence function is any value other than 1.0, the inputs are not correlated and the frequency response functions can be calculated.

$$COH_{ik} = \frac{|GFF_{ik}|^2}{GFF_{ii} GFF_{kk}} \quad (55)$$

Where:

- GFF_{ik} = Cross power spectrum between inputs i and k
- GFF_{ii} = Auto power spectrum of input i
- GFF_{kk} = Auto power spectrum of input k

Next consider F_1 as a reference spectrum, and eliminate from $F_2 \dots F_{N_1}$, in a least squares sense, all linear dependence on F_1 . For F_2 the pertinent equations are Equation 56 and Equation 57.

$$F_2^1 = F_2 - L_{21} F_1 \quad (56)$$

$$L_{21} = \frac{GFF_{12}}{GFF_{11}} \quad (57)$$

In these equations, F_2^1 represents what is left from F_2 after eliminating the linear dependence on F_1 in a least squares sense. The superscripts refer to the number of times a particular element has been conditioned. The auto power spectrum of F_2^1 represented by GFF_{22}^1 , can be calculated from Equation 58 or Equation 59. This equation also defines the first step of a Gauss elimination on the input cross spectra matrix $[GFF]$ applied to element GFF_{22} . If COH_{12} equals 1.0, then from Equation 59 GFF_{22}^1 equals 0.0; a zero diagonal element is generated during the first step of the Gauss elimination on the input cross spectra matrix $[GFF]$. Therefore, the input cross spectra matrix $[GFF]$ is singular and F_1 and F_2 are correlated.

$$GFF_{22}^1 = GFF_{22} - \frac{|GFF_{12}|^2}{GFF_{11}} \quad (58)$$

$$GFF_{22}^1 = GFF_{22} (1 - COH_{12}) \quad (59)$$

If COH_{12} is smaller than 1.0, F_1 and F_2 are not linearly dependent. Next consider F_2^1 as the reference spectrum and eliminate out of $F_3 \dots F_{N_1}$ all linear dependence on F_2^1 . This yields Equation 60 and Equation 61.

$$F_3^2 = F_3^1 - L_{32} F_2^1 \quad (60)$$

$$L_{32} = \frac{GFF_{23}^1}{GFF_{22}^1} \quad (61)$$

The partial coherence function between F_2^1 and F_3^1 , COH_{23}^1 is defined by Equation 62. If the partial coherence is equal to 1, then F_2^1 and F_3^1 are linearly dependent.

$$COH_{23}^1 = \frac{|GFF_{23}^1|^2}{GFF_{22}^1 GFF_{33}^1} \quad (62)$$

From Equation 63 or Equation 64 it follows that GFF_{33}^2 is 0.0, implying that the input cross spectra matrix $[GFF]$ is singular and that $F_2 \dots F_{N_i}$ are correlated. If COH_{23}^1 is less than 1.0, then F_3^2 can be taken as the next reference spectrum. Sequentially, then, a total of N_i-1 functions is generated. If COH_{12} or any $COH_{k+1, k+2}^k$, defined by Equation 65, equals 1.0 then the input cross spectra matrix $[GFF]$ is singular and the input forces are correlated at that frequency and unique frequency response functions cannot be calculated at that frequency.

$$GFF_{33}^2 = GFF_{33}^1 - \frac{|GFF_{23}^1|^2}{GFF_{22}^1} \quad (63)$$

$$GFF_{33}^2 = GFF_{33}^1 (1 - COH_{23}^1) \quad (64)$$

$$COH_{k+1, k+2}^k = \frac{|GFF_{k+1, k+2}^k|^2}{GFF_{k+1, k+1}^k GFF_{k+2, k+2}^k} \quad (65)$$

$$k = 1, 2, \dots, m-2$$

6.2.1.1 Vector Representation

To better visualize the concept of ordinary and partial coherence, the inputs can be represented by vectors at any frequency. Figure 42 shows a three input case where the inputs at a given frequency are represented by three vectors.

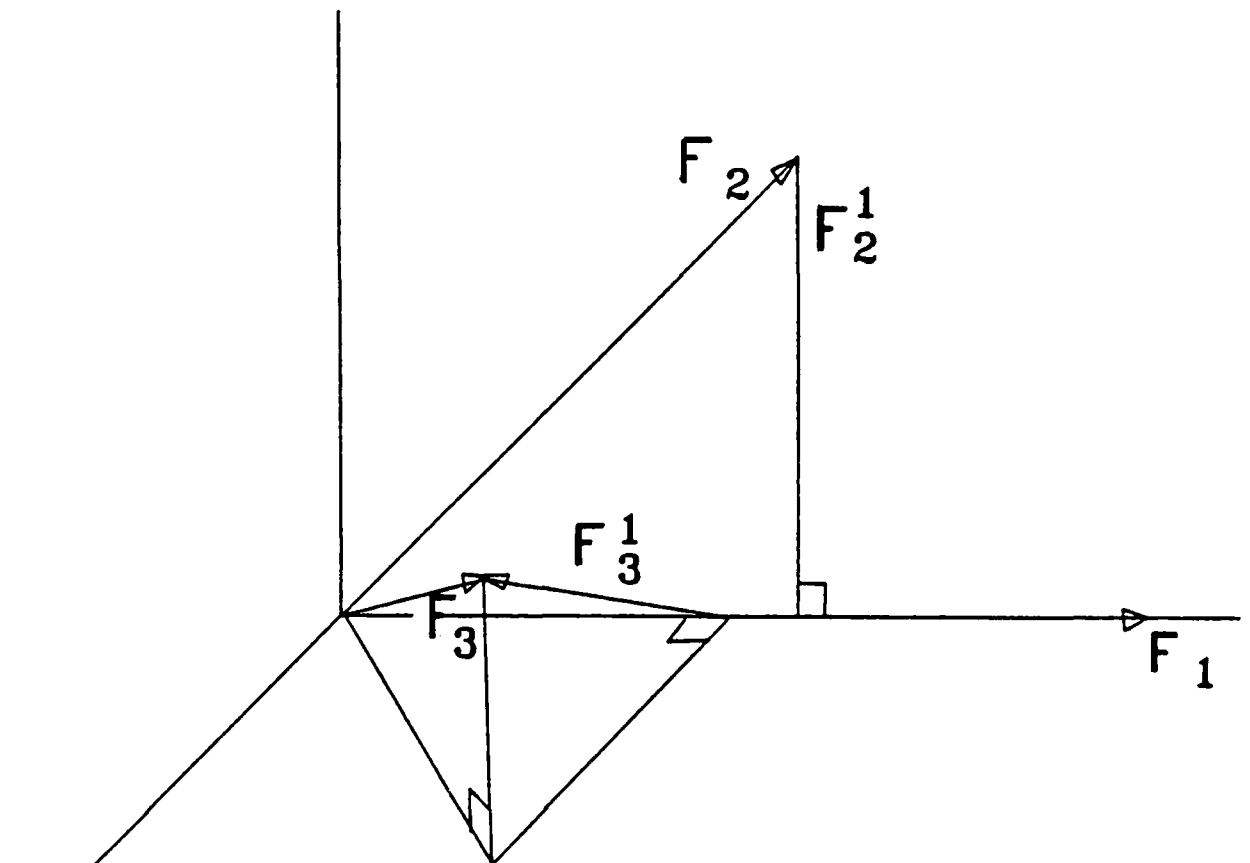
By considering F_1 as the reference spectrum, the ordinary coherence between inputs 1 and 2 and between inputs 1 and 3 can be defined as:

$$COH_{12} \approx \frac{F_{21}}{F_2} \quad (66)$$

$$COH_{13} \approx \frac{F_{31}}{F_3} \quad (67)$$

Where F_{21} is the perpendicular distance of the projection of F_2 on F_1 and F_{31} is the perpendicular distance of the projection of F_3 on F_1 . This is equivalent to eliminating F_1 from F_2 and F_3 . Therefore, if either F_2 or F_3 was in the same direction as F_1 , the perpendicular distance divided by the original length would be 1 indicating perfect correlation. If the vectors were at right angles, the value would be zero, indicating no correlation.

Next, the vectors F_2^1 and F_3^1 , which are the part remaining after eliminating F_1 , are used to compute



$$\text{COH}_{12} = .71$$

$$\text{COH}_{13} = .70$$

Figure 42. Three Inputs As Vectors - F_1 Used As The Reference

the conditioned partial coherence. Figure 43 shows these two vectors.

The partial coherence between inputs 2 and 3 after eliminating input 1 is defined as:

$$COH_{23}^1 = \frac{F_{32}^1}{F_3^1} \quad (68)$$

This is equivalent to finding the perpendicular distance of the projection of F_3^1 on F_2^1 .

To demonstrate that the order of conditioning has an effect on the magnitude of the coherence, the three forces are shown again in Figure 44, now using F_2 as the reference vector. The ordinary coherence between inputs 2 and 1 and between inputs 2 and 3 are now defined by Equations 69 and 70.

$$COH_{21} = \frac{F_{12}}{F_1} \quad (69)$$

$$COH_{23} = \frac{F_{32}}{F_3} \quad (70)$$

Next, the vectors F_1^1 and F_3^1 , which are the part remaining after eliminating F_2 , are used to compute the conditioned partial coherence. Figure 45 shows these two vectors.

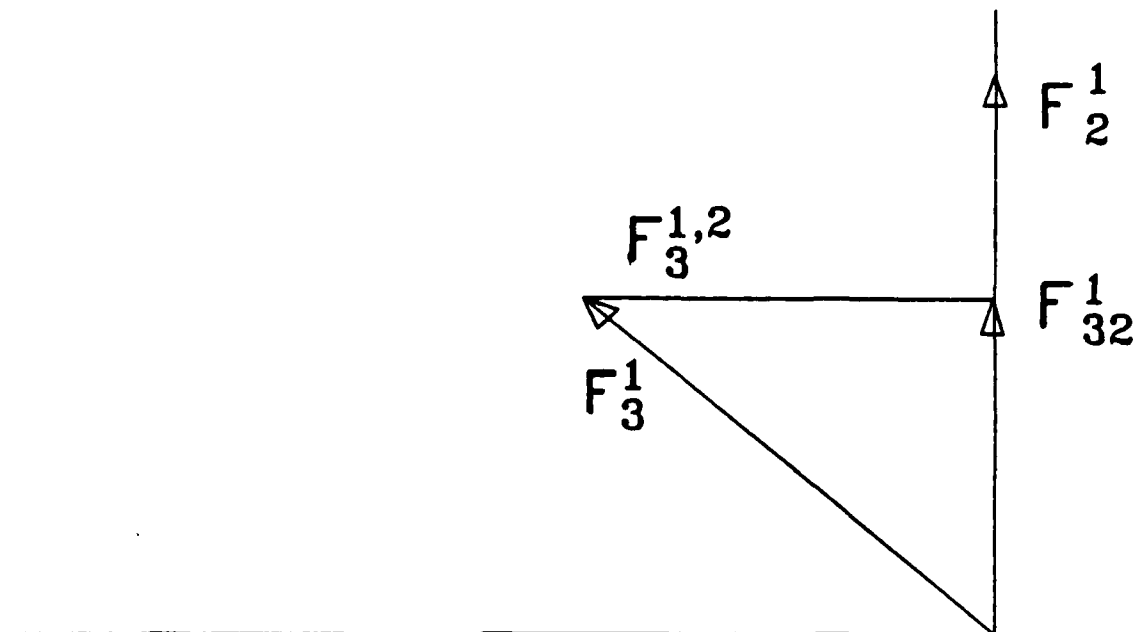
The partial coherence between inputs 1 and 3 after eliminating input 2 is defined as follows.

$$COH_{13}^1 = \frac{F_{31}^1}{F_3^1} \quad (71)$$

As can be seen by comparing Figures 42 through 45, the values of the coherence functions are different for the different conditioning sequence.

6.2.2 Principal Input Forces

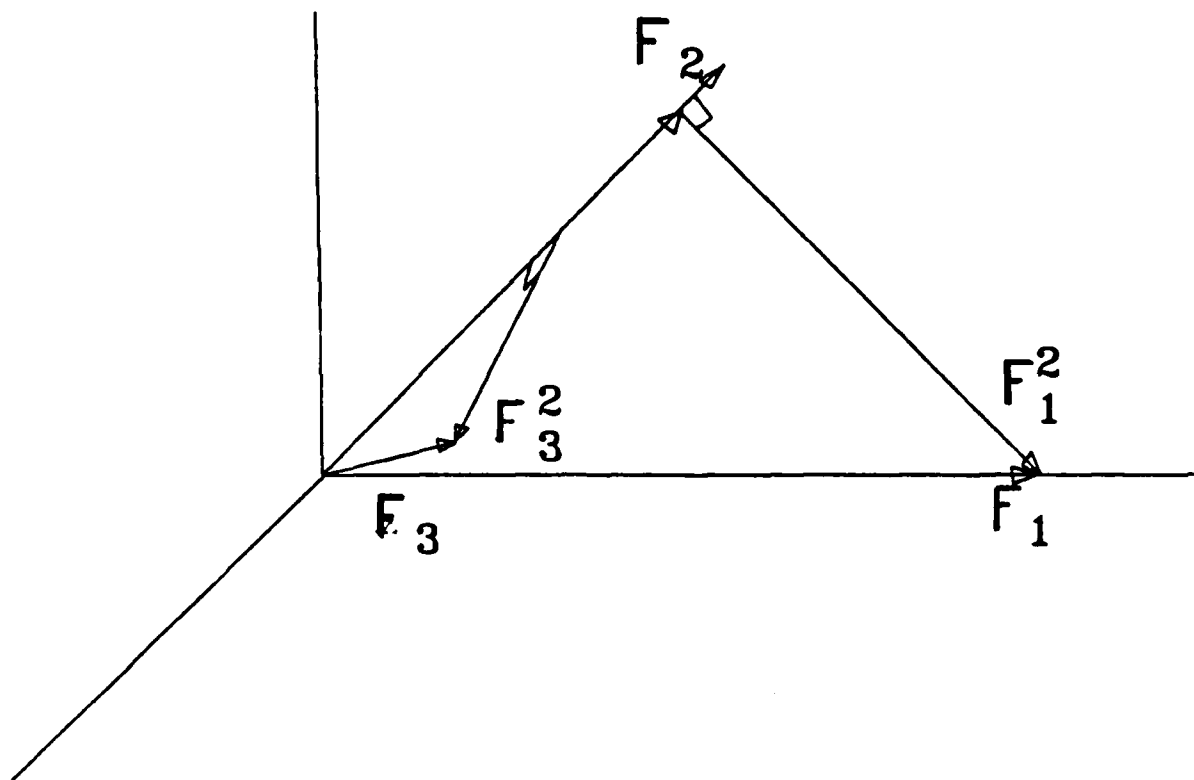
A more critical and concise technique can be formulated if $F_1 \dots F_{N_i}$ represent the spectra of N_i independent, fully non-correlated input forces from which the spectra of the measured input forces can be derived by linear combinations, as shown by Equation 72. The input cross spectra matrix $[GFF]$ can now be expressed by Equation 73. $[GFF]$ is a diagonal matrix with the auto power spectra of the principal forces on the diagonal; the diagonal elements are referred to as the principal auto power spectra.



$$\text{COH}_{23}^1 = .64$$

$$X_3^{1,2} = .42$$

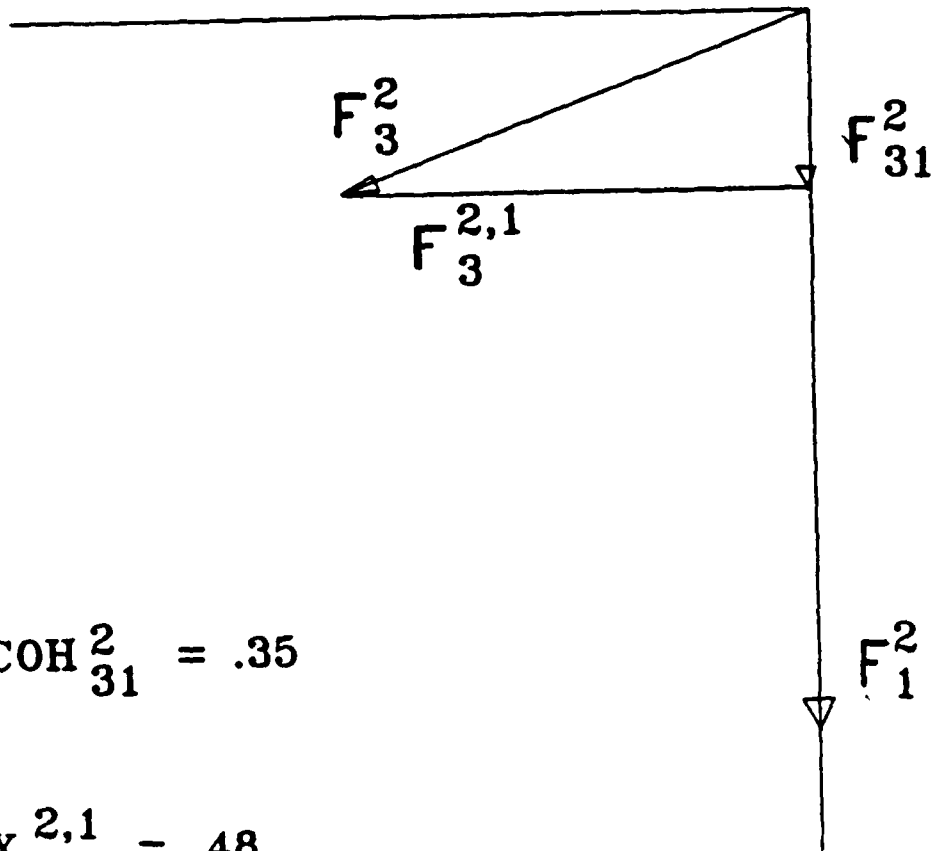
Figure 43. Remaining Vectors - F_1 Used As The Reference



$$\text{COH}_{21} = .71$$

$$\text{COH}_{23} = .69$$

Figure 44. Three Inputs As Vectors - F_2 Used As The Reference



$$\text{COH}_{31}^2 = .35$$

$$X_{31}^{2,1} = .48$$

Figure 45. Remaining Vectors - F_2 Used As The Reference

$$[F_1 \dots F_{N_i}] = [F_{\cdot 1} \dots F_{\cdot N_i}] [U] \quad (72)$$

$[U]$: complex matrix, dimension $m \times m$

$$GFF_{\cdot ik} = \sum F_{\cdot i} * F_{\cdot k} = 0 \quad i=k$$

$$[GFF] = [U]^H [GFF_{\cdot}] [U] \quad (73)$$

Notice that Equation 73 defines the eigenvalue decomposition of the input cross spectra matrix $[GFF]$. From this point of view, $[GFF_{\cdot}]$ represents the eigenvalues and $[U]$ the eigenvectors of the input cross spectra matrix $[GFF]$. This eigenvalue decomposition is always defined since the input cross spectra matrix $[GFF]$ is Hermitian. The eigenvectors are independent, so that $[U]$ is not singular. Therefore, when some of the eigenvalues of the input cross spectra matrix $[GFF]$ are 0, or negligible, then the input cross spectra matrix $[GFF]$ is singular. Or, in other words, when some of the principal auto power spectra are negligible and therefore the corresponding principal input forces insignificant, then the measured input forces are correlated.

This procedure is similar to transforming the inertia matrix of a structure to the principal moments of inertia or to transforming the stress tensor to the principal stress direction.

6.3 Examples

To investigate the potential of the ordinary and partial coherence, the determinant, and the principal input forces to detect the presence of either zero's in the auto power spectrum of the forces or to detect correlated forces, it is again beneficial to start with the dual input case. Again, the data were collected from the body-in-white using the same input locations as in Figure 34. In some of the data in this section, potential failures in the data collection were purposely introduced into the estimation of the frequency response function.

Figure 46 shows the ordinary coherence function between the input forces for the two input case. As can be seen, the highest degree of correlation is at the rigid body bounce mode. But, because the correlation is below unity, the frequency response function can still be estimated uniquely at all frequencies in the frequency range of interest.

Figure 47 shows the principal auto power spectra of the same input forces. Since there are two spectra, each of significant value, there is little correlation between the forces. But, at the rigid body bounce mode, the second spectra has a fairly significant drop. This indicates the same correlation as the ordinary coherence function at the same frequency.

To check for zeros in the input auto power spectrum, either the auto power spectra themselves may be checked, or the value of the determinant of the input cross spectra matrix may be checked. Figure 48 shows the two input auto power spectrums. The auto power spectra are both flat with no significant drops. Figure 49 is the determinant of the input cross spectra matrix. This function also has no significant drop. These functions indicate that there are no zeros in the auto power spectra. Therefore, the frequency response functions can be estimated for the entire frequency range of interest. Figure 50 shows the frequency response estimates.

Next, one exciter system was turned off, simulating an exciter system failure during the test. Since the

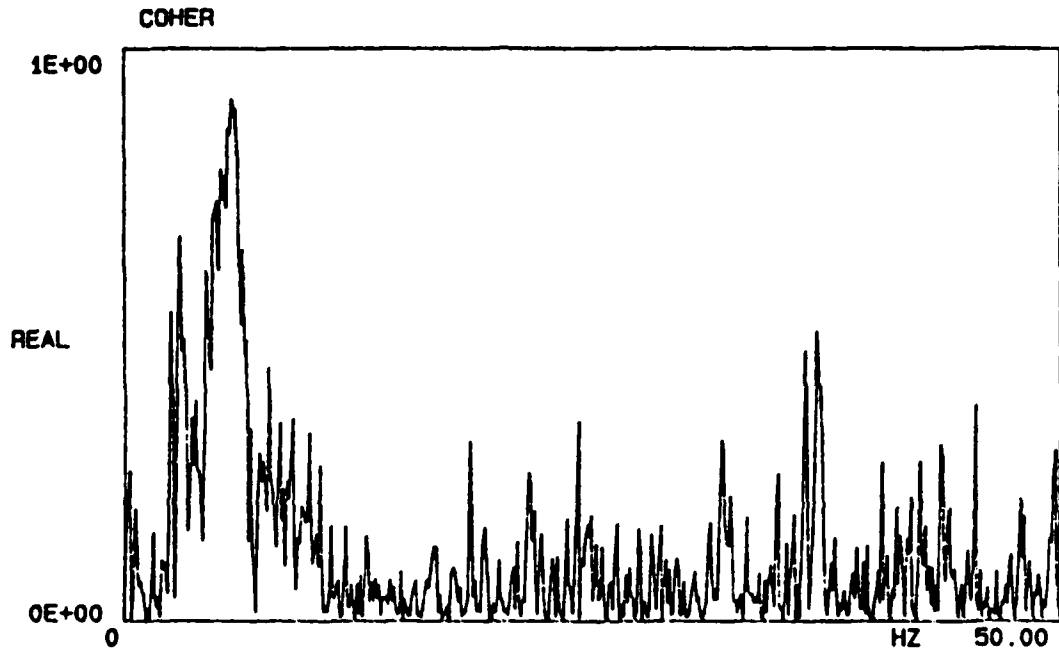


Figure 46. Ordinary Coherence Function Between Forces Dual Input Case

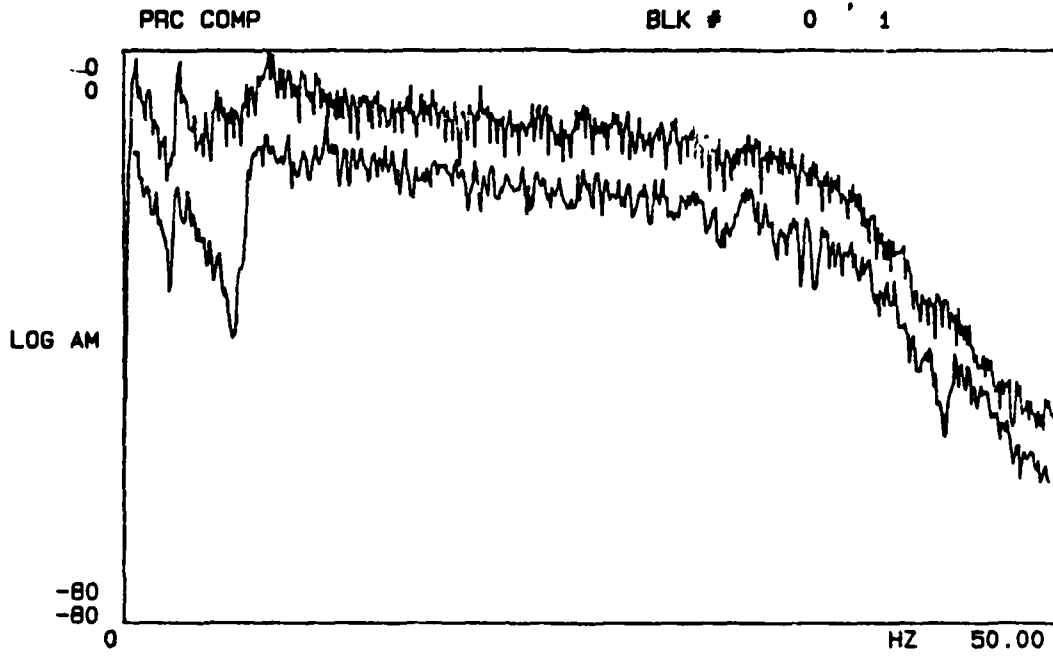


Figure 47. Principal Auto Power Spectra of Input Forces Dual Input Case

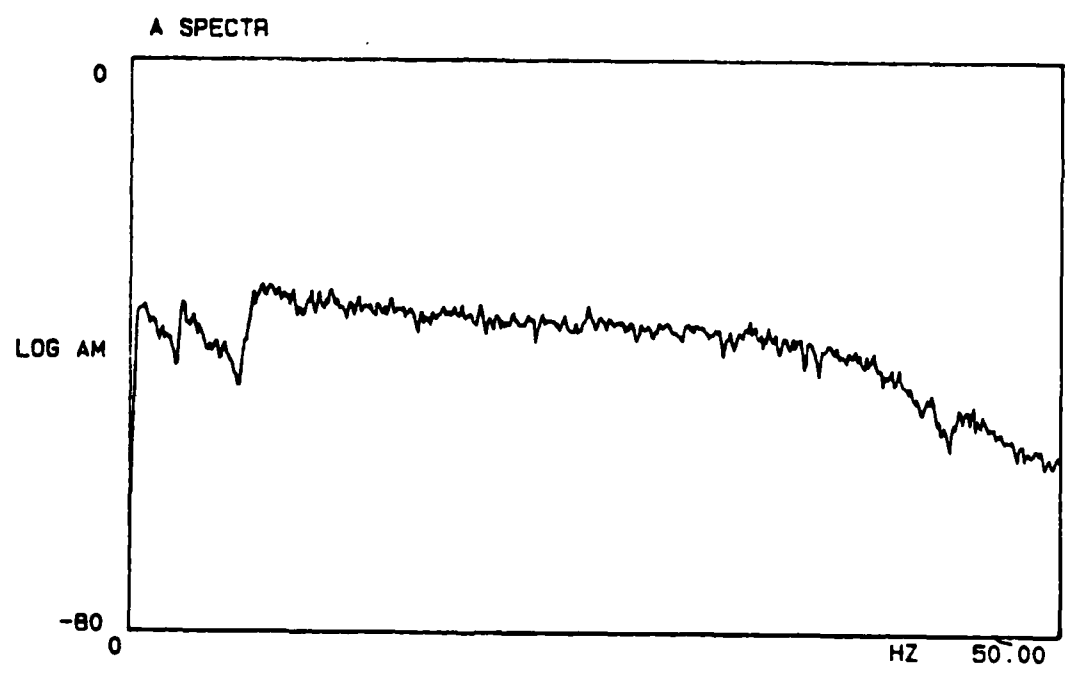
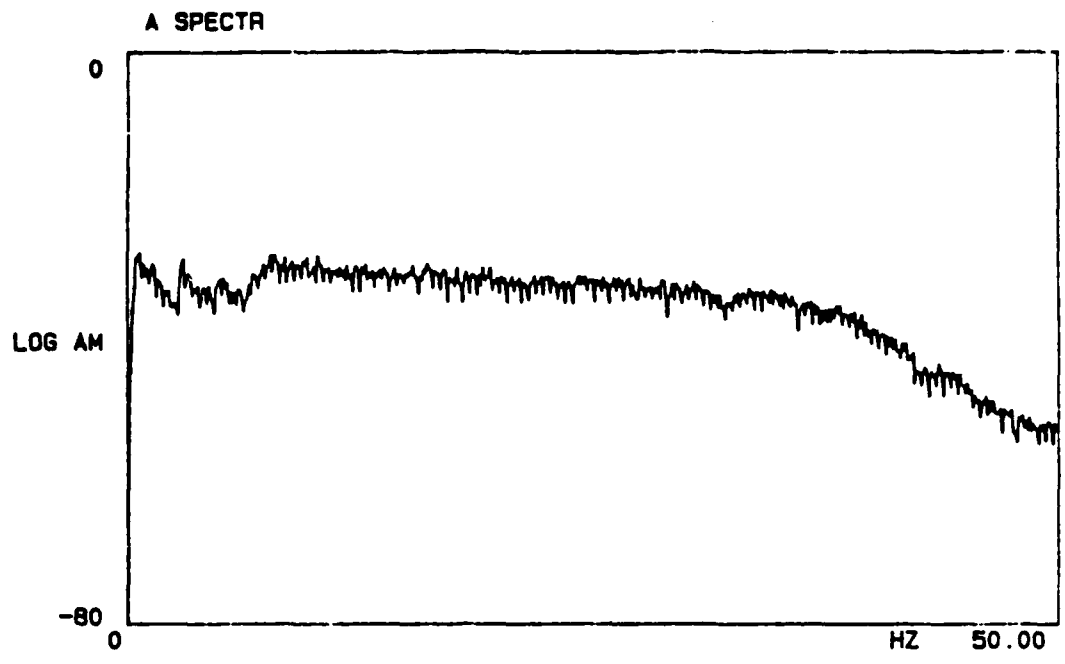


Figure 48. Input Auto Power Spectrum Dual Input Case

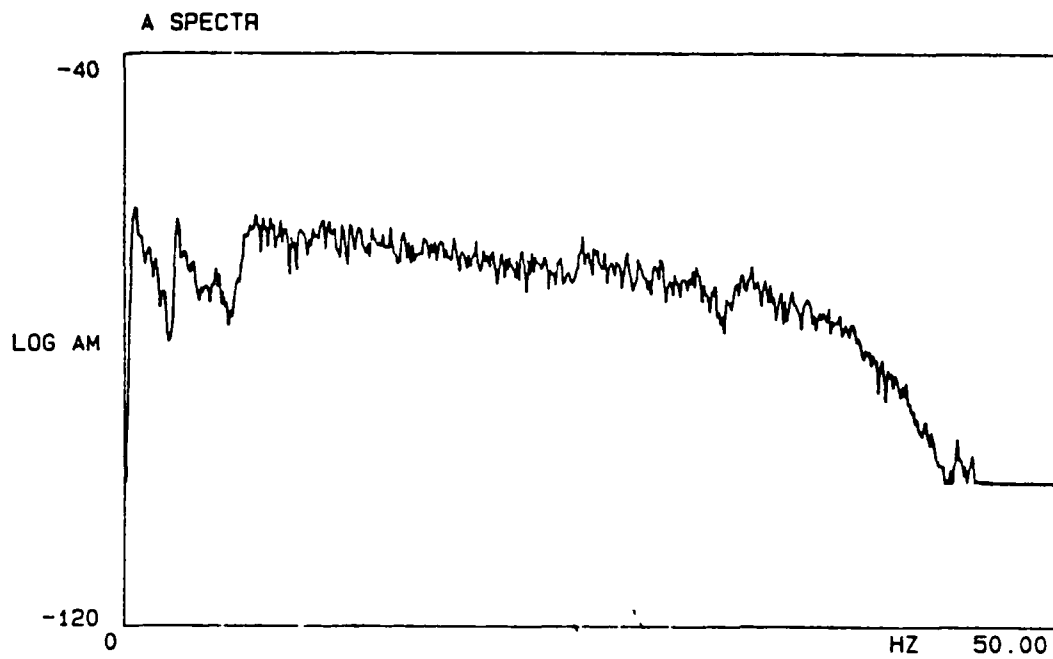


Figure 49. Determinant of Input Cross Spectrum Matrix Dual Input Case

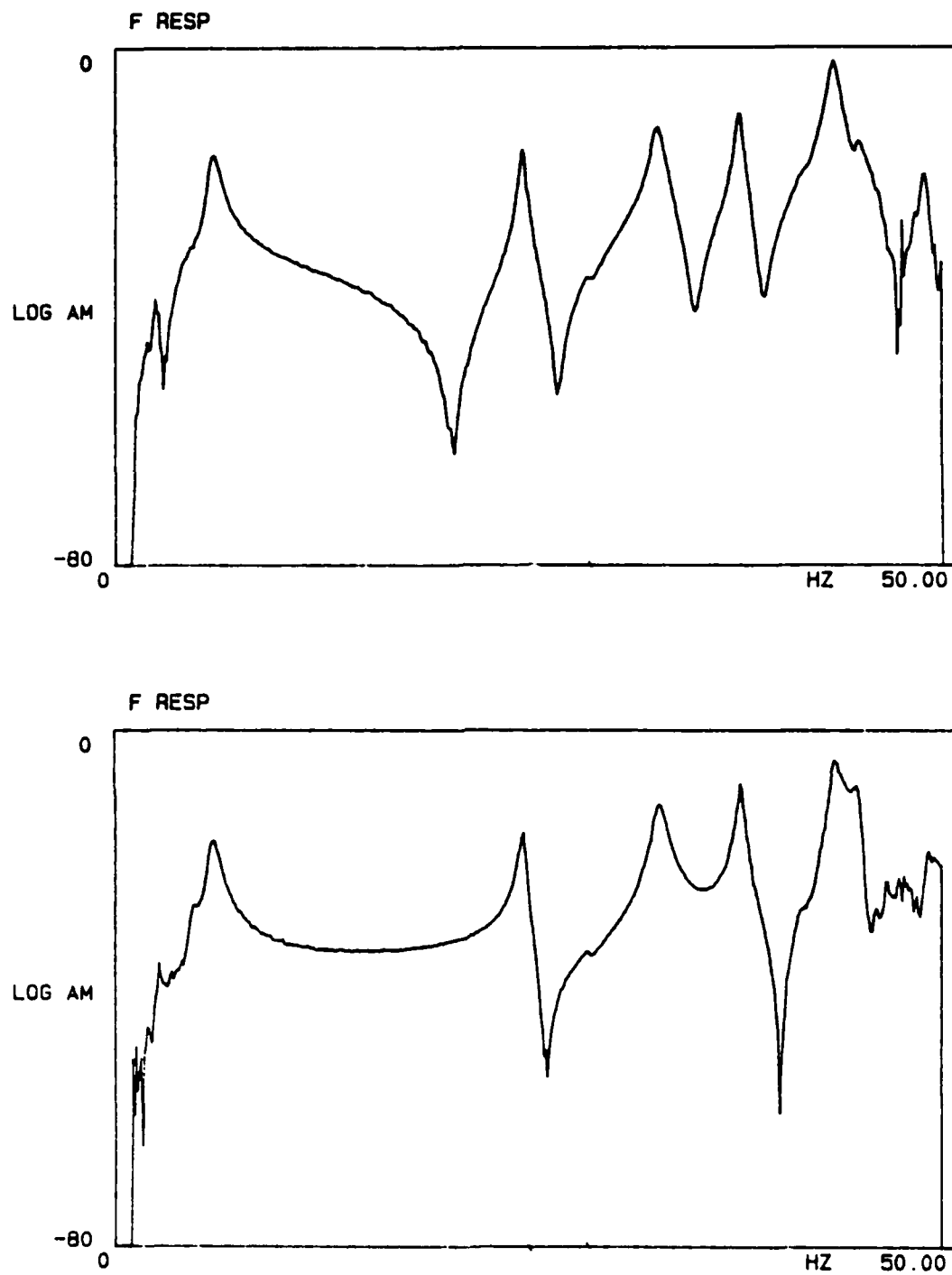


Figure 50. Frequency Response Estimates Dual Input Case

load cell was still attached to the system, that load cell measured a force that was caused by the motion of the structure due to the other exciter. The measured force will look similar to an acceleration signal, since the load cell, with the mass of the structure on top of it, will be similar to an accelerometer. Figure 51 shows the input auto power spectra of the forces. The top function is for the input that was driven. The bottom is for the input that had the shaker turned off. The top function is similar to the previous auto power spectrum. The bottom function, much lower in magnitude, shows the location of resonances, similar to an auto power spectrum of acceleration.

Figure 52 shows the ordinary coherence function between these two signals. The function is unity at many locations and approaches unity at most frequencies. This function should look like the function in Figure 46. Figure 53 is the principal auto power spectra for this case. There is now only one spectra that has significant value indicating one independent force. Figure 54 is the determinant function which is much lower in value than the function in Figure 49 and also has many zero's. Figure 55 is the estimate of the frequency response functions for this case.

The general form of a frequency response function can be seen in these functions but, the data is of unacceptable quality.

To show the problems with correlated inputs, the same signal was used to drive both exciter systems. Figure 56 shows the input auto power spectra of the two input forces. Because of the difference in the impedance at the two locations, the auto power spectra appear different. Therefore, there is no way to detect correlation by looking at the auto power spectra.

Figure 57 shows the ordinary coherence function between these two forces. The value of the ordinary coherence function is unity throughout virtually the entire data block. Figure 58 is the principal auto power spectra for the same case. Again, there is only one spectra of significant value in this function. Figure 59 shows the frequency response estimates for this case. Again, these are of unacceptable quality. For the three input case, the value of the coherence functions and the principal input spectra becomes more obvious. As the number of inputs increase, so too do the number of functions. It is important to realize that the order of removal has an effect on the value of the partial coherence functions.

First, a three input case with all shakers operable was used. Figure 60 shows the ordinary coherence function between input 1 and input 2. The function shows some correlation at the rigid body bounce mode but is not unity at any frequency in the range of interest. Figure 61 shows the conditioned partial coherence function between input 2 and input 3 with the effects of input 1 removed. This function also shows no correlation between forces. Figure 62 shows the principal auto power spectra of input forces. There are three spectra of significant value indicating three, uncorrelated forces. Therefore, the frequency response functions can be estimated.

To demonstrate the difficulty of interpretation of the coherence functions and the conciseness of the principal forces, the signal to input 2 was turned off but the load cell was left on. Figure 63 shows the ordinary coherence function between input 1 and input 2. Figure 64 shows the conditioned partial coherence function between input 2 and input 3 with the effects of input 1 removed. Figure 65 is the principal auto power spectra of inputs. All three functions show that there is correlation between forces. The coherence functions indicate correlation by the fact that they are unity for a good portion of the data block. The principal auto power spectra by the fact that there are only two spectra of significant value.

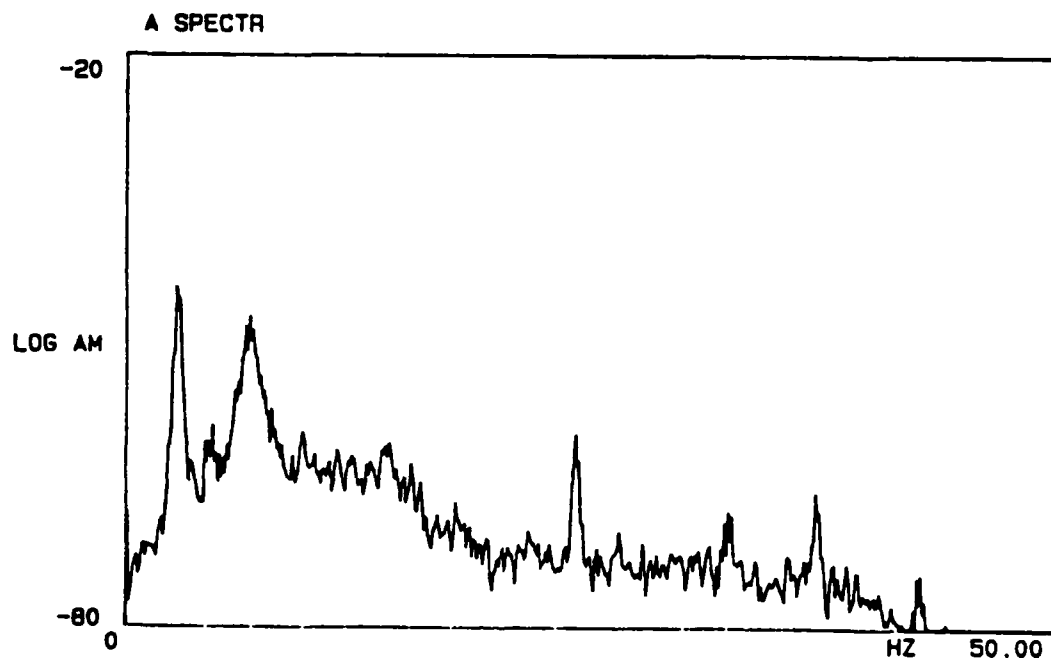
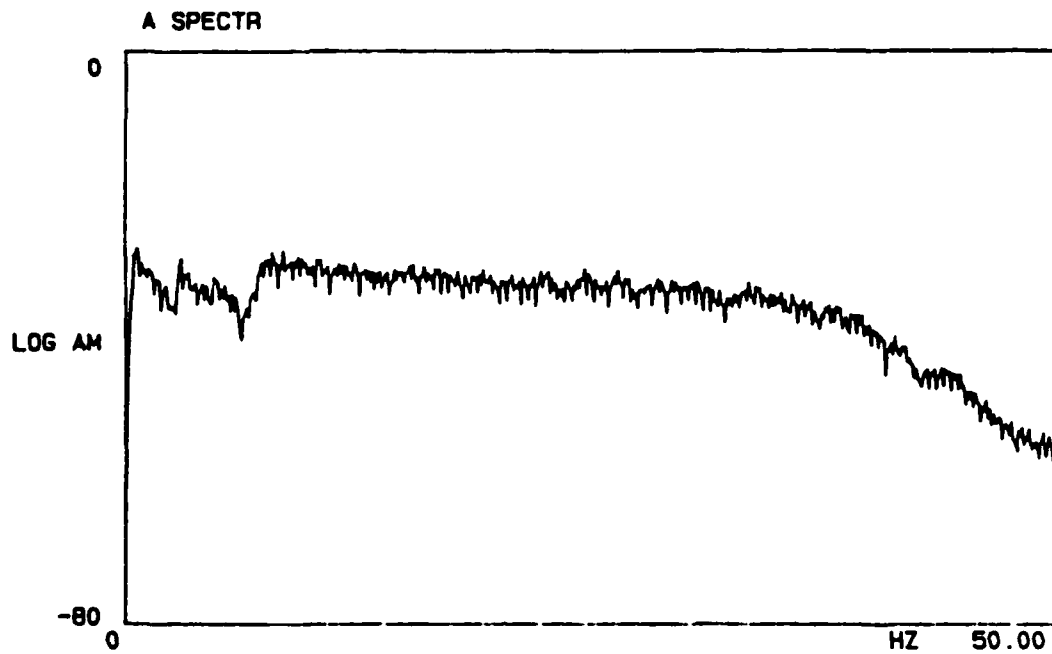


Figure 51. Input Auto Power Spectrum, One Input Not Driven, Dual Input Case

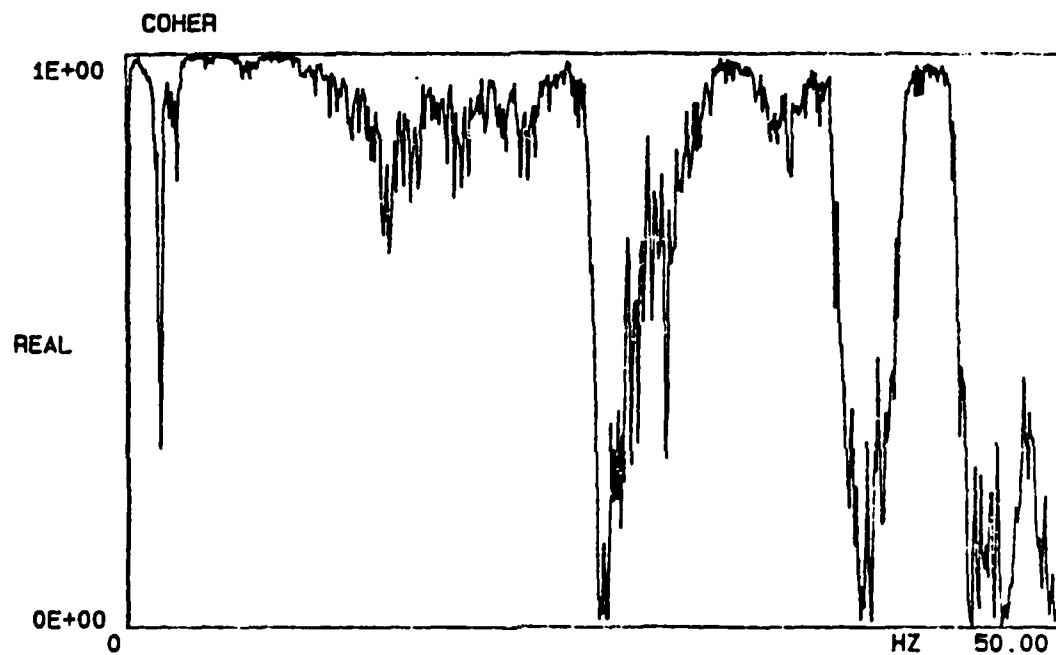


Figure 52. Ordinary Coherence Function Between Forces One Input Not Driven, Dual Input Case

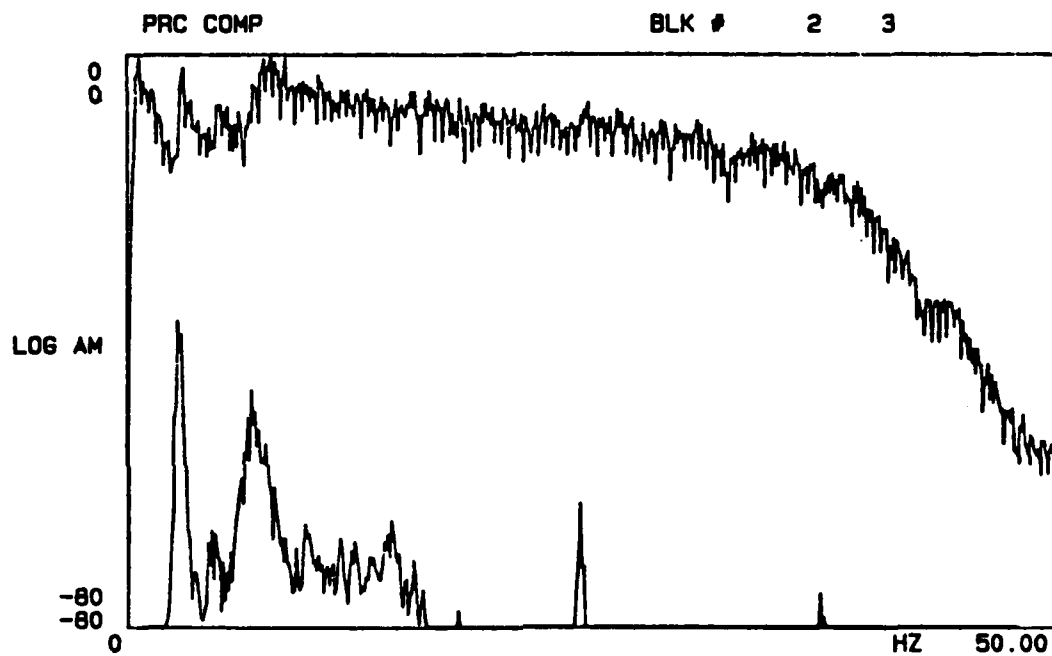


Figure 53. Principal Auto Power Spectra of the Input Forces, One Input Not Driven, Dual input Case

Next, input 2 was made active and the signal to input 3 was turned off. Figure 66 shows the ordinary coherence between input 1 and input 2. Figure 67 shows the conditioned partial coherence function between input 2 and input 3 with the effects of input 1 removed. Figure 68 is the principal auto power spectra for this case. The ordinary coherence between input 1 and input 2 shows no potential problems with correlation. But, the conditioned partial coherence show a definite correlation between inputs. This is also seen in the principal auto power spectra because there is only two spectra of significant value.

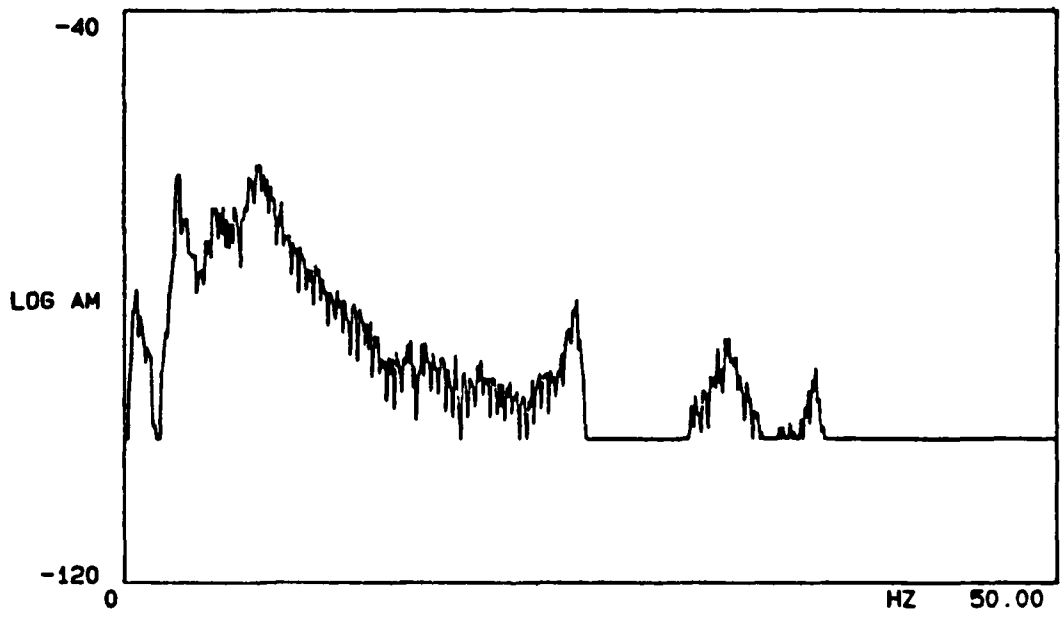


Figure 54. Determinant Function, One Input Not Driven, Dual Input Case

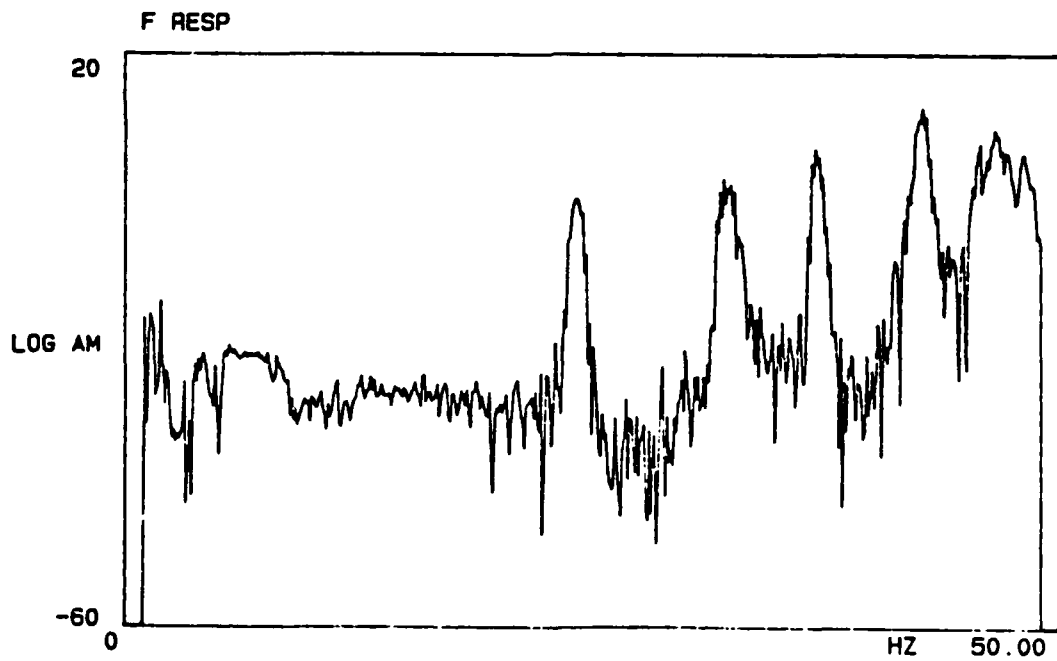
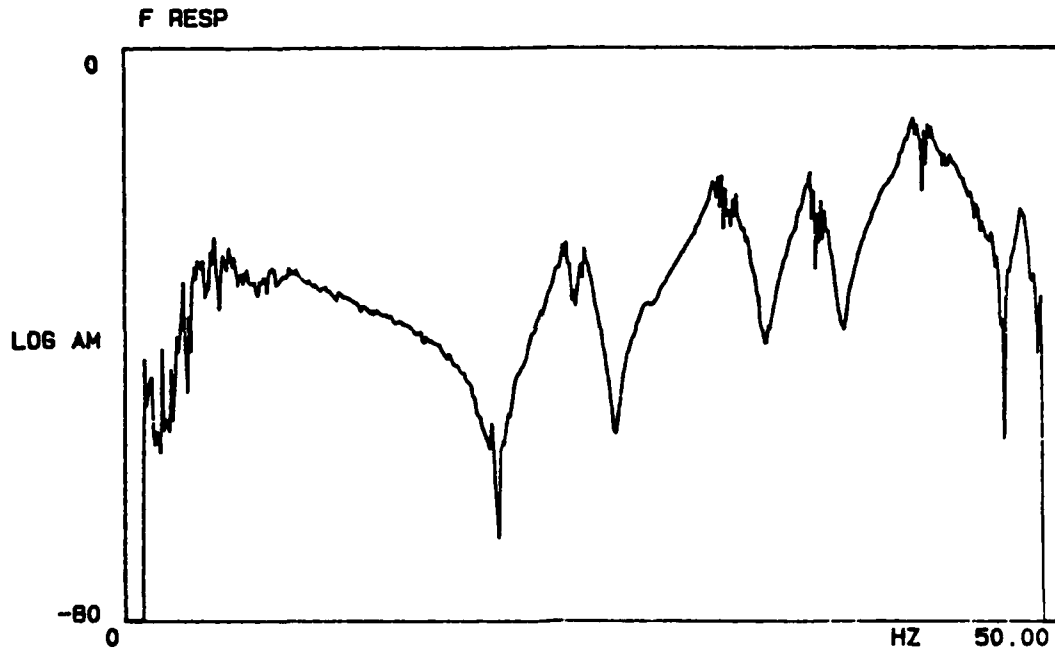


Figure 55. Frequency Response Estimates, One Input Not Driven, Dual Input Case

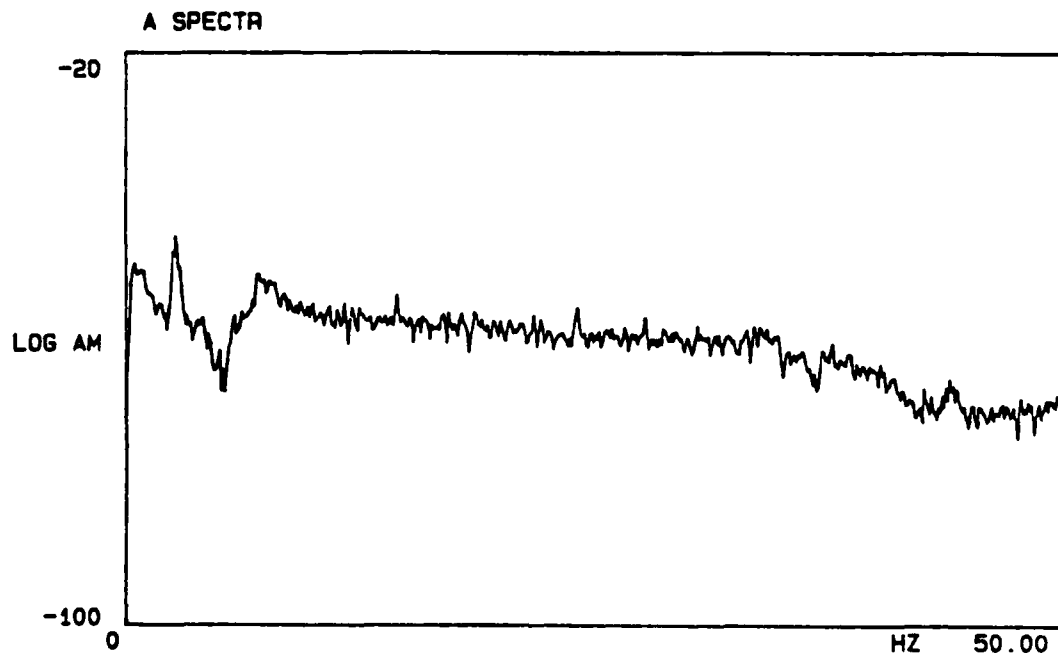
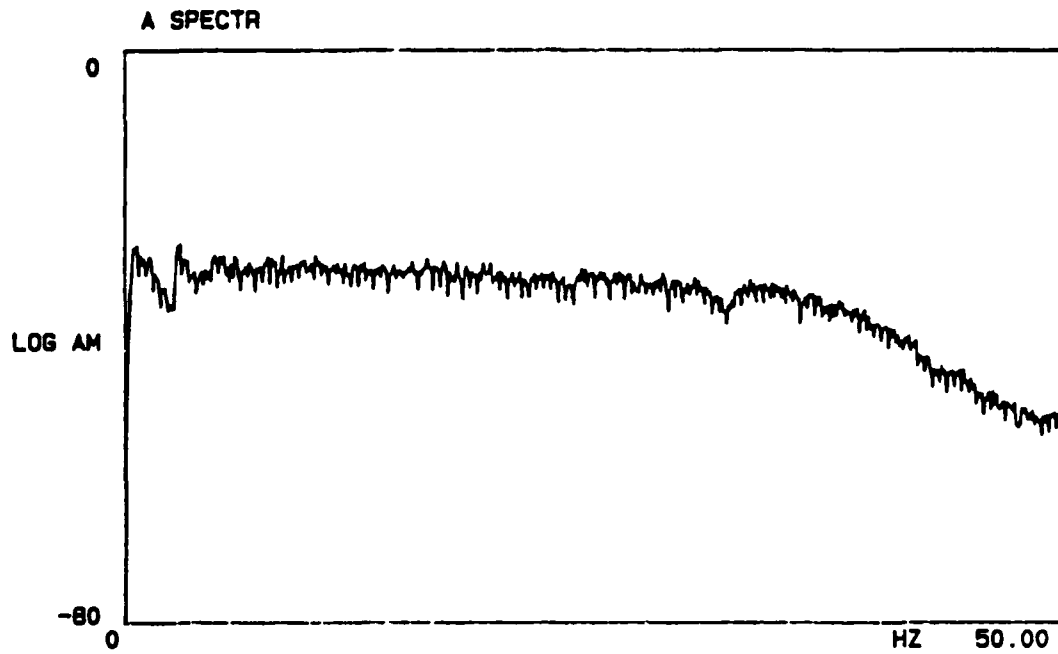


Figure 56. Auto Power Spectrum of Inputs, Same Signal Driving Both Exciters, Dual Input Case

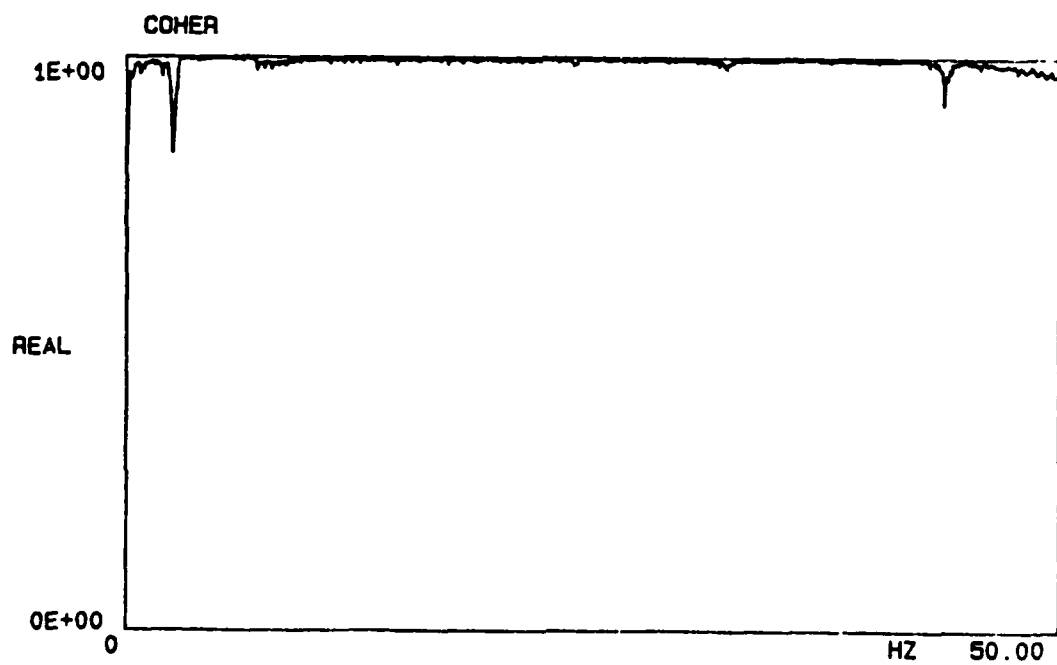


Figure 57. Ordinary Coherence Between Forces, Same Signal Driving Both Exciters, Dual Input Case

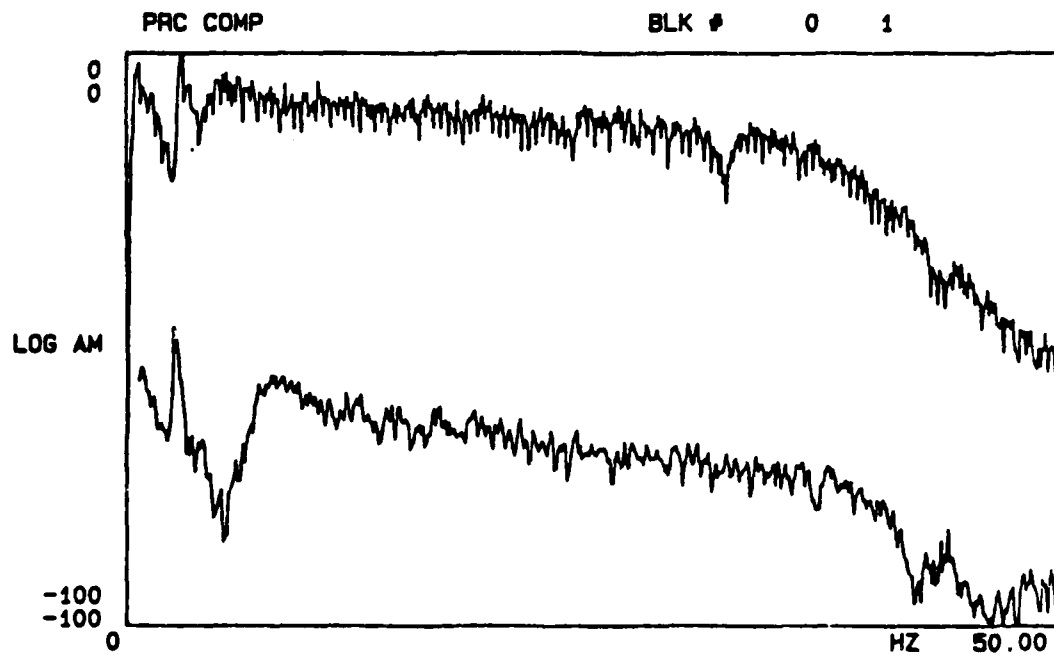


Figure 58. Principal Auto Power Spectra of Inputs, Same Signal Driving Both Exciters, Dual Input Case

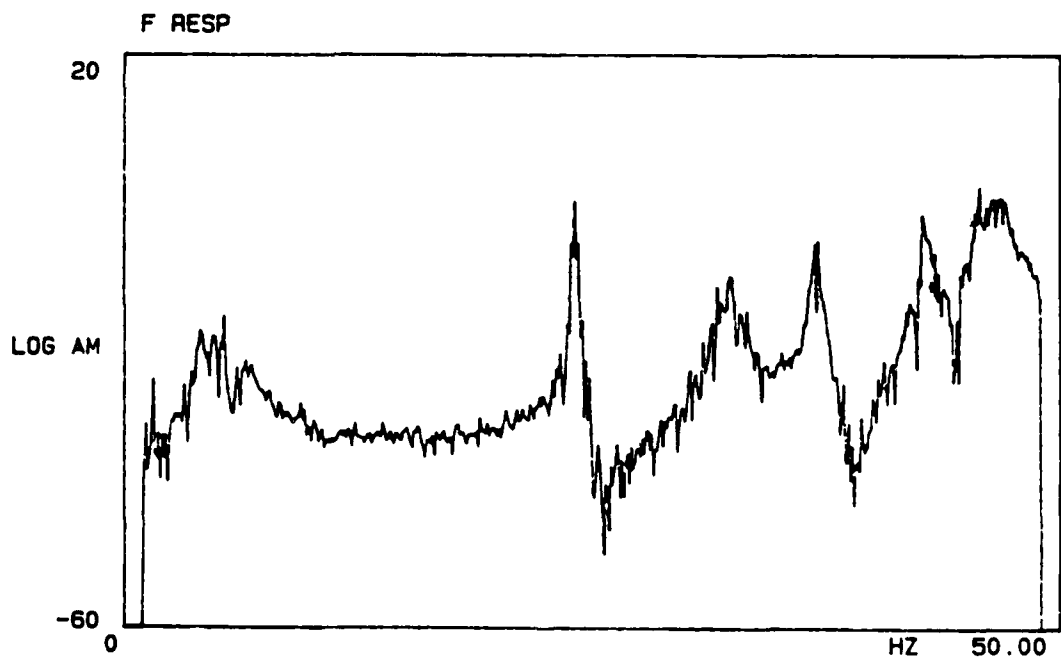
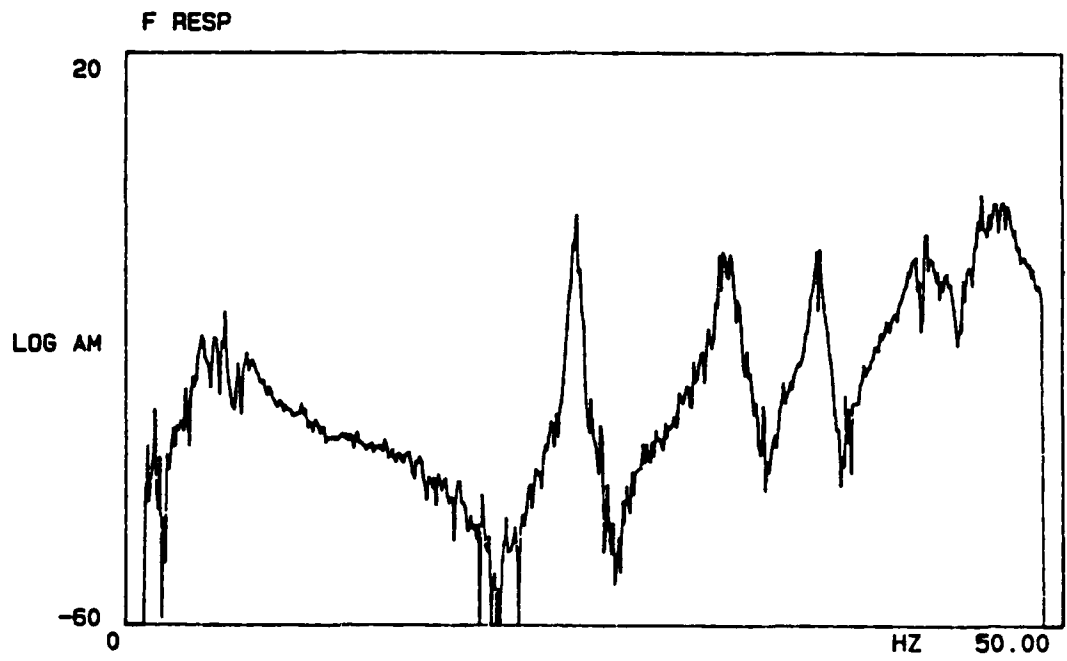


Figure 59. Frequency Response Estimates, Same Signal Driving Both Exciters, Dual Input Case

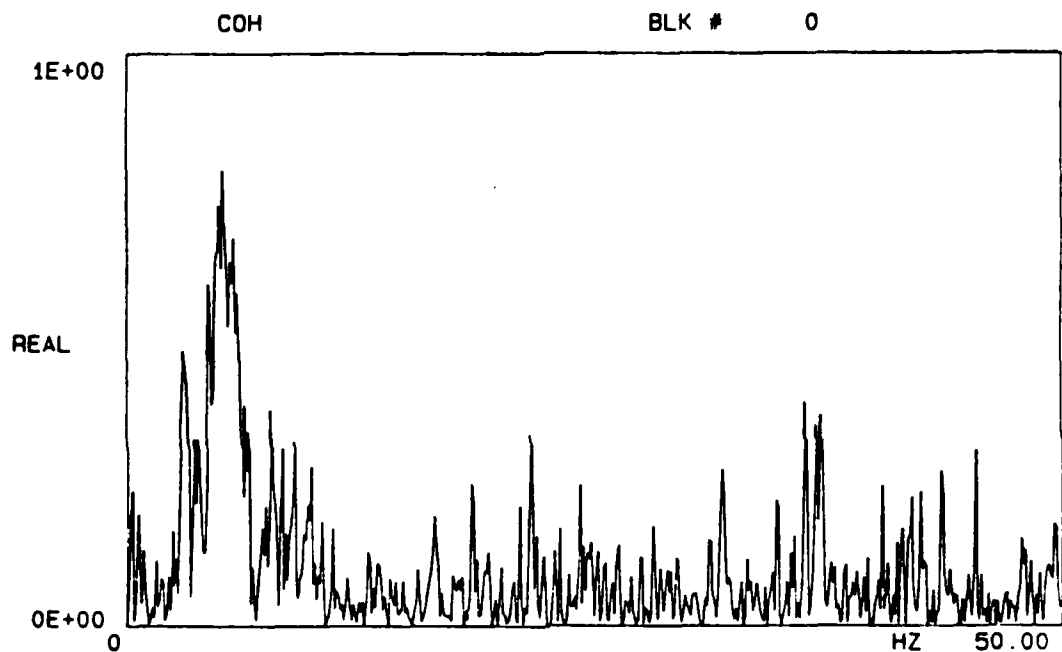


Figure 60. Ordinary Coherence Function COH_{12} Three Input Case

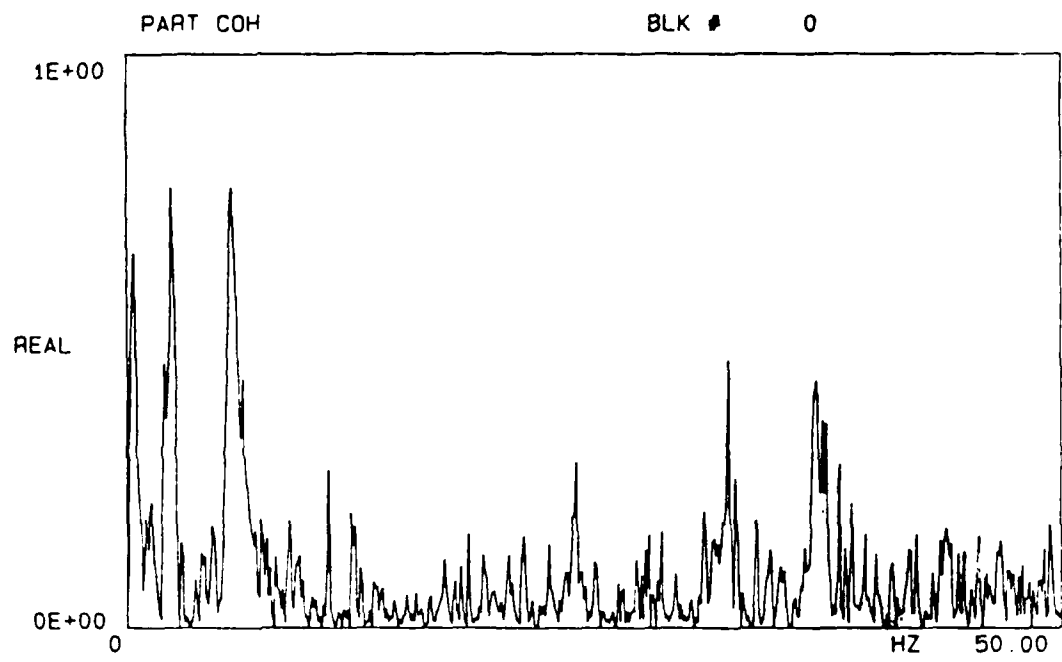


Figure 61. Conditioned Partial Coherence COH_{23}^1 Three Input Case

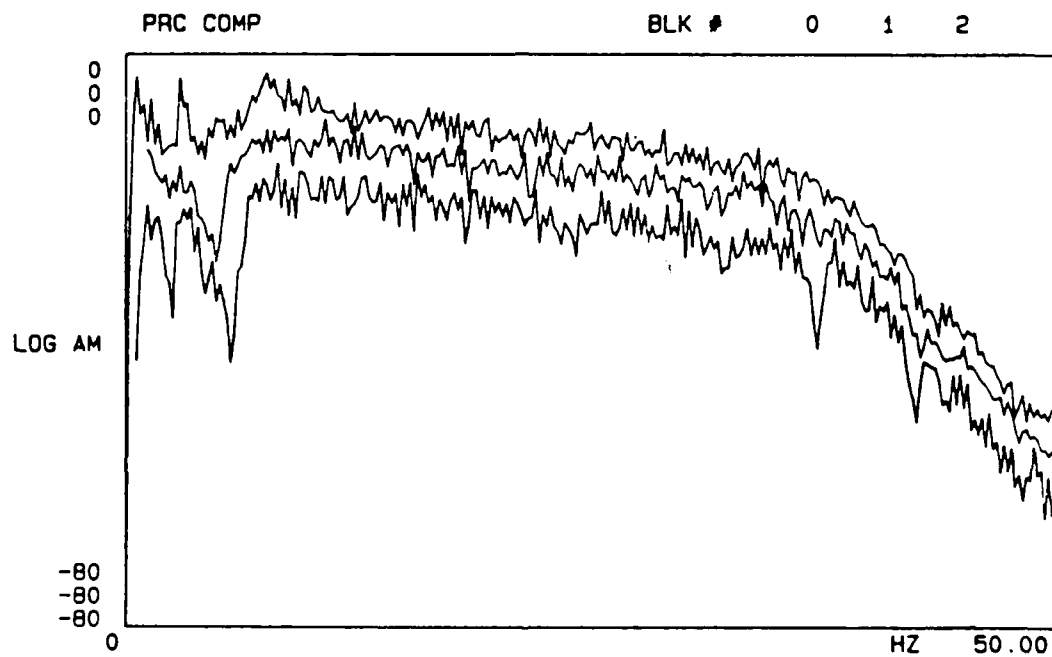


Figure 62. Principal Auto Power Spectra of Inputs, Three Input Case

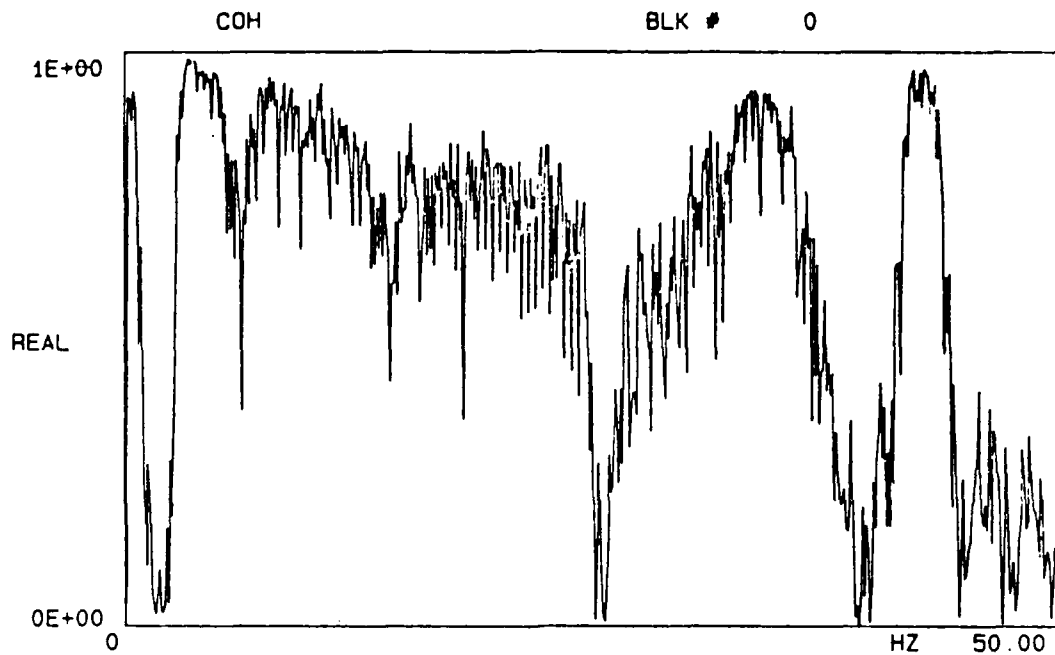


Figure 63. Ordinary Coherence Function COH_{12} Input 2 off, Three Input Case

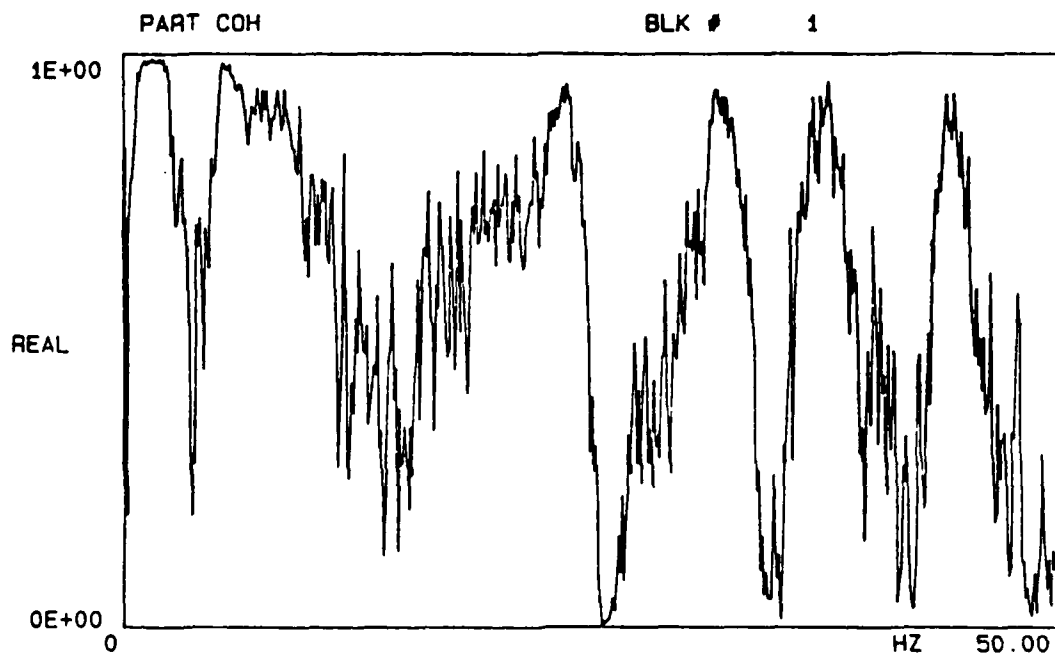


Figure 64. Conditioned Partial Coherence COH_{23}^1 Input 2 off, Three Input Case

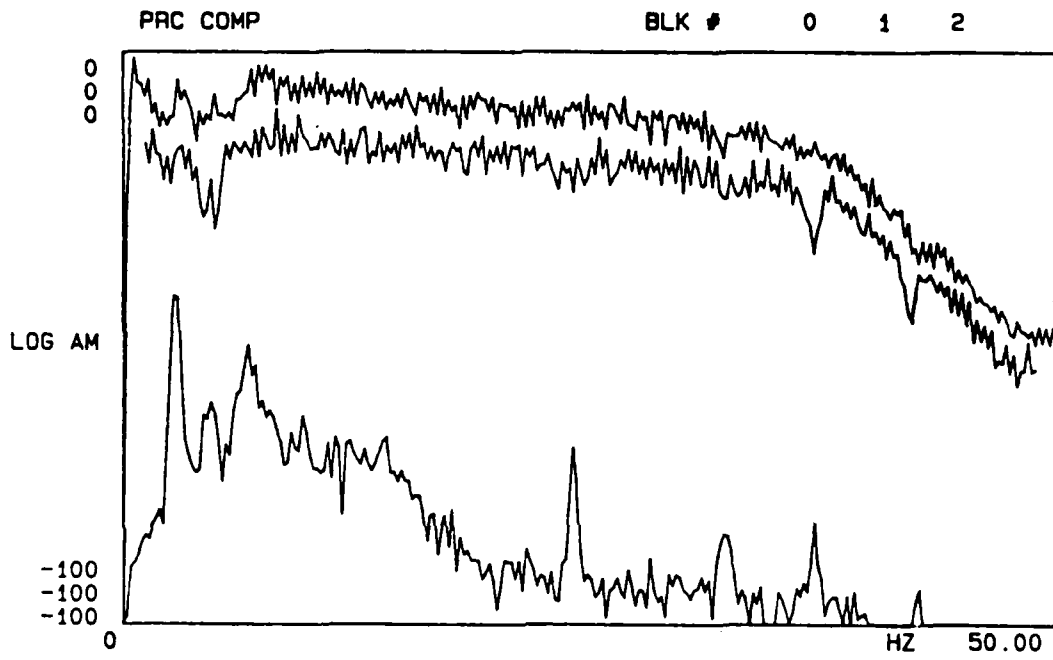


Figure 65. Principal Auto Power Spectra of Inputs, Shaker 2 off, Three Input Case

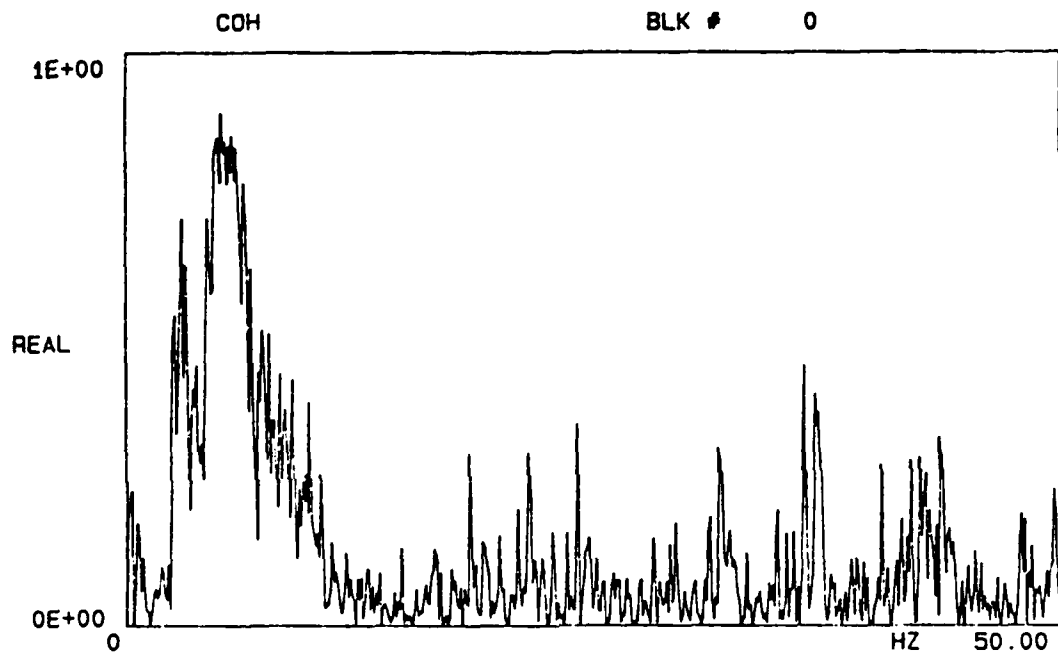


Figure 66. Ordinary Coherence Function COH_{12} , Input 3 off, Three Input Case

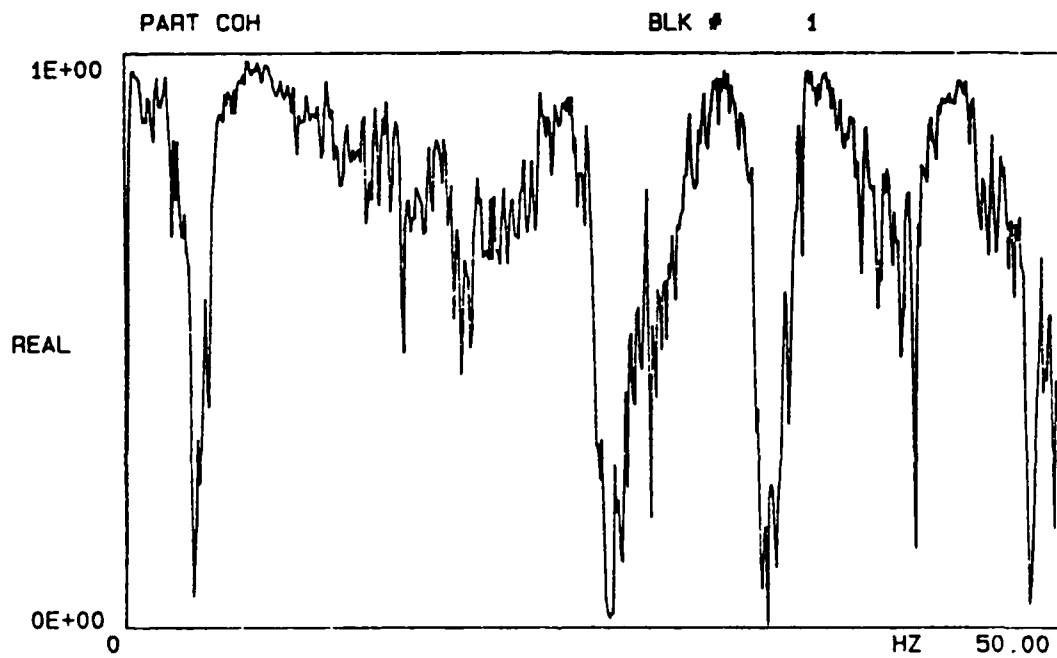


Figure 67. Conditioned Partial Coherence COH_{23}^1 , Input 3 Off, Three Input Case

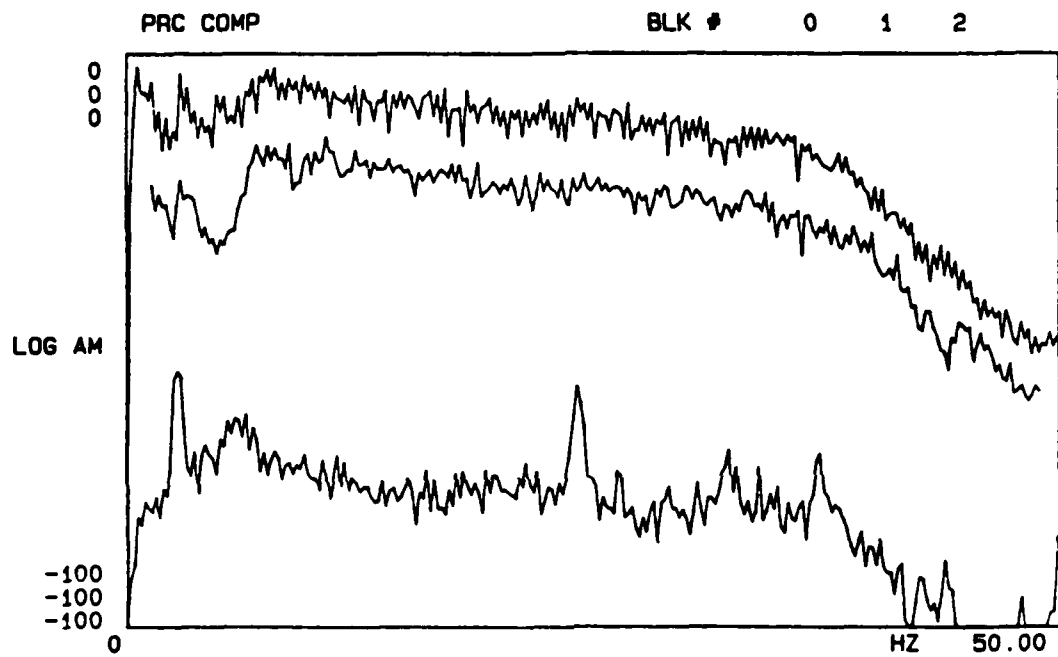


Figure 68. Principal Auto Power Spectra of Inputs, Input 3 off, Three Input Case

7. NON-LINEAR CONSIDERATIONS

7.1 Overview

The vibration of structures is a very natural phenomenon and although much work has been dedicated to the analysis and understanding of it, there exist an infinite number of vibrational problems which cannot be predicted. Because of this, experimental testing is needed to describe the vibrational characteristics of many structures. In this research, a linear system will be defined as a system in which the responses are linearly proportional to the input forces. A nonlinear system will be defined as having responses that are not linearly proportional to the input forces. In the analysis of linear systems, the responses can be predicted and an explicit mathematical model can be generated to represent the physical characteristics of the system. In the analysis of nonlinear systems, the responses can not adequately predict the measured dynamic characteristics.

It is accepted that most real structures exhibit nonlinear characteristics. Practical experience suggest that in many cases, this nonlinear term is negligible and a linear system can be assumed. However, as structures become more complicated and more accurate results are required, the nonlinear component is no longer negligible.

In modal analysis, frequency response functions are calculated based on a linear model of the structure. Thus, it is important to first accurately determine the contribution of the nonlinear components to the system. As described in Figure 69, the contribution of nonlinear components varies from system to system. At position "A", there exist a totally linear system having no contamination of nonlinear components. Between positions "A" and "B" the system is composed of linear and nonlinear terms; however, the nonlinear component in this case is small enough to be negligible. Between positions "B" and "C", the nonlinear term can no longer be negligible - the system should not be assumed to be linear. Finally, past position "C" the system is considered to highly nonlinear ^[49].

7.2 Research Objectives

One of the primary objectives of this research is to investigate previous studies dealing with nonlinearities as related to the modal analysis field. A review of current studies which deal with nonlinearities was made in terms of a literature search. Because of the difficulty involved in creating a physical structure with a known nonlinearity, most of the past research has only dealt with basic mathematical nonlinear structures having only one or two degrees of freedom.

Because of the increasing utilization of the multiple input estimation technique, it is the ultimate goal of this research to investigate a method for detecting nonlinearities in a system when using the multiple input estimation technique combined with random excitation signals. What is eventually desired is a detection method which could be programmed into the modal acquisition software and accessed to evaluate the degree of nonlinearity within a test structure.

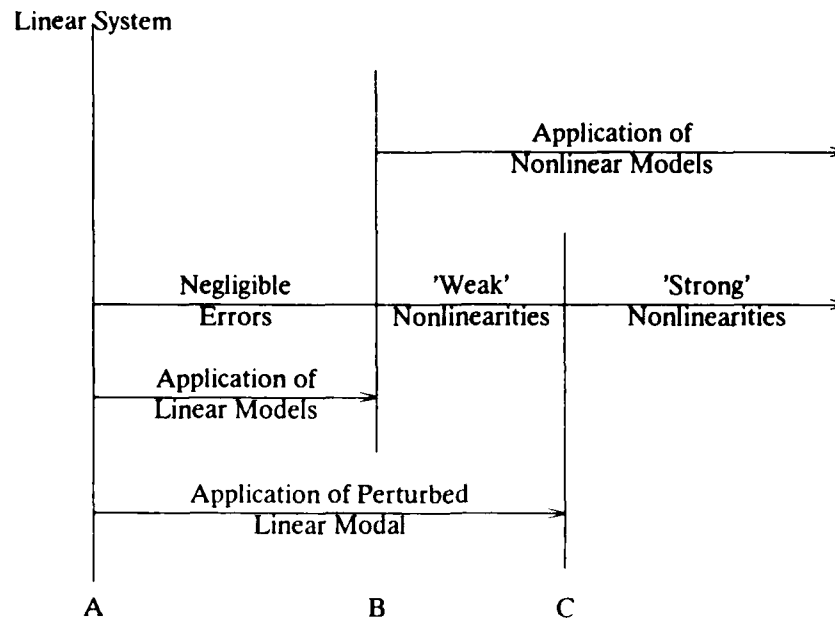


Figure 69. Evaluation of Linear and Nonlinear Systems

7.3 Modal Analysis and Nonlinearities

7.3.1 System Assumptions

In the field of experimental modal analysis there are three basic assumptions that are made about a structure. First, the structure is assumed to be time invariant. This means that the modal parameters that are to be determined will be constants of the structure. In general, a structure will have components whose mass, stiffness, or damping depend on factors which are not measured or included in the model. For example, in some structures, the components could be temperature dependent. In this case, temperature could be described as a time varying parameter; therefore, each of the temperature dependent components would be considered to be time varying. Thus, for a time varying structure, the same measurements made at different times would be inconsistent.

The second basic assumption is that the structure is observable. By observable, it is meant that the input/output measurements that are made contain enough information to generate an adequate behavioral model of the structure. For example, if a structure has several degrees of freedom of motion that are not measured, then the structure is considered to be not observable. Such a case would be that of a partially filled tank of liquid when sloshing of the fluid occurs^[50].

Finally, the third basic assumption is that the structure is either linear or can be approximated as linear over a certain frequency range. This essentially means that the response of the structure due to the simultaneous application of two or more excitation forces is a linear combination of the responses from each of the input forces acting separately. This relationship is shown in Figure 70. If a particular input signal, $a(t)$, causes an output signal, $A(t)$, and a second input signal, $b(t)$, causes a different

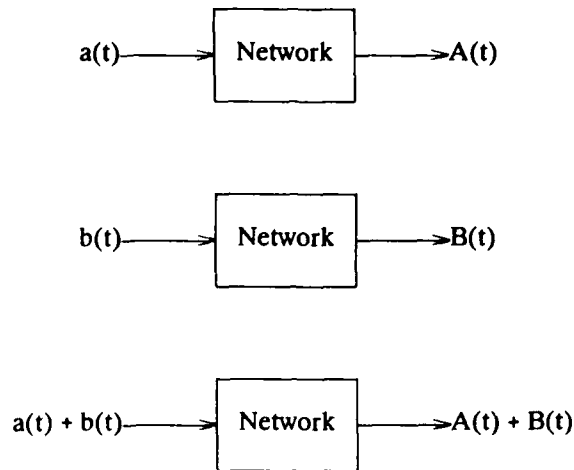


Figure 70. Linear Network

output signal, $B(t)$; then, if both input signals, $a(t)$ and $b(t)$, are applied to a linear system, the output signal will be the summation of the individual signals, $A(t) + B(t)$ ^[51].

7.3.2 Basic Nonlinear Systems

A linear system with several degrees of freedom can be modeled completely by a frequency response function which can be defined as the Fourier transform of the output signal divided by the Fourier transform of the input signal. In mechanical systems, the input signal is a type of force while the output signal is a quantity such as displacement, velocity, or acceleration. The frequency response function of these different output quantities are referred to as receptance, mobility, or compliance respectively, see Table 2.

As was previously stated, a linear structure can be characterized by its frequency response function and, as long as the structure does not physically change, this function will remain constant. This is not the case for a nonlinear structure; the system is no longer characterized by a single response function. In this case, the structure is very dependent to the time varying variables in the inputs of the system.

Although there exist very linear systems, most real structures have nonlinear components. Practical experience shows that the degree of nonlinearity of a structure varies according to the characteristics of the system. That is, welded structures will usually exhibit a linear response; where a riveted or spot welded structure exhibits a very nonlinear response ^[52].

As an example of a nonlinear system, consider a simple pendulum of length " l " having a bob of mass " m ", as shown in Figure 71. The equation of motion of this simple pendulum can be written as:

TABLE 2. Frequency Response Measurements

Receptance	$\frac{\text{Acceleration}}{\text{Force}}$
Effective Mass	$\frac{\text{Force}}{\text{Acceleration}}$
Mobility	$\frac{\text{Velocity}}{\text{Force}}$
Impedance	$\frac{\text{Force}}{\text{Velocity}}$
Dynamic Compliance	$\frac{\text{Displacement}}{\text{Force}}$
Dynamic Stiffness	$\frac{\text{Force}}{\text{Displacement}}$

$$m l^2 \ddot{\Theta} + m g l \Theta = 0 \quad \text{or} \quad \ddot{\Theta} + \frac{g}{l} \Theta = 0 \quad (74)$$

This equation only holds for small oscillations, such that:

$$\sin \Theta \approx \Theta \quad (75)$$

The exact equation of motion is nonlinear and can be written as:

$$m l^2 \ddot{\Theta} + m g l \sin \Theta = 0 \quad \text{or} \quad \ddot{\Theta} + \frac{g}{l} \Theta - \frac{g}{6l} \Theta^3 + \frac{g}{120l} \Theta^5 - \dots = 0 \quad (76)$$

A simple spring-mass system is shown in Figure 72. This system can be characterized by the equation:

$$m \ddot{x} + k x = 0 \quad (77)$$

This equation is based on the assumption that the elastic spring in the system obeys Hooke's Law; which states that the spring force is proportional to the spring deformation. In this case, the relationship between the spring force versus the spring deformation is a straight line, as shown in

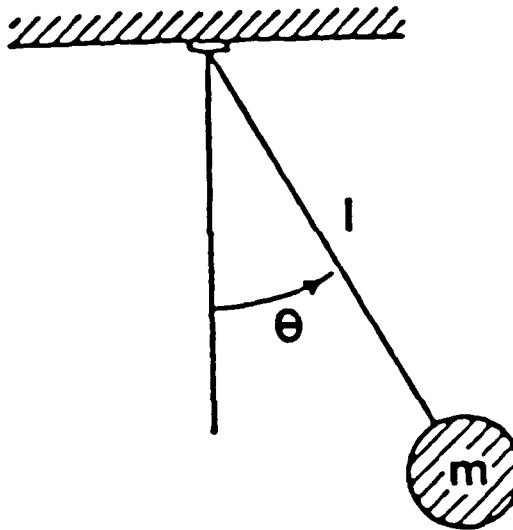


Figure 71. Simple Pendulum

Figure 73. However, this linear characteristic property is not found in many systems. In a simple coil spring, a nonlinear behavior will occur when the spring is overly compressed or extended. In either case, the elastic spring will exhibit a nonlinear characteristic such that the spring force increases more rapidly than the spring deformation; this is referred to as a hardening spring. On the other hand, certain systems such as the simple pendulum exhibit a softening characteristic. Both of these nonlinear properties are shown in Figure 73. A system which exhibits a hardening or softening effect can be described by the following equation of motion:

$$m \ddot{x} + k (x \pm \mu^2 x^3) = 0 \quad (78)$$

where the nonlinear term is positive for a hardening effect and negative for a softening effect. These are both examples of nonlinear stiffness in a structure. For the hardening effect, the natural frequency will increase with the amplitude of the oscillation, where the frequency will decrease with amplitude for a softening effect. These nonlinear properties are also shown in Figure 74. As the frequency of the input force is swept up, the frequency response would follow the curve from location 1, to location 2, to location 3. At location 3, a small increase in frequency would result in an immediate jump of the response down to location 5. From location 5, the response would follow the curve through location 6 as the frequency increased. If the input force was to begin at a high frequency and then decrease, the response would follow the curve from location 6 to location 5 and continue on to location 4. At location 4, a small decrease in frequency would result in an immediate jump up to location 2. From location 2 the response would follow the curve to location 1.

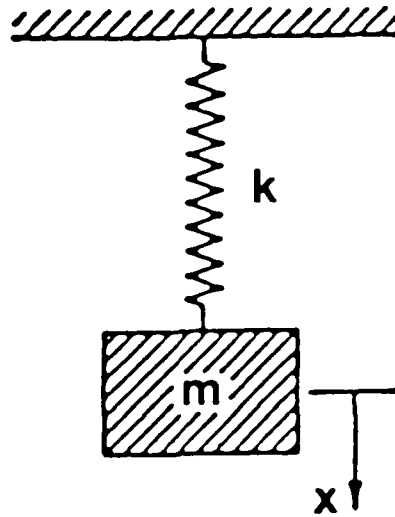


Figure 72. Simple Spring-Mass System

The previous examples have all exhibited nonlinearities in the elastic component. When considering a simple mass system with a dashpot as the damping component, as shown in Figure 75, certain assumptions must be made. The spring component must be linear and the force due to the resistance of the dashpot must be proportional to the velocity; thus, the equation of motion is linear. However, in many cases, the dashpot resistance is more accurately described by a term which is proportional to the square of the velocity. Furthermore, the resistance is always opposing the motion.

This nonlinear equation of motion is written as:

$$m \ddot{x} + c |\dot{x}| \dot{x} + kx = 0 \quad (79)$$

This is an example of nonlinear damping within a structure ^[53].

Nonlinear behavior in structures can be related to such characteristics as backlash, nonlinear stiffness, nonlinear damping, nonlinear material properties, or friction. These nonlinearities can be classified as "limited" or "nonlimited" nonlinearities. In the "limited" case, the nonlinearity is limited within a particular force level range. Nonlinearities due to backlash could be classified as a "limited" nonlinearity. "Nonlimited" nonlinearities refer to those nonlinearities which are independent of force level. Nonlinear damping is an example of a "nonlimited" nonlinearity ^[54].

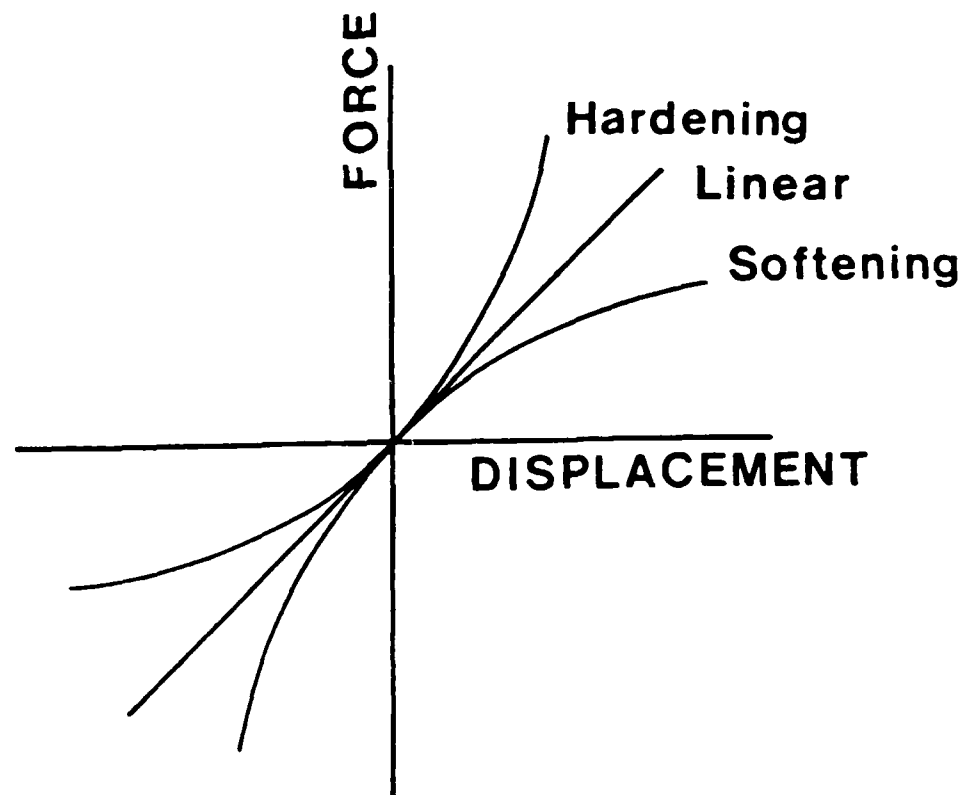


Figure 73. Force Characteristic Curves

7.3.3 Excitation Techniques

When a structure is to be tested to determine the modal parameters, one of the most important considerations is the excitation method to be used. For a linear structure, the frequency response function is independent of the amplitude and type of the excitation signal. This is not the case for a nonlinear structure; the selection is crucial since the method of excitation can either minimize or enhance the nonlinear behavior of the structure. The different excitation signals can be divided into two classifications; the deterministic excitation signals and the random excitation signals.

The deterministic signal is one which can be described by an explicit mathematical relationship. These signals are then divided into two other classifications, periodic or non-periodic. A signal is periodic if it repeats itself at equal time intervals. Frequency response functions that result from deterministic signals are dependent upon the signal level and type. Therefore, these signals are very useful in detecting nonlinearities in structures. Table 3 gives a summary of the different excitation signals and their classification.

The use of a sine wave, which is a deterministic signal, to excite a structure is very common [55]. The main advantage of a swept sine test is that the input force can be precisely controlled. It is this characteristic that makes this method particularly useful when trying to identify nonlinear systems. If a particular system is nonlinear, by varying the input force levels, one can compare several frequency response functions and identify inconsistencies. A major disadvantage with this method is that it gives a very poor linear approximation of a nonlinear system. This causes a serious problem if the data is to be used to estimate modal parameters. Therefore, this method is adversely affected by

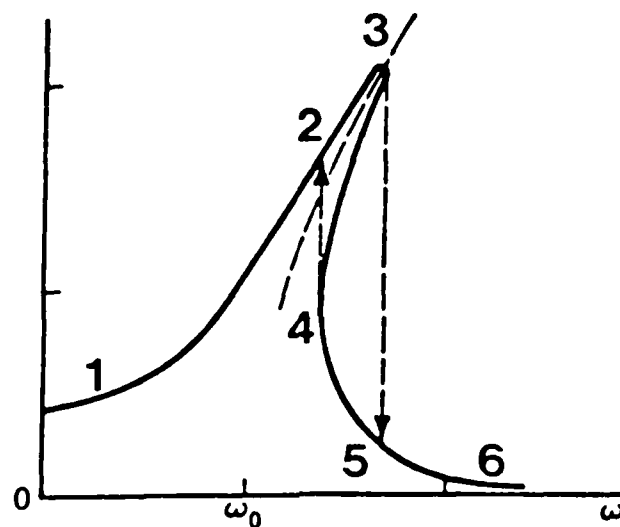


Figure 74. F.R.F. of a Hardening and Softening Spring

nonlinearities.

Another deterministic excitation signal is an impact signal. The impact testing technique is very useful for trouble-shooting and preliminary modal surveys. However, this technique should not be utilized with nonlinear structures because of the difficulties in controlling the impact force and insufficient energy to properly excite the structure^[56].

The random signal is one which can only be described by its statistical properties over a given time period; no explicit mathematical relationship exists. For structures with small nonlinearities, the frequency response functions from a random signal will not differ greatly from that of a deterministic signal. However, as the nonlinearity in the structure increases, the random excitation gives a better linear approximation of the system, since the nonlinearities tend to be averaged out. The random excitation signal has been increasingly useful since it enables the structure to be investigated over a wide frequency range, unlike the sine wave^[9].

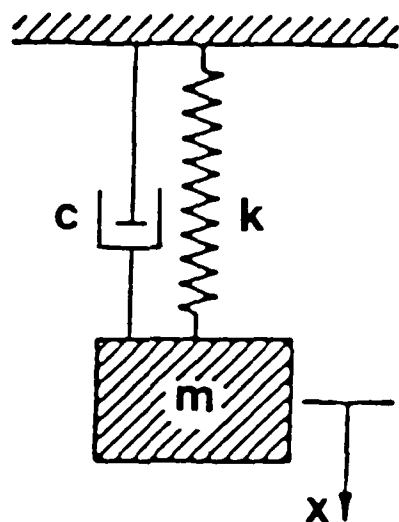


Figure 75. Simple Spring-Mass System with Dashpot

TABLE 3. Excitation Signal Summary

Deterministic Excitation	Random Excitation
Slow Sinusoidal Sweep Fast Sinusoidal Sweep Periodic Chirp Impulse (Impact) Step Relaxation	True (Pure) Random Pseudo Random Periodic Random Burst Random (Random Transient)

7.4 Nonlinear Detection Techniques

7.4.1 Distortion of The Characteristic Function

Mathematically, linearity can be expressed by the superposition theorem which states:

$$\text{If } a(t) \rightarrow A(t) \text{ and } b(t) \rightarrow B(t) \text{ Then } a(t) + b(t) \rightarrow A(t) + B(t) \quad (80)$$

To be utilized experimentally, each measured frequency response function would be required to be checked for the validity of Equation 80. Since this would be an impractical process, only several representative functions are checked. If Equation 80 is valid, the structure is assumed to be linear under the given test conditions^[57]. Typically, only the driving point measurements are evaluated. Other response locations, which allow the nonlinear characteristics to be excited, need also to be evaluated.

7.4.1.1 The Nyquist Plot

One of the earliest methods for detecting nonlinearities in test structures utilized the characteristics of the Nyquist plot. From a strict control systems definition, the Nyquist plot is a polar plot of the open-loop transfer function. The original approach for the "circle fit" parameter estimation routine which utilizes the Nyquist plot, was developed by Kennedy and Pancu^[58]. The Nyquist plot is another way of displaying the frequency response function; it plots the real part of the function versus the imaginary part of the function. As is shown for a single degree of freedom system in Figure 76, the horizontal axis is the real part and the vertical axis is the imaginary part. At the starting frequency for a linear system, the phase angle is close to zero and the magnitude is one over the static stiffness. In the Nyquist plot the frequency increases in a clockwise direction. As the frequency approaches resonance, the real part of the function decreases while the imaginary part increases. At the point where the rate of change of the arc length with respect to frequency is a maximum, the curve crosses the imaginary axis. At that point the real part goes to zero and the complex number is a pure imaginary value and that frequency is resonance. Beyond the resonance, the curve continues on a circular arc and reaches the origin at an infinite frequency.

In models which are comprised of nonlinear elements or signal processing errors, the Nyquist plot is no longer a circular arc. In these cases the resulting plots are elliptical or a combination of circles with distorted regions^[59]. These distortions are due to the fact that the linearized equation, which is represented as a complex value, can no longer be represented as a circle.

Not only do the plots distort, but the lines that join points of constant frequency for different excitation levels (isochrones) also distort for nonlinear systems. The distortion of the isochrones is dependent upon the type of nonlinearity. Figure 77 gives several examples of these distortions. It should be noted that the plots in Figure 77 are only the response of the system. The isochrones are more sensitive to nonlinearities than the actual Nyquist plots; thus, the pattern of these lines could be a better detection and identification technique for nonlinearities. Methods for identifying the nonlinear systems have proved to be successful^[60]; however, prior assumptions about the form of the nonlinearity must be made. Another limitation is that the algorithm which is utilized to estimate the

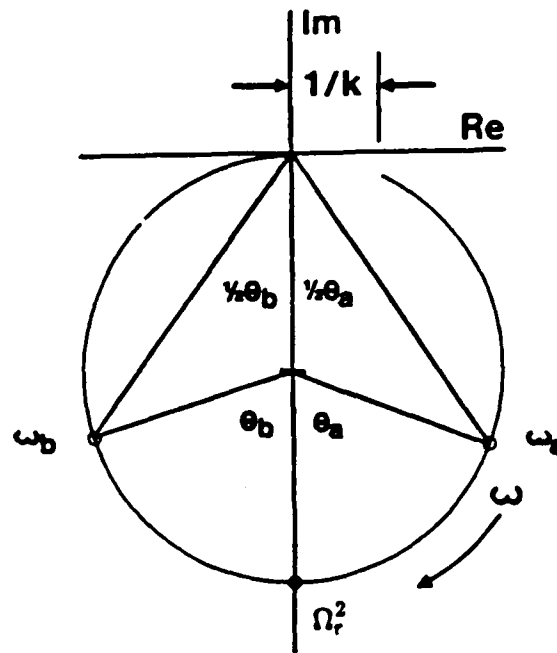


Figure 76. Nyquist Plot

frequency response function influences the shape of the Nyquist plot. As in the case where the H_1 algorithm is utilized for the estimate, the amplitude at resonance is underestimated. When the H_2 algorithm is utilized, the amplitude at resonance is overestimated. In both cases, the estimation error causes the Nyquist plot to be elongated. For the isochrones to be useful, the modes of vibrations of the system must be lightly coupled and the nonlinearity must be simple [61].

7.4.1.2 Damping Values

As an extension to the Nyquist distortion detection method, the damping values computed from a single mode of vibration has proven to be useful as a linearity detection technique. As represented in Figure 76, an estimate of the damping of a single degree of freedom linear system can be calculated from a Nyquist plot by the following equation [62].

$$\delta_r = \frac{\omega_a^2 - \omega_b^2}{\Omega_r^2} \frac{1}{\tan \frac{\theta_a}{2} + \tan \frac{\theta_b}{2}} \quad (81)$$

By utilizing several frequencies before and after the resonant frequency, several independent damping

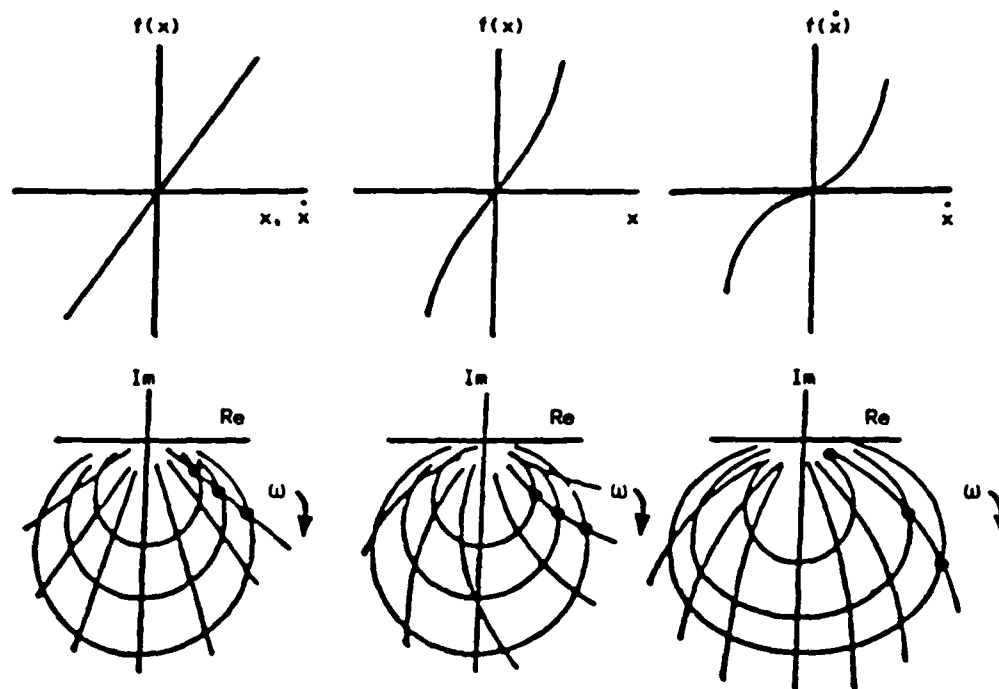


Figure 77. Distorted Nyquist Plots

estimates can then be produce a three-dimensional carpet plot. Figure 78 represents a linear system. The damping estimates are constant for each of the different combination of frequencies before and after the resonance; thus producing a flat contour. Figure 79 compares two nonlinear cases and shows how the three-dimensional carpet plots varies from a linear case [63]. Again, this method is easy to implement; however, only lightly coupled modes of vibration can be accurately examined. This method also has no means of linearizing the response for the modal analysis test.

7.4.2 Reciprocity

The theorem of reciprocity states that the dynamic response of the p^{th} displacement co-ordinate, due to any time-varying force of the q^{th} co-ordinate is equal to the response of the q^{th} co-ordinate due to the same force of the p^{th} co-ordinate [64].

Mathematically it is expressed as:

$$\frac{X_p}{F_q} = \frac{X_q}{F_p} \quad (82)$$

Reciprocity is often used as a linearity indicator; however, it does not define linearity. A symmetric

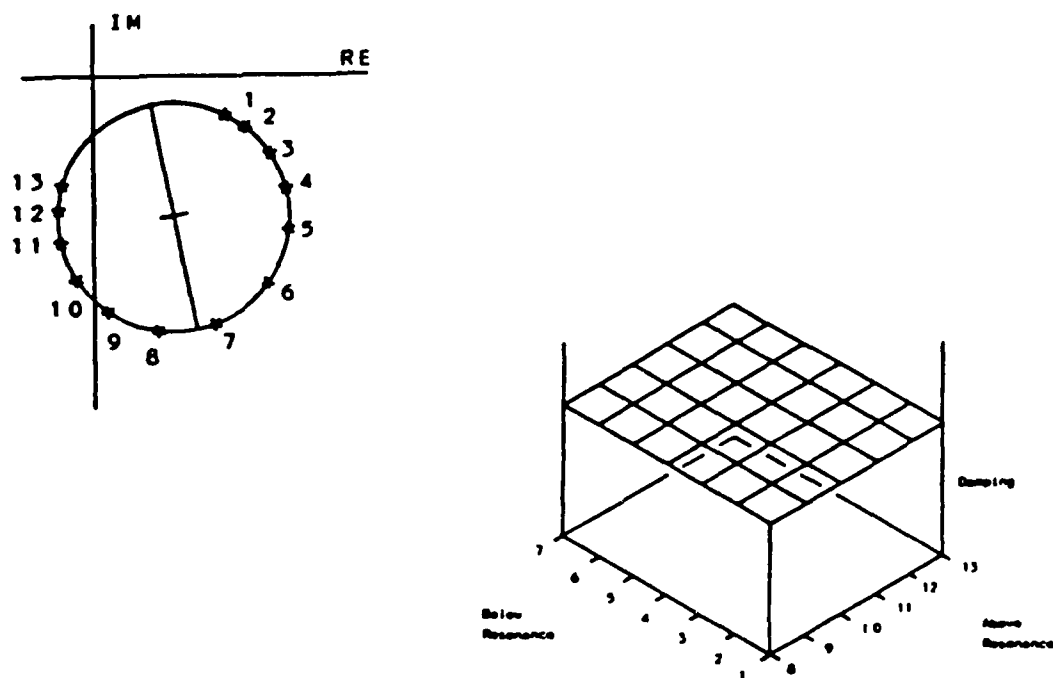


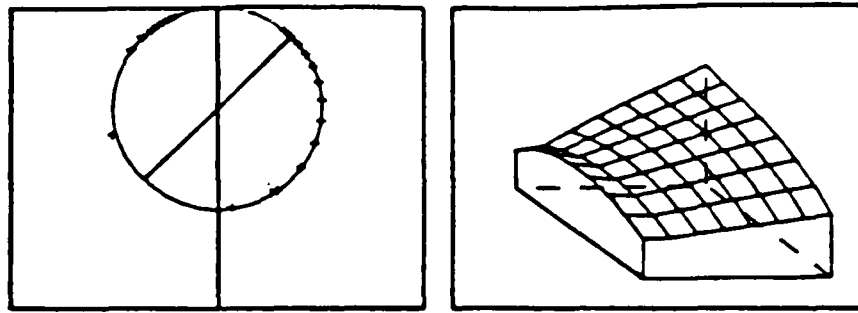
Figure 78. Carpet Plot of a Linear System

nonlinear system may exhibit reciprocity while not satisfying the superposition principle ^[61]. It has been shown that reciprocity only strictly applies to the ratio of statically applied forces and the resulting response displacements and not to dynamically applied forces. For the reciprocity theorem to be valid the stiffness matrix $[k]$, the mass matrix $[m]$, and the system matrix $[k]^{-1} [m]$ must be symmetric; these conditions are not commonly found in real structures.

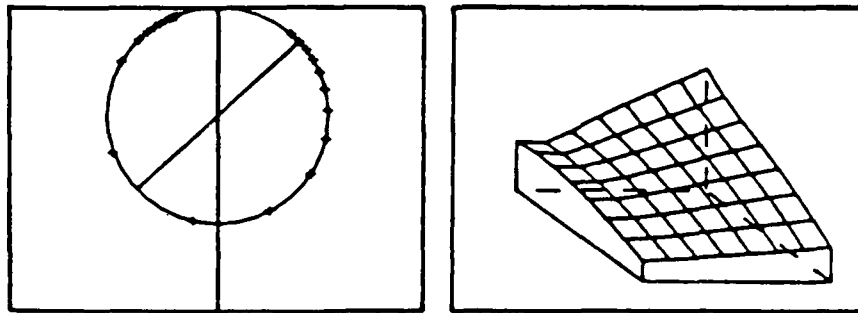
7.4.3 Coherence

The measured coherence function is also often used as a linearity indicator. The coherence function is defined as a measure of the degree of causality between a system input and output. It describes the division of the output power into coherent and incoherent parts with respect to the input. The coherence function is a good indicator of uncorrelated noise on the input or output signals; however, it does not necessarily indicate that the test structure is nonlinear. It has been shown that even though the coherence functions are nearly unity, when the frequency response functions are overlaid, shifts in frequency occur - indicating a nonlinear structure ^[57]. The ability to differentiate between nonlinearities and the effects of leakage is often difficult and many nonlinearities may be phase coherent when a periodic random excitation signal is used.

Although these are the most common ways of detecting nonlinearities, none of these techniques are definitive indicators of linearity within a structure. Other methods do exist that not only give a better indication of linearity but also can aid in the identification of nonlinearities.



Cubic Stiffness



Backlash

Figure 79. Carpet Plots of Nonlinear Systems

7.4.4 The 'Sig-function'

The 'sig-function' is a new method that was developed as a nonlinearity detector for the time domain and is still in the development stages at the University of Leuven, Belgium. A time domain detecting technique could be advantageous for several reasons. As in the case of a sinusoidal excitation, the common practice is to only utilize the fundamental harmonics of the output to calculate the frequency response function and neglect all the other sub and post harmonics. The 'sig-function' utilizes the total energy of the harmonic distortion of the output signal.

The 'sig-function' describes the energy of the harmonic distortion of the output signal, as related to the total energy, as a function of frequency. It is mathematically defined for a sinusoidal excitation as follows:

$$\text{sigf}(\omega) = \frac{\int_0^T (x(t) - x'(t))^2 dt}{\int_0^T x(t)^2 dt} \quad (83)$$

where:

$x(t)$ represents the total response signal
 $x'(t)$ represents the fundamental filtered time signal

In this equation, $x(t)$, is the total response due to some input force at the fundamental frequency (ω). The term $x'(t)$ is the portion of $x(t)$ that is occurring at the fundamental frequency. The numerator, which is the difference of these values, represents the response that does not occur at the fundamental frequency. This calculation is made at each frequency between some minimum and maximum bandwidth. Once calculated, the magnitude of the function will range from 0 to 1, where 0 represents a linear system with no nonlinear characteristics and 1 represents a system which is totally nonlinear.

This 'sig-function' method is mainly a detection technique rather than a identification method. The biggest advantage of this technique is that it does not use reduced data. Most other nonlinear detection techniques usually require the estimation of frequency response functions. These techniques are based upon the fundamental harmonic in which the output is filtered such that it contains only the excitation frequency. Because of this, there is a reduction in the available data [61]. There are however two disadvantages with the 'sig-function' method namely; its sensitivity for noise and the restriction for sinusoidal excitation. This technique has also not yet been applied to multi-mode systems.

7.4.5 The Hilbert Transform

One of the most promising methods for detecting nonlinearities is one which uses a version of the Hilbert transform to provide a relationship between the real and imaginary parts of the measured complex frequency response function. The initial application of the Hilbert transform to the field of modal analysis was done by Professor T. Vinh of the Institute Supérieur des Matériaux et de la Construction Mécanique, St. Ouen, France. Vinh and his associates, A. Haoui and Y. Chevalier, are currently utilizing the Hilbert transform in the time domain [66-67], while M. Simon, G.R. Tomlinson, and N.E. Kirk, of Simon Engineering Laboratories and the University of Manchester - Manchester, England, are making applications of the Hilbert transform in the frequency domain [69-70]. The following mathematical description of the Hilbert transform and its application to nonlinearities is a combination of the previous references.

The Hilbert transform is a mathematical way to describe a causal physical system. By causal physical system it is meant that the system can only react to inputs after the inputs have been applied. If the analytic functions of a complex variable are examined, certain relationships between the real and imaginary parts of the functions are found. Given the imaginary part of a complex variable, the real part could be uniquely determined. The same holds true for the real part; that is, if the real part of a

complex variable is given, the imaginary part could be uniquely determined. This relationship between the real and imaginary parts is a version of the Hilbert transform. Likewise, for a linear mechanical system, the imaginary part of the frequency response function is uniquely determined from the real part or the phase of a frequency response function uniquely gives the amplitude. This only applies to a frequency response function that corresponds to a causal system; therefore, the Hilbert transform is applied to a frequency response function to determine if this relationship between the imaginary and real parts exists. If this relationship does not exist, the system under investigation is not a linear causal system.

The Hilbert transform of a real-valued time signal, $f(t)$, is defined as:

$$\mathbb{H}\{f(t)\} = \frac{1}{\pi} \int_{-\infty}^{\infty} \frac{f(\tau) d\tau}{t - \tau} \quad (84)$$

To redefine the Hilbert transform, let $G(z)$ be a function of a complex variable, z . Cauchy's formula states that if G is analytic everywhere within and on a simple closed contour, C , taken in the positive sense and z_0 is any point interior to C , then:

$$G(z_0) = \frac{1}{2\pi j} \int_C \frac{G(z) dz}{z - z_0} \quad (85)$$

In terms of the quantity Mobility, the measured complex analytic function, $\hat{H}(\omega)$, can be written in the frequency domain as:

$$\hat{H}(\omega) = \sum_{r=1}^N \frac{j\omega X_r}{\omega_r^2 (1 + j\delta_r) - \omega^2} \quad (86)$$

This equation can also be written as a function of complex frequency such that $z = \alpha + j\xi$. If this series is expressed as the ratio of two polynomials, the function becomes:

$$\hat{H}(z) = jzA \frac{(z - a_1)(z - a_2) \dots (z - a_{2m-2})}{(z - b_1)(z - b_2) \dots (z - b_{2m})} \quad (87)$$

where A is a constant; a and b are the zeros and poles of the function representing the antiresonances and resonances of the system. The mapping of these poles and zeros onto the complex frequency plane is shown in Figure 80. The poles are in the top half of the plane but the zeros can be in any part of the plane. The contour, C , for the integration of Equation 84 needs to be chosen such that it avoids the poles. Figure 80 shows this contour which is a semicircle in the lower half of the z -plane and a section on the real axis, with a slight detour to avoid the extra poles located at $\omega = \pm \omega_c$ on the real axis. Because of this contour selection, the integral of Equation 85 can be broken up into two separate integrals.

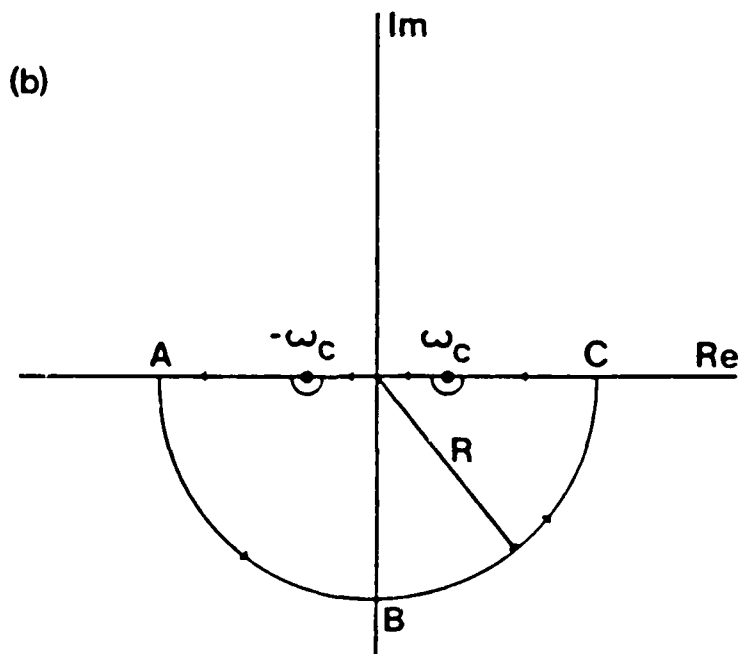
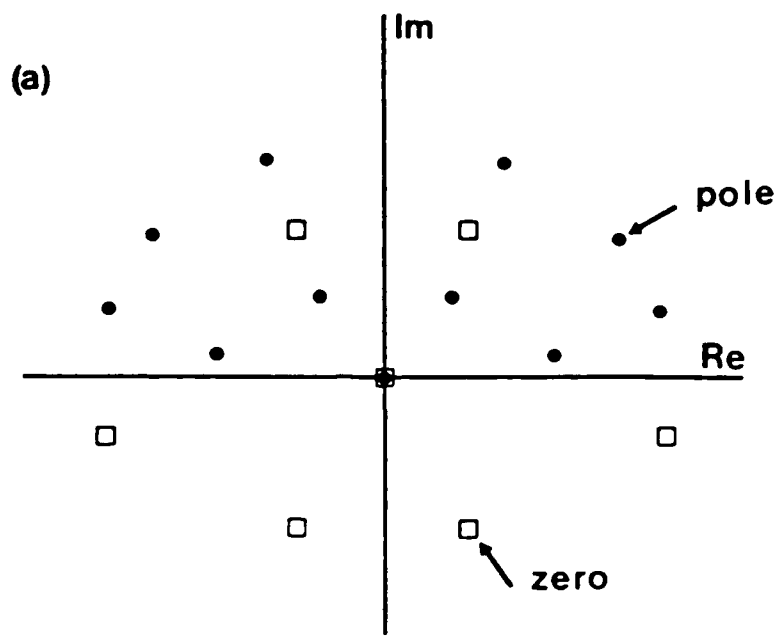


Figure 80. Complex Frequency Plane

$$\int_C = \int_{ABC} + \int_{CA} \quad (88)$$

The first integral approaches zero as the radius of the semicircle, R , approaches infinity. For this case, the integral of Equation 85 is only the line integral which lies on the real axis and can be written as:

$$\hat{H}(\omega_c) = -\frac{1}{\pi j} PV \int_{-\infty}^{\infty} \frac{\hat{H}(\omega) d\omega}{\omega - \omega_c} \quad (89)$$

where PV indicates that the Cauchy Principal Value of the integral has been taken and ω_c represents the current frequency in the frequency response function. This equation is of the same form as Equation 85; therefore, it can be written as:

$$H\{\hat{H}(\omega_c)\} = H'(\omega_c) = -\frac{1}{\pi j} PV \int_{-\infty}^{\infty} \frac{\hat{H}(\omega) d\omega}{\omega - \omega_c} \quad (90)$$

where $H'(\omega_c)$ represents the Hilbert transform of the measured complex analytic function, $H\{\hat{H}(\omega_c)\}$. As could be done with Equation 85, Equation 90 can be split into its real and imaginary parts; which are as follows:

$$\text{Re } H'(\omega_c) = -\frac{1}{\pi} PV \int_{-\infty}^{\infty} \frac{\text{Im } \hat{H}(\omega) d\omega}{\omega - \omega_c} \quad (91)$$

$$\text{Im } H'(\omega_c) = -\frac{1}{\pi} PV \int_{-\infty}^{\infty} \frac{\text{Re } \hat{H}(\omega) d\omega}{\omega - \omega_c} \quad (92)$$

These relations define the Hilbert transform pair which relate the real and imaginary parts of $\hat{H}(\omega)$.

If $\hat{H}(\omega)$ is the Fourier transform of a real signal $h(t)$, which is the unit impulse response of a linear system, such that:

$$\hat{H}(\omega) = \int_{-\infty}^{\infty} h(t) e^{-2\pi j\omega t} dt \quad (93)$$

then from the properties of the analytic Fourier kernel, $e^{-2\pi j\omega t}$, the real part of $\hat{H}(\omega)$ is an even function and the imaginary part of $\hat{H}(\omega)$ is an odd function. This can be stated mathematically as:

$$\hat{H}(-\omega) = \hat{H}^*(\omega) \quad (94)$$

Equations 91 and 92 can be rewritten as:

$$\operatorname{Re} H'(\omega_c) = -\frac{1}{\pi} PV \left\{ \int_{-\infty}^0 \frac{\operatorname{Im} \hat{H}(\omega) d\omega}{\omega - \omega_c} + \int_0^{\infty} \frac{\operatorname{Im} \hat{H}(\omega) d\omega}{\omega - \omega_c} \right\} \quad (95)$$

$$\operatorname{Im} H'(\omega_c) = -\frac{1}{\pi} PV \left\{ \int_{-\infty}^0 \frac{\operatorname{Re} \hat{H}(\omega) d\omega}{\omega - \omega_c} + \int_0^{\infty} \frac{\operatorname{Re} \hat{H}(\omega) d\omega}{\omega - \omega_c} \right\} \quad (96)$$

Using the following properties which define odd and even functions:

$$\operatorname{Re} \hat{H}(-\omega) = \operatorname{Re} \hat{H}(\omega) \quad (97)$$

$$\operatorname{Im} \hat{H}(-\omega) = -\operatorname{Im} \hat{H}(\omega) \quad (98)$$

Equation 95 can be rewritten as:

$$\begin{aligned} \operatorname{Re} H'(\omega_c) &= -\frac{1}{\pi} PV \left\{ \int_{-\infty}^0 \frac{\operatorname{Im} \hat{H}(\omega) d\omega}{-\omega - \omega_c} + \int_0^{\infty} \frac{\operatorname{Im} \hat{H}(\omega) d\omega}{\omega - \omega_c} \right\} \quad (99) \\ &= -\frac{1}{\pi} PV \left\{ \int_0^{\infty} \frac{\operatorname{Im} \hat{H}(\omega) d\omega}{\omega + \omega_c} + \int_0^{\infty} \frac{\operatorname{Im} \hat{H}(\omega) d\omega}{\omega - \omega_c} \right\} \\ &= -\frac{2}{\pi} PV \int_0^{\infty} \frac{\omega \operatorname{Im} \hat{H}(\omega) d\omega}{\omega^2 - \omega_c^2} \end{aligned}$$

Equation 96 can also be rewritten as:

$$\begin{aligned}
 \text{Im } H'(\omega_c) &= \frac{1}{\pi} PV \left\{ \int_{-\infty}^0 \frac{-\text{Re } \hat{H}(\omega) d\omega}{-\omega - \omega_c} + \int_0^{\infty} \frac{\text{Re } \hat{H}(\omega) d\omega}{\omega - \omega_c} \right\} \\
 &= \frac{1}{\pi} PV \left\{ - \int_0^{\infty} \frac{\text{Re } \hat{H}(\omega) d\omega}{\omega + \omega_c} + \int_0^{\infty} \frac{\text{Re } \hat{H}(\omega) d\omega}{\omega - \omega_c} \right\} \\
 &= \frac{2\omega_c}{\pi} PV \int_0^{\infty} \frac{\omega \text{Re } \hat{H}(\omega) d\omega}{\omega^2 - \omega_c^2}
 \end{aligned} \tag{100}$$

It is these two Equations, 99 and 100, which are so called the Kramer - Kronig version of the Hilbert transform. They are continuous forms of the Hilbert transform and can be used to relate the real and imaginary parts of a frequency response function of a linear system. A new form of the Hilbert transform is currently being developed by using the inverse Fourier transform. It will replace Equations 99 and 100 to reduce the speed limitation in the frequency domain calculation.

As earlier defined, the frequency response function is the ratio of the Fourier transform of the output signal over the Fourier transform of the input signal.

$$\hat{H}(\omega) = \frac{\mathbf{F}\{y(t)\}}{\mathbf{F}\{x(t)\}} = \text{Re } \hat{H}(\omega) + j \text{Im } \hat{H}(\omega) \tag{101}$$

The Hilbert transform of the measured complex function, $\hat{H}(\omega)$ is defined as:

$$\mathbf{H}\{\hat{H}(\omega)\} = H'(\omega) = \text{Re } H'(\omega) + j \text{Im } H'(\omega) \tag{102}$$

where $\text{Re } H'(\omega)$ represents the real part of the Hilbert transform and $\text{Im } H'(\omega)$ represents the imaginary part of the Hilbert transform as defined in Equations 99 and 100. Thus, for a linear system the Hilbert transform of a system's frequency response function, $\mathbf{H}\{\hat{H}(\omega)\}$ equals the original frequency response function, $\hat{H}(\omega)$. This can be mathematically written as:

$$H'(\omega) = \hat{H}(\omega) \tag{103}$$

Thus, for a linear system, the Hilbert transform can be used to calculate the real part of $\hat{H}(\omega)$ from knowing the imaginary part and visa versa, by using Equations 99 and 100. In practical terms, when a frequency response function is obtained through a particular testing technique, the procedure is to compute the imaginary part of the frequency response function by taking the Hilbert transform of the real part. This calculated imaginary part is then compared to the actual measured imaginary part. The same type of procedure is also applied to the real part of the functions. If the correlation between the calculated and the actual measured parts are good then the system is classified as a linear system.

However, when the measured frequency response function is contaminated by nonlinearities, the correlation is poor. In this case, there exist the condition whereby the relationship between Equations 99 and 100 no longer hold true. This condition can be expressed as:

$$\mathbf{H}\{\hat{H}(\omega)\} = H'(\omega) \neq \hat{H}(\omega) \quad (104)$$

Therefore, it can be stated that for a causal system to exist $H'(\omega)$ must equal $\hat{H}(\omega)$, and if $H'(\omega)$ does not equal $\hat{H}(\omega)$ the system is classified as being nonlinear.

Thus, the following statements must be valid for a structure to be linear:

$$H'(\omega) = \hat{H}(\omega) \quad (105)$$

$$\mathbf{F}^{-1}[\hat{H}(\omega)] = h(t) \quad (106)$$

It should be noted that the same conclusions have been derived by Vinh ^[66] using Parseval's theorem, which states that the energy in the frequency domain is equal to that in the time domain.

Because one can only consider a limited frequency range, one can derive a useful algorithm for discrete frequency response functions from Equations 99 and 100.

Assume that $\hat{H}(\omega)$ is defined at n number of frequencies, $\omega_1 \dots \omega_n$ (where $\omega_n = n\Delta\omega$), and that:

$$\hat{H}(\omega) = 0 \text{ for } \omega < \omega_1, \omega > \omega_n \quad (107)$$

The discrete form of the Hilbert transform is then:

$$\text{Re } H'(\omega) = H'_R(\omega) = -\frac{2}{\pi} \sum_{k=1}^n \frac{\hat{H}_I(\omega_k) \omega_k \Delta\omega}{\omega_k^2 - \omega^2} \quad (108)$$

$$\text{Im } H'(\omega) = H'_I(\omega) = \frac{2\omega}{\pi} \sum_{k=1}^n \frac{\hat{H}_R(\omega_k) \omega_k \Delta\omega}{\omega_k^2 - \omega^2} \quad (109)$$

where:

$$\Delta\omega = \omega_k - \omega_{k-1} = \frac{(\omega_n - \omega_1)}{(n - 1)}$$

Since these functions are exactly linear, they will obey the equality condition where:

$$\mathbf{H}\{\hat{H}_R\} = \hat{H}_I \quad (110)$$

$$\mathbf{H}\{\hat{H}_I\} = \hat{H}_R$$

However, when the magnitude of the real or imaginary part of $\hat{H}(\omega)$ does not equal zero at the frequency limits such that Equation 110 is not satisfied, errors in the transformed data are found due to the fact that the Hilbert transform is based upon an integral from $-\infty$ to ∞ . To correct for these errors correction terms can be introduced to account for the transformed data outside the limited frequency range; however, a preliminary estimation of the natural frequencies within the desired frequency band is required.

These correction terms are derived by first assuming the data is represented as a mobility frequency response function such that:

$$\hat{H}(\omega) = \sum_{r=1}^N \frac{j \omega X_r}{\omega^2 - \omega_r^2 (1 + j \delta_r)} \quad (111)$$

Considering only one degree of freedom, the continuous Hilbert transform is broken up into three frequency ranges:

$$H'_{Re}(\omega_c) = -\frac{2}{\pi} PV \left\{ \int_0^{\omega_h} \frac{\omega \hat{H}_I(\omega) \partial \omega}{\omega^2 - \omega_c^2} + \int_{\omega_l}^{\omega_h} \frac{\omega \hat{H}_I(\omega) \partial \omega}{\omega^2 - \omega_c^2} + \int_{\omega_h}^{\infty} \frac{\omega \hat{H}_I(\omega) \partial \omega}{\omega^2 - \omega_c^2} \right\} \quad (112)$$

$$H'_{Im}(\omega_c) = \frac{2\omega_c}{\pi} PV \left\{ \int_0^{\omega_l} \frac{\omega \hat{H}_R(\omega) \partial \omega}{\omega^2 - \omega_c^2} + \int_{\omega_l}^{\omega_h} \frac{\omega \hat{H}_R(\omega) \partial \omega}{\omega^2 - \omega_c^2} + \int_{\omega_h}^{\infty} \frac{\omega \hat{H}_R(\omega) \partial \omega}{\omega^2 - \omega_c^2} \right\} \quad (113)$$

The first and last terms are the corrections terms for the low and high frequency range. In these ranges, ω is assumed to influence any resonant frequencies, ω_r . Therefore, for the lightly damped case:

$$\omega^2 - \omega_r^2 (1 + j \delta) \approx \omega^2 - \omega_r^2 \quad (114)$$

The correction terms can then be written as:

$$A_R(\omega_c) = -\frac{2}{\pi} \int_0^{\omega_1 - \epsilon} \frac{\omega X_R}{(\omega^2 - \omega_r^2)} - \frac{\omega d\omega}{(\omega^2 - \omega_c^2)} \quad (115)$$

$$B_R(\omega_c) = -\frac{2}{\pi} \int_{\omega_k + \epsilon}^{\infty} \frac{\omega X_R}{(\omega^2 - \omega_r^2)} - \frac{\omega d\omega}{(\omega^2 - \omega_c^2)} \quad (116)$$

$$A_I(\omega_c) = \frac{2\omega_c}{\pi} \int_0^{\omega_1 - \epsilon} \frac{\omega X_I}{(\omega^2 - \omega_r^2)} - \frac{d\omega}{(\omega^2 - \omega_c^2)} \quad (117)$$

$$B_I(\omega_c) = \frac{2\omega_c}{\pi} \int_{\omega_k + \epsilon}^{\infty} \frac{\omega X_I}{(\omega^2 - \omega_r^2)} - \frac{d\omega}{(\omega^2 - \omega_c^2)} \quad (118)$$

When there is more than one mode in the response between ω_1 and ω_n the correction is made by summing the individual terms for each mode. Therefore, the discrete Hilbert transform formula are:

$$H'_R(\omega_1) = -\frac{2}{\pi} \sum_{k=1}^n \frac{\hat{H}_I(\omega_k) \omega_k \Delta\omega}{\omega_k^2 - \omega_1^2} + A_R + B_R \quad (119)$$

$$H'_I(\omega_1) = \frac{2\omega_1}{\pi} \sum_{k=1}^n \frac{\hat{H}_R(\omega_k) \Delta\omega}{\omega_k^2 - \omega_1^2} + A_I + B_I \quad (120)$$

with

$$\Delta\omega = \frac{\omega_n - \omega_1}{(n - 1)}$$

Utilization of the Hilbert transform for the identification of nonlinearities has proven to be useful in the case of a sinusoidal excitation. However, in the case where a random or transient excitation signal is desired, using the Hilbert transform to detect nonlinearities would not be valid since the use to the Fourier transform results in frequency response functions which satisfy the equality condition $\hat{H}(\omega) = H'(\omega)$, and thus a nonlinearity could not be detected [68].

One disadvantage with this particular application to detect nonlinearities is that the Hilbert transform in the frequency domain is a continuous transform over all frequencies. When a discrete transform is defined, errors are introduced and there is a loss of information in the resonant frequency region, particularly in the case of a lightly damped mode.

7.4.6 Volterra and Wiener Functional Series

Volterra first suggested that the input/output relationship of a nonlinear system could be expressed as a functional series in 1887 [71].

The expression for the system response from a stationary random excitation can be written as:

$$x(t) = x_1(t) + x_2(t) + \eta(t) \quad (121)$$

where

- $x(t)$ = Total measured response
- $x_1(t)$ = Linear response term
- $x_2(t)$ = Nonlinear response term
- $\eta(t)$ = extraneous uncorrelated noise term

If a particular system is linear and time-invariant, then the output can be expressed as the convolution of the input with the system's unit impulse response:

$$x(t) = \int_{-\infty}^{\infty} h(\tau) f(t - \tau) d\tau \quad (122)$$

In the nonlinear system case, the output can be expressed in a Taylor series as:

$$x(t) = h_0 + \int_{-\infty}^{\infty} h_1(\tau) f(t - \tau) d\tau_1 + \int_{-\infty}^{\infty} \int_{-\infty}^{\infty} h_2(\tau_1, \tau_2) x(t - \tau_1) x(t - \tau_2) d\tau_1 d\tau_2 + \quad (123)$$

$$\int_{-\infty}^{\infty} \int_{-\infty}^{\infty} \int_{-\infty}^{\infty} h_3(\tau_1, \tau_2, \tau_3) x(t - \tau_1) x(t - \tau_2) x(t - \tau_3) d\tau_1 d\tau_2 d\tau_3 + \dots$$

In this equation, $h_n(\tau_1 \dots \tau_n)$ are terms which are referred to as the Volterra Kernels which represent the higher order characteristic terms of a nonlinear system. As a linear time-invariant system is completely characterized by its unit impulse response, so a nonlinear system, which can be represented by a Volterra series, is completely characterized by its Volterra Kernels.

By taking the Fourier transform of Equation 123, the series can be represented in the frequency domain as:

$$X_n(\omega_1, \omega_2, \dots, \omega_n) = H_n(\omega_1, \omega_2, \dots, \omega_n)F(\omega_1)F(\omega_2)\dots F(\omega_n) \quad (124)$$

This equation indicates that by using the higher order calculated frequency response functions, nonlinear systems can be identified and characterized. Because the Volterra equation is a Taylor series, it has several limitations. One problem is the convergence of the Volterra series. Another limitation is encountered in determining the maximum number of terms required in the Volterra expansion.

The Wiener functional series, an alternative functional series, can be written as:

$$x(t) = \sum_{n=0}^{\infty} \int_{(n)} g_n(\tau_1, \tau_2, \dots, \tau_n) H_n(f; t - \tau_1, t - \tau_2, \dots, t - \tau_n) d\tau_1 d\tau_2 \dots d\tau_n \quad (125)$$

A system of a certain general class is characterized by a set of functions called Wiener kernels which are determined by analyzing the system response to a white Gaussian time function. In Wiener's technique, the coefficients of an orthogonal expansion of the Wiener kernels are determined. This leads to the general Wiener model. The Wiener theory is limited to system characterizations with non-white Gaussian inputs and several non-Gaussian waveforms. Wiener eliminated the limitations that are present in the Volterra series by forming the orthogonal set of functions. The advantage of this form is that the estimates of the kernel functions can be obtained by a correlation technique. This method utilizes the orthogonality of the Hermite functions when the excitation is gaussian white noise [72-76].

7.4.7 Bispectral Analysis

In the classical linear spectral analysis, only the statistical relationships between the auto and cross spectra are used in the analysis. The first extension of the linear spectral analysis to higher order investigations is bispectral analysis. This method is utilized as a technique of detecting quadratic nonlinearities. The advantage of this higher order investigation is that it is able to measure the extent of statistical dependency of various combinations of three spectral components. Because of this, the bispectral technique has proven very useful in the nonlinear study of vibrations.

The cross bispectrum (C.B.S.) is one type of bispectrum which evaluates the quadratic statistical relationship among three spectral components. Mathematically, the cross bispectrum can be expressed as:

$$B_c(\omega_1, \omega_2) = \langle X(\omega_1)X(\omega_2)U^*(\omega_3) \rangle \quad (126)$$

where:

$$\omega_1 + \omega_2 = \omega_3$$

The relationship, $\omega_1 + \omega_2 = \omega_3$ denotes that the interaction of two complex spectral components generates a third spectral component. In this spectrum, a peak is present when the spectral components, $X(\omega_1)$ and $X(\omega_2)$, are statistically dependent on $U(\omega_3)$. The height of the peak is dependent on the amplitude of the three spectral components. Because of this dependency, a normalized measurement of the statistical dependency is required which is independent of the spectra component's amplitude. This normalized measure is referred to as the cross bicoherence squared (C.B.C.) and is mathematically defined as:

$$b_c^2(\omega_1, \omega_2) = \frac{|B_c(\omega_1, \omega_2)|^2}{\langle |X(\omega_1)X(\omega_2)|^2 \rangle \langle |U(\omega_3)|^2 \rangle} \quad (127)$$

When complete statistical dependency exist between $U(\omega_3)$, $X(\omega_1)$ and $X(\omega_2)$, the cross bicoherence squared will equal unity. If there is no dependency at all the C.B.C. is equal to zero.

The bispectrum therefore measures the extent of statistical dependency between those three spectral components with respect to amplitude. The bicoherence squared is then a normalized measure of the statistical dependency independent of amplitudes; thus, peaks in the spectrum will exist even though the spectral amplitudes are small, if there is significant statistical dependency^[77-80]. Figure 81 shows the sensitivity of the cross bispectrum to quadratic nonlinearities.

7.5 Nonlinearities and Multiple Inputs

7.5.1 The Multiple Input Estimation Technique

Because of the Gaussian probability distribution of the random signal, nonlinearities are difficult to detect through conventional detection methods. When using a deterministic excitation, such as in a slow swept sine signal, nonlinearities can be detected by varying the force level and comparing the frequency response functions. When nonlinearities are present, the frequency response functions obtained will be different, because the force amplitude is not constant throughout the frequency range. To investigate a method for the detection of nonlinearities through the use of a random excitation signal coupled with the multiple inputs, one should review the multiple input theory as described by the Structural Dynamics Research Laboratory at the University of Cincinnati^[18,30,33,43,48]. Section 5 is a complete presentation of multiple input theory.

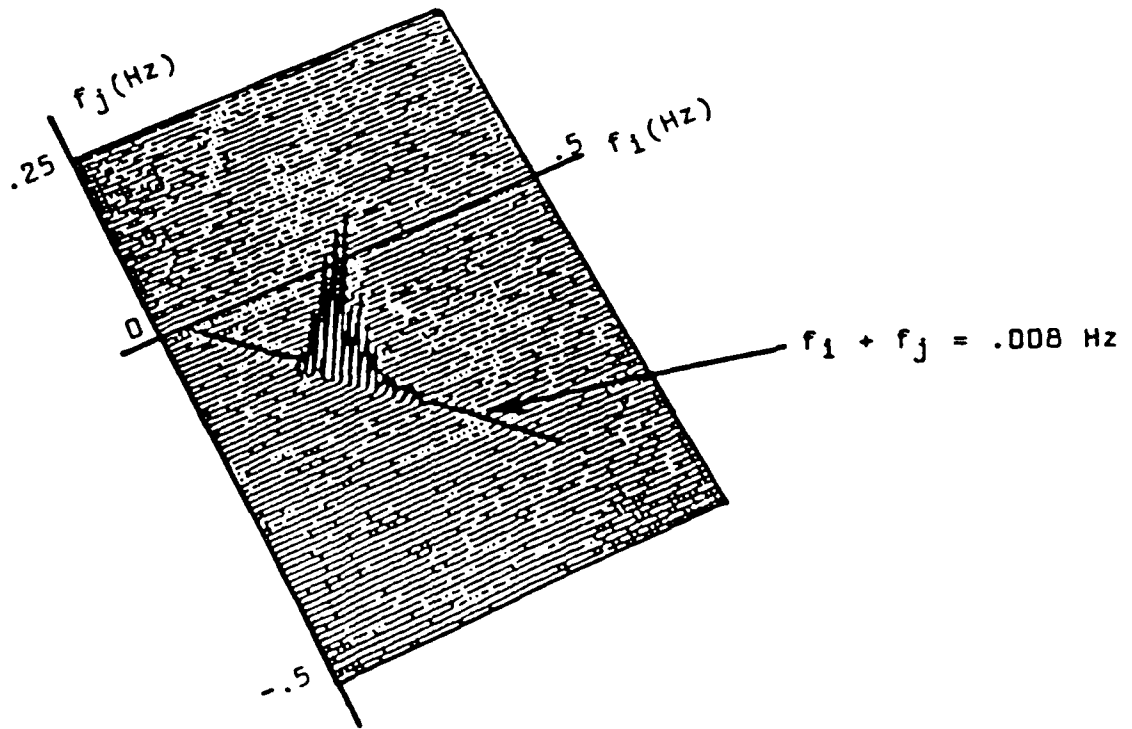


Figure 81. Cross Bispectrum Plot

7.5.2 Higher Order Function Estimates

In most typical mechanical systems, the response which is due to a given excitation is dictated by both linear and nonlinear mechanisms. In many cases, the linear response dominates over the nonlinear response. The nonlinear response is of a higher order and often is assumed to be negligible. However, even weak nonlinear terms can be instrumental in the input/output relationship of the system. It is the intent of this thesis to investigate a procedure for the detection of nonlinearities in structures by using higher order frequency response function estimates that are calculated when using multiple inputs.

Consider the case of a single input and a single output measured during a modal test. The system model assumed is:

$$X(\omega) = H(\omega) * F(\omega) + v(\omega) \quad (128)$$

where:

$X(\omega)$ = Spectrum of the output

$F(\omega)$ = Spectrum of the input

$H(\omega)$ = Frequency response function of the output with respect to the input

$v(\omega)$ = Spectrum of the noise component of X not linearly related to F

If the structure under investigation was a noise-free perfect linear system containing no nonlinearities, Equation 128 could be reduced to:

$$X = H F \quad (129)$$

As nonlinearities are added to the system, Equation 129 becomes increasingly incorrect. To correct for these nonlinearities additional higher order terms could be added, as described in Equation 130.

$$X = H F + \sum_{k=2}^n H_k F^k + \sum_{l=2}^n H_l F^{\frac{1}{l}} \quad (130)$$

This equation should mathematically describe a linear system with any number of nonlinearities. Because of computer limitations and the mathematical complexities involved, this thesis will concentrate on the following simplified estimate.

$$X = H_1 F + H_2 F^2 + H_3 F^3 + H_4 F^4 \quad (131)$$

In this equation, there is only a single input (F) and a single response (X). One could say that the first term of Equation 131 represents the linear portion of the system, while the following terms represents a squared, cubic, and quadratic nonlinear term. By considering the measured input signal F, to be one force along with F^2 , F^3 , and F^4 also representing forces, the multiple input theory can be utilized assuming the forces are uncorrelated. Therefore, four frequency response functions can be calculated. After mathematically manipulating them, these four frequency response functions can be normalized and utilized as nonlinearity detection functions.

7.5.3 Research Approach

Because of the difficulty of creating a physical system with a single known nonlinearity, this thesis will

concentrate on a computer simulated approach to the investigation. The first step is to digitally simulate a dynamic system, by using the computer program BOSS.

BOSS (Block Oriented System Simulator) is a time sharing FORTRAN IV program developed for simulation of dynamic systems by T.R. Comstock of the University of Cincinnati and V.T. Nicolas of Structural Dynamics Research Corporation. The system to be simulated is described by a series of blocks similar to those employed in control systems analysis. Since BOSS is capable of solving first and second order differential equations, the user need not prepare an "analog computer wiring diagram". This feature, combined with unique integrating routines and program logic, results in less time required to define the system, simplified input/output, increased accuracy, and on-line adjustment of all system parameters and time variables.

BOSS provides the capability of simulating systems requiring up to ninety-nine blocks. Twenty-six standard linear and nonlinear block types are available. The user may also generate up to six special block types. BOSS contains an ordering routine that automatically assures that the correct sequence of calculations will be performed^[81].

As input to the BOSS program, a file which contained characteristic properties of a particular system was created. Upon termination of the BOSS program, an output file which contained the filtered digital force and response values for the time domain signals were generated. This dual channel, time domain data was then written to disc. By modifying the existing data acquisition program, the necessary filtered data was obtained directly from disc. The existing data acquisition program was modified as to first obtain the simulated force and response signals from the disc in blocks of 1024 digital time points. A Hanning window was then applied to both signals as a corrective measure for the error, leakage, which smears energy throughout the frequency range. Both the force and response data blocks were then Fourier transformed. Once the blocks were transformed into the frequency domain, the simulated force block was squared, cubed, and quadrupled in order to create the additional input forces. The necessary auto and cross spectra were calculated. These functions were required to calculate the four frequency response functions and multiple coherence function, utilizing the multiple input theory. In order to use the frequency response functions as nonlinear detection functions, each of the functions were first multiplied by its complex conjugate; resulting in individual response power functions. These functions were then normalized by multiplying the function by its corresponding input power spectrum; thus, creating functions which represent the response due to the four inputs. Individually, the higher order functions were meaningless; however, once normalized and compared, the functions could be used as nonlinearity detection functions. Schematically, this process is depicted in Figure 82.

From these functions, one can detect nonlinearities in the test structure. If the structure is linear, the effect of the higher order terms should be negligible and the estimated higher order detection functions should not be significant when they are overlaid. However, as the nonlinearity in the test structure increases, the estimated higher order functions are needed to describe the response of the nonlinear system. Thus, these normalized higher order functions become more significant as the nonlinearity in the test structure increases.

7.5.4 Research Application

As was previously discussed, the BOSS program allowed both linear and nonlinear systems to be simulated digitally. Several different systems with different characteristics were simulated and compared. Table 4 gives a brief description of each of the systems that were analyzed. For each of the systems analyzed (Figures 85-110). plots of the normalized nonlinearity detection functions (top), the real and imaginary parts of the estimated frequency response function due to the actual force (middle), and the multiple coherence function were plotted for comparison purposes. Each of

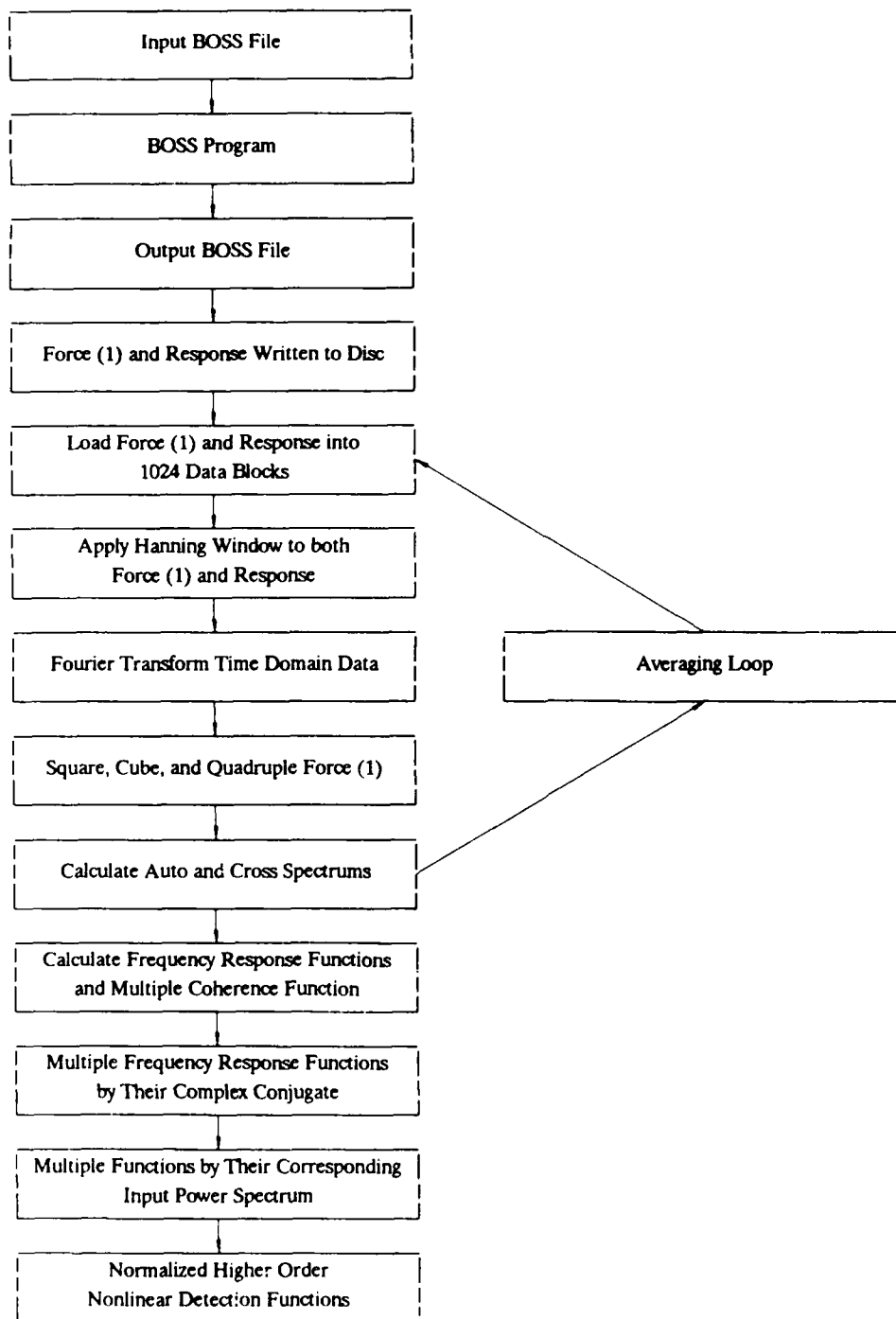


Figure 82. Process Flow Diagram

these plots are identified by their associated BOSS input file names and are referenced in Table 4.

File	Linear/ Nonlinear	Type of Nonlinearity	Nonlinearity	Excitation Signal	Force Level	Number of Averages	Figure
BLRA	Linear		$\beta = 0.0$	Random	1000	100	85
BNRA	Nonlinear	Duffing	$\beta = 1 \times 10^4$	Random	1000	100	86
BNRC	Nonlinear	Duffing	$\beta = 8 \times 10^4$	Random	1000	100	87
BLBA	Linear		$\beta = 0.0$	Burst	1000	100	88
BNB100	Nonlinear	Duffing	$\beta = 8 \times 10^4$	Burst	1000	100	89
BLBA	Linear		$\beta = 0.0$	Burst	1000	25	90
BNBA	Nonlinear	Duffing	$\beta = 1 \times 10^4$	Burst	1000	25	91
BNBB	Nonlinear	Duffing	$\beta = 6 \times 10^4$	Burst	1000	25	92
BNBC	Nonlinear	Duffing	$\beta = 8 \times 10^4$	Burst	1000	25	93
BNBD	Nonlinear	Duffing	$\beta = 10 \times 10^4$	Burst	1000	25	94
BLBLF	Linear		$\beta = 0.0$	Burst	100	25	95
BNLF1	Nonlinear	Duffing	$\beta = 1 \times 10^4$	Burst	100	25	96
BNLF8	Nonlinear	Duffing	$\beta = 8 \times 10^4$	Burst	100	25	97
BLHF0	Linear		$\beta = 0.0$	Burst	5000	25	98
BNHF1	Nonlinear	Duffing	$\beta = 1 \times 10^4$	Burst	5000	25	99
BNHF8	Nonlinear	Duffing	$\beta = 8 \times 10^4$	Burst	5000	25	100
BLK2	Linear		$e_0 = 0.0$	Burst	1000	25	103
BNK21	Nonlinear	Clearance	$e_0 = 0.0001\text{m}$	Burst	1000	25	104
BNK25	Nonlinear	Clearance	$e_0 = 0.0005\text{m}$	Burst	1000	25	105
BLK2H0	Linear		$e_0 = 0.0$	Burst	5000	25	106
BNK2H1	Nonlinear	Clearance	$e_0 = 0.0001\text{m}$	Burst	5000	25	107
BNK2H5	Nonlinear	Clearance	$e_0 = 0.0005\text{m}$	Burst	5000	25	108
BNDA	Nonlinear	Damping	$c \dot{x} ^n$	Burst	1000	25	110

TABLE 4. BOSS Input Files

7.5.4.1 Duffing's Equation Simulated

The first system which was simulated was a single degree-of-freedom system as shown in Figure 83. In this model, the stiffness is proportional to the displacement cubed as in Duffing's equation. Figure 84 shows a block diagram of the BOSS input file for this system. For this simulated system the following parameters were used.

$$\begin{aligned} \text{mass (m)} &= 5 \text{ Kg} \\ \text{damping (c)} &= 100 \text{ N-s/m} \\ \text{stiffness (k)} &= 150,000 \text{ N/m} \end{aligned}$$

In this system, β represents the amount of nonlinearity; as β increases, the amount of nonlinearity in the model also increases. A linear system of this type has a theoretical resonant frequency at 27.5 Hz. and a damping value of 5.8 %.

In the initial investigation, the excitation signal was a pure random signal with a multiplication gain of 1000. A constant 100 averages were also taken for the analysis. Three different systems were then simulated as β equaled 0, 10000, and 80000. As was to be expected, when $\beta = 0$, a linear case existed and the normalized detection functions gave no indication of a nonlinearity being present. As β increased both the frequency response and multiple coherence functions became more distorted. As shown in the nonlinearity detection functions, as β increases the higher order nonlinear terms better

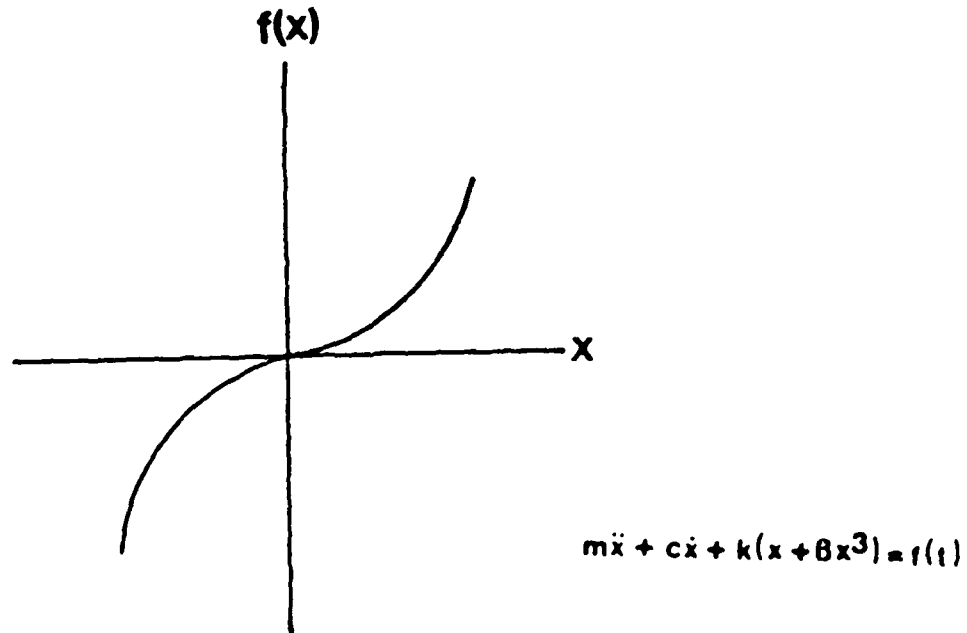


Figure 83. Nonlinear Stiffness Model

describe the nonlinear behavior of the system and have a greater effect on the entire response of the model. Although the nonlinearity simulated was a theoretical cubic nonlinearity, no single higher order term was dominant in describing the nonlinearity (reference Figures 85, 86, 87).

7.5.5 Effects of Varying Test Parameters

The same model was used to investigate the effect of varying the excitation signal, number of averages, and excitation force level. When the excitation signal was changed from a pure random signal to a burst random signal, there was no significant improvement in the quality of the measurement for the linear or nonlinear case. The major advantage of the burst random signal over the pure random signal is the capability of the burst random signal to minimize the "leakage" error.

$$m\ddot{x} + c\dot{x} + k(x + \beta x^3) = f(t)$$

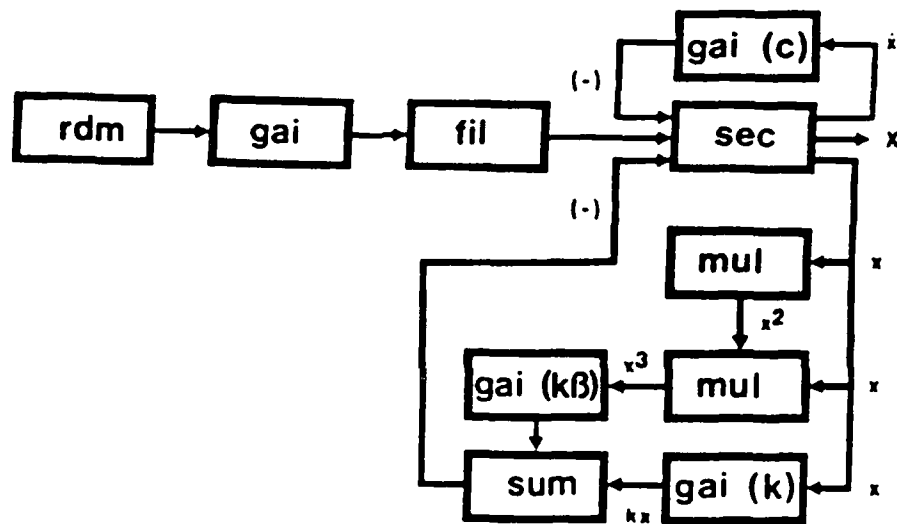


Figure 84. BOSS Nonlinear Stiffness Model

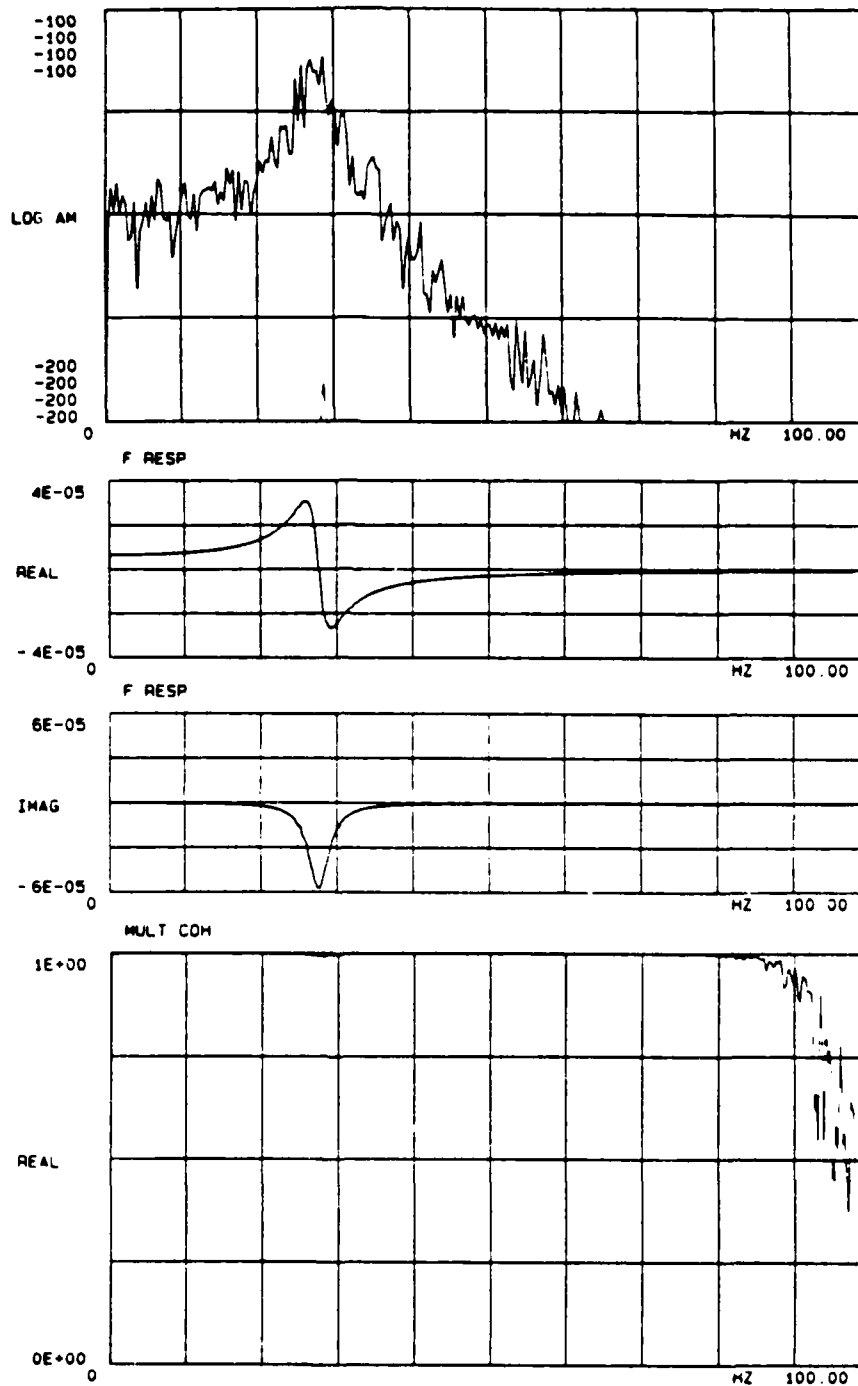


Figure 85. Linear Stiffness Model - BLRA

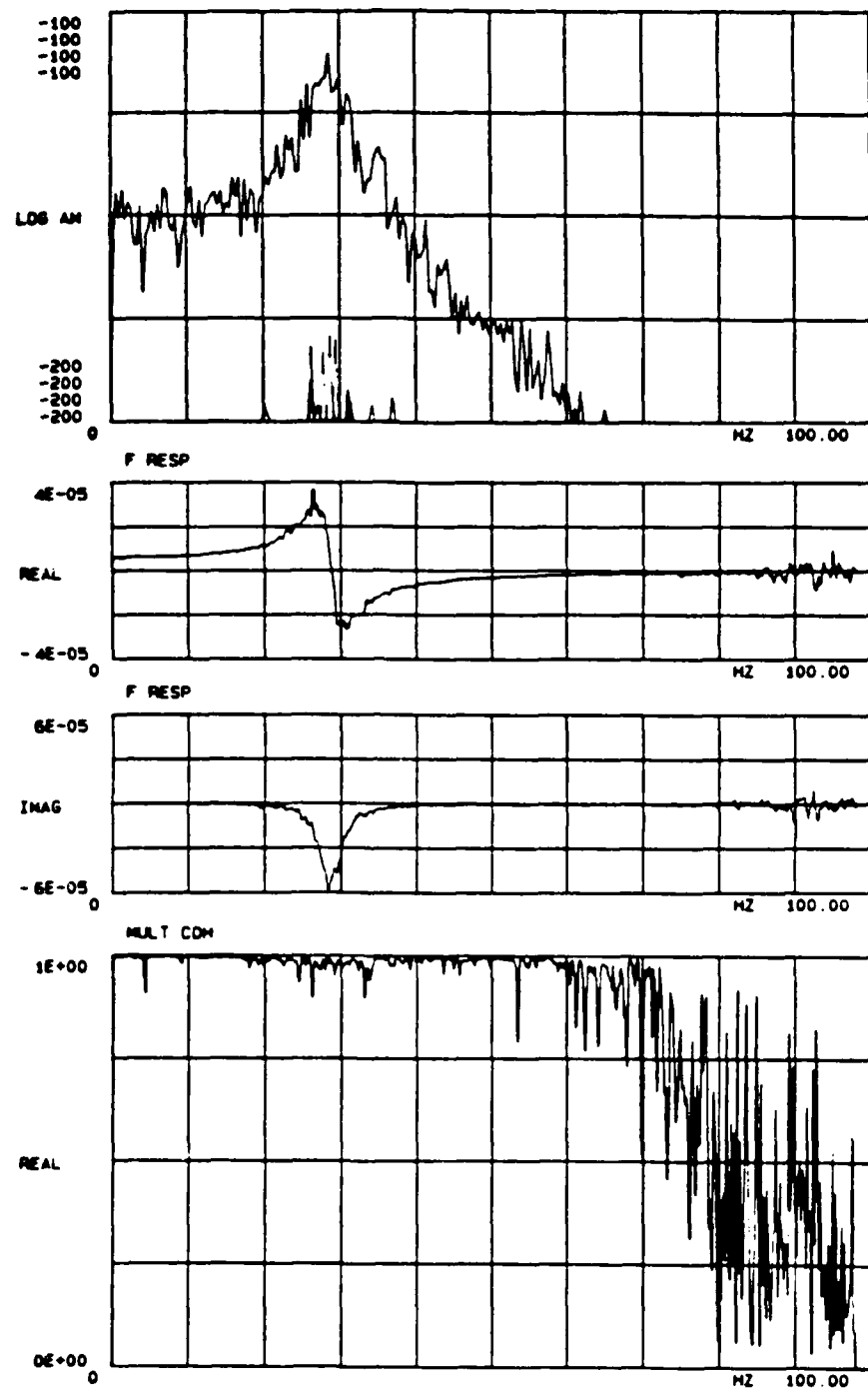


Figure 86. Nonlinear Stiffness Model - BNRA

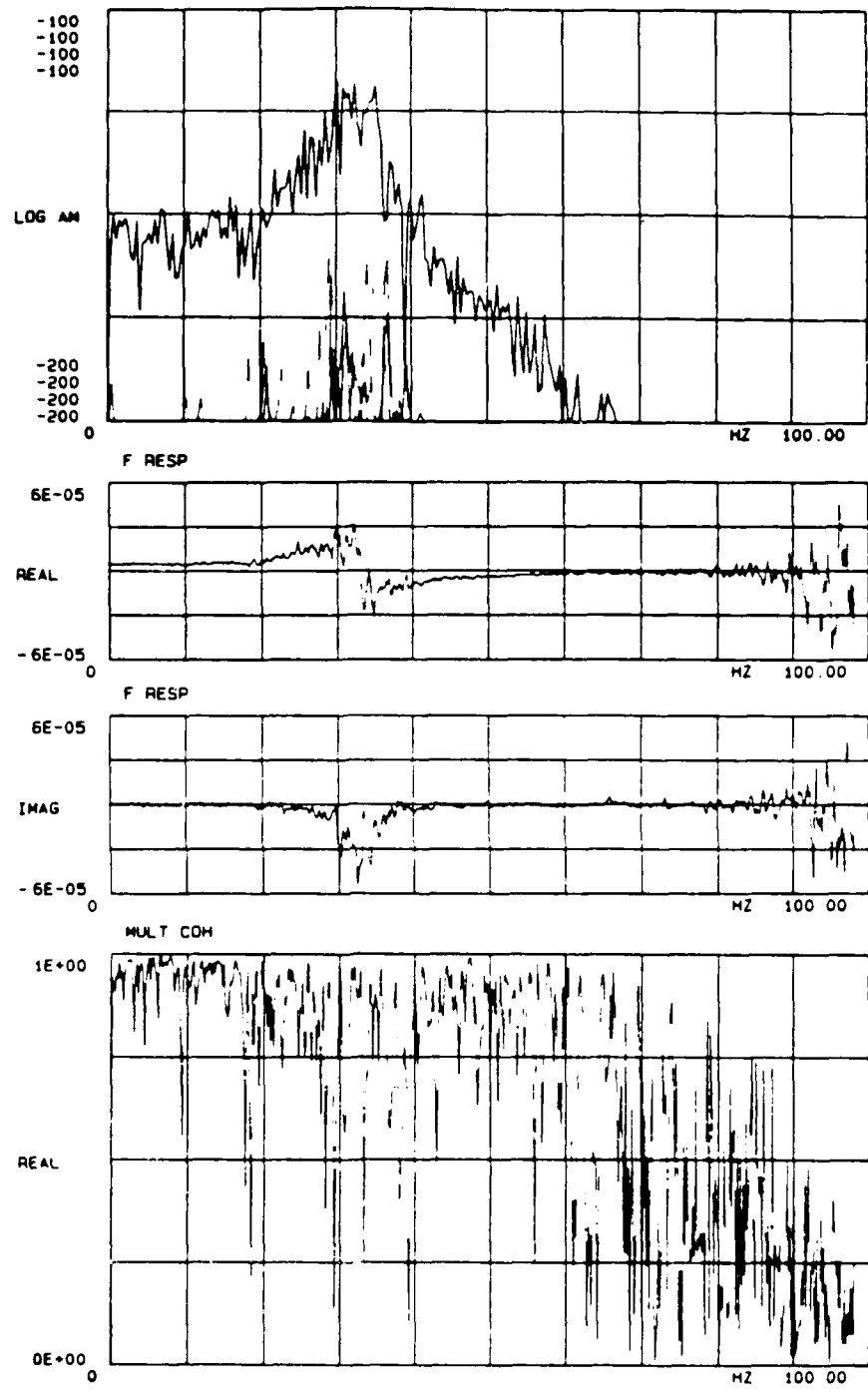


Figure 87. Nonlinear Stiffness Model - BNRC

However, when simulating the system, β was set to 0 and 80000 to simulate a linear and nonlinear case. After comparing the burst random functions with the pure random functions, no significant changes were found (reference Figures 88, 89). After analyzing the synthesized data, decreasing the number of averages from 100 to 25 had little to no effect on the quality of the measurement in both the linear and nonlinear cases (reference Figures 90, 91, 92, 93, 94). This is inconsistent with actual experience which shows that decreasing the number of averages deteriorates the measured functions. The fact that the measurements did not deteriorate, could indicate that the random generator within the BOSS program was not creating a pure random signal.

However, it should be noted that in physical structures, it is possible to minimize the effect of noncoherent noise by increasing the number of averages with a type of random excitation. Utilizing a burst random excitation signal with 25 averages yielded the same results as in the previous nonlinear system. As β was increased the frequency response and multiple coherence functions became more distorted. As in the random excitation case, the higher order nonlinear terms became more dominant as the nonlinearity, β , increased (reference Figures 90, 91, 92, 93, 94).

Using the same model, the force level was decreased by a factor of 10. Three systems were simulated where β equaled 0, 10000, and 80000. In each case, the normalized detection functions indicated a linear system; the higher order terms had little to no effect on the synthesized system because of the low force level. Furthermore, none of the frequency response or the multiple coherence functions demonstrated any distortions. Even though the systems had known nonlinearities, they could be represented as linear systems (reference Figures 95, 96, 97).

Using the same β increment values, the system was simulated at a high force level; 5 times that of the original level. At this high level, even the linear model ($\beta = 0.0$) indicated characteristics of a nonlinearity being present. The higher order terms became somewhat influential in the system. This is most likely due to numerical problems within the BOSS program. As β increased in magnitude, the nonlinearity increased and the higher order detection terms became more dominant (reference Figures 98, 99, 100).

7.5.6 Dead Zone Gap Simulated

To further investigate the proposed detection technique, another nonlinear system was simulated. As shown in Figure 101, the nonlinear parameter in this case is the magnitude of the dead zone gap (e_0). As the dead zone increases, the nonlinearity of the system becomes more severe. Figure 102 shows a block diagram of the BOSS input file for this system. This single degree-of-freedom model used the following parameters.

$$\begin{aligned}\text{mass (m)} &= 5 \text{ Kg} \\ \text{damping (c)} &= 20 \text{ N-s/m} \\ \text{stiffness (k)} &= 75,000 \text{ N/m}\end{aligned}$$

A linear system of this type has a theoretical resonant frequency at 27.5 Hz. and a damping value of 1.2 %.

Initially, a linear case was analyzed where there was no dead zone gap (e_0). As before, the linear system showed no distortions in the frequency response and multiple coherence functions. The detection functions gave no indications of any higher order terms being influenced. A dead zone gap was then introduced at both 10000 m and 50000 m. Again, each of the functions demonstrated that as the nonlinearity of the system increased, the contribution of the higher order terms also increased (reference Figures 103, 104, 105).

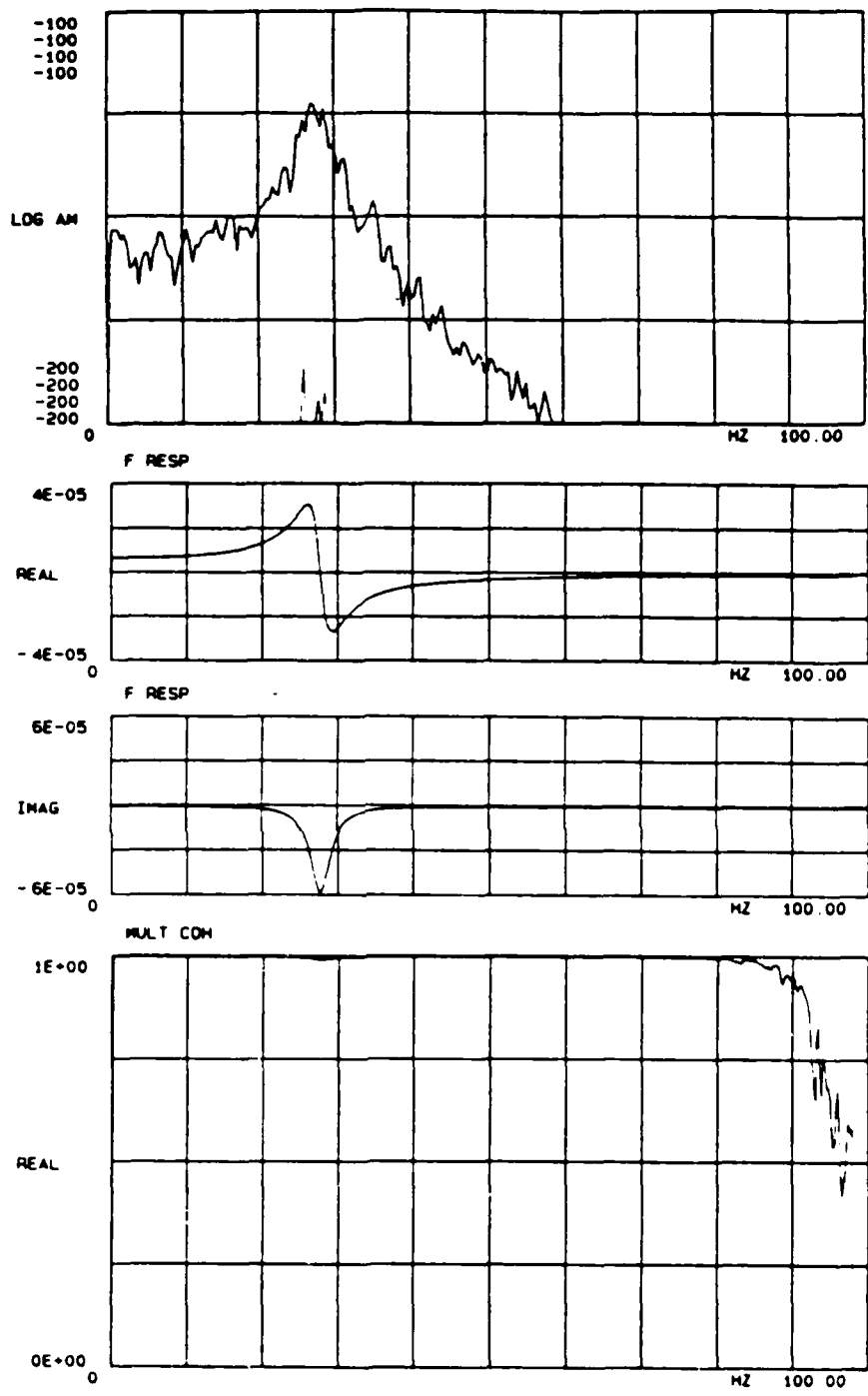


Figure 88. Linear Stiffness Model - BLBA

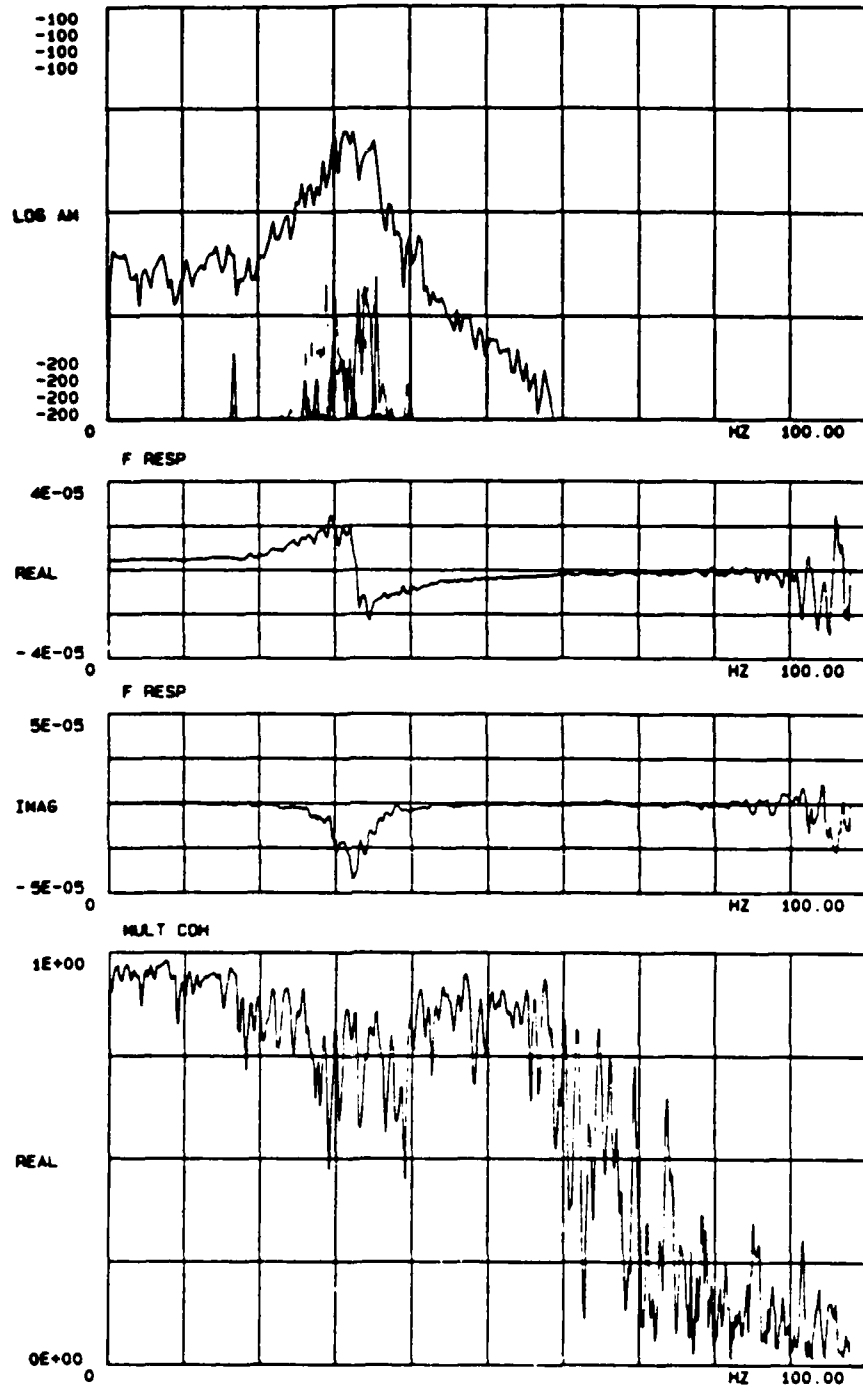


Figure 89. Nonlinear Stiffness Model - BNB100

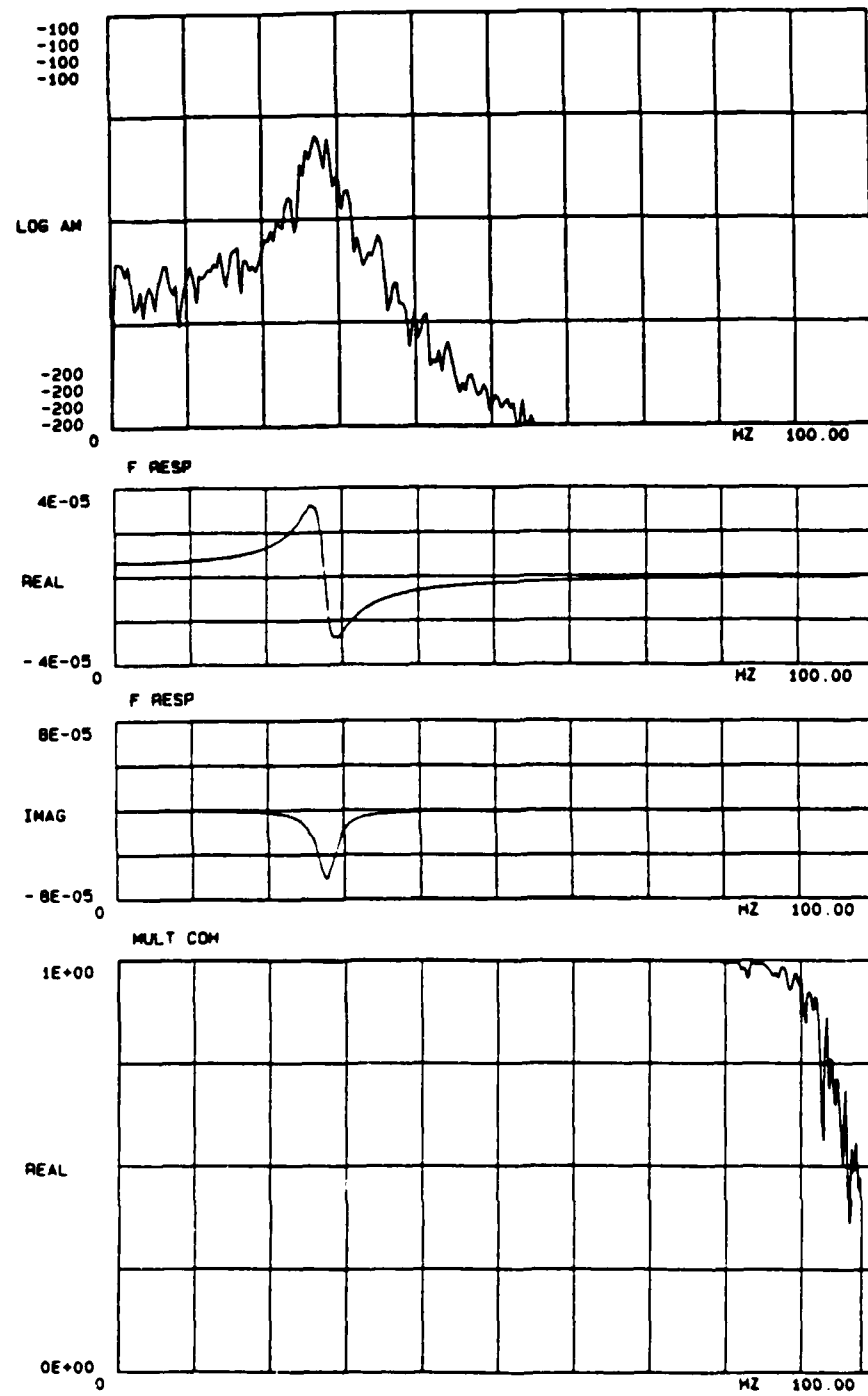


Figure 90. Linear Stiffness Model - BLBA

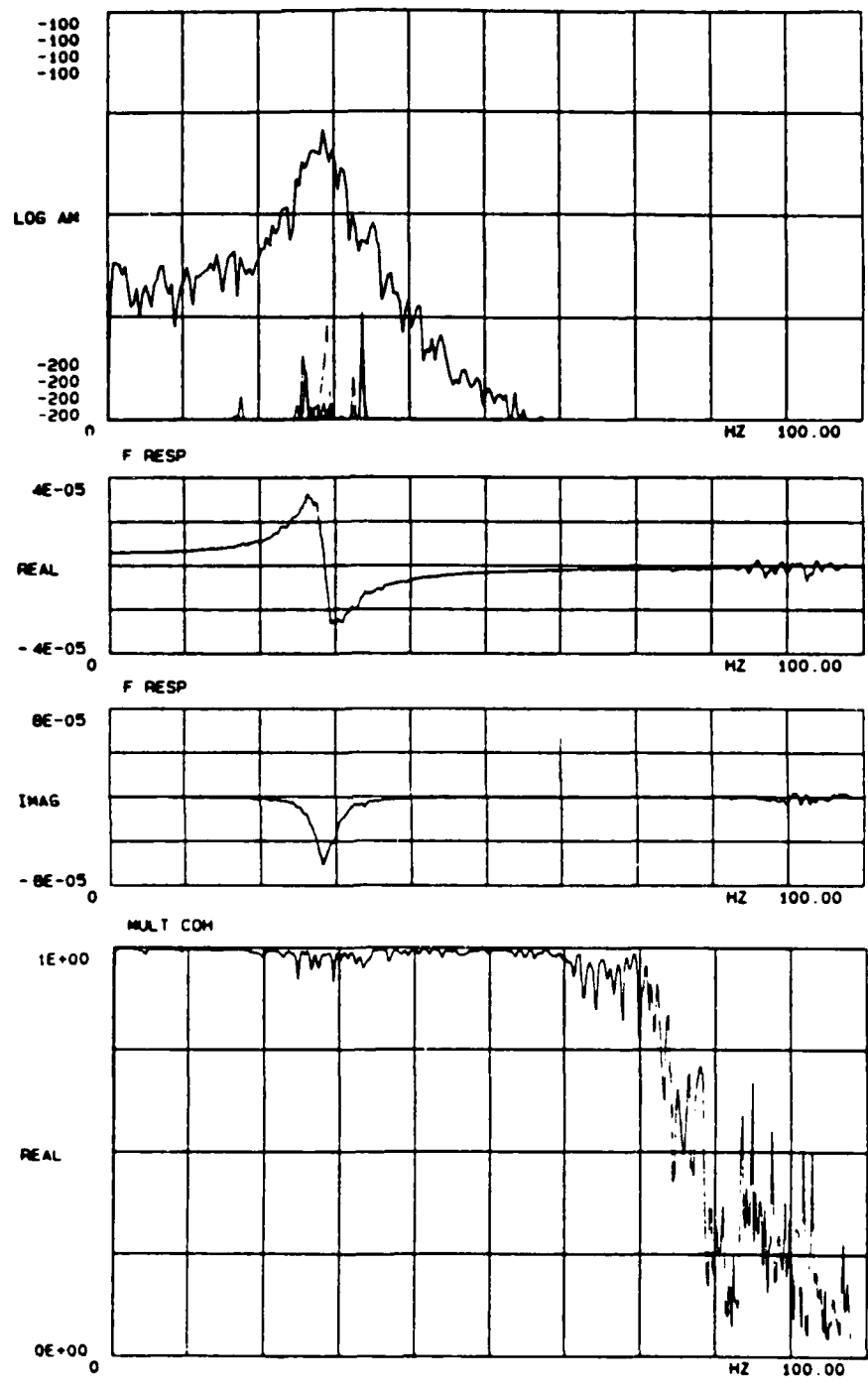


Figure 91. Nonlinear Stiffness Model - BNBA

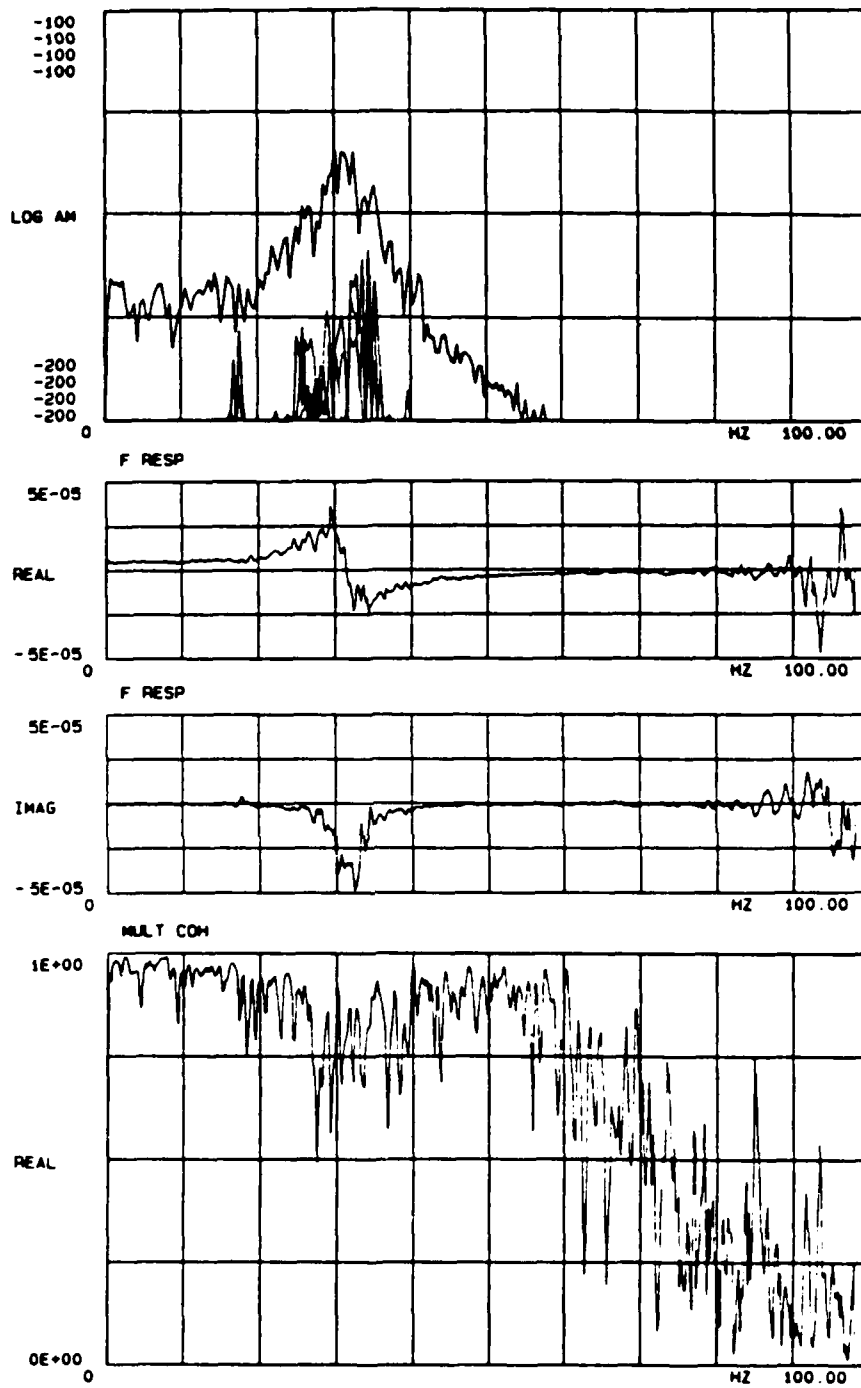


Figure 92. Nonlinear Stiffness Model - BNBB

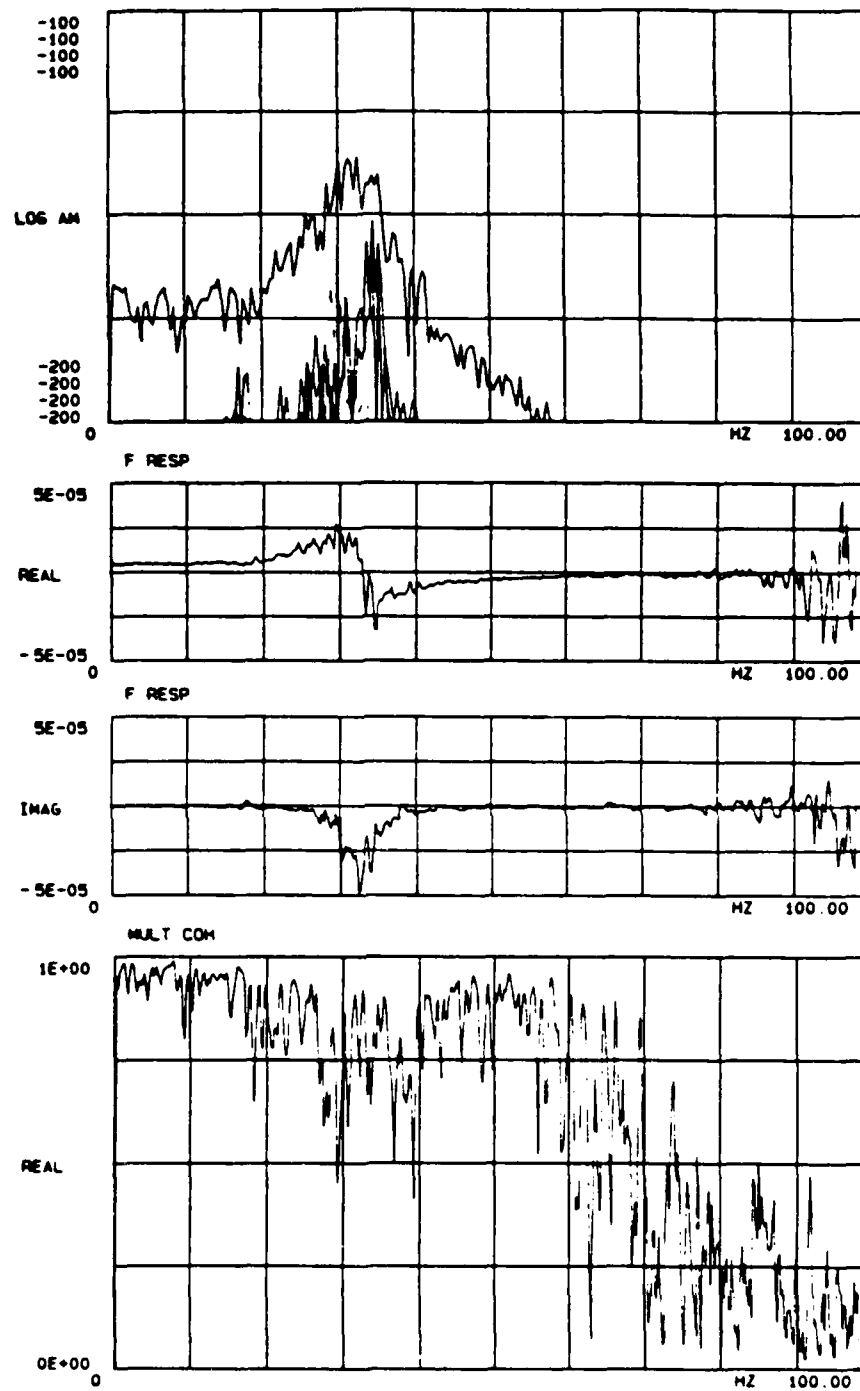


Figure 93. Nonlinear Stiffness Model - BNBC

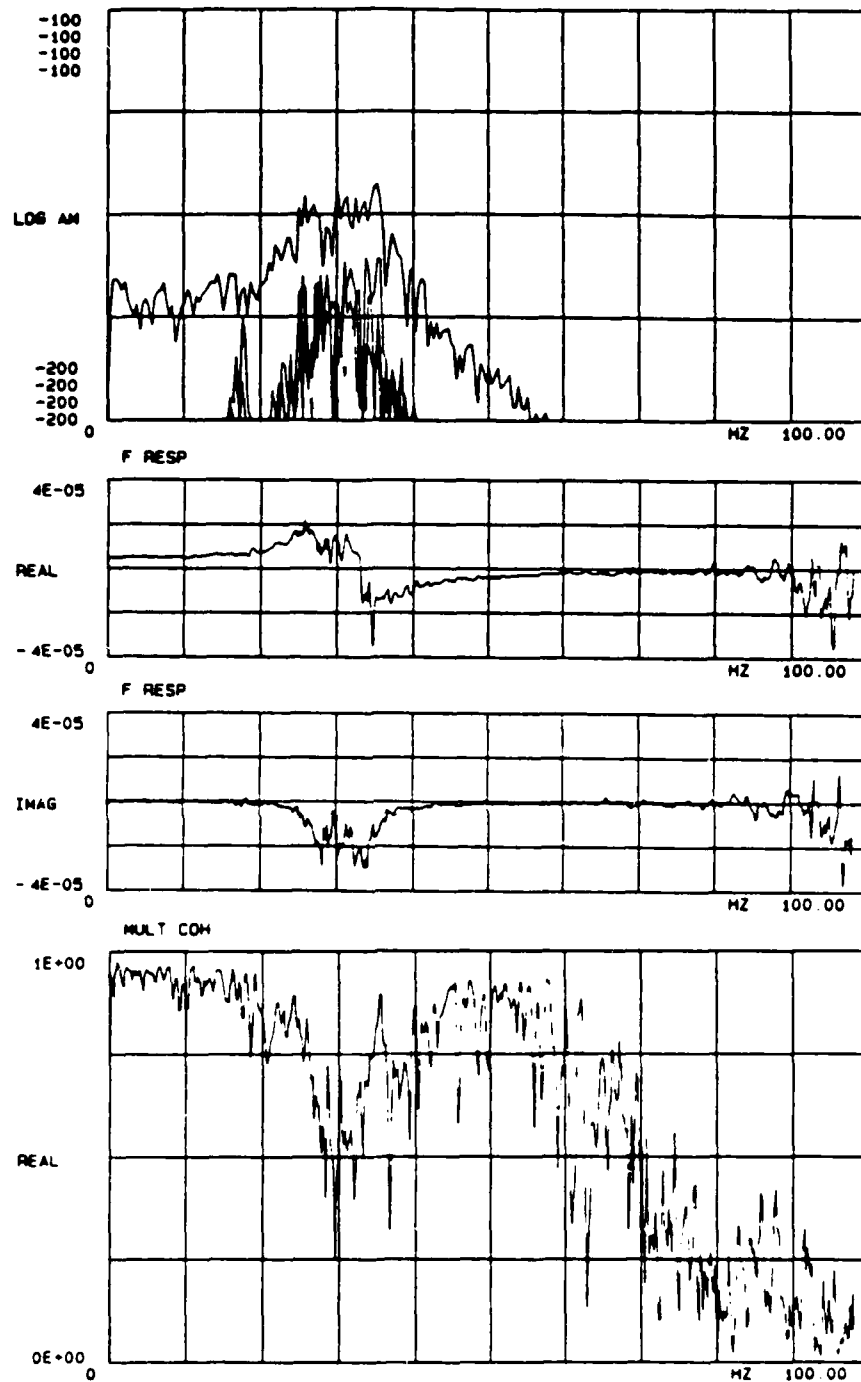


Figure 94. Nonlinear Stiffness Model - BNBD

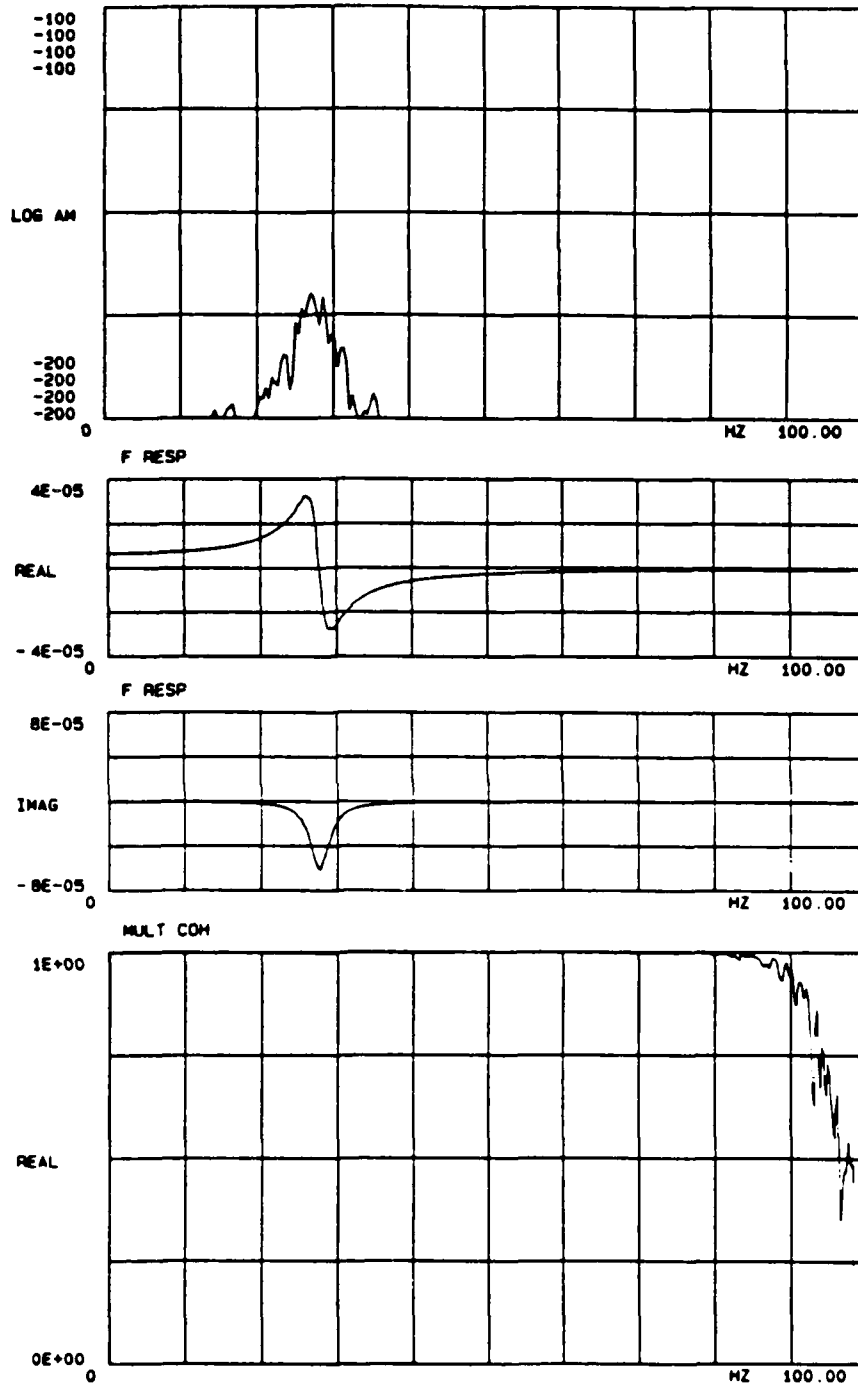


Figure 95. Linear Stiffness Model - BLBLF

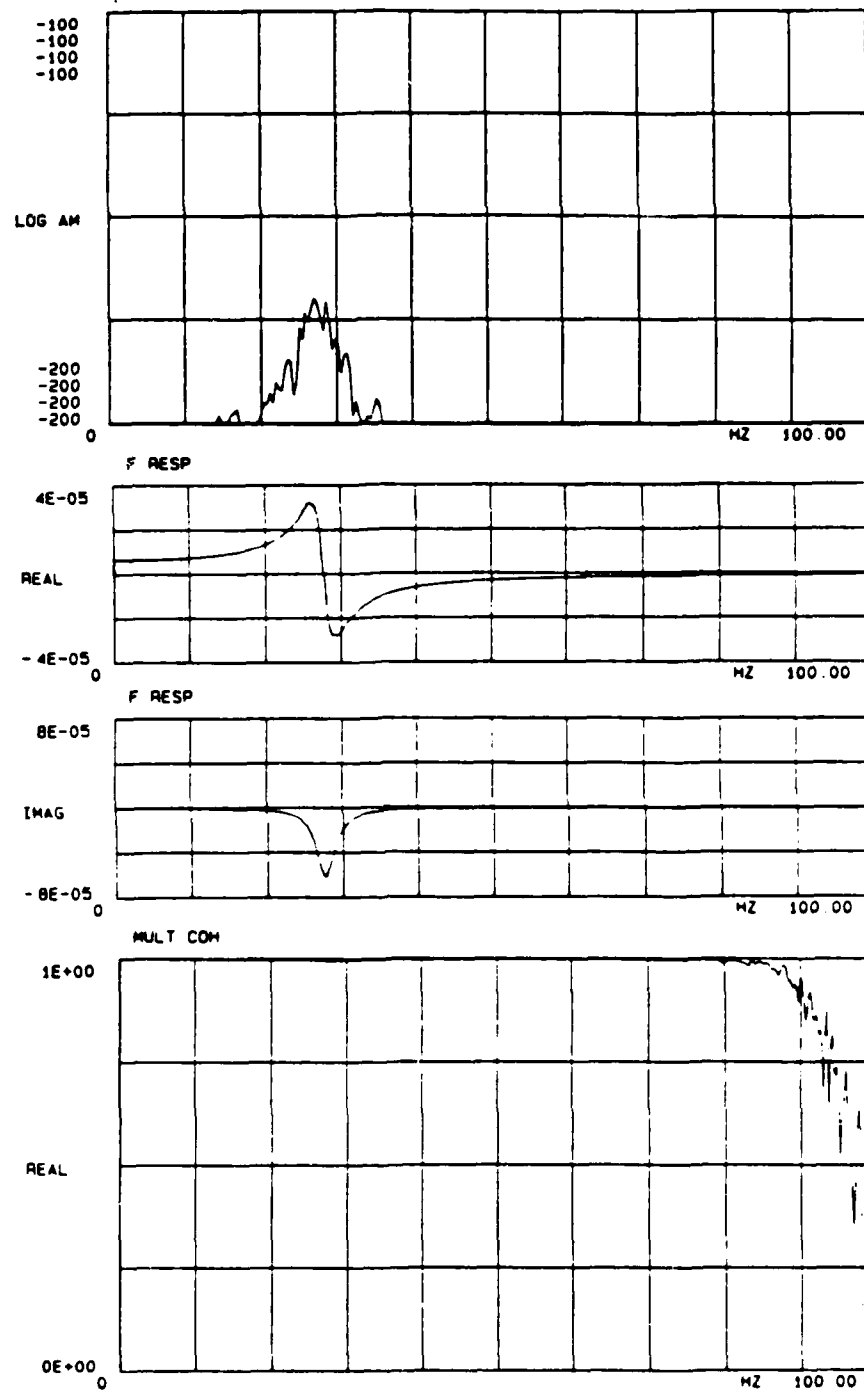


Figure 96. Nonlinear Stiffness Model - BNLF1

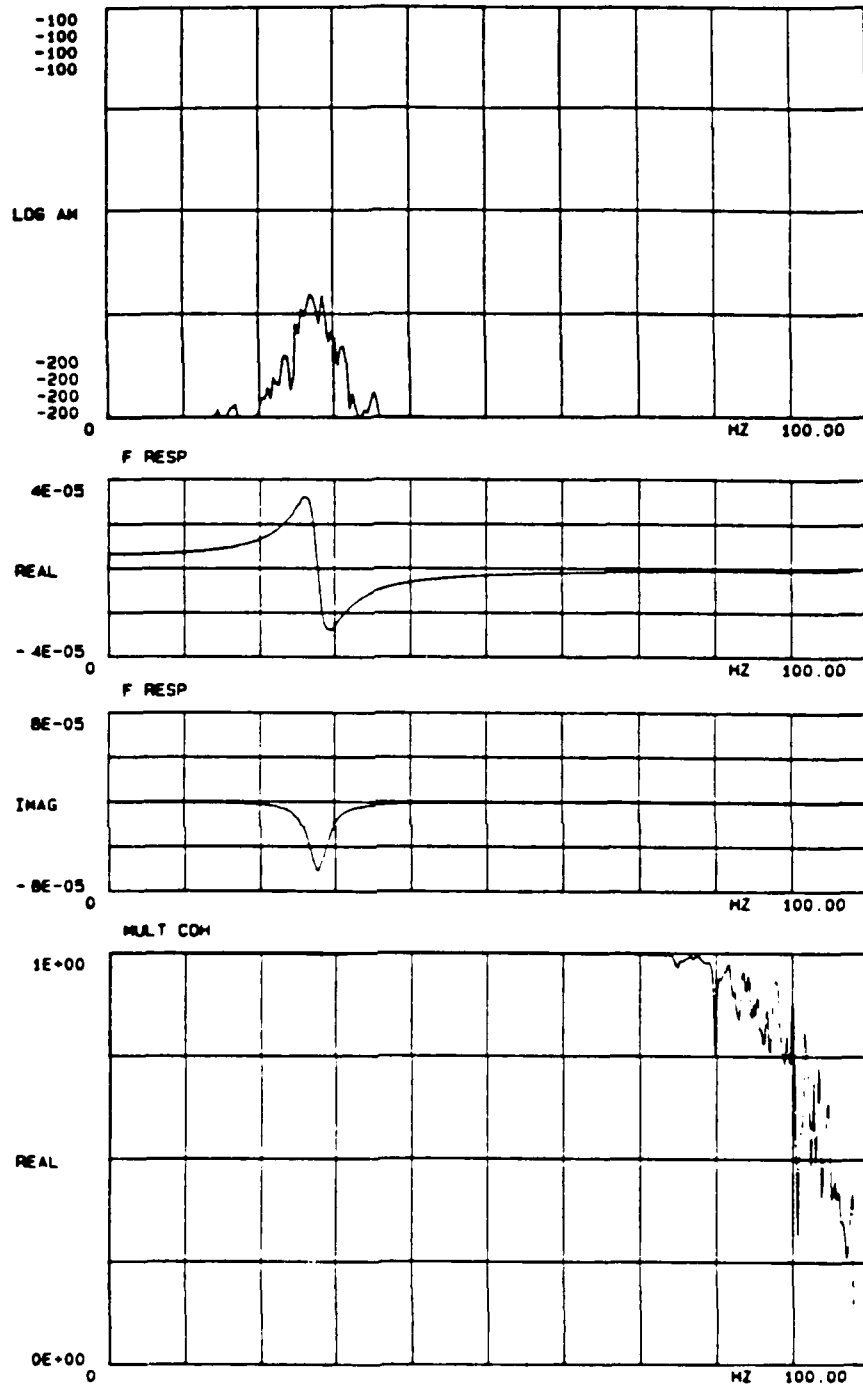


Figure 97. Nonlinear Stiffness Model - BNLF8

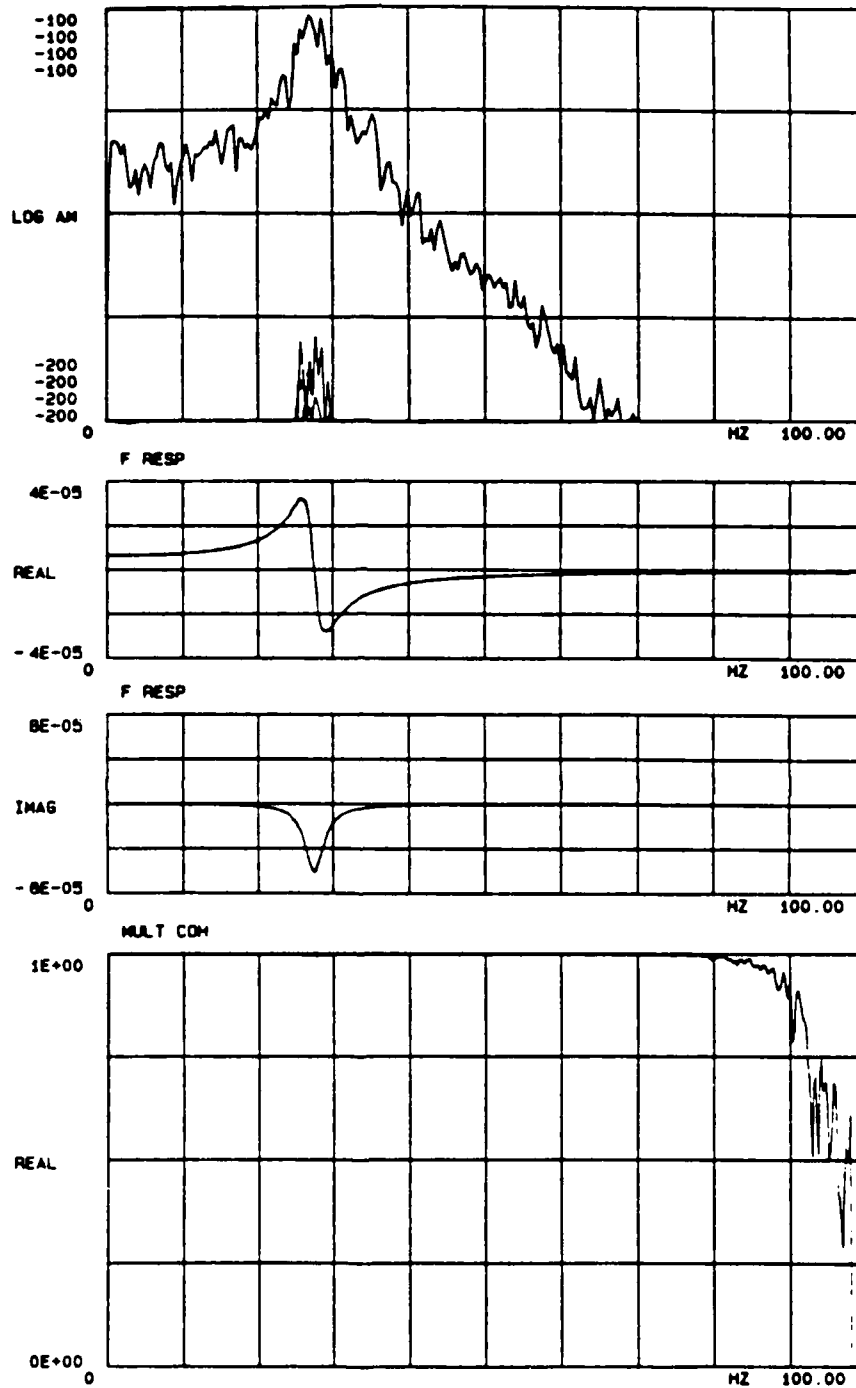


Figure 98. Linear Stiffness Model - BNHF0

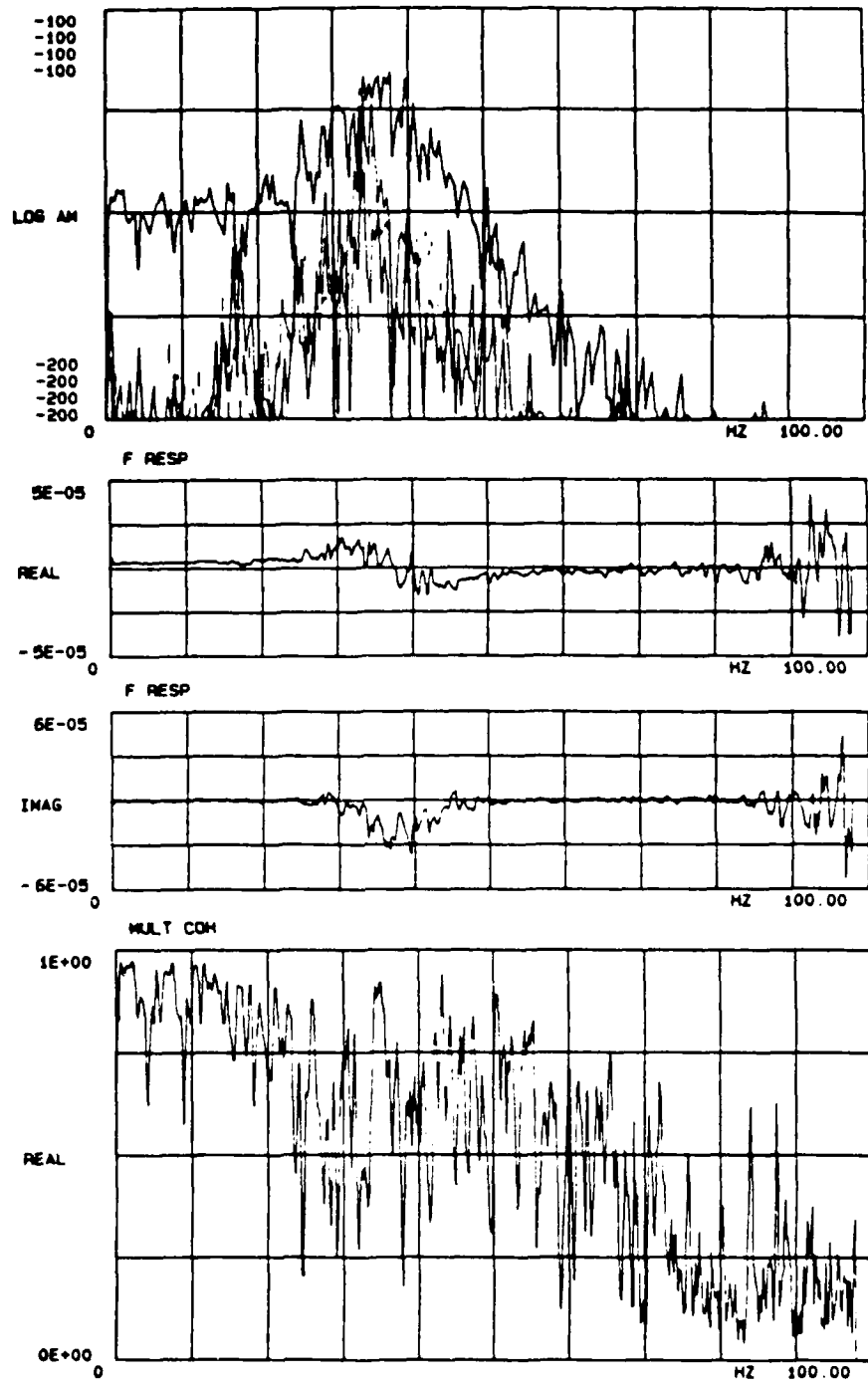


Figure 99. Nonlinear Stiffness Model - BNHF1

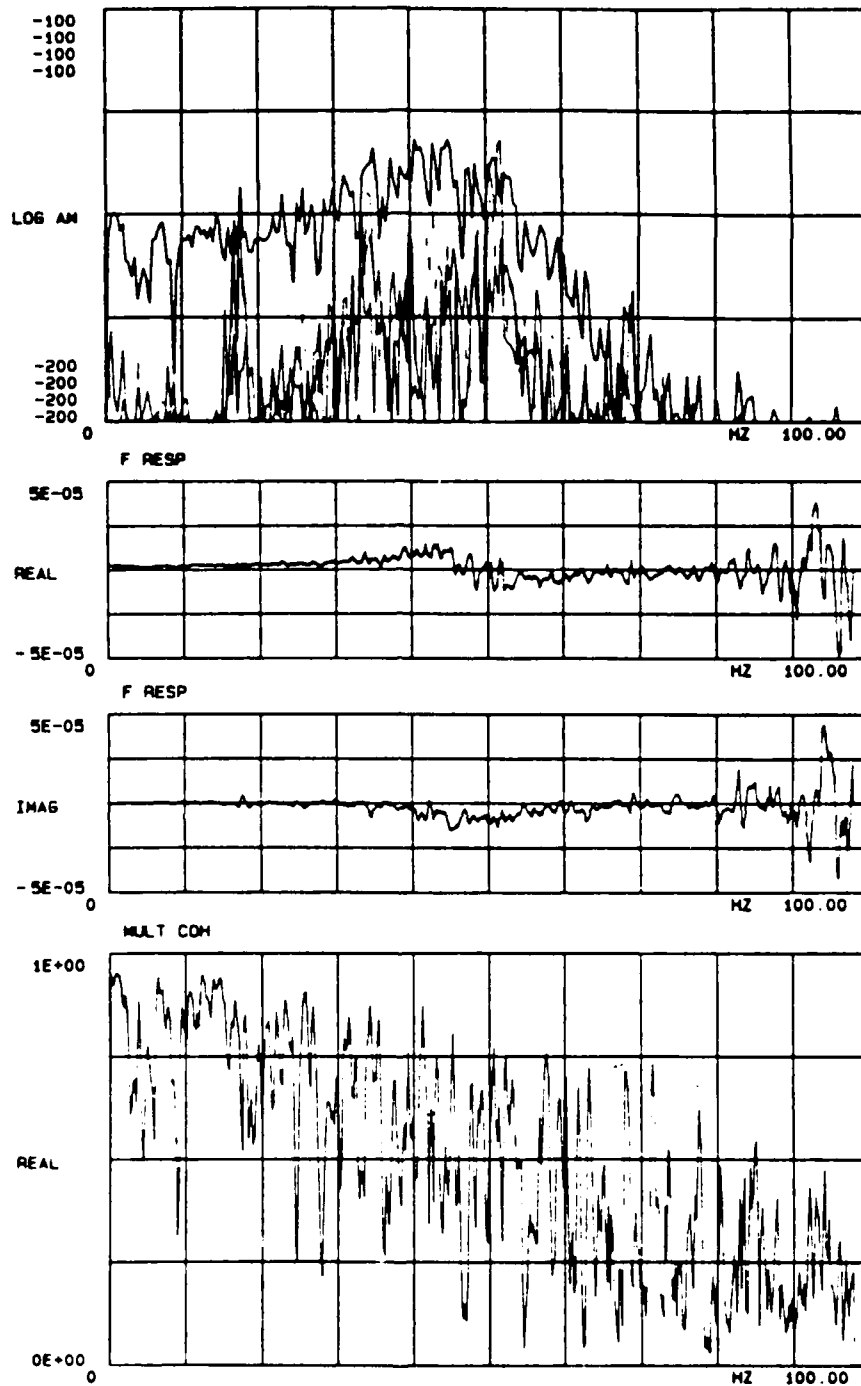
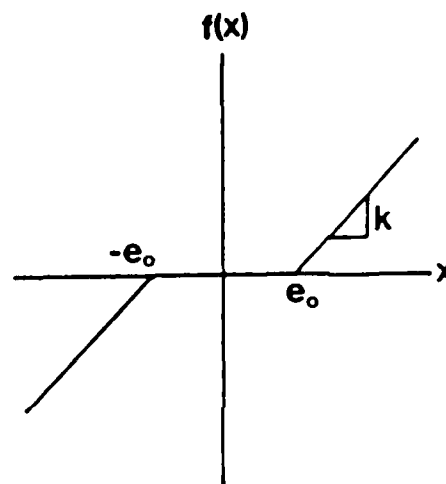
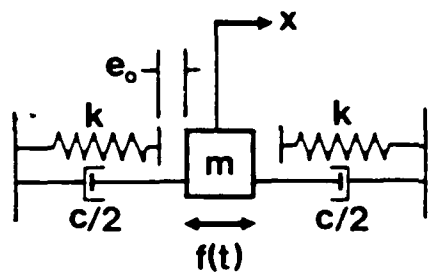


Figure 100. Nonlinear Stiffness Model - BNHF8



- if $x < -e$ \longrightarrow $m\ddot{x} + c\dot{x} + k(x+e) = f(t)$
- if $-e \leq x \leq e$ \longrightarrow $m\ddot{x} + c\dot{x} = f(t)$
- if $e < x$ \longrightarrow $m\ddot{x} + c\dot{x} + k(x-e) = f(t)$

Figure 101. Nonlinear Clearance Model

if $x < -e$ \rightarrow $m\ddot{x} + c\dot{x} + k(x+e) = f(t)$
 if $-e \leq x \leq e$ \rightarrow $m\ddot{x} + c\dot{x} = f(t)$
 if $e < x$ \rightarrow $m\ddot{x} + c\dot{x} + k(x-e) = f(t)$

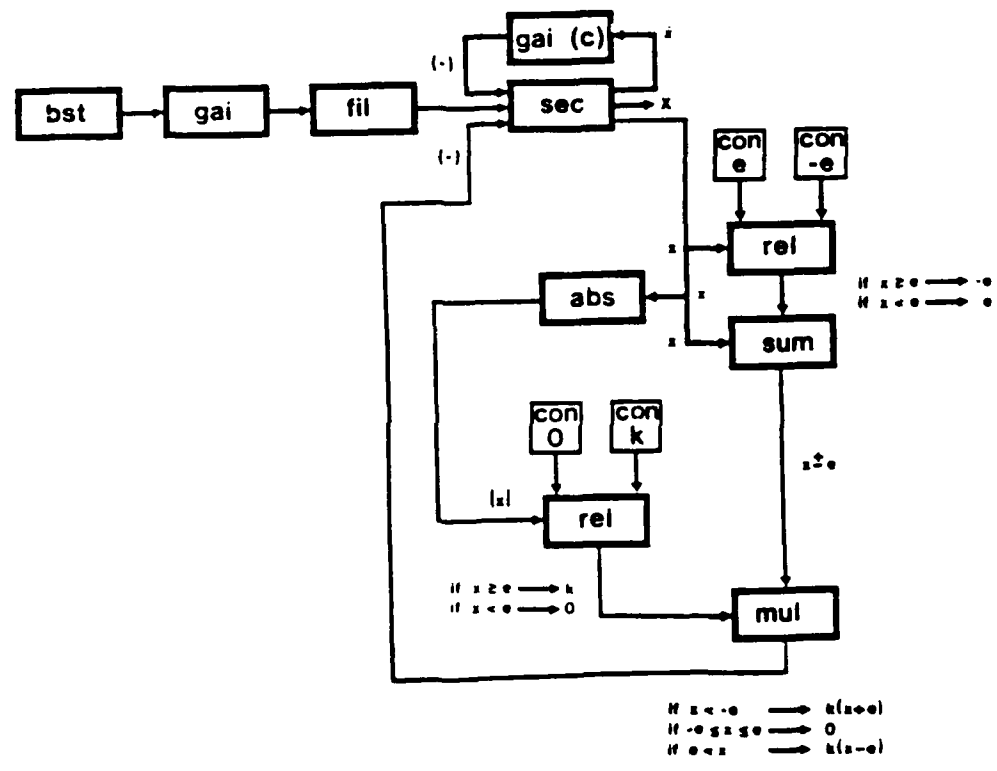


Figure 102. BOSS Nonlinear Clearance Model

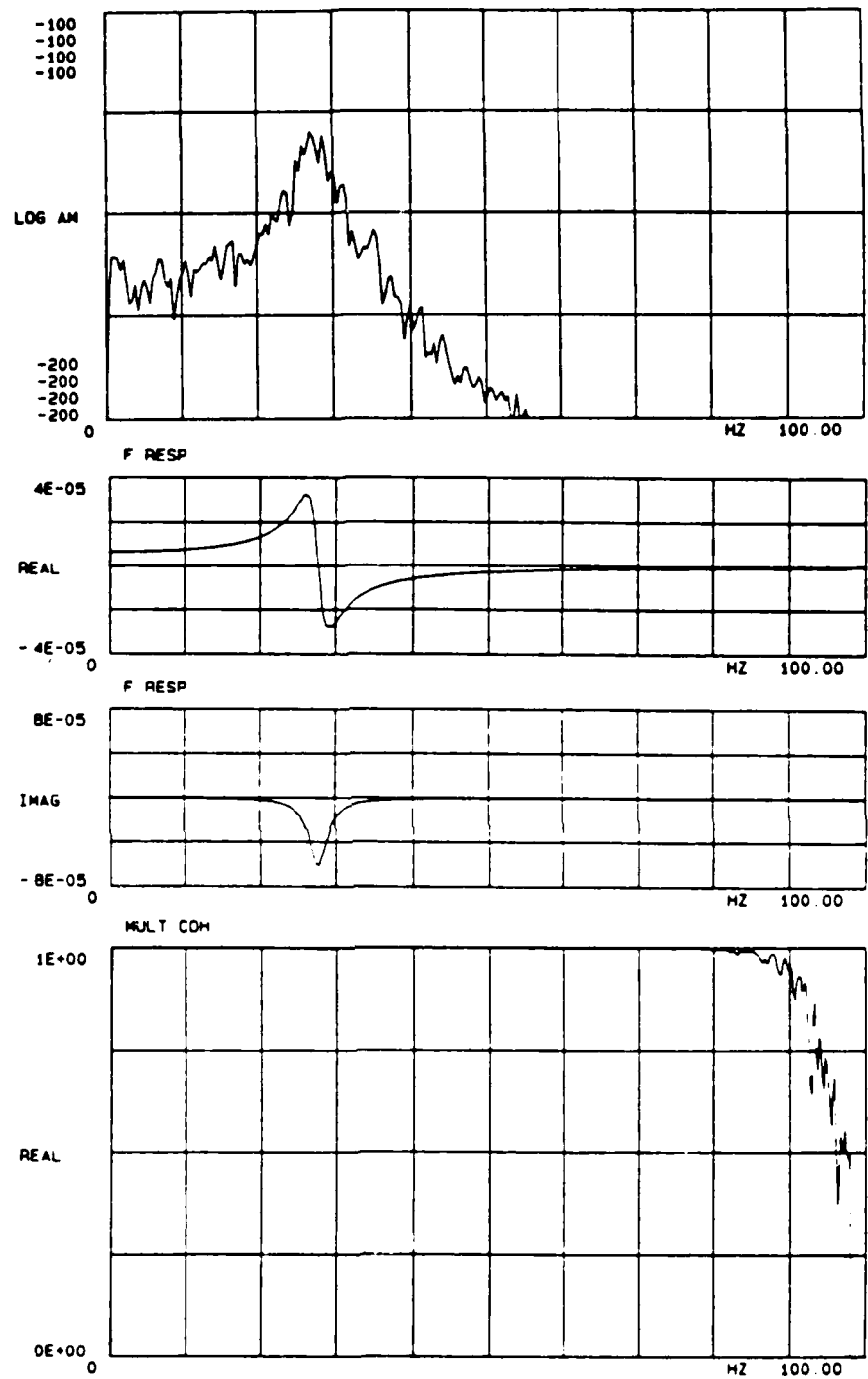


Figure 103. Linear Clearance Model - BLK2

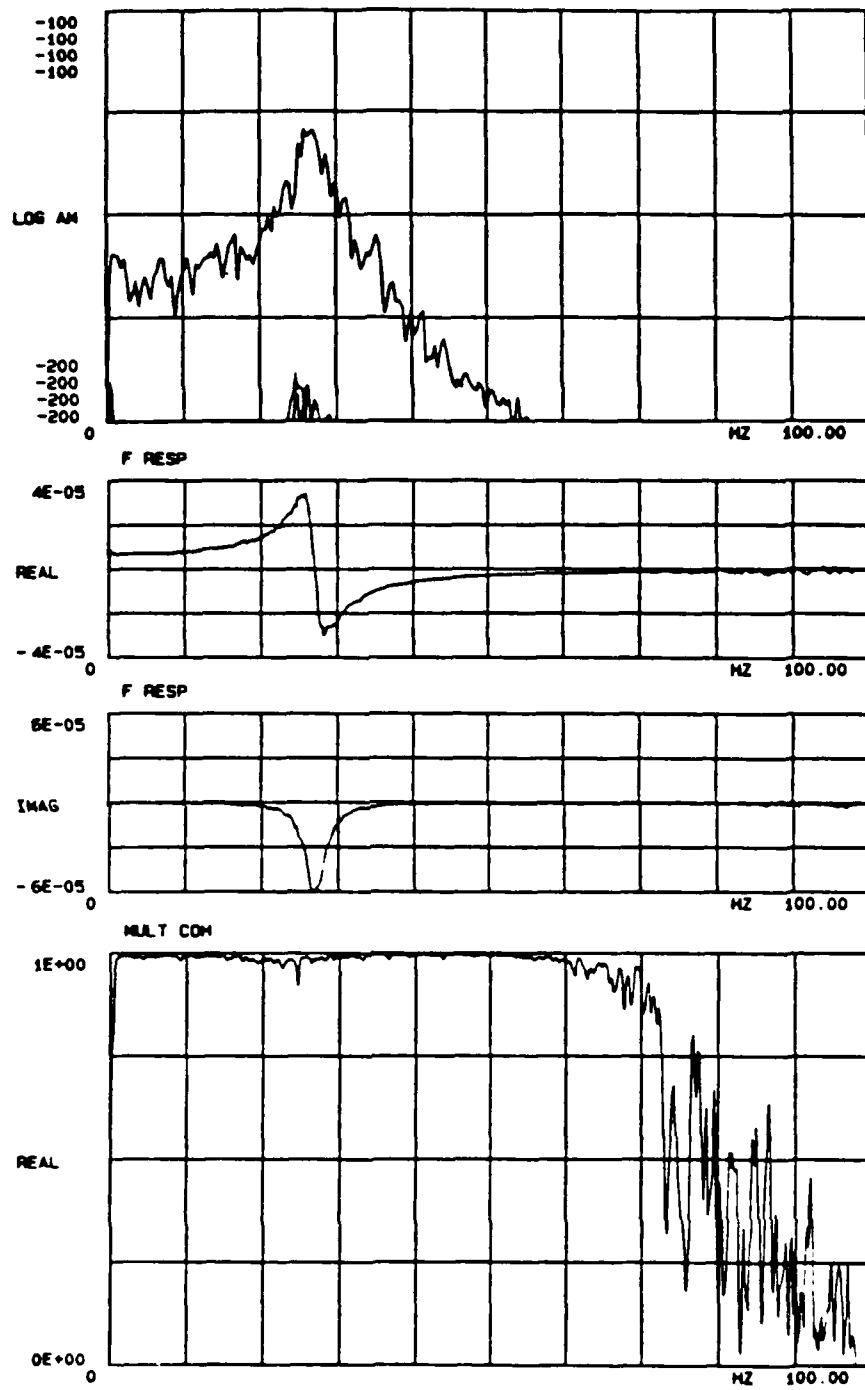


Figure 104. Nonlinear Clearance Model - BNK21

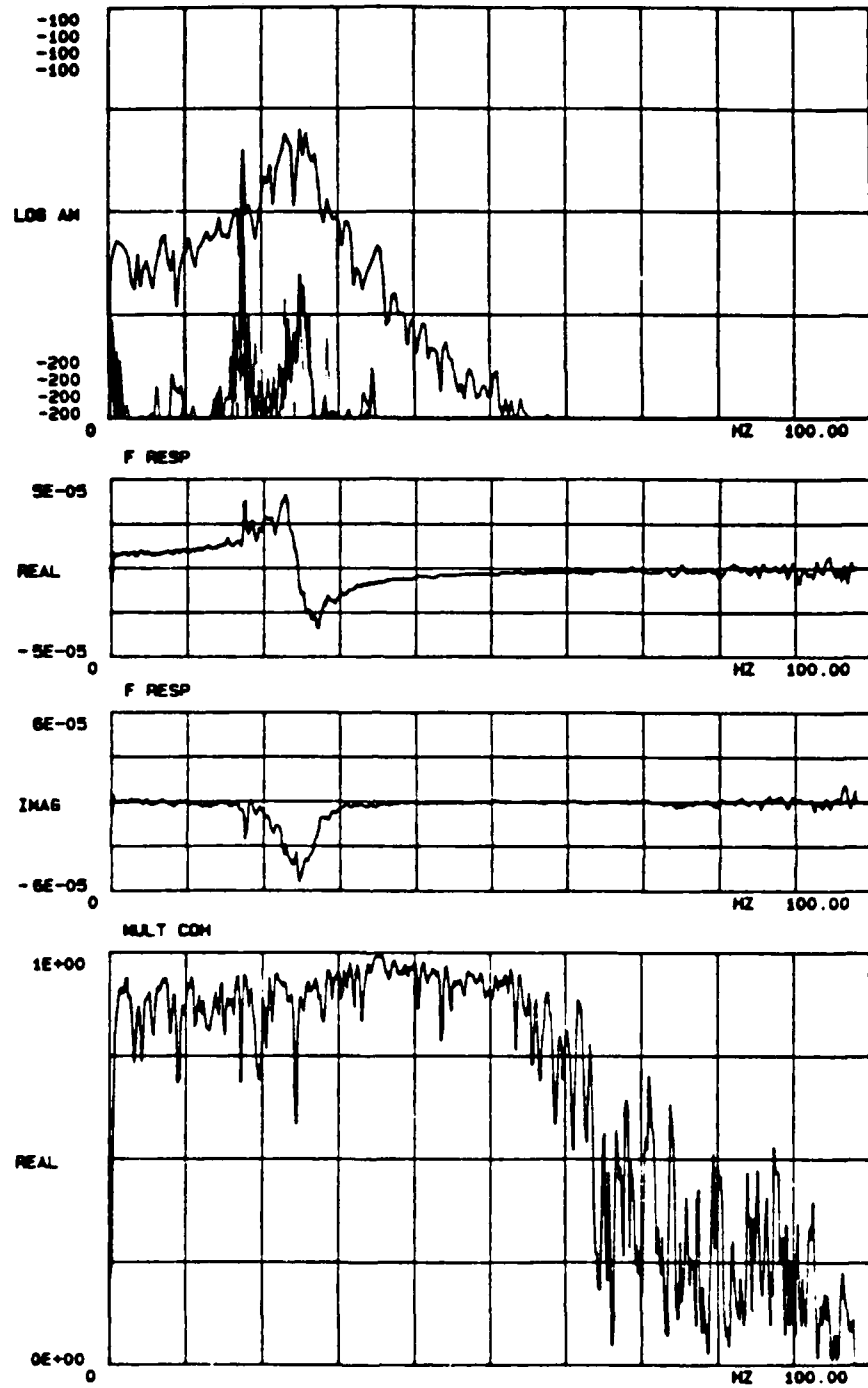


Figure 105. Nonlinear Clearance Model - BNK25

Using the same increments for e_0 , the force level was increased by a factor of five. As was previously demonstrated, at this higher force level the linear case indicated contributions of small nonlinear higher order terms. As the gap increased, the contribution of the higher order terms became more significant (reference Figures 106, 107, 108).

7.5.7 Nonlinear Damping Effects Simulated

To evaluate a nonlinear damping system, a single degree-of-freedom model in which the damping is proportional to the square of the velocity was generated. In this model, the damping is always opposing the motion of the system and is mathematically expressed as:

$$m \ddot{x} + c |\dot{x}| \dot{x} + kx = f(t) \quad (132)$$

This model consisted of the following system parameters:

$$\begin{aligned} \text{mass (m)} &= 5 \text{ Kg} \\ \text{damping (c)} &= 100 \text{ N-s/m} \\ \text{stiffness (k)} &= 150,000 \text{ N/m} \end{aligned}$$

As before, a theoretical linear system of this type has a resonant frequency at 27.5 Hz. and a damping value of 5.8 %. Figure 109 shows a block diagram of the BOSS input file for this nonlinear system.

After simulating the nonlinear system, the higher order detection functions indicated that a nonlinearity was present even though the frequency response and multiple coherence functions did not demonstrate any drastic distortions (reference Figure 110).

7.5.8 Two Degree of System Simulated

As an alternative to evaluating a system simulated by the BOSS program, a Hewlett Packard Mechanical Transfer Function Simulator (HP 05423-60002) was used to generate a linear model. A pure random excitation signal was utilized as the input signal to the function simulator. The simulator was then able to generate a linear two degree-of-freedom response signal. At this point, the modified data acquisition program was used to generate the nonlinear detection functions; however, the time domain input and response signals were obtained as "real time" data from the function simulator.

Once calculated, the nonlinear detection functions indicated the presence of a type of nonlinearity at the resonant frequencies. However, the frequency response and multiple coherence functions did not demonstrate any nonlinear distortions (reference Figure 111). This seems to be an inconsistency with the linear function simulator and should be further researched.

As a second evaluation, the force level was increased and a new set of functions were calculated. The increased force level made the higher order terms of the detection functions become more dominate. Although, the frequency response and coherence functions remained unchanged; implying a linear system exist (reference Figure 112).

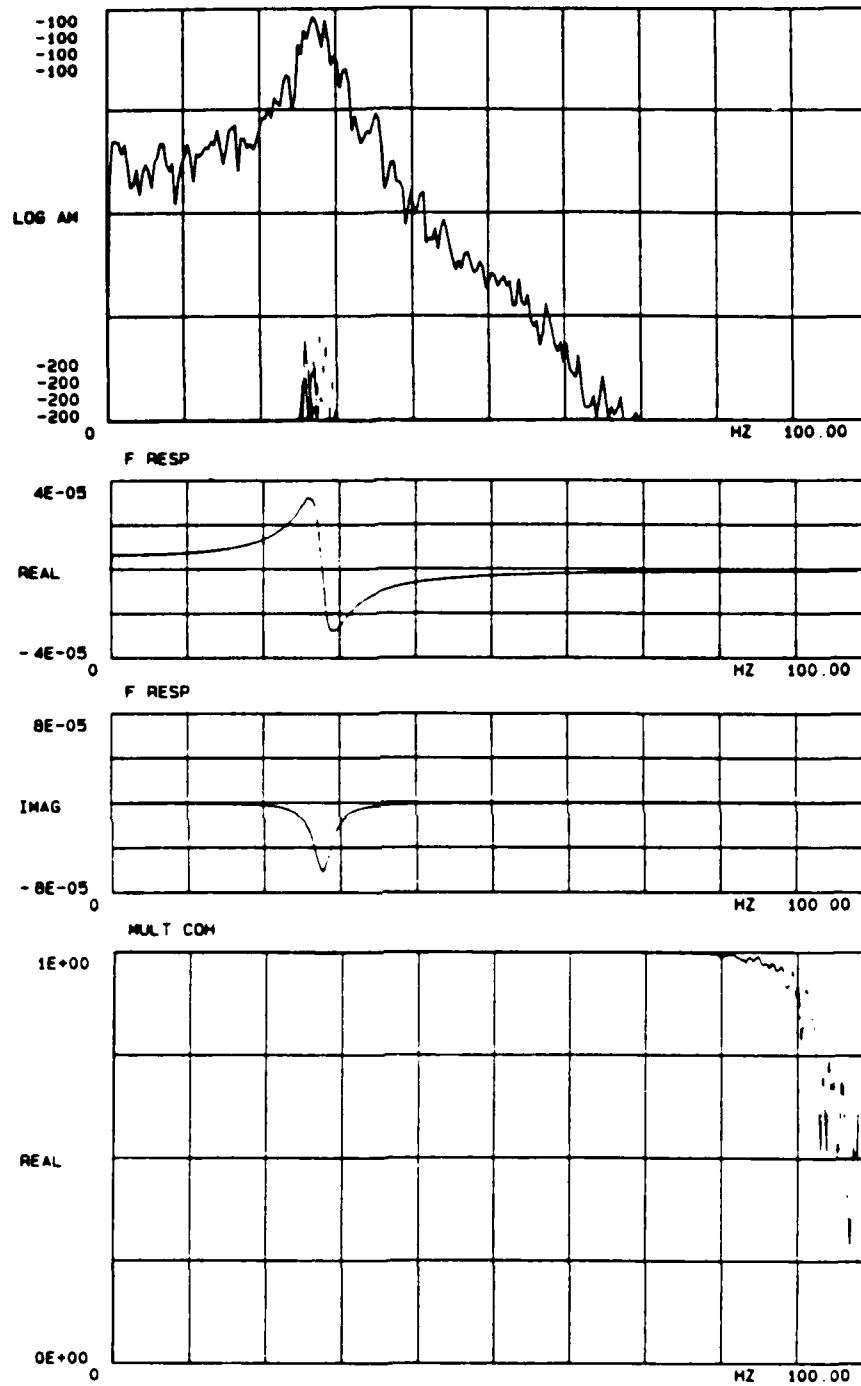


Figure 106. Linear Clearance Model - BLK2H0

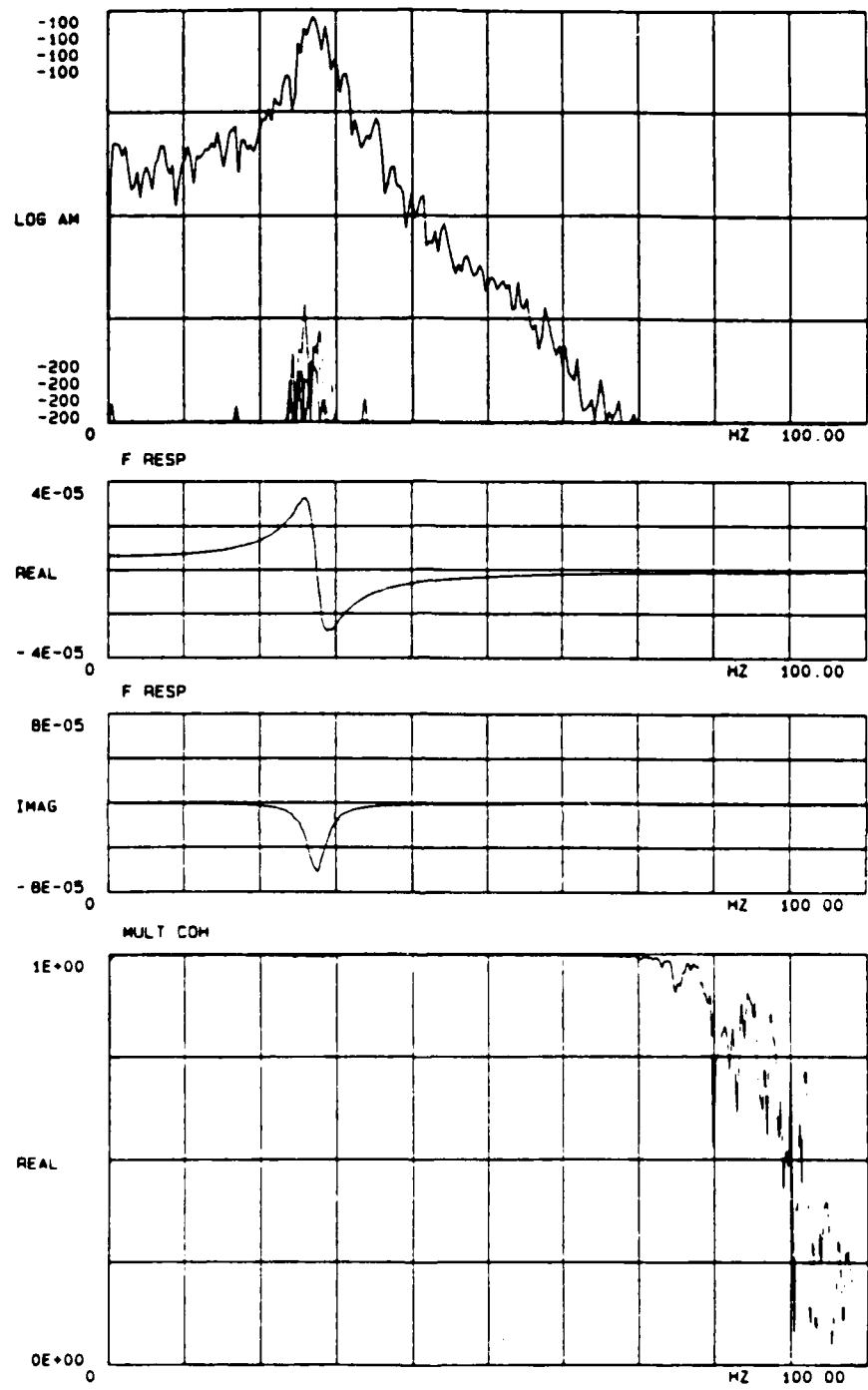


Figure 107. Nonlinear Clearance Model - BNK2H1

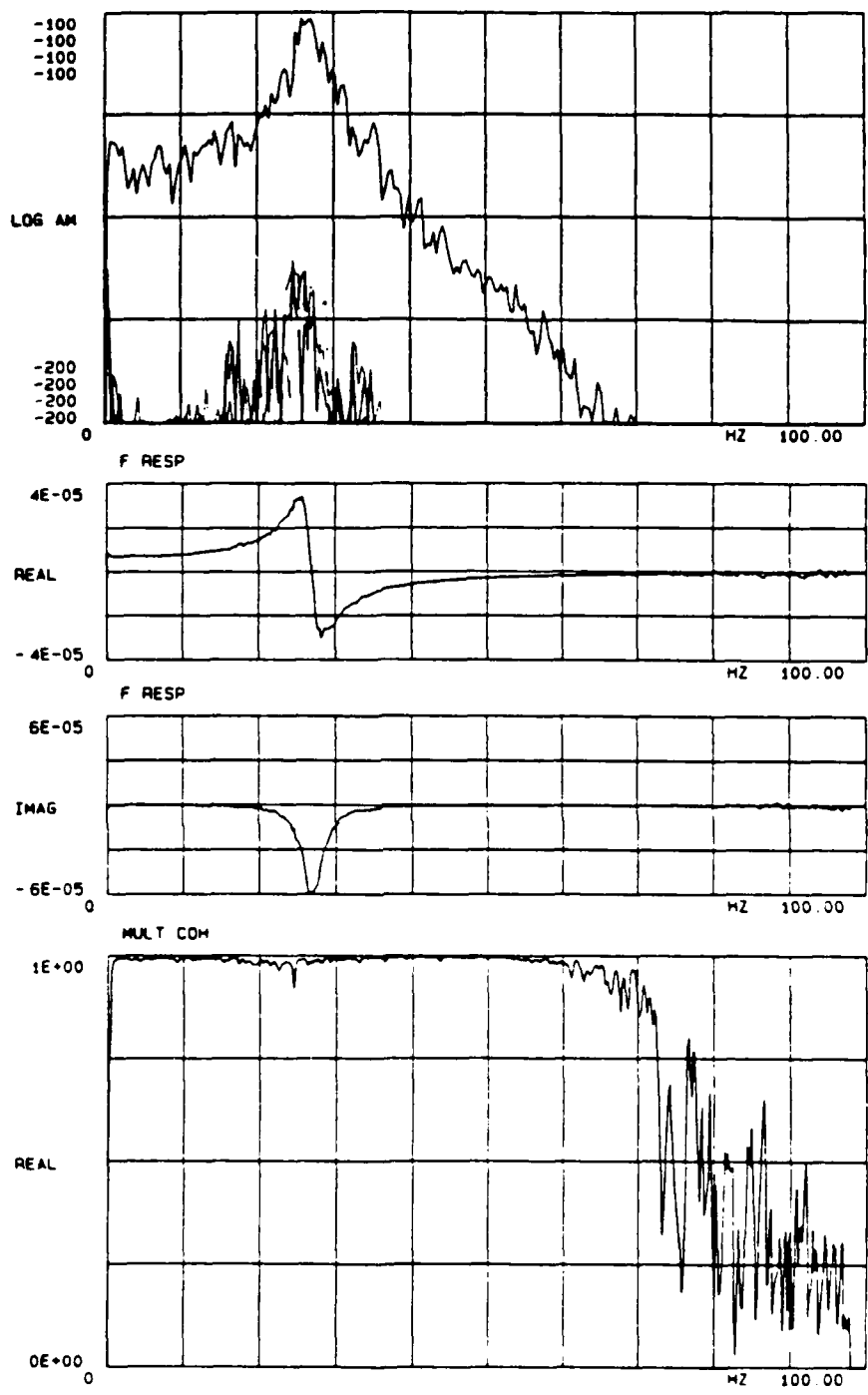


Figure 108. Nonlinear Clearance Model - BNK2H5

$$m\ddot{x} + c|\dot{x}| + kx = f(t)$$

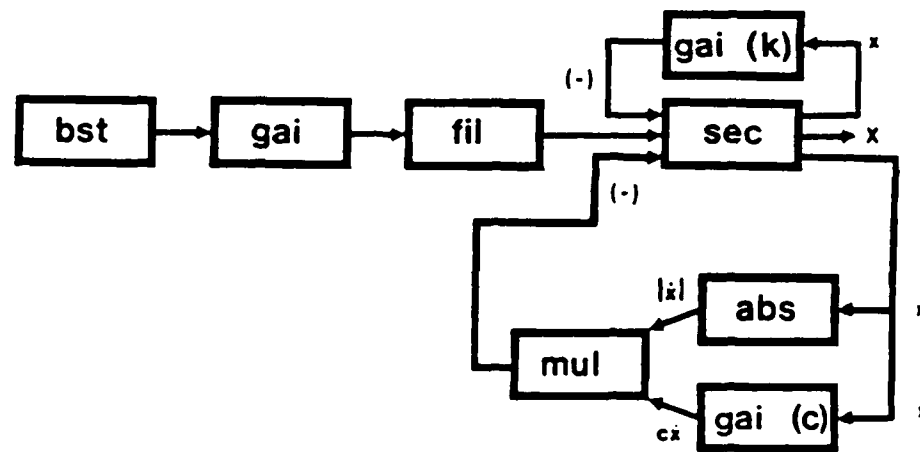


Figure 109. BOSS Nonlinear Damping Model

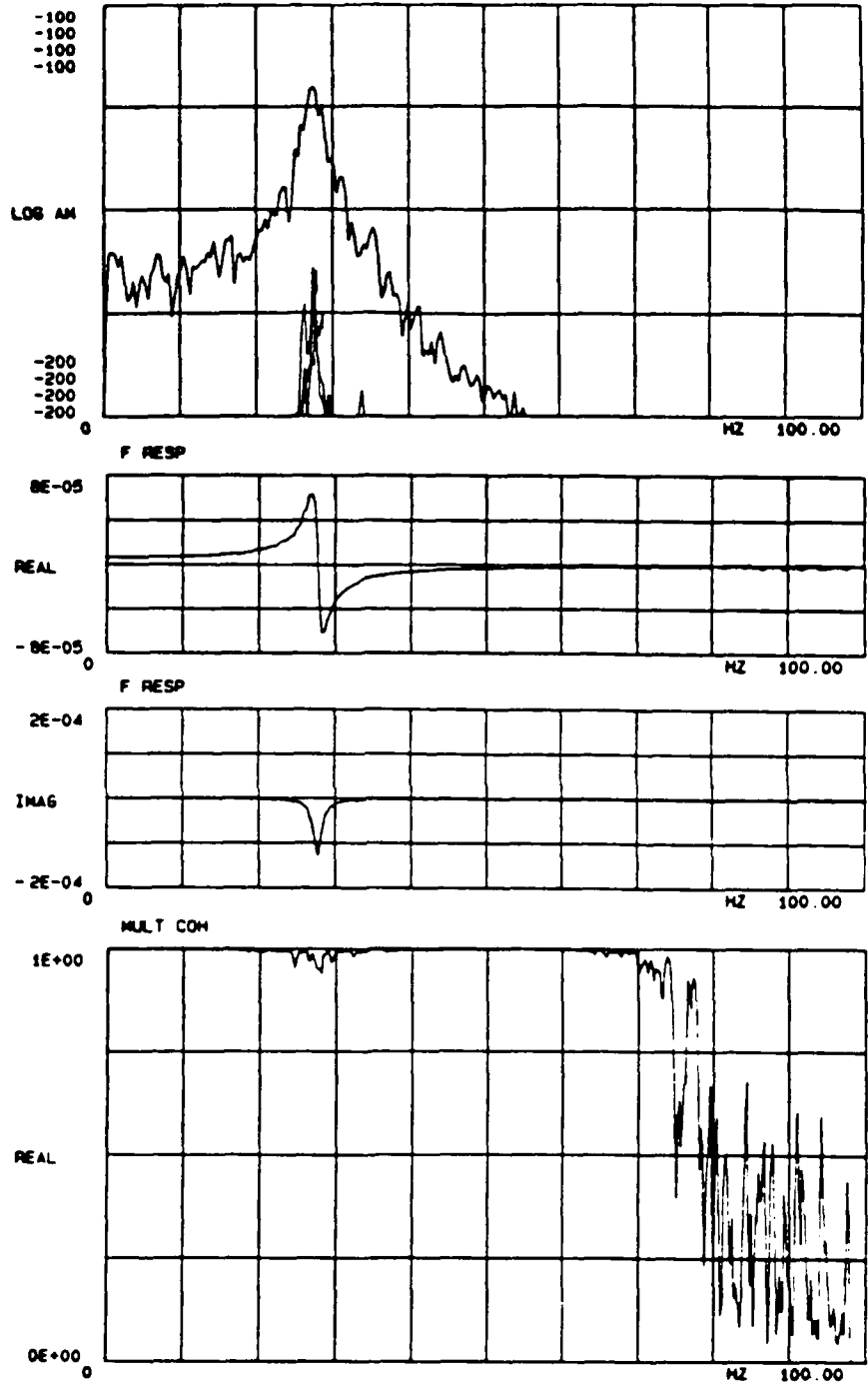


Figure 110. Nonlinear Damping Model - BNDA

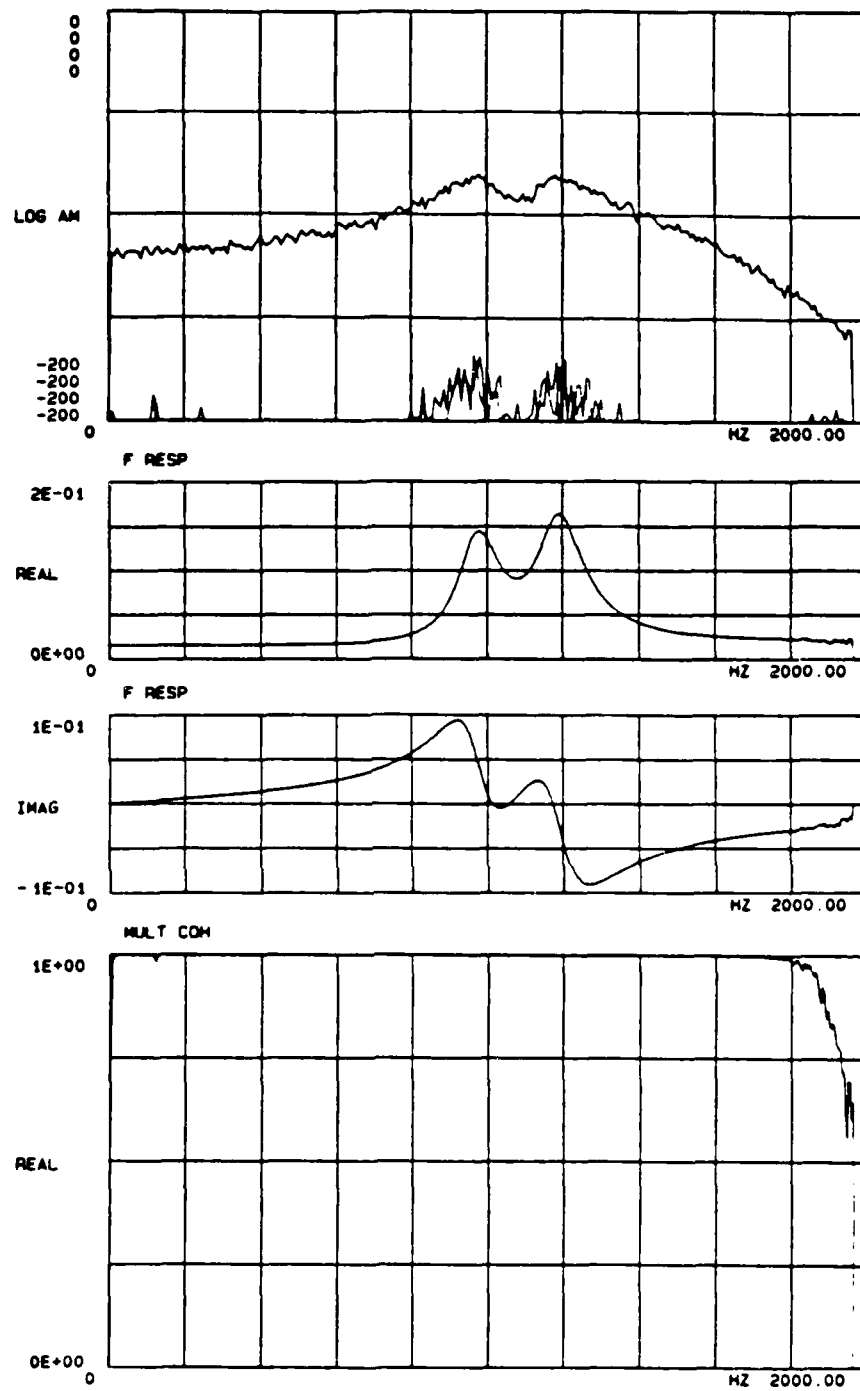


Figure 111. Function Simulator - Low Force

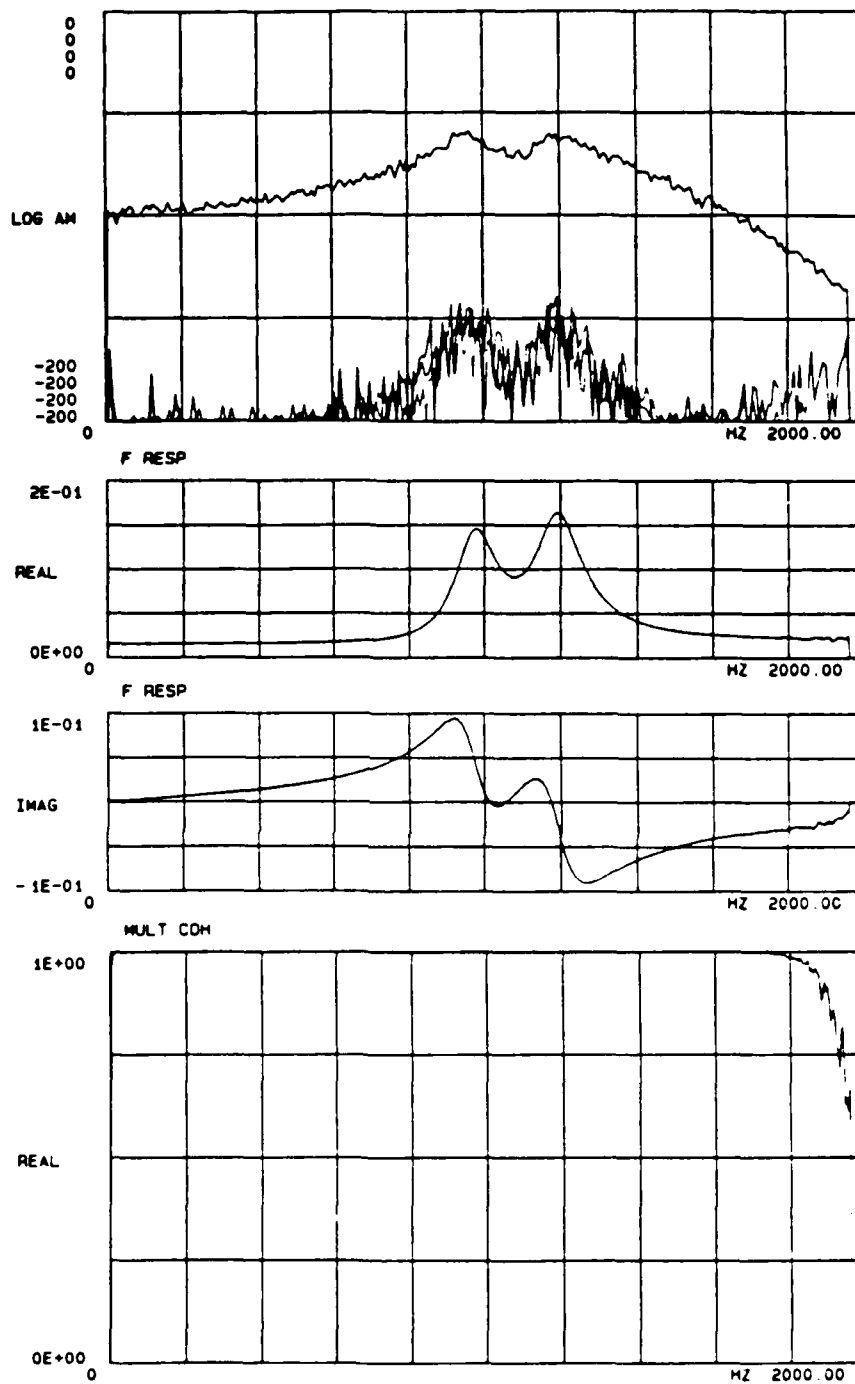


Figure 112. Function Simulator - High Force

7.5.9 Application to Physical Systems

Two physical structures were used to evaluate this detection method. The first structure was a modified body-in-white in which the rear of the vehicle was removed from the "B" pillars and the floor was removed up to the "A" pillar section joints. This modified structure is referred to as a "buck". The second structure evaluated was a 1986 Jeep in which the front and rear suspensions were removed. A single electrodynamic shaker was attached to the front rail through a stinger configuration. A load cell which measured the input force was attached between the stinger and the rail. An accelerometer, which measured the response of the structure, was located at the excitation point in the excitation direction. These two signals were then used as inputs to the data acquisition program. A pure random excitation signal was used to excite the structure at three different force levels, 2.5, 5, and 10 lbs. rms.

At each of these force levels, four nonlinear detection functions were calculated along with the frequency response and multiple coherence functions. In each of the three different detection plots, the higher order terms are represented at a constant level except in two ranges. At the ranges 0-10 Hz. and 20-30 Hz., the plots indicate peaks in the higher order nonlinear terms. The only significant difference in the frequency response functions at the different force levels occurs at 20-30 Hz. In this range, the resonant frequencies not only show a change in amplitude but also a frequency shift which could indicate nonlinear behavior (reference Figures 113, 114, 115).

As was the case in the "buck" test, a single electrodynamic shaker was attached to the front rail of the Jeep through a stinger configuration. A pure random excitation signal was used to excite the structure at three different force levels, 5, 10, and 15 lbs. rms. A load cell measured the input force while an accelerometer measured the response at the driving point in the excitation direction. These two signals were then used as "real time" inputs to the modified data acquisition program.

At each of the different force levels, four nonlinear detection functions were calculated; which is a single linear function and three nonlinear functions. The linear frequency response and multiple coherence functions were also calculated for each force level. Again, the nonlinear higher order functions remained at a somewhat constant amplitude except in several frequency ranges. In each of the three different nonlinear detection plots, peaks in the nonlinear higher order functions were found at 4-6 Hz., 15-21 Hz., and 24-32 Hz. After comparing the calculated frequency response functions, for each of the different force levels, the peaks in the nonlinear detection functions corresponded to resonant frequencies. At approximately 28 Hz., the frequency response functions demonstrated not only a change in amplitude but also a shift in the resonant frequency which indicates nonlinear behavior (reference Figures 116, 117, 118).

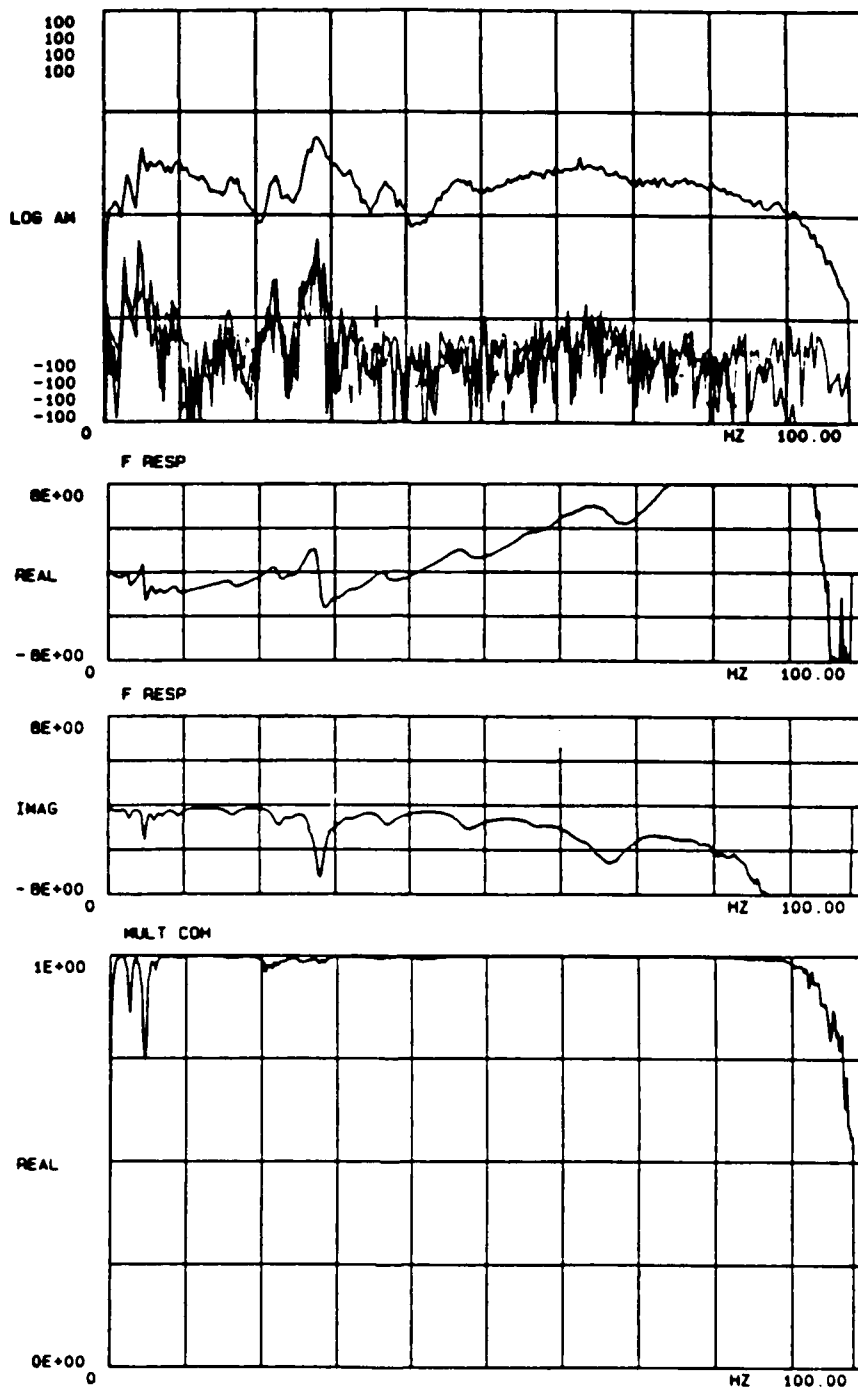


Figure 113. Modified Body-in-White - 2.5 lbs

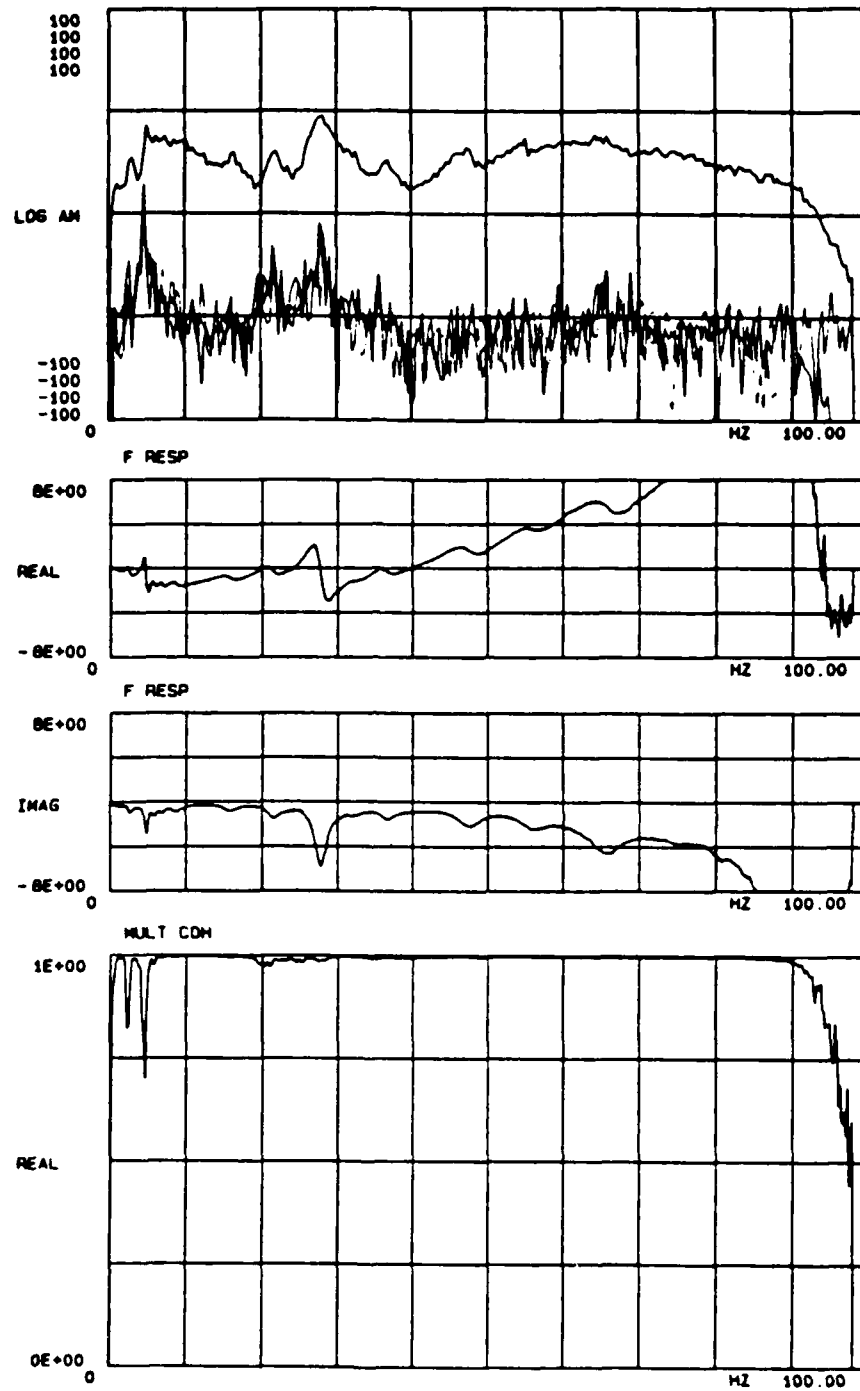


Figure 114. Modified Body-in-White - 5.0 lbs

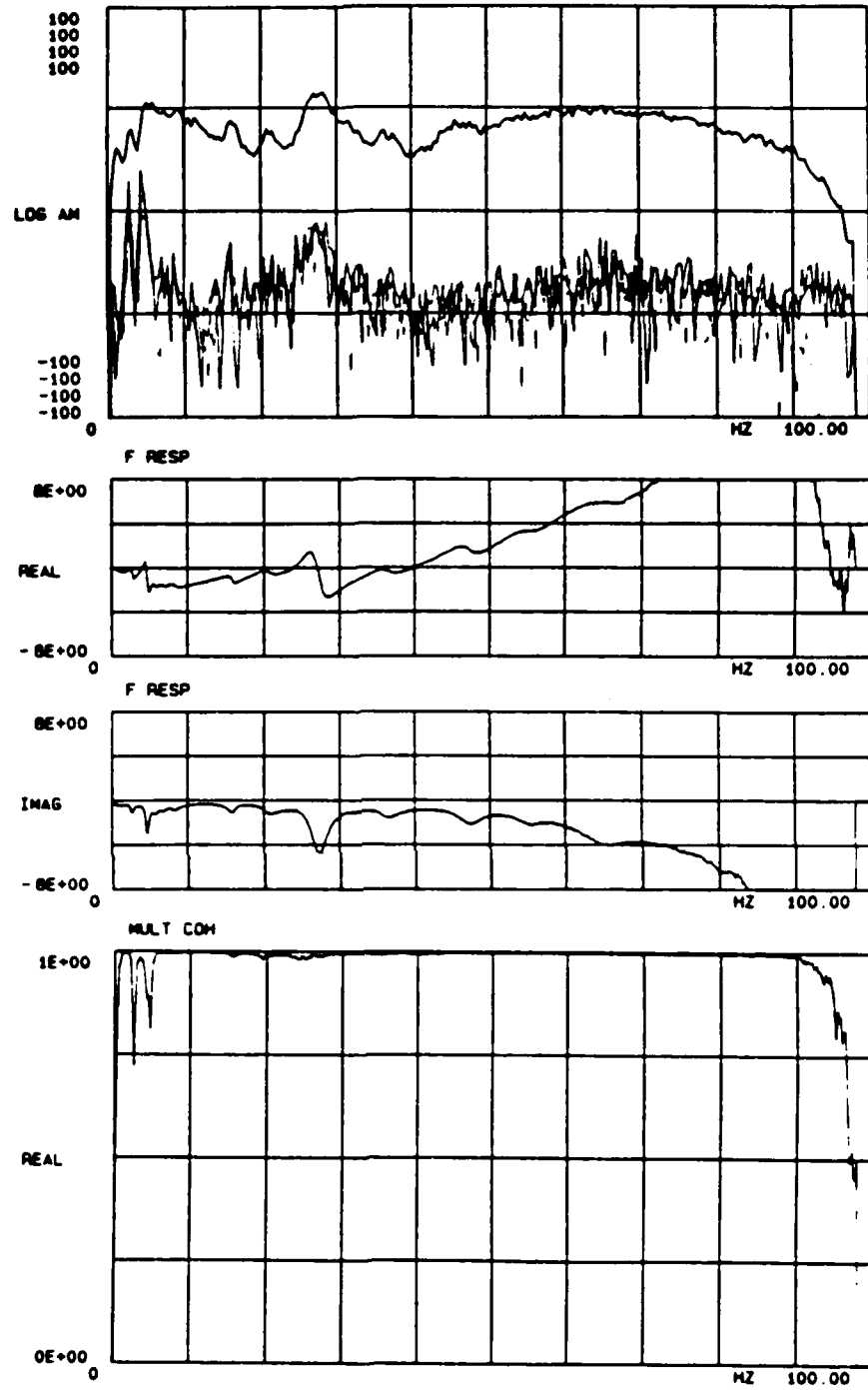


Figure 115. Modified Body-in-White - 10.0 lbs

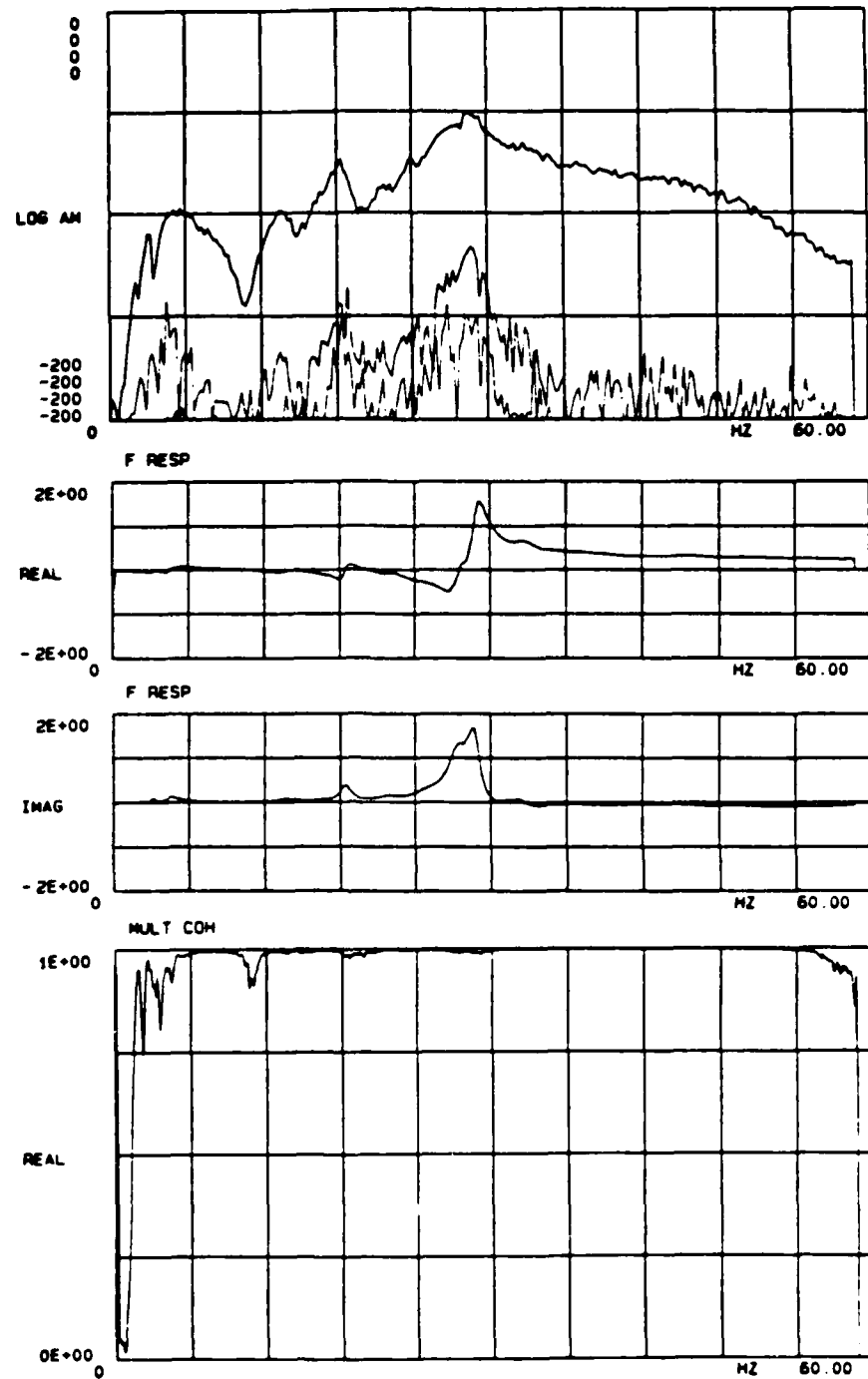


Figure 116. AMC Jeep - 5.0 lbs

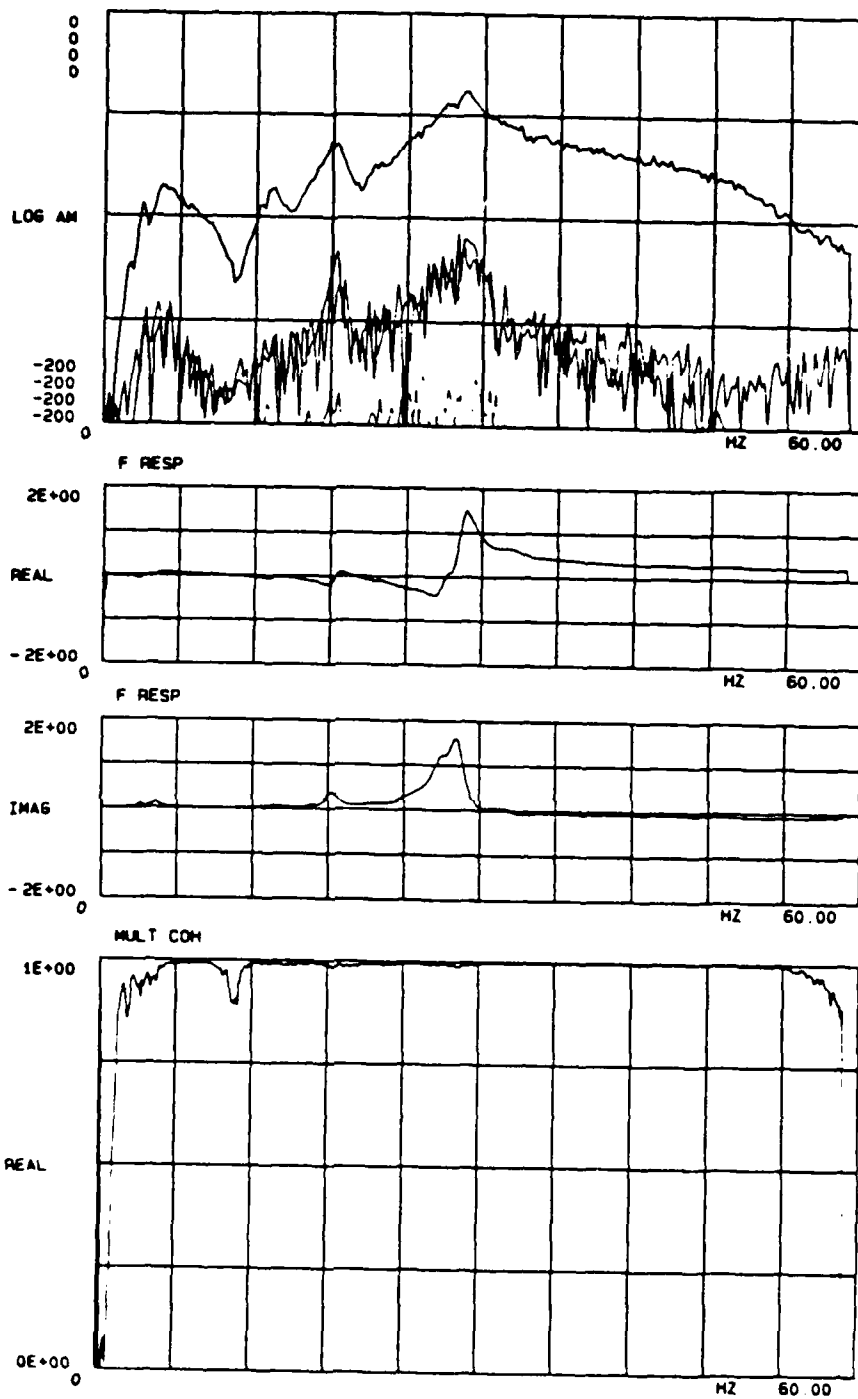


Figure 117. AMC Jeep - 10.0 lbs

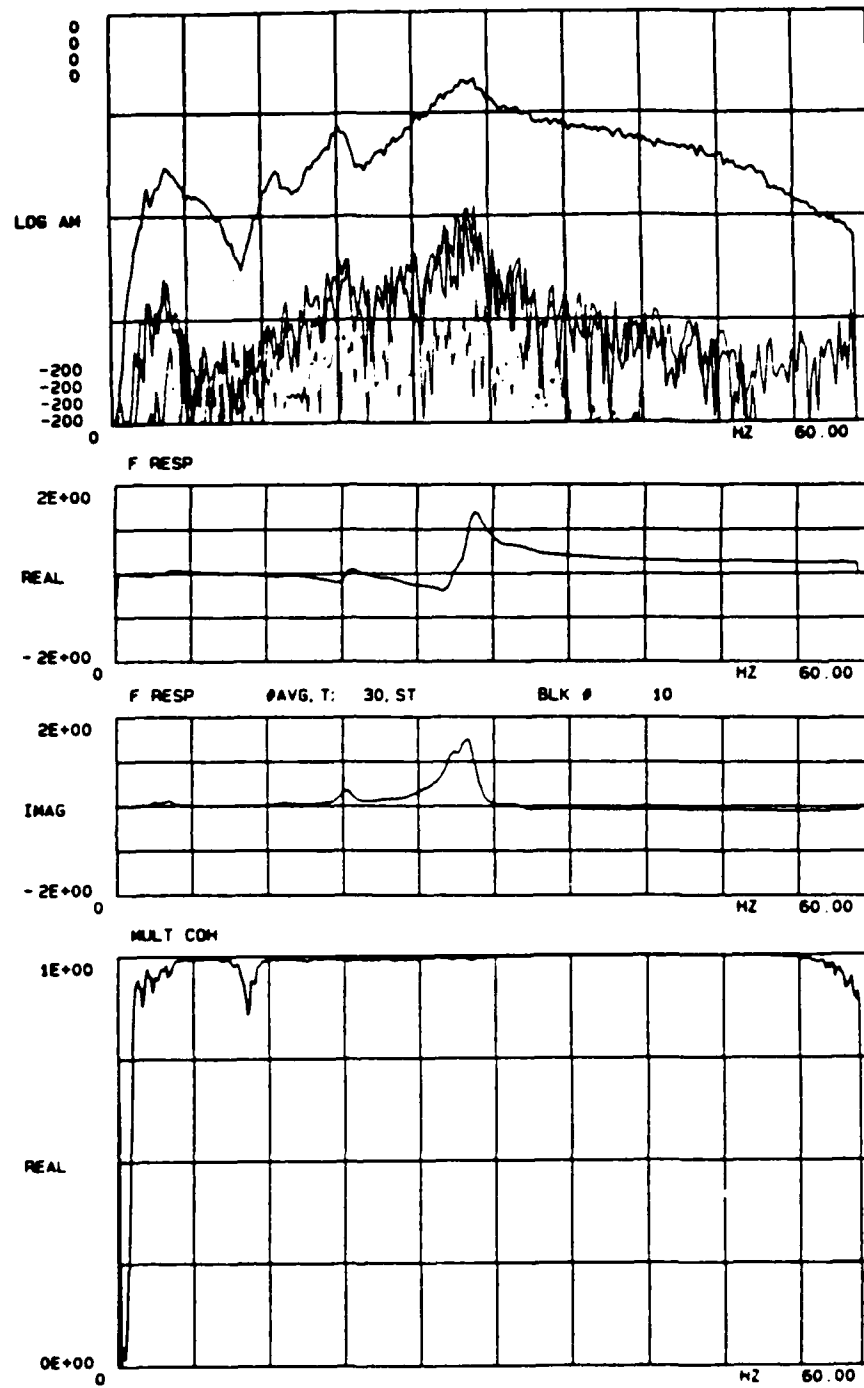


Figure 118. AMC Jeep - 15.0 lbs

7.6 CONCLUSIONS AND RECOMMENDATIONS

It is apparent that in physical mechanical systems, there exist a linear and nonlinear response due to some force input. In many cases, this nonlinear behavior can be neglected. However, in other cases, the nonlinear response cannot be ignored. It is and has been essential to perform some type of linearity check in order to make this evaluation. As the use of dynamic models based on experimental data becomes more extensive, the detection and eventually the characterization of nonlinearities becomes even more important.

The initial presented work provides several nonlinearity detection methods which are currently being implemented. Each of these different techniques has certain limitations which effect the accuracy of the detection method. As an alternative detection method, this work researched the possibility of detecting nonlinearities by utilizing higher order terms in conjunction with the multiple input/output estimation theory. By using higher order terms of a measured input force, the nonlinear behavior of a system can be detected. This alternative technique was researched as a fast and valid method to give an indication of the linearity of a system when implementing a random type of excitation signal.

This research demonstrated that for a theoretical single degree-of-freedom system, as the amount of nonlinearity increases, the nonlinear detection functions become more predominant. This preliminary study indicates that this nonlinear detection technique is sensitive to different types of nonlinearities if the correct number of higher order nonlinear terms are utilized. Further research is needed to determine the actual number of higher order terms necessary to accurately model a particular nonlinear system. To further validate this detection technique, the frequency response functions which are estimated utilizing the multiple input theory should be compared to the frequency response functions estimated by a single input/output algorithm. Although initial investigations demonstrated that the utilized forces were uncorrelated in the frequency domain, additional research is needed to study the relationship between these forces. As in most cases, this detection method is only valid for the measured response and input force points; it is still necessary to check several critical points of the structure for linearity and then assume the entire system behaves accordingly. The higher order detection technique does however eliminate having to perform a linearity check at different force levels for comparison purposes. The technique will give an indication of the amount of nonlinearity present in the structure at a particular force level. Further research is needed to evaluate an acceptable level at which linearity within the system can be assumed.

REFERENCES

- [1] Bendat, J.S.; Piersol, A.G., *Random Data: Analysis and Measurement Procedures*, John Wiley and Sons, Inc., 1971, 407 pp.
- [2] Otne, R.K., Enochson, L., *Digital Time Series Analysis*, John Wiley and Sons, Inc., 1972, 467 pp.
- [3] Bendat, J. S., Piersol, A. G., *Engineering Applications of Correlation and Spectral Analysis*, John Wiley, New York, 302 pp., 1980
- [4] Lecture Notes, Experimental Modal Analysis Short Course, Structural Dynamics Research Laboratory, Department of Mechanical and Industrial Engineering, University of Cincinnati, Cincinnati, OH., 1977-1984.
- [5] "Measuring Vibration," Breul and Kjaer Pamphlet Number BR0094, Breul and Kjaer Instruments, Inc., 1980.
- [6] Lally, R. W., "Transduction," PCB Piezotronics, Inc., Depew, New York
- [7] Zimmerman, R. D., "7110 Hammer Calibration Standard, User's Manual," Document 57110, QUIXOTE Measurement Dynamics, Inc., Cincinnati, OH.
- [8] "Petro Wax for Accelerometer Mounting," Data Sheet 08024284, PCB Piezotronics, Inc., Depew, New York
- [9] Dally, J.W.; Riley, W.F.; McConnell, K.G., *Instrumentation for Engineering Measurements*, John Wiley & Sons, Inc., New York, 1984.
- [10] Durrani, T.S.; Nightingale, J.M., "Data Windows for Digital Spectral Analysis," Institution of Electrical Engineers Proceedings, Volume 119, 1972, pp. 343-352.
- [11] Potter, R.W., "Compilation of Time Windows and Line Shapes for Fourier Analysis," Hewlett-Packard Company, 1972, 26 pp.
- [12] Cole, H.A., Jr., "On-the-Line Analysis of Random Vibrations," AIAA Paper Number 68-288, April, 1968
- [13] Cole, H.A., Jr., "Failure Detection of a Space Shuttle Wing Flutter Model by Random Decrement," NASA TM X-62, 041, May, 1971
- [14] Cole, H.A., Jr., "On-Line Failure Detection and Damping Measurement of Aerospace Structures by Random Decrement Signatures," NASA CR-2205, March, 1973
- [15] Hammond, C.E., Doggett, R.V., Jr., "Determination of Subcritical Damping by Moving-Block/Randomdec Applications," Flutter Testing Techniques, NASA-SP-415, October, 1975, pp. 59-76
- [16] Reed, R.E., "Analytical Aspects of Randomdec Analysis," AIAA Paper Number 79-0828, 1979, pp. 404-409
- [17] Brown, D.L., Carbon, G.D., Ramsey, K., "Survey of Excitation Techniques Applicable to the Testing of Automotive Structures," SAE Paper Number 770029, 1977
- [18] Allemang, R.J., Rost, R.W., Brown, D.L., "Multiple Input Estimation of Frequency Response Functions: Excitation Considerations," ASME Paper Number 83-DET-73, 1983, 11 pp.
- [19] Allemang, R.J., Brown, D.L., Zimmerman, R.D., "Determining Structural Characteristics from Response Measurements," University of Cincinnati, College of Engineering, Research Annals, Volume 82, Number MIE-110, 39 pp., 1982.

- [20] Allemang, R.J., Brown, D.L., Zimmerman, R.D., "Techniques for Reducing Noise in Frequency Response Function Measurements," University of Cincinnati, College of Engineering, Research Annals, Volume 82, Number MIE-112, 56 pp., 1982.
- [21] Halvorsen, W.G., Brown, D.L., "Impulse Technique for Structural Frequency Response Testing," Sound and Vibration, November, 1977, pp. 8-21
- [22] Stenger, G., "Step Relaxation Method for Structural Dynamic Excitation," Master of Science Thesis, Department of Mechanical Engineering, University of Cincinnati, 1979, 54 pp.
- [23] Olsen, N., "A Comparison of Excitation Techniques for Modal Analysis," Proceedings, International Modal Analysis Conference, 1982, pp. 200-210.
- [24] Moriwaki, T., Iwata, K., Veno, S., "Optimizing Dynamic Force in Shock Excitation Testing," Annals of the CIRP, Volume 26, 1977, pp. 427-434
- [25] Potter, R. W., "Matrix Formulation of Multiple and Partial Coherence," Journal of the Acoustic Society of America, Volume 66, Number 3, March 1977, pp. 776-781
- [26] Dodds, C.J., Robson, J.D., "Partial Coherence in Multivariate Random Processing," Journal of Sound and Vibration, Volume 42, Number 2, 1975, pp. 243-249
- [27] Bendat, J.S., "Solutions for the Multiple Input/Output Problem," Journal of Sound and Vibration, Volume 44, Number 3, 1976, pp.311-325
- [28] Piersol, A.G., "Physical Applications of Correlation and Coherence Analysis," Journal of Acoustical Society of America, Volume 55, Number 2, 1975, 29 pp.
- [29] Akaike, H., "On the Statistic Estimation of the Frequency Response Function of a System Having Multiple Inputs," Annals of the Institute of Statistical Mathematics, Volume 17, Number 2, 1965
- [30] Allemang, R. J., "Investigation of Some Multiple Input/Output Frequency Response Function Experimental Modal Analysis Techniques," Doctor of Philosophy Dissertation, University of Cincinnati, Mechanical Engineering Department, 1980, 358 pp.
- [31] Allemang, R.J., Rost, R.W., Brown, D.L., "Dual Input Estimation of Frequency Response Functions for Experimental Modal Analysis of Aircraft Structures," Proceedings, International Modal Analysis Conference, pp.333-340, 1982.
- [32] Carbon, G.D., Brown, D.L., Allemang, R.J., "Application of Dual Input Excitation Techniques to the Modal Testing of Commercial Aircraft," Proceedings, International Modal Analysis Conference, pp.559-565, 1982.
- [33] Allemang, R.J., Brown, D.L., Rost, R.W., "Dual Input Estimation of Frequency Response Functions for Experimental Modal Analysis of Automotive Structures," SAE Paper Number 820193.
- [34] Allemang, R.J., Brown, D.L., Rost, R.R., "Multiple Input Estimation of Frequency Response Functions for Experimental Modal Analysis," U.S. Air Force Report Number AFATL-TR-84-15, 1984, 185 pp.
- [35] Rost, R.W. "Investigation of Multiple Input Frequency Response Function Estimation Techniques for Modal Analysis," Doctor of Philosophy Dissertation University of Cincinnati Mechanical Engineering Department 1985, 219 pp.
- [36] Hunt, D., Peterson, E., "Multishaker Broadband Excitation for Experimental Modal Analysis," SAE Paper Number 831435, 1983, 10 pp.
- [37] Robinson, E., *Least Squares Regression Analysis in Terms of Linear Algebra*, Goose Pond Press, 1981, 508 pp.
- [38] Jennings, A., *Matrix Computation for Engineers and Scientists*, John Wiley & Sons, 1977, 330 pp.

- [39] Noble, B., Daniel, J.W., *Applied Linear Algebra*, Prentice-Hall, Inc., 1977, 476 pp.
- [40] Allemang, R.J., Rost, R.W., Brown, D.L., "Multiple Input Estimation of Frequency Response Functions," Proceedings, International Modal Analysis Conference, 1982, pp. 710-719.
- [41] Mitchell, L. "Improved Methods for Fast Fourier Transform (FFT) Calculation of Frequency Response Functions," ASME Journal of Mechanical Design, Vol. 104/2, pp.277-279.
- [42] Vold, H., Crowley, J., Rocklin, G. "A Comparison of H_1, H_2, H_∞ , Frequency Response Functions," Proceedings of the 3rd International Modal Analysis, 1985, pp.272-278. 1977, pp. 427-434
- [43] Rost, R.W., Leuridan, J., "A Comparison of Least Squares and Total Least Squares for Multiple Input Estimation of Frequency Response Functions," ASME Paper Number 85-DET-105, 1985.
- [44] Golub, G., Van Loan, C., "An Analysis of the Total Least Squares Problem," SIAM Journal of Numerical Analysis, Volume 17/6, 1985, pp. 883-893.
- [45] Van Huffel, S., et al, "The Total least Squares Problem: Properties, Application, and Generalization," SIAM Journal of Numerical Analysis, 1984, 33 pp.
- [46] Lawson, C., Hanson, R., *Solving Least Squares Problems* Prentice-Hall, Inc., 1974, 340 pp.
- [47] Wicks, A., Vold, H., "The H_∞ Frequency Response Estimator," Proceedings, International Modal Analysis Conference, 1986, pp. xxx-yyy.
- [48] Rost, R.W.; Leuridan, J.M., "Multiple Input Estimation of Frequency Response Functions: Diagnostic Techniques for the Excitation," The American Society of Mechanical Engineers, ASME paper no. 85-DET-107, 5 pp.
- [49] Leuridan, J.M., Lecture notes from The Advance Modal Analysis Course, Structural Dynamics Research Lab, University of Cincinnati, August 1984.
- [50] Goyder, H.G.D., "On the Measurement of Frequency Response Functions in the Presence of Nonlinearities and Noise," United Kingdom Atomic Energy Authority, Harwell, OX11 ORA, England, 26 pp.
- [51] Hewlett Packard, "The Fundamentals of Signal Analysis," Application Note 243, November 1981, p. 6.
- [52] Kirshenboim, J.; Ewins, D.J., "A Method for Recognizing Structural Nonlinearities in Steady-State Harmonic Testing," Journal of Vibration, Acoustics, Stress, and Reliability in Design, Volume 106, January 1984, pp. 49 - 52.
- [53] Harris, C.M.; Crede, C.E., *Shock and Vibrational Handbook*, McGraw-Hill Book Company, Second Edition, 1976, pp. 4-1 - 4-8.
- [54] Mertens, M.; Van Der Auweraer, H.; Vanherck, P.; Snoeys, R., "Detection of Nonlinear Dynamic Behavior of Mechanical Structures," Proceedings of the Fourth International Modal Analysis Conference , 1986, pp. 712-719.
- [55] Ewins, D.J., "Measurement and Application of Mechanical Impedance Data," Journal of the Society of Environmental Engineers, Part 1, Dec. 75, pp. 3 - 13, Part 2, Mar. 76, pp. 23 - 33, Part 3, Jun. 76, pp. 7 -17.
- [56] Ramsey, K.A., "Effective Measurements for Structural Dynamics Testing," Part II, Sound and Vibration, October 1976, pp. 18-31.
- [57] Tomlinson, G.R.; Ahmed, I., "Frequency and Damping Estimates from a Non-linear Structure - Causalisation and Random Excitation," Proceedings of the Tenth International Seminar on Modal Analysis, K.U. Leuven, Belgium, Part IV, 1985.

- [58] Kennedy, C.C.; Pancu, C.D.P., "Use of Vectors in Vibration Measurement and Analysis," *Journal of Aeronautical Sciences*, Volume 14, Number 11, 1947, pp. 603-625.
- [59] Tomlinson, G.R.; Hilbert, J.H., "Identification of the Dynamic Characteristics of a Structure with Coulomb Friction," *Journal of Sound and Vibration*, 64 (2), 1979, pp. 233-242.
- [60] Rades, M., "Identification of the Dynamic Characteristics of a Simple System with Quadratic Damping," *Serie de Mecanique Appliquee*, 28 (4), 1983, pp. 439-446.
- [61] Tomlinson, G.R., "Detection, Identification, and Quantification of Nonlinearity in Modal Analysis - A Review," *Proceedings of the Fourth International Modal Analysis Conference*, 1986, pp. 837-843.
- [62] Ewins, D.J., "Measurement and Application of Mechanical Impedance Data," *Journal of the Society of Environmental Engineers*, June 1976, pp. 7-17.
- [63] Ewins, D.J.; He, J., "Critical Assessment of the Accuracy of Modal Parameter Extraction," *Imperial College of Science and Technology, London Dynamics Group Mechanical Engineering*, Report Number 85003, October 1985.
- [64] Hans, E.L., "No Reciprocal Theorem For Dynamic Displacements," *Journal of Sound and Vibration*, 64 (2), 1979, pp. 275-276.
- [65] Mertens, M.; Van Der Auweraer, H.; Vanherck, P.; Snoeys, R., "Basic Rules of a Reliable Detection Method for Nonlinear Dynamic Behavior," *Proceedings of the Tenth International Seminar on Modal Analysis*, K.U. Leuven, Belgium, Part IV, 1985.
- [66] Vinh, T.; Haoui, A.; Chevalier, Y., "Modal Analysis of Structures with Applications to the Mechanics of Materials," *University of Manchester, Euromech 168*, 1983.
- [67] Vinh, T.; Haoui, A.; Chevalier, Y., "Extension of Modal Analysis to Nonlinear Structures by Using the Hilbert Transform," *Proceedings of the Second International Modal Analysis Conference*, 1984, pp. 852-857.
- [68] Simon, M.; Tomlinson, G.R., "Modal Analysis of Linear and Nonlinear Structures Employing the Hilbert Transform," *Proceeding of the Second International Conference on Recent Advances in Structural Dynamics*, Volume II, pp. 495-510.
- [69] Tomlinson, G.R.; Kirk, N.E., "On the Identification of Nonlinearities in Modal Testing Employing the Hilbert Transform," *Simon Engineering Laboratories, University of Manchester - Manchester, England*, 32 pp.
- [70] Tomlinson, G.R.; Kirk, N.E., "Modal Analysis and Identification of Structural Nonlinearity," *Simon Engineering Laboratories, University of Manchester - Manchester, England*, 21 pp.
- [71] Billings, S.A., "Identification of Nonlinear Systems - A Survey," *IEE Proceedings*, Volume 127, Part D, Number 6, November 1980, pp. 272-288.
- [72] Marmarelis, V.Z., "Practicable Identification of Nonstationary Nonlinear Systems," *IEE Proceedings*, Volume 128, Part D, Number 5, September 1981, pp. 211-214.
- [73] Schetzen, M., "A Theory of Nonlinear System Identification," *Int. J. Control*, Volume 20, Number 4, 1974, pp. 577-592.
- [74] Barrett, J.F., "Formula for Output Autocorrelation and Spectrum of a Volterra System with Stationary Gaussian Input," *IEE Proceedings*, Volume 127, Part D, Number 6, November 1980, pp. 286-288.
- [75] Lawrence, P.J., "Estimation of the Volterra Functional Series of a Nonlinear System Using Frequency Response Data," *IEE Proceedings*, Volume 128, Part D, Number 5, September 1981, pp. 206-210.
- [76] Schetzen, M., "Nonlinear System Modeling Based on the Wiener Theory," *IEEE Proceedings*, Volume 69, Number 12, December 1981, pp. 1557-1573.

- [77] Kim, Y.C.; Powers, E.J., "Digital Bispectral Analysis and its Applications Nonlinear Wave Interactions," IEEE Transactions on Plasma Science, Volume PS-7, Number 2, June 1979, pp. 120-131.
- [78] Choi, D.; Chang, J.; Stearman, R.O.; Powers, E.J., "Bispectral Identification of Nonlinear Mode Interactions," University of Texas at Austin, College of Engineering.
- [79] Choi, D.; Chang, J.; Stearman, R.O.; Powers, E.J., "Bispectral Analysis of Parametric and Nonlinear Systems," University of Texas at Austin, College of Engineering.
- [80] Choi, D.; Miksad, R.W.; Powers, E.J.; Fischer, F.J., "Application of Digital Cross bispectral Analysis Techniques to Model the Nonlinear Response of a Moored Vessel System in Random Seas," Journal of Sound and Vibration, 99 (3), 1985, pp. 309-326.
- [81] Comstock, T.R.; Nicolas, V.T., "Introduction to BOSS," BOSS User Manual.

BIBLIOGRAPHY

- [1] *Lecture Notes, Experimental Modal Analysis Short Course*, Structural Dynamics Research Lab, Dept. of Mechanical and Industrial Engineering, University of Cincinnati, Cincinnati, Ohio, 1977-1984.
- [2] Abramson, H. N., *Nonlinear Vibration*, Shock and Vibration Handbook, 2nd Edition, pp. 4-1 - 4-8.
- [3] Adshima N., *Measurement of Nonlinear Vibration by Signal Compression Method*, Journal of the Acoustical Society of America, Vol. 76, Num. 3, September 1984, pp. 794-901.
- [4] Andronikou, A. M., Bekey G. A., and Hadaegh F. Y., *Identifiability of Nonlinear Systems with Hysteretic Elements*, Journal of Dynamic Systems, Measurement and Control, Vol. 105, Num. 4, December 1983, pp. 209-214.
- [5] Anonymous, *Petro Wax for Accelerometer Mounting*, PCB Piezotronics, Inc., Data Sheet 08024284 (Depew, New York).
- [6] Anonymous, *Measuring Vibration*, Breul and Kjaer Pamphlet No. BR0094, Breul and Kjaer Instruments, Inc., 1980.
- [7] Anonymous, *Parameter Estimation Applications of Modal 3.0/6.0*, SMS Technical Information, September 1984, 12 pp.
- [8] Ballard W. C., Casey, S. L., Clausen, J. D., *Vibration Testing with Mechanical Impedance Methods*, Sound and Vibration, January 1969, 0.
- [9] Barden, M., *The Development of a Digitally Controlled Mechanical Transfer Function System*, Institute of Environmental Science, Proceedings, Vol. 2, 1975, pp. 60-66.
- [10] Barrett, J. F., *Formula for Output Autocorrelation and Spectrum of a Volterra System with Stationary Gaussian Input*, IEE Proceedings, Vol. 127, Num. 6, November 1980, pp. 286-288.
- [11] Baruch, M., *Methods of Reference Basis for Identification of Linear Dynamic Structures*, AIAA Journal, Vol. 22, Num. 4, April 1984, pp. 561-564. Baruch, M., *Selective Optimal Orthogonalization of Measured Modes*, AIAA Journal, Vol. 17, Num. 1, January 1979, pp. 120-121.
- [12] Baruch, M. and Bar Itzhack, I. Y., *Optimal Weighted Orthogonalization of Measured Modes*, AIAA Journal, Vol. 16, Num. 4, April 1978, pp. 346-351.
- [13] Bendat, J. S., *Statistical Errors for Non-linear System Measurements Involving Square-Law Operations*, Journal of Sound and Vibration, Vol. 90, Num. 2, 1983, pp. 275-282.
- [14] Bendat, J. S. and Piersol, A. G., "Engineering Applications of Correlation and Spectral Analysis," John Wiley (New York), 1980, 302 pp.
- [15] Bendat, J. S. and Piersol, A. G., *Spectral Analysis of Non-Linear Systems Involving Square-Law Operations*, Journal of Sound and Vibration, Vol. 81, Num. 2, 1982, pp. 199-213.
- [16] Bennett, R. M., Desmarais, R. N., *Curve Fitting of Aeroelastic Transient Response Data with Exponential Functions*, NASA-SP-415, 1976, pp. 43-58.
- [17] Bergman, L. A. and Hale, A. L., *Linear System Identification via Poisson Moment Functionals*, AIAA Journal, Vol. 22, Num. 4, April 1984, pp. 566-568.
- [18] Bergman, L. A., Hale, A. L., and Goodding, J. C., *Identification of Linear Systems by Poisson Moment Functionals in the Presence of Noise*, AIAA Journal, Vol. 23, Num. 8, August 1985, pp. 1234-1235.

- [19] Berman, A., *Limitations on the Identification of Discrete Structural Dynamic Models*, 9 pp.
- [20] Berman, A., *Comment on "Optimal Weighted Orthogonalization of Measured Modes"*, AIAA Journal, Vol. 17, Num. 8, August 1979, pp. 927-928.
- [21] Berman, A., Giasanter, N., Bartlett, F. D., Jr., *An Evaluation of a Constrained Test Method for Obtaining Free Body Responses*, NASA-CR-2307, 1973, 55 pp.
- [22] Billinger, D. R., *The Identification of Polynomial Systems by means of Higher Order Spectra*, Journal of Sound and Vibration, Vol. 12, Num. 3, 1970, pp. 301-313.
- [23] Billings, S. A., *Identification of Nonlinear Systems - A Survey*, IEE Proceedings, Vol. 127, Num. 6, November 1980, pp. 272-285.
- [24] Billings, S. A. and Fakhouri, S. Y., *Theory of Separable Processes with Applications to the Identification of Nonlinear Systems*, IEE Proceedings, Vol. 125, Num. 9, pp. 1051-1058.
- [25] Billings, S. A. and Voon, W. S. F., *Least Squares Parameter Estimation Algorithms for Non-linear Systems*, Int. J. Systems Sci., Vol. 15, Num. 6, 1984, pp. 601-615.
- [26] Bishop, R. E. D. and Gladwell, G. M. L., *An Investigation Into The Theory of Resonance Testing*, Philosophical Transactions, Royal Society of London Series A, Vol. 255, Num. A1055, 1963, pp. 241-280.
- [27] Bodson, B. J., *A Straight-Line Technique for Extracting Modal Properties from Frequency Response Data*, Mechanical Systems and Signal Processing, Vol. 1, Num. 1, January 1987, pp. 29-40.
- [28] Brandon, J. A. and Cowley, A., *A Weighted Least Squares Method for Circle Fitting to Frequency Response Data*, Journal of Sound and Vibration, Vol. 89, Num. 3, August 8 1983, pp. 419-424.
- [29] Breitbach, E., Dr., *Identification of Nonlinear Systems*, CISM Courses and Lectures, International Centre for Mechanical Sciences, Num. 272, pp. 373-403.
- [30] Broadbent, E. G., *Vector Plotting as an Indication of the Approach to Flutter*, Flight Flutter Testing Symposium NASA-SP-385, 1958, pp. 31-40.
- [31] Brown, D. L., Allemang, R. J., Zimmerman, R. and Mergeay, M., *Parameter Estimation Techniques for Modal Analysis*, SAE Paper# 790221, 1979.
- [32] Brown, K. T., *Measurement of Modal Density: An Improved Technique for Use on Lightly Damped Structures*, Journal of Sound and Vibration, Vol. 96, Num. 1, Sept. 8, 1984, pp. 127-132.
- [33] Caruso, H., *Practical Experience in Vibration Testing External Avionics Systems*, Institute of Environmental, Sciences Proceedings,(A78-32101 12-31), 1977, pp. 362-364.
- [34] Cheng-Xun S., Hua L., and Wen-hu H., *Identification of Vibrating System Parameters By Maximum Likelihood Method*, ASME Publication #. 85-Det-112, 5 pp.
- [35] Chen, S. and Fuh, J., *Application of the Generalized Inverse in Structural System Identification*, AIAA Journal, Vol. 22, Num. 12, December 1984, pp. 1827-1828.
- [36] Choi, D., Chang, J., Stearman, R., and Powers, E., *Bispectral Identification of Nonlinear Mode Interactions*, University of Texas at Austin, College of Engineering, 8 pp.
- [37] Choi, D., Miksad, R. W., Powers, E. J., and Fischer, F. J., *Applctn. of Digital Cross-Bispectral Analysis Technqs. to Model the Nonlinear Response of a Moored Vessel System in Random Seas*, Journal of Sound and Vibration, Vol. 99, Num. 3, 1985, pp. 309-326.
- [38] Choi, D., Powers, E. J., Chang, J.-H., and Stearman, R. O., *Bispectral Analysis of Parametric and Nonlinear Systems*, University of Texas at Austin, College of Engineering, Austin, Texas 78712, 1983, 6 pp.

- [39] Chouychai, T. and Vinh, T., *Analysis of Nonlinear Structure by Programmed Impact Testing and Higher Order Transfer Function*, Proceedings/Fourth International Modal Analysis Conference, 1986, pp. 743-747.
- [40] Cole, H. A., Jr., *On-Line Failure Detection and Damping Measurement of Aerospace Structures by Random Decrement Signatures* NASA CR-2205, March 1973.
- [41] Cole, H. A., Jr., *On-the-Line Analysis of Random Vibrations*, AIAA Paper No. 68-288, April 1968.
- [42] Cole, H. A., Jr., *Failure Detection of a Space Shuttle Wing Flutter Model by Random Decrement*, NASA TM X-62, 041, May 1971.
- [43] Collins, J. D., Hart, G. C., Hasselman, T. K. and Kennedy, B., *Statistical Identification of Structures*, AIAA Journal, Vol. 12, Num. 2, 1974, pp. 185-190.
- [44] Coppolino, R. N., *A Simultaneous Frequency Domain Technique for Estimation of Modal Parameters from Measured Data*, SAE Technical Paper Series # 811046 Presented @ Aerospace Congress and Exposition, October 5-8 1981, 7 pp.
- [45] Craig, R. R., Chung, Y., and Blair, M., *Modal Vector Estimation for Closely-Spaced-Frequency Modes*, Center for Aeronautical Research Report CAR 82-1, Feb 1, 1982, 39 pp.
- [46] Croker, M. D., *Experimental Modal Analysis of Non-linear Structures*, Proceedings/Tenth International Seminar on Modal Analysis, K.U. Leuven, Belgium, Part IV, 1985.
- [47] Curtis, A. J., Tinling, N. G., and Abstein H. T., Jr., *Selection and Performance of Vibration Tests*, Shock and Vibration Information Center, U.S., Dept. of Defense SVM-8, 1971, 218 pp.
- [48] Dally, J. W., Riley, W. F., and McConnell, K. G., "Instrumentation for Engineering Measurements," John Wiley and Sons, Inc. (New York), 1984.
- [49] Dat, R., *Structural and Thermal Tests Their Evolution and Present Trends, Volume I: Structural and Mechanical Tests*, European Space Research Organization, June 1973, pp. 85-102.
- [50] Dat, R., *Determination of a Structure's Eigen Modes by a Vibration Test with Non-Selective Excitation*, European Space Research Organization ESRO-TT-6 (N74-23517), 1974, pp. 97-118.
- [51] Dat, R., *Developments in Structural Vibration Testing Methods*, La Recherche Aerospatiale. No. 1983-6, 1983, pp. 41-59.
- [52] Dat, R. and Meurzec, J., *The Application of a Smoothing Technique to Analyse Frequency Response Measurements For A Linear System*, Royal Aircraft Establishment RAE-LIB-TRANS-1703 (N73-26616), 1973, 21 pp.
- [53] Dat, R., *Experimental Methods used in France For Flutter Prediction*, O.N.E.R.A. Report No. TP-1428, 1974, 22 pp.
- [54] De Vries G., *The Analysis of the Responses of a Mechanical Structure in Global Vibration Test*, Aeronautical Research Labs, Translation ARL/SM-28 (N68-29059), 1967, 15 pp.
- [55] Ensminger, R. R. and Turner, M. J., *Structural Parameter Identification from Measured Vibration Data*, AIAA Journal Paper # 79-0829, pp. 410-416.
- [56] Ewins, D. J., *Measurement and Application of Mechanical Impedance Data, Part 2*, Journal of the Society of Environmental Engineers, March 1976, pp. 23-33.
- [57] Ewins, D. J., *Measurement & Application of Mechanical Impedance Data Part 3 - Interpretation and Application of Measured Data*, Journal of the Society of Environmental Engineers, June 1976, pp. 7-17.
- [58] Ewins, D. J. and He, J., *Critical Assessment of the Accuracy of Modal Parameter Extraction*, Imperial College London; Dynamics Groups Mechanical Engineering Report #85003.

Presented @ 10th I.M.A.S., October 1985.

- [59] Ewins, D. J. and Kirshenboim, J., *A Method for Recognizing Structural Nonlinearities in Steady State Harmonic Testing*, Journal of Vibration, Acoustics, Stress, and Reliability, Vol. 106, January 1984, pp. 49-52.
- [60] Fillod R. and Piranda, J., *Identification of Eigensolutions by Galerkin Technique*, ASME Publication 79-DET-35.
- [61] Fillod, R., Lallement, G. and Piranda, J., *Is a Structure Nonlinear? If Yes, How Perform its Modal Identification?*, Proceedings/Tenth International Seminar on Modal Analysis, K.U. Leuven, Belgium, Part IV, 1985.
- [62] Flannelly, W. G. and Berman, A., *The State of The Art of System Identification or Aerospace Structures*, System Identification of Vibrating Structures ASME, 1972, pp. 121-131.
- [63] Frachebourg, A., *Comparison of Excitation Signals: Sensitivity to Nonlinearity and Ability to Linearize Dynamic Behavior*, Proceedings/Tenth International Seminar on Modal Analysis, K.U. Leuven, Belgium, Part V, 1985.
- [64] Fritzen, C., *Identification of Mass, Damping, and Stiffness Matrices of Mechanical Systems*, ASME Publication No. 85-DET-91, 8 pp.
- [65] Gaukroger, D. R. and Copley, J. C., *Methods for Determining Undamped Normal Modes and Transfer Functions from Receptance Measurements*, Royal Aircraft Establishment, TR 79071, Departmental Reference: Structures BF/B/0793, 1979, pp. 1-31.
- [66] Gaukroger, D. R., Heron, K. H. and Skingle, C.W., *The Processing of Response Data To Obtain Modal Frequencies and Damping Ratios*, Journal of Sound and Vibration, Vol. 35, Num. 4, 1974, pp. 559-571.
- [67] Gersch, W., *Estimation of the Autoregressive Parameters of a Mixed Autoregressive Moving-Average Time Series*, IEEE Transactions on Automatic Control, October 1970, pp. 583-588.
- [68] Gersch, W., *On the Achievable Accuracy of Structural System Parameter Estimates*, Journal of Sound and Vibration, Vol. 34, Num. 1, 1974, pp.63-79.
- [69] Gersch, W. and Foutch, D. A., *Least Squares Estimates of Structural System Parameters Using Covariance Function Data*, IEEE Transactions on Automatic Control, Vol. AC-19, Num. 6, December 1974, pp. 898-903.
- [70] Gersch, W., Nielsen, N. N. and Akaike, H., *Maximum Likelihood Estimation of Structural Parameters from Random Vibration Data*, The Journal of Sound and Vibration, Vol. 31, Num. 3, 1973, pp. 295-308.
- [71] Gold, R. R. and Hallauer, W. L., Jr., *Modal Testing with Asher's Method Using a Fourier Analyzer and Curve Fitting*, Submitted to 25th International Instrumentation, pp. 1-21.
- [72] Goyder, H. G. D., *On the Measurement of Frequency Response Functions in the Presence of Nonlinearities and Noise*, United Kingdom Atomic Energy Authority, Harwell, OX11 ORA, England, 26 pp.
- [73] Haidl, G., *Non-Linear Effects in Aircraft Ground and Flight Vibration Tests*, Advisory Group for Aerospace Research and Development AGARD-R-652, 1976, 24 pp.
- [74] Hallauer, W. L., Jr. and Franck, A., *On Determining the Number of Dominant Modes in Sinusoidal Structural Response*, The Shock & Vibration Bulletin, Vol. 49, September 1979.
- [75] Hallauer, W. L., Jr. and Stafford, J. F., *On the Distribution of Shaker Forces in Multiple-Shaker Modal Testing*, Shock & Vibration Bulletin, Vol. 48, Num. 1, 1978, pp. 49-63.
- [76] Hammond, C. E. and Doggett, R. V., Jr., *Determination of Subcritical Damping by Moving-Bloc/Randomdec Applications*, Flutter Testing Techniques NASA-SP-415, 1975, pp. 59-76.

- [77] Hanagud, S. V., Meyyappa, M. and Craig, J. I., *Method of Multiple Scales and Identification of Nonlinear Structural Dynamic Systems*, AIAA Journal, May 1985, pp. 802-807.
- [78] Hanagud, S., Meyyappa, M., Cheng, Y. P., and Craig, J. I., *Identification of Structural Dynamic Systems with Nonproportional Damping*, AIAA Journal, November 1986, pp. 1880-1882.
- [79] Hans, E. L., *No Reciprocal Theorem for Dynamic Displacements*, Journal of Sound and Vibration, Vol. 64, Num. 2, 1979, pp. 275-276.
- [80] Harris, C. M. and Crede, C. E., "Shock and Vibrational Handbook," (Second Edition), McGraw-Hill Book Company, 1976, pp. 4-1 - 4-8.
- [81] Huan, S.-L., McInnis, B. C., and Denman, E. D., *Identification of Structural Systems Using Naturally Induced Vibration Data in the Presence of Measurement Noise*, Computer Methods in Applied Mechanics & Engineering, Vol. 41, Num. 2, 1983, pp. 123-128.
- [82] Ibanez, P., *Identification of Dynamic Parameters of Linear and Non-Linear Structural Models from Experimental Data*, Nuclear Engineering and Design, Vol. 25, 1973, pp. 30-41.
- [83] Ibanez, P., *Methods for the Identification of Dynamic Parameters of Mathematical Structural Models from Experimental Data*, Nuclear Engineering and Design, Vol. 27, Num. 2, 1974, pp. 209-219.
- [84] Ibrahim, S. R., *Modal Identification Techniques Assessment and Comparison*, pp. 831-839.
- [85] Ibrahim, S. R., *Double Least Squares Approach for Use in Structural Modal Identification*, AIAA Journal, Vol. 24, Num. 3, March 1986, pp. 499-503.
- [86] Ibrahim, S. R., *Ibrahim Time Domain Modal Vibration Testing Technique*, Seminar Sponsored by Old Dominion University School of Continuing Studies.
- [87] Ibrahim, S. R. and Mikuckik, E. C., *A Method for the Direct Identification of Vibration Parameters from the Free Response*, Shock & Vibration Bulletin, Vol. 47, Num. 4, 1977, pp. 183-198.
- [88] Idelsohn, S. R. and Cardona, A., *Recent Advances in Reduction Methods in Non Linear Structural Dynamics*, Proceedings of the 2nd International Conference on Recent Advances in Structural Dynamics, Vol. II, pp. 475-482.
- [89] Isenberg, J., *Progressing from Least Squares to Bayesian Estimation*, Submitted to ASME Paper No. 79-WA/DSC-16 Dynamic Systems & Control Division.
- [90] Ito, H., Kobayashi, E., and Murai, S., *Non-Linear System Simulation by the Modal Method*, Proceedings/2nd International Modal Analysis Conference (Orlando, Florida), February 1984, pp. 528-534.
- [91] Jennings, A., *Eigenvalue Methods for Vibration Analysis II*, The Shock & Vibration Digest, January 1984, pp. 25-33.
- [92] Jezequel, L., *Three New Methods of Modal Identification*, ASME Publication No. 85-DET-92, 9 pp.
- [93] Jezequel, L., *Modal Synthesis of Large Structures with Nonlinear Joints from Vibration Tests*, 18 pp.
- [94] Juang, J. and Pappa, R. S., *Effects of Noise on ERA-Identified Modal Parameters*, AAS/AIAA Astrodynamics Specialist Conference, Vail, Colorado, Paper No. AAS 85-422, Aug. 12-15 1985, 23 pp.
- [95] Juang, J. and Pappa, R. S., *An Eigensystem Realization Algorithm (ERA) for Modal Parameter Identification and Model Reduction*, June 4-6 1984, 20 pp.
- [96] Kennedy, C. C. and Pancu, C. D. P., *Use of Vectors in Vibration Measurement and Analysis*, Journal of Aeronautical Sciences, Vol. 14, Num. 11, 1947, pp. 603-625.

- [97] Kim, Y. C. and Powers, E. J., *Digital Bispectral Analysis and its Applications to Nonlinear Wave Interactions*, IEEE Transactions on Plasma Science, Vol. PS-7, Num. 2, June 1979, pp. 120-131.
- [98] Kirshenboim, J. and Ewins, D. J., *A Method for Recognizing Structural Nonlinearities in Steady-State Harmonic Testing*, Journal of Vibration, Acoustics, Stress and Reliability in Design, Vol. 106, January 1984, pp. 49-52.
- [99] Kirshenboim, J. and Ewins, D. J., *A Method for the Derivation of Optimal Modal Parameters from Several Single-Point Excitation Tests*, IMAC II, pp. 991-997.
- [100] Klosterman, A., *On the Experimental Determination and Use of Modal Representations of Dynamic Characteristics*, Ph.D. Dissertation, University of Cincinnati, Mechanical Engineering Department, 1971, 184 pp.
- [101] Knight, Jr., N. F., *Nonlinear Structural Dynamic Analysis Using A Modified Modal Method*, AIAA Journal, Vol. 23, Num. 10, October 1985, pp. 1594-1601.
- [102] Kortum, W. and Niedbal, N., *Application of Modern Control Theory to Modal Survey Techniques*.
- [103] Lang, G. F., *Anti-Resonant Analysis... An Often Overlooked Alternative*, 10 pp.
- [104] Leuridan, J. and Vold, H., *A Time Domain Linear Model Estimation Technique for Global Modal Parameter Identification* 9 pp.
- [105] Leuridan, J. M., *Lecture Notes from the Advance Modal Analysis Course*, Structural Dynamics Research Lab, University of Cincinnati, Cincinnati, Ohio 45221, August 1984.
- [106] Leuridan, J. M., Brown, D. L. and Allemang, R. J., *Direct System Parameter Identification of Mechanical Structures with Application to Modal Analysis*, 9 pp.
- [107] Leuridan, J. M., Brown, D. L. and Allemang, R. J., *Time Domain Parameter Identification Methods for Linear Modal Analysis: A Unifying Approach*, Journal of Vibration, Acoustic, Stress, and Reliability in Design PaperNo. 85-DET-90, 8 pp.
- [108] Link, M. and Volland, A., *Identification of Structural System Parameters From Dynamic Response Data*, Z Flugwiss, Weltraum Forsch. , Vol. 2, Num. 3, 1978, pp. 165-174.
- [109] Marchand, M., *Parameter Estimation From Flight Test Data By Means of Statistical Methods in the Frequency Domain*, European Space Research Organization ESRO - TT - 104, 1974, pp.213-223.
- [110] Marmarelis, V. Z., *Practicable Identification of Nonstationary Nonlinear Systems*, IEE Proceedings, Vol. 128, Num. 5 (D), September 1981, pp. 211-214.
- [111] Marples, V., *The Derivation of Modal Damping Ratios From Complex-Plane Response Plots*, Journal of Sound and Vibration, Vol. 31, Num. 1, 1973, pp. 105-117.
- [112] Masri, S. F. and Caughey, T. K., *A Nonparametric Identification Technique for Nonlinear Dynamic Problems*, Journal of Applied Mechanics, Vol. 46, June 1979, pp. 433-447.
- [113] Masri, S. F. and Stott, S. J., *Random Excitation of a Nonlinear Vibration Neutralizer*, Journal of Mechanical Design, Vol. 100, October 1978, pp. 681-689.
- [114] Masri, S. F., Miller, R. K., and Sassi, H., *Time Domain Analysis of Nonlinear Vibration Data*, Proceedings of the 2nd International Conference on Recent Advances in Structural Dynamics, Vol. II, pp. 511-520.
- [115] Masri, S. F., Sassi, H., and Caughey, T. K., *Nonparametric Identification of Nearly Arbitrary Nonlinear Systems*, Journal of Applied Mechanics, Vol. 49, September 1982, pp. 619-628.
- [116] Maymon, G., *Experimental Determination of Linear Damping Coefficients in Elastic Structures with Geometric Nonlinearity*, Israel Journal of Technology, Vol. 16, 1978, pp. 64-69.

- [117] Mertens, M., Van Der Auweraer, H., Vanherck, P., and Snoeys, R., *Basic Rules of a Reliable Detection Method for Nonlinear Dynamic Behavior*, Proceedings/Tenth International Seminar on Modal Analysis, K.U. Leuven, Belgium, Part IV, 1985.
- [118] Mertens, V., Van Der Auweraer, H., Vanherck, P., and Snoeys, R., *Detection of Nonlinear Dynamic Behavior of Mechanical Structures*, Proceedings/Fourth International Modal Analysis Conference, 1986, pp. 712-719.
- [119] Miramand N., Billaud J.F., Leleux F., Kernevez J.P., *Identification of Structural Modal Parameters By Dynamic Tests at a Single Point*, Shock and Vibration Bulletin, Vol. 46, Num. 5, 1976, pp. 197-212.
- [120] Mustain, R. W., *Survey of Modal Vibration Test/Analysis Techniques*, SAE Aerospace Engineering and Manufacturing Meeting, Town and Country, San Diego, Nov. 29 - Dec. 2, 1976, Pub. #760870, 16 pp.
- [121] Natke, H. G and Rotert, D., *Determination of Normal Modes from Identified Complex Modes*, Z. Flugwiss. Weltraumforsch.g., Heft 2, 1985, pp. 82-88.
- [122] Natke, H. G., *Remarks on Essential Modern Modal Test Methods*, ESRO, Structural and Thermal Tests (N74-14537), Vol. 1, 1973, pp. 1-22.
- [123] Nayfeh, A. H., *The Response of Multidegree of Freedom Systems with Quadratic Nonlinearities to a Harmonic Parametric Response*, Journal of Sound and Vibration, Vol. 90, Num. 2, 1983, pp. 237-244.
- [124] Nieman, R. E., Fisher, D. G. and Seborg, D. E., *A Review of Process Identification and Parameter Estimation Techniques*, International Journal of Control, Vol. 13, Num. 2, 1971, pp.209-264.
- [125] Okubo, N., *The Effect of Non-Linearity on Transfer Function Measurement*, Sound and Vibration, November 1982, pp. 34-37.
- [126] Otnes, R. K. and Enochson, L., "Digital Time Series Analysis," John Wiley and Sons, Inc., 1972, 467 pp.
- [127] Pandit, S. M. and Mehta, N. P., *Data Dependent Systems Approach to Modal Analysis Via State Space*, Journal of Dynamic Systems, Measurement, and Control, Vol. 107, June 1985, pp. 132-138.
- [128] Pandit, S. M. and Suzuki, H., *Application of Data Dependent Systems to Diagnostic Vibration Analysis*, ASME Publication No. 79-DET-7, 1979, 9 pp.
- [129] Pappa, R. S., *Some Statistical Performance Characteristics of the "ITD" Modal Identification Algorithm* AIAA Paper No. 82-0768, 1982, 19 pp.
- [130] Pappa, R. S. and Ibrahim, S. R., *A Parametric Study of the "ITD" Modal Identification Algorithm*, Preliminary Review Copy, 11/13/80.
- [131] Pappa, R. S. and Juang, J., *Companison of the ERA and Polyreference Modal Identification Techniques (abstract)* 3rd SDRC I-Deas; User's Conf., Oct. 20-23,1986, 11 pp.
- [132] Pendered, J. W. and Bishop, R. E. D., *A Critical Introduction to Some Industrial Resonance Testing Techniques*, Journal of Mechanical Engineering Science, Vol. 5, Num. 4, 1963, pp. 345-367.
- [133] Pendered, J. W. and Bishop, R. E. D., *The Determination of Modal Shapes in Resonance Testing*, Journal of Mechanical Engineering Science, Vol. 5, Num. 4, 1963, pp. 379-385.
- [134] Pessen, D. W., *Mechanism Animation on a Personal Computer*, Mechanical Engineering, October 1984, pp. 33-35.
- [135] Peterson, E. L. and Klosterman, A. L., *Obtaining Good Results From an Experimental Modal Survey*, Society of Environmental Engineers, Symposium, London England, 1977, 22 pp.

- [136] Potter, R. and Richardson, M., *Mass, Stiffness, and Damping Matrices from Measured Modal Parameters* ISA-74 (International Instrumentation-Automatical Conference & Exhibit) Paper No. 74-630, 1974.
- [137] Potter, R. W., *A General Theory of Modal Analysis for Linear Systems*, Shock and Vibration Digest, Vol. 7, Num. 11, 1975, 8 pp.
- [138] Rades, M., *Identification of the Dynamic Characteristics of a Simple System with Quadratic Damping*, Serie de Mecanique Appliquee, Vol. 28, Num. 4, 1983, pp. 439-446.
- [139] Rades, M., *Methods for the Analysis of Structural Frequency Response Measurement Data*, 1975, pp.73-87.
- [140] Rades, M., *System Identification Using Real-Frequency-Dependent Modal Characteristics*, The Shock and Vibration Digest, Vol. 18, Num. 8, August 1986, pp. 3-10.
- [141] Ramsey, K. A., *Effective Measurements for Structural Dynamics Testing, Part II*, Sound and Vibration, October 1976, pp. 18-31.
- [142] Ramsey, K. A. and Firmin, Dr. A., *Experimental Modal Analysis, Structural Modifications and FEM Analysis-Combining Forces on a Desktop Computer*, SMS Litature to be presented @ 1st Annual Modal Analysis Conference, Nov. 8-10, 1982, pp. 581-606.
- [143] Rao, D. K., *Interactive Modal Imaging Proacess for Vibrating Structures*, ASME Publication No. 85-DET-110, 12 pp.
- [144] Reed, R. E., *Analytical Aspects of Randomdec Analysis*, AIAA Paper No. 79-0828, 1979, pp. 404-409.
- [145] Reiter, W.F., and Hodgson T.H., *Data Acquisition in Vibration Testing*, Vibration Testing-Instrumentation and Data Analysis, ASME, AMD, Vol. 12, 1975, pp. 1-24.
- [146] Richardson, M. and Kniskern, J., *Identifying Modes of Large Structures from Multiple Input and Response Measurements*, SAE Paper No. 760875, 1976, 12 pp.
- [147] Richardson, M. and Potter, R., *Identification of the Modal Properties of an Elastic Structure from A,Measured Transfer Function Data*, Instrument Society of America ISA ASI 74250, 1974, pp. 239-246.
- [148] Richardson, M. H. and Formenti, D. L., *Parameter Estimation from Frequency Response Measurements Using Rational Fraction Polynomials*, SMS Literature (Structural Measurement Systems), pp. 167-181.
- [149] Riad, H. D., *Nonlinear Response Using Normal Modes*, AIAA Paper No. 74-138, 1974, 6 pp.
- [150] Roberts, V. B., *Techniques for Nonlinear Random Vibration Problems*, The Shock and Vibration Digest, Vol. 16, Num. 9, September 1984, pp. 3-14.
- [151] Rosenberg, R. M., *The Normal Modes of Nonlinear n-Degree-of-Freedom Systems*, Journal of Applied Mechanics, March 1962, pp. 7-14.
- [152] Rost, B. and Leuridan, J., *A Comparison of Least Squares and Total Least Squares for Multiple Input Estimation of Frequency Response Functions*, ASME Publication No. 85-DET-105, 6 pp.
- [153] Schetzen, M., *A Theory of Non-Linear System Identification*, Int. J. Control, Vol. 20, Num. 4, 1974, pp. 577-592.
- [154] Schetzen, M., *Nonlinear System Modeling Based on the Wiener Theory*, IEEE Proceedings, Vol. 69, Num. 12, December 1981, pp. 1557-1573.
- [155] Singh, R. P. and Likins, P. W., *Singular Value Decomposition for Constrained Dynamical Systems*, Journal of Applied Mechanics, Vol. 52, Num. 4, December 1985, pp. 943-948.
- [156] Singh, R., Nopporn, C., and Busby, H., *Feasibility of Using Modal Analysis Techniques for Nonlinear Multidegree of Freedom Systems*, Proceedings of the 2nd International Conference

- on Recent Advances in Structural Dynamics, Vol. II, pp. 483-493.
- [157] Smiley, R. G., *Getting the Most Out of Commercial Modal Systems*.
 - [158] Snyder, V. W., Meeuwse, G. L., and Shapton, W. R., *Interactive Design Using Eigenvalue Modification, A Comparison of Experimental & Theoretical Modal Analysis*, SAE Technical Paper Series No. 820191 Presented @ International Congress and Exposition (Detroit, Michigan), Feb. 22-26 1982, 8pp.
 - [159] Stahle, C. V., *Modal Test Methods and Applications*, Journal of Environmental Sciences, Jan/Feb 1978, 4 pp.
 - [160] Szemplinska-Stupnicka, W., *The Modified Single Mode Method in the Investigations of the Resonant Vibrations of Non-Linear Systems*, Journal of Sound and Vibration, Vol. 63, Num. 4, 1979, pp. 475-489.
 - [161] Targoff, W. P., *Orthogonality Check and Correction of Measured Modes*, AIAA Journal, Vol. 14, Num. 2, 1976, pp. 164-167.
 - [162] Tomlinson, G. R., *Detection, Identification, and Quantification of Nonlinearity in Modal Analysis - A Review*, Proceedings/Fourth International Modal Analysis Conference, 1986, pp. 837-843.
 - [163] Tomlinson, G. R., *Using the Hilbert Transform with Linear and Non-linear Multi-mode Systems*, Proceedings/Third International Modal Analysis Conference, 1985, pp. 255-265.
 - [164] Tomlinson, G. R., *An Analysis of the Distortion Effects of Coulomb Damping on the Vector Plots of Lightly Damped Systems*, Journal of Sound and Vibration, Vol. 71, Num. 3, 1980, pp. 443-451.
 - [165] Tomlinson, G. R. and Ahmed, I., *Frequency and Damping Estimates from a Non-linear Structure - Causalisation and Random Excitation*, Proceedings/Tenth International Seminar on Modal Analysis, K.U. Leuven, Belgium, Part IV, 1985.
 - [166] Tomlinson, G. R. and Hilbert, J. H., *Identification of the Dynamic Characteristics of a Structure with Coulomb Friction*, Journal of Sound and Vibration, Vol. 64, Num. 2, 1979, pp. 233-242.
 - [167] Tomlinson, G. R. and Kirk, N. E., *Modal Analysis and Identification of Structural Non-Linearity*, Proceedings of the 2nd International Conference on Recent Advances in Structural Dynamics, Vol. II, pp. 495-510.
 - [168] Tomlinson, G. R. and Kirk, N. E., *Modal Analysis and Identification of Structural Non-Linearity*, Simon Engineering Laboratories, University of Manchester, Manchester, England, 21 pp.
 - [169] Tomlinson, G. R. and Lam, J., *Frequency Response Characteristics of Structures with Single and Multiple Clearance Type Nonlinearity*, Journal of Sound and Vibration, Vol. 96, Num. 1, 1984, pp. 111-125.
 - [170] To, C. W. S., *The Response of Nonlinear Structures to Random Excitation*, The Shock and Vibration Digest, April 1984, pp. 13-33.
 - [171] Trubert, M. R., *Use of Analog Computer for the Equalization of Electro Magnetic Shakers in Transient Testing*, NASA-CR-95095, 1968, 23 pp.
 - [172] Tso, W. K. and Asmis, K. G., *Multiple Parametric Resonance in a Non-Linear Two Degree of Freedom System*, 1974, pp. 269-277.
 - [173] Tumanov, Y. A., Lavrov, V. Y., and Markov, Y. G., *Identification of Nonlinear Mechanical Systems*, Prikladnaya Mekhanika, Vol. 17, Num. 9, September 1981, pp. 106-110.
 - [174] Tustin, W., *Minicomputer Control of Vibration, Shock and Acoustical Tests*, Test Engineering Management, Vol. 35, Num. 1-2, 1976, 4 pp.

- [175] Ulm, S. C. and Morse, I. E., *Recognizing System Nonlinearities Using Modal Analysis Tests*, ASME Publication No. 82-DET-138, 8 pp.
- [176] Van Loon P., *Modal Parameters of Mechanical Structures*, Ph. D., Dissertation, Catholic University of Leuven, Belgium, 1974, 183 pp.
- [177] Vigneron, F. R., *A Natural Modes Formulation and Modal Identities for Structures with Linear Viscous Damping*, Communications Research Center, January 1985, 24 pp.
- [178] Vinh, T., Haoui, A., and Chevalier, Y., *Modal Analysis of Structures with Applications to the Mechanics of Materials*, University of Manchester, Euromech 168, 1983.
- [179] Vonhanacker, I. P., *Use of Modal Parameters of Mechanical Structures in Sensitivity Analysis, System Synthesis and System Identification Methods*, Katholieke Universiteit te Leuven, September 1980, 33 pp.
- [180] Wang, Z. and Fang, T., *A Time-Domain Method for Identifying Modal Parameters*, Journal of Applied Mechanics, Vol. 53, Num. 1, March 1986, pp. 28-32.
- [181] White, R. G., *Effects of Non-Linearity Due to Large Deflections in the Resonance Testing of Structures*, Journal of Sound and Vibration, Vol. 16, Num. 2, 1971, pp. 255-267.
- [182] Wittmeyer, H., "Ein iteratives, experimental-rechnerisches Verfahren zur Bestimmung der dynamischen...", *Zeitschrift für Flugwissenschaften*, Vol. 19, 1971, pp. 229-241.
- [183] Wittmeyer, H., *Ground Resonance Test of a Structure with Damping Coupling and Frequency Neighborhood (German)*, Gedanken zur Entwicklung der Plastizitätstheorie, Vol. 24, Num. 3, 1976, pp. 139-151.
- [184] Wolf, B., *Identification of Linear Structures*, Journal of Dynamic Systems, Measurement, and Control, Vol. 106, December 1984, pp. 300-304.
- [185] Wysocki, E. M. and Rugh, W. J., *An Approximation Approach to the Identification of Nonlinear Systems Based on Frequency-Response Measurements*, Int. J. Control, Vol. 79, Num. 1, 1979, pp. 113-123.
- [186] Yarcho, W. B., *Survey of Vibration Test Procedures in Use by the Air Force*, Shock and Vibration Bulletin, Vol. 42, Num. 1, 1972, pp. 11-17.
- [187] Yar, M. and Hammond, J. K., *Spectral Analysis of a Randomly Excited Duffing System*, Proceedings/Fourth International Modal Analysis Conference, 1986, pp. 736-742.
- [188] Zecher, J. E., *Developing a Desktop Computer-Based Three-Dimensional Modeling System*, Mechanical Engineering, November 1983, pp. 50-61.
- [189] Zhang, L., Kanda, H., Brown, D. L. and Allemang, R. J., *A Polyreference Frequency Domain Method for Modal Parameter Identification*, ASME Publication #85-DET-106, 5 pp.
- [190] Zimmerman, R. D., *7110 Hammer Calibration Standard, User's Manual*, QUIXOTE Measurement Dynamics, Inc., Document 57110, Cincinnati, Ohio.

Nomenclature

Matrix Notation

$\{..\}$	braces enclose column vector expressions
$\{..\}^T$	row vector expressions
$[..]$	brackets enclose matrix expressions
$[..]^H$	complex conjugate transpose, or Hermitian transpose, of a matrix
$[..]^T$	
$[..]^{-1}$	inverse of a matrix
$[..]^+$	generalized inverse (pseudoinverse)
$[..]_{q \times p}$	size of a matrix: q rows, p columns
$[..]$	diagonal matrix

Operator Notation

A^*	complex conjugate
F	Fourier transform
F^{-1}	inverse Fourier transform
H	Hilbert transform
H^{-1}	inverse Hilbert transform
\ln	natural logarithm
L	Laplace transform
L^{-1}	inverse Laplace transform
$\text{Re} + j\text{Im}$	complex number: real part "Re", imaginary part "Im"
\dot{x}	first derivative with respect to time of dependent variable x
\ddot{x}	second derivative with respect to time of dependent variable x
\bar{y}	mean value of y
\hat{y}	estimated value of y
$\sum_{i=1}^n A_i B_i$	summation of $A_i B_i$ from $i = 1$ to n
$\frac{\partial}{\partial t}$	partial derivative with respect to independent variable "t"
$\det[..]$	determinant of a matrix
$\ .. \ _2$	Euclidian norm

Roman Alphabet

A_{pqr}	residue for response location p, reference location q, of mode r
C	damping
COH	ordinary coherence function†
COH_{ik}	ordinary coherence function between any signal i and any signal k†
COH^c	conditioned partial coherence†
e	base e (2.71828...)
F	input force
F_q	spectrum of q^{th} reference†
GFF	auto power spectrum of reference†
GFF_{qq}	auto power spectrum of reference q†

GFF_{ik}	cross power spectrum of reference i and reference k†
$[GFFX]$	reference power spectrum matrix augmented with the response/reference cross power spectrum vector for use in Gauss elimination
GXF	cross power spectrum of response/reference†
GXX	auto power spectrum of response†
GXX_{pp}	auto power spectrum of response p†
$h(t)$	impulse response function†
$h_{pq}(t)$	impulse response function for response location p, reference location q †
$H(s)$	transfer function†
$H(\omega)$	frequency response function, when no ambiguity exist, H is used instead of $H(\omega)$ †
$H_{pq}(\omega)$	frequency response function for response location p, reference location q, when no ambiguity exist, H_{pq} is used instead of $H_{pq}(\omega)$ †
$H_1(\omega)$	frequency response function estimate with noise assumed on the response, when no ambiguity exist, H_1 is used instead of $H_1(\omega)$ †
$H_2(\omega)$	frequency response function estimate with noise assumed on the reference, when no ambiguity exist, H_2 is used instead of $H_2(\omega)$ †
$H_S(\omega)$	scaled frequency response function estimate, when no ambiguity exist, H_S is used instead of $H_S(\omega)$ †
$H_v(\omega)$	frequency response function estimate with noise assumed on both reference and response, when no ambiguity exist, H_v is used instead of $H_v(\omega)$ †
$[I]$	identity matrix
j	$\sqrt{-1}$
K	stiffness
L	modal participation factor
M	mass
M_r	modal mass for mode r
$MCOH$	multiple coherence function†
N	number of modes
N_i	number of references (inputs)
N_o	number of responses (outputs)
p	output, or response point (subscript)
q	input, or reference point (subscript)
r	mode number (subscript)
R_I	residual inertia
R_F	residual flexibility
s	Laplace domain variable
t	independent variable of time (sec)
t_k	discrete value of time (sec)
	$t_k = k \Delta t$
T	sample period
x	displacement in physical coordinates
X	response
X_p	spectrum of p^{th} response†
z	Z domain variable

Greek Alphabet

$\delta(t)$	Dirac impulse function
Δf	discrete interval of frequency (Hertz or cycles/sec)
Δt	discrete interval of sample time (sec)
ϵ	small number
η	noise on the output

λ_r	r^{th} complex eigenvalue, or system pole $\lambda_r = \sigma_r + j\omega_r$
$[\Lambda]$	diagonal matrix of poles in Laplace domain
ν	noise on the input
ω	variable of frequency (rad/sec)
ω_r	imaginary part of the system pole, or damped natural frequency, for mode r (rad/sec) $\omega_r = \Omega_r \sqrt{1 - \zeta_r^2}$
Ω_r	undamped natural frequency (rad/sec) $\Omega_r = \sqrt{\sigma_r^2 + \omega_r^2}$
ϕ_{pr}	scaled p^{th} response of normal modal vector for mode r
$\{\phi\}_r$	scaled normal modal vector for mode r
$[\Phi]$	scaled normal modal vector matrix
$\{\psi\}$	scaled eigenvector
ψ_{pr}	scaled p^{th} response of a complex modal vector for mode r
$\{\psi\}_r$	scaled complex modal vector for mode r
$[\Psi]$	scaled complex modal vector matrix
σ	variable of damping (rad/sec)
σ_r	real part of the system pole, or damping factor, for mode r
ζ	damping ratio
ζ_r	damping ratio for mode r
†	vector implied by definition of function

Appendix A: Least Squares Method

A.1 Least Squares Method

The process of determination of a mathematical model for a group of variables is known as the parameter estimation process. One of the more popular approaches used in parameter estimation is the *Least Squares Method*.

In its simplest form the least squares method will be illustrated in this section. Suppose that the relationship between two group of variables x and y can be best described by the equation of a straight line:

$$y = a_1 x + a_0 \quad (A1)$$

One could arbitrarily choose two sets of x and y quantities and solve for the two unknown parameters a_1 and a_0 . Yet, the line constructed by the computed a_1 and a_0 parameters might not pass through some sets of x and y , since the information associated with those points were not used in computing a_1 and a_0 .

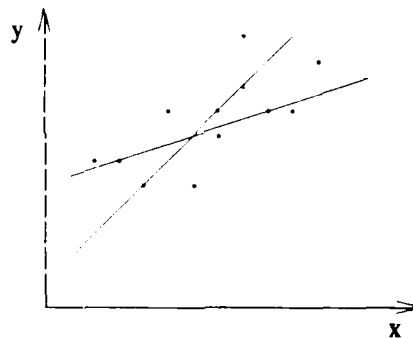


Figure 119. Straight Lines Fitting the Data

The reasons for all the points not being located on one straight line could be:

- Errors in data set
- Inaccurate model for the data set.

The least squares criterion requires that the sum of the squares of the deviations separating the data points from the curve will be minimum. These deviations are simply the difference between the estimated values of y (hereafter denoted by \hat{y}_r) from Eq. (A1) and the actual measured values of y (y_r). In other words, the deviations are the errors associated with the value of y predicted by the model and the actual measured data. The least squares method approach will use information associated with all of the x and y sets, to determine the "best" estimates of a_1 and a_0 .

$$E = \sum_{r=1}^N e_r^2 = \sum_{r=1}^N [y_r - \hat{y}_r]^2 = \sum_{r=1}^N [y_r - (a_1 x_r + a_0)]^2 \quad (A2)$$

Minimization of error, Eq. (A2), with respect to a_1 and a_0 results in the following equations which are called the *normal equations for the least squares problem*:

$$\frac{\partial E}{\partial a_1} = \sum_{r=1}^N 2 \left[y_r - (a_1 x_r + a_0) \right] [-x_r] = 0 \quad (\text{A3})$$

$$\frac{\partial E}{\partial a_0} = \sum_{r=1}^N 2 \left[y_r - (a_1 x_r + a_0) \right] [-1] = 0 \quad (\text{A4})$$

Equations (A3) and (A4) can be solved for the unknown parameters a_1 and a_0 .

$$a_1 = \frac{N \sum_{r=1}^N x_r y_r - \left(\sum_{r=1}^N x_r \right) \left(\sum_{r=1}^N y_r \right)}{N \sum_{r=1}^N x_r^2 - \left(\sum_{r=1}^N x_r \right)^2} \quad (\text{A5})$$

$$a_0 = \frac{\left(\sum_{r=1}^N y_r \right) \left(\sum_{r=1}^N x_r^2 \right) - \left(\sum_{r=1}^N x_r \right) \left(\sum_{r=1}^N x_r y_r \right)}{N \sum_{r=1}^N x_r^2 - \left(\sum_{r=1}^N x_r \right)^2} \quad (\text{A6})$$

The a_1 and a_0 values computed from Eqs. (A5) and (A6) represent the characteristics of a straight line which would "best" describe the x and y sets of values.

Similarly, one could compute a_1 and a_0 parameters with the criterion that the sum of the square of errors in the x (e_x) would be minimum. Another approach could be the minimization of the sum of the square of errors in the x and y (e_v).

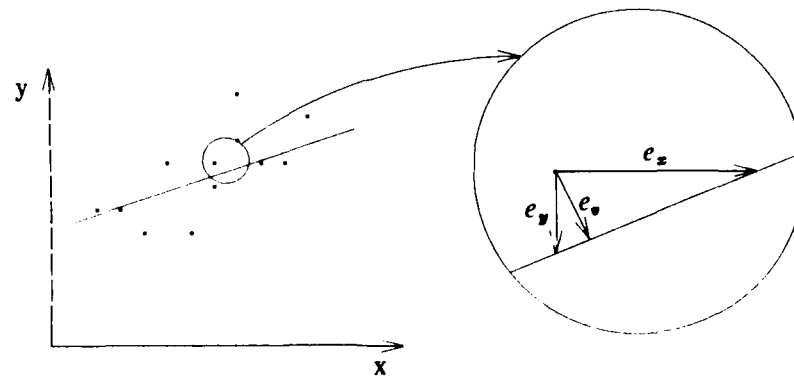


Figure 120. Errors in Least Squares Estimation

The least squares problem can be formulated in matrix notation as:

$$\{Y\} = [X]\{A\} \quad (\text{A7})$$

where,

$$\{Y\} = \begin{Bmatrix} y_1 \\ y_2 \\ \vdots \\ y_N \end{Bmatrix} \quad [X] = \begin{bmatrix} x_1 & 1 \\ x_2 & 1 \\ \vdots & \vdots \\ x_N & 1 \end{bmatrix} \quad \{A\} = \begin{Bmatrix} a_1 \\ a_0 \end{Bmatrix}$$

The equations presented by matrix Eq. (A7) are in general a set of inconsistent and overdetermined equations. Inconsistent, since it is not usually possible to find $\{A\}$ that would satisfy all the individual equations of Eq. (A7), and overdetermined, since the number of equations is larger than the number of unknowns. The least square solution of Eq. (A7) is:

$$[X]^T\{Y\} = [X]^T[X]\{A\} \quad (\text{A8})$$

and solving for unknown vector $\{A\}$

$$\{A\} = \left([X]^T[X]\right)^{-1} [X]^T\{Y\} \quad (\text{A9})$$

provided that $([X]^T[X])^{-1}$ exists. In the case that the inverse of $([X]^T[X])$ does not exist, one could use numerical techniques to solve for vector $\{A\}$.

In a more general case where matrices A, X, and Y are complex valued, the transpose notation, T, must be replaced with hermitian notation, H, in Eqs. (A8) and (A9). Where the hermitian operator, H, is the complex conjugate transpose. Hence, the unknown vector $\{A\}$ is given by:

$$\{A\} = \left([X]^H[X]\right)^{-1} [X]^H\{Y\} \quad (\text{A10})$$

Individual equations in matrix Eq. (A7) could be multiplied by a weighting factor to give that equation more or less weight in the computation. The weighting factors could be presented in form of a diagonal ($N \times N$) matrix, W. The diagonal element in row i represents the weighting factor corresponding to equation i, and the off diagonal terms are all zero. Matrix W is pre-multiplied to both sides of Eq. (A7):

$$[W]\{Y\} = [W][X]\{A\} \quad (\text{A11})$$

where,

$$[W] = \begin{bmatrix} w_1 & 0 & \dots & 0 \\ 0 & w_2 & \dots & 0 \\ \vdots & \vdots & \ddots & \vdots \\ 0 & 0 & \dots & w_N \end{bmatrix}$$

Solving for vector $\{A\}$ in Eq. (A11):

$$\{A\} = \left([X]^H[W]^H[W][X]\right)^{-1} [X]^H[W]^H[W]\{Y\} \quad (\text{A12})$$

In general the relationship of Eq. (1.1) could be in the form of:

$$y = a_N x^N + a_{N-1} x^{N-1} + \dots + a_1 x + a_0 \quad (\text{A13})$$

A set of equations similar to the formulation above could be written and solved to obtain the least squares estimation of unknown parameters $a_N, a_{N-1}, \dots, a_1, a_0$.

The least squares method stated above could easily be extended to problems involving more than one

independent variable. For example, z could be expressed in terms of x and y :

$$z = a_2 y + a_1 x + a_0 \quad (\text{A14})$$

The corresponding normal equations for the least squares problem of Eq. (A14) are:

$$\frac{\partial E}{\partial a_2} = \sum_{r=1}^N 2[z_r - (a_2 y_r + a_1 x_r + a_0)] [-y_r] = 0 \quad (\text{A15})$$

$$\frac{\partial E}{\partial a_1} = \sum_{r=1}^N 2[z_r - (a_2 y_r + a_1 x_r + a_0)] [-x_r] = 0 \quad (\text{A16})$$

$$\frac{\partial E}{\partial a_0} = \sum_{r=1}^N 2[z_r - (a_2 y_r + a_1 x_r + a_0)] [-1] = 0 \quad (\text{A17})$$

Equations (A15) - (A17) can be solved for the unknown parameters a_2 , a_1 , and a_0 . The computed values a_2 , a_1 , and a_0 represent the characteristics of a plane which would "best" describe the x , y , and z sets of values.

The above theory and formulation could be expanded to least squares estimation of a surface and eventually to higher order dimensions.

A.2 Correlation Coefficient

The "goodness" of the least squares estimation process is measured by the coefficient of correlation parameter which is defined in terms of *total variation* and *explained variation*. The total variation of y is defined as $\sum_{r=1}^N (y_r - \bar{y})^2$, which is the sum of the squares of the deviations of y_r from the mean value, \bar{y} . Total variation consists of two parts: (1) the explained variation, $\sum_{r=1}^N (\hat{y}_r - \bar{y})^2$; and (2) the unexplained variation, $\sum_{r=1}^N (y_r - \hat{y}_r)^2$. The terms explained variation and unexplained variation are used to denote the fact that the deviations $\hat{y}_r - \bar{y}$ have a definite pattern, while, the deviations $y_r - \hat{y}_r$ are random and unpredictable.

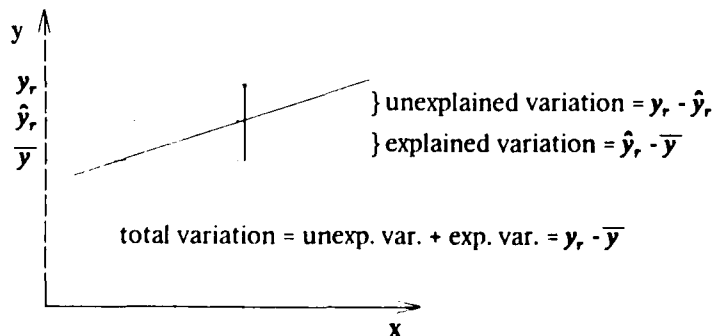


Figure 121. Variations in Data

Therefore, the coefficient of correlation γ^2 , is defined as:

$$\gamma^2 = \frac{\left(\sum_{r=1}^N (\hat{y}_r - \bar{y})^2 \right)}{\left(\sum_{r=1}^N (y_r - \bar{y})^2 \right)} \quad (\text{A18})$$

The magnitude of γ^2 varies between 0 and 1. A value of 0 indicates no correlation between dependent and independent variable(s), while a value of 1 indicates perfect correlation.

It should be pointed out that the coefficient of correlation computed for a set of data and a assumed model, only indicates the relationship of data based on the assumed model. That is, the coefficient of correlation measures the degree to which the assumed model describes the relationship for a set of data

A.3 Examples

A.3.1 Example 1

For the data given in Table 5 and the assumed model equation:

$$y = a_1 x + a_0 \quad (\text{A19})$$

x	65	63	67	64	68	62	70	66	68	67	69	71
y	68	66	68	65	69	66	68	65	71	67	68	70

TABLE 5. x and y Values for Least Squares Fit

- Find the least squares solution of a_1 and a_0 .
- Find the coefficient of correlation.

Solution:

- The following normal equations must be solved for a_1 and a_0

$$a_0 N + a_1 \sum_{r=1}^N x_r = \sum_{r=1}^N y_r \quad (\text{A20})$$

$$a_0 \sum_{r=1}^N x_r + a_1 \sum_{r=1}^N x_r^2 = \sum_{r=1}^N x_r y_r \quad (\text{A21})$$

substituting the appropriate terms in Eqs. (A20) and (A21):

$$\begin{aligned} 12 a_0 + 800 a_1 &= 811 \\ 800 a_0 + 53418 a_1 &= 54107 \end{aligned}$$

from which we find $a_1 = 0.476$ and $a_0 = 35.82$ or

$$y = 0.476x + 35.82 \quad (\text{A22})$$

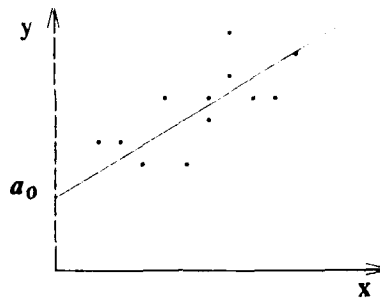


Figure 122. Least Squares Fit of Data

$$\text{b) Explained variation} = \sum_{r=1}^N (\hat{y}_r - \bar{y})^2 = 19.22$$

$$\text{Total variation} = \sum_{r=1}^N (y_r - \bar{y})^2 = 38.92$$

$$\text{Coefficient of correlation} = \gamma^2 = \frac{19.22}{38.92} = 0.7027$$

A.3.2 Example 2

Given the model for the sampled impulse response function between two points on a structure as,

$$h(t_k) = \sum_{r=1}^{2N} A_r e^{\lambda_r t_k} \quad (\text{A23})$$

where,

$$k = 0, 1, 2, \dots, 2N$$

Δt = value of time subinterval

$$t_k = k \Delta t$$

and the known pole information λ_r , formulate the least squares solution of estimating the residues, A_r .

Solution:

For simplicity and conciseness let,

$$z_r = e^{\lambda_r \Delta t}$$

and therefore Eq. (A23) can be rewritten as,

$$h(t_k) = \sum_{r=1}^{2N} A_r z_r^k \quad (\text{A24})$$

expanding Eq. (A24) for time values of t_0 to t_{2N-1} will result in the following $2N$ equations

$$\begin{aligned} h(t_0) &= A_1 + A_2 + \cdots + A_{2N} \\ h(t_1) &= A_1 z_1 + A_2 z_2 + \cdots + A_{2N} z_{2N} \\ h(t_2) &= A_1 z_1^2 + A_2 z_2^2 + \cdots + A_{2N} z_{2N}^2 \\ &\vdots \\ h(t_{2N-1}) &= A_1 z_1^{2N-1} + A_2 z_2^{2N-1} + \cdots + A_{2N} z_{2N}^{2N-1} \end{aligned} \quad (\text{A25})$$

presenting the $2N$ equations of Eq. (A25) in matrix form gives,

$$\begin{bmatrix} 1 & 1 & \cdots & 1 \\ z_1 & z_2 & \cdots & z_{2N} \\ z_1^2 & z_2^2 & \cdots & z_{2N}^2 \\ \vdots & \vdots & \ddots & \vdots \\ z_1^{2N-1} & z_2^{2N-1} & \cdots & z_{2N}^{2N-1} \end{bmatrix} \begin{Bmatrix} A_1 \\ A_2 \\ \vdots \\ A_{2N} \end{Bmatrix} = \begin{Bmatrix} h(t_0) \\ h(t_1) \\ h(t_2) \\ \vdots \\ h(t_{2N-1}) \end{Bmatrix} \quad (\text{A26})$$

or,

$$[z]\{A\} = \{h\} .$$

Solving Eq. (A26) with more than $2N$ rows for vector $\{A\}$ will result in the least squares solution of the residues.

A.4 References

- [1] Ben Nobel, James W. Daniel, *Applied Linear Algebra*, Prentice-Hall, Inc., 1977.
- [2] Gibert Strang, *Introduction to Applied Mathematics*, Wellesley-Cambridge press, 1986.
- [3] Murray R. Spiegel, *Schaum's outline series "Statistics"*, McGraw-Hill Book, 1961.

Appendix B: Singular Value Decomposition

B.1 Singular Value Decomposition

The singular value decomposition will decompose a matrix into the simplest possible form, that being diagonal. This decomposition will always be possible regardless of the rank, or dimension, of the matrix^[1].

Consider the right and left eigenvectors of the $m \times n$ matrix $[A]$, which is of rank k .

$$[A] \{v\} = \{u\} \sigma \quad (\text{B1})$$

$$[A]^H \{u\} = \{v\} \sigma \quad (\text{B2})$$

where:

- $\{u\} = m \times 1$ left singular vector
- $\{v\} = n \times 1$ right singular vector
- $\sigma =$ scalar singular value

By substituting Eq. (B1) into Eq. (B2) for $\{u\}$, the right singular vectors can be determined from:

$$[A]^H [A] \{v\} = \{v\} \sigma^2 \quad (\text{B3})$$

$$| [A]^H [A] - \sigma^2 [I] | = 0$$

where:

- $i = 1 \rightarrow k \quad \sigma_i^2 > 0$
- $i = k+1 \rightarrow n \quad \sigma_i^2 = 0$
- $[V] = [\{v\}_1 \{v\}_2 \{v\}_3 \cdots \{v\}_n]$ right singular unitary matrix.

By substituting Eq. (B2) into Eq. (B1) for $\{v\}$, the left singular vectors can be determined from:

$$[A] [A]^H \{u\} = \{u\} \sigma^2 \quad (\text{B4})$$

$$| [A] [A]^H - \sigma^2 [I] | = 0$$

where:

- $i = 1 \rightarrow k \quad \sigma_i^2 > 0$
- $i = k+1 \rightarrow m \quad \sigma_i^2 = 0$
- $[U] = [\{u\}_1 \{u\}_2 \{u\}_3 \cdots \{u\}_m]$ left singular unitary matrix.

If the eigenvector matrices $[U]$ and $[V]$ are unitary ($[U]^H = [U]^{-1}$ and $[V]^H = [V]^{-1}$), that is, both columns and rows form an orthonormal set, the linear transformation will preserve both angles and lengths. Interpreted geometrically, linear transformations defined by unitary matrices behave like simple rotations in space. The matrix $[A]$, can now be decomposed into diagonal form by appending the eigenvector matrices to Eq. (B1) and premultiplying by $[U]^H$, forming the matrix product:

$$[S] = [U]^H [A] [V] = \begin{bmatrix} \{u\}_1^H \\ \vdots \\ \{u\}_k^H \\ \vdots \\ \{u\}_m^H \end{bmatrix} \begin{bmatrix} \{u\}_1 \sigma_1 & \cdots & \{u\}_k \sigma_k & \{0\}_{k+1} & \cdots & \{0\}_n \end{bmatrix} . \quad (B5)$$

Using the unitary matrix property, $[U]^H [U] = [I]$, the right hand side can be further simplified as:

$$[S] = [U]^H [A] [V] = \begin{bmatrix} \sigma_1 & 0 & 0 & \cdots & 0 \\ 0 & \sigma_2 & 0 & \cdots & 0 \\ 0 & 0 & \sigma_3 & & 0 \\ \vdots & \vdots & & & \vdots \\ 0 & 0 & 0 & \cdots & \sigma_k \\ - & \{0\} & - & - & - \\ & & & & \{0\} \end{bmatrix} \begin{bmatrix} [0] \\ [0] \end{bmatrix} = \begin{bmatrix} [\Sigma] & [0] \\ [0] & [0] \end{bmatrix} . \quad (B6)$$

Thus, the original matrix, $[A]$, is decomposed into the matrix $[S]$, with the singular values on the diagonal, by the unitary matrices $[U]$ and $[V]$.

Then the singular value decomposition of $[A]$ is defined by:

$$[A] = [U][S][V]^H \quad (B7)$$

Noting the partitioning of the matrix $[S]$ of Eq. (B6), the unitary transformation matrices $[U]$ and $[V]$ can be partitioned in the same way to yield:

$$[A] = [U][S][V]^H = \begin{bmatrix} [U]_1 & [U]_2 \end{bmatrix} \begin{bmatrix} [\Sigma] & [0] \\ [0] & [0] \end{bmatrix} \begin{bmatrix} [V]_1^H \\ [V]_2^H \end{bmatrix} \quad (B8)$$

Thus, the singular value decomposition of $[A]$ can be further reduced to:

$$[A] = [U]_1 [\Sigma] [V]_1^H \quad (B9)$$

where:

- $[U]_1$ = left singular submatrix of size $m \times k$
- $[\Sigma]$ = diagonal singular value matrix of size $k \times k$
- $[V]_1^H$ = right singular submatrix of size $k \times n$.

The (Moore-Penrose) generalized inverse (pseudoinverse) ^[1-3], $[A]^\dagger$, of $[A]$ is:

$$[A]^\dagger = [V]_1 \begin{bmatrix} [\Sigma]^{-1} & [0] \\ [0] & [0] \end{bmatrix} [U]_1^H = [V]_1 [\Sigma]^{-1} [U]_1^H .$$

where:

- $[A]^\dagger$ = $n \times m$ generalized inverse of $[A]$
- $[V]_1$ = right singular submatrix of size $n \times k$.
- $[\Sigma]^{-1}$ = inverse of diagonal singular value matrix of size $k \times k$
- $[U]_1^H$ = left singular submatrix of size $k \times m$.

B.2 References

- [1] Ben Nobel, James W. Daniel, *Applied Linear Algebra*, Prentice-Hall, Inc., 1977, pp. 323-337.
- [2] Gibert Strang, *Introduction to Applied Mathematics*, Wellesley-Cambridge Press, 1986.
- [3] Gibert Strang, *Linear Algebra and Its Applications*, Academic Press, 1980.